Fluid Reabsorption Across Pig Urinary Bladder

Marian Manso

Department of Health and Applied Sciences

University of the West of England

September 2019

A thesis submitted in partial fulfilment of the requirements of the University of the West of England, Bristol for the degree of Doctor of Philosophy.

This work was funded by Ferring Pharmaceuticals and University of Bristol

Copyright disclaimer

This copy has been supplied on the understanding that it is copyright material and that no quotation from the thesis may be published without proper acknowledgement.

Acknowledgements

5; Trust in the Lord with all your heart and lean not on your understanding; 6 in all your ways submit to him and he will make your path straight.

Proverbs 3:5-6

This thesis and research contained within could not have been achieved without my friends, colleagues and supervisory team. I would like to take a moment to thank them all for everything they have done for me.

Firstly, I would like to thank my director of studies Dr Bahareh Vahabi for giving me the opportunity of a lifetime. I am grateful for her support, guidance, advice and encouragements. This opportunity has created a career path for me that I normally wouldn't have been able to dream of and for that I am forever grateful. Thank you for all the lessons you have thought over the past four years (five years including placement year).

I would also like to thank all my second supervisors, Prof. Marcus Drake, Prof. Christopher Fry, Prof. John Hancock, Prof. Myra Conway for their continuous support and guidance. I am grateful for the opportunity and I am also grateful to have been supervised by them. Their hard work has made this possible.

I would also like to thank Ferring Pharmaceuticals, Bristol University and Prof. Marcus Drake for the funding they provided for this research.

Finally (but very importantly) I would like to thank my dad, Prince Kwame Manso for being my backbone in life and motivating me to always aim high. Thank you for all your sacrifices. I would also like to thank my mom, Matilda Abora Manso, my siblings: Theresa Manso, Micheal Manso, Priscilla Manso, Joey Manso, Deborah Manso, for simply being my safety net whenever I needed one.

I would also like to thank two important people who have stood by me through everything: Nana Gyimah Baffour and Rosemary Boateng. Thank you for putting up with me all these years. None of this would have been possible without both of you.

I would like to thank my husband Robert Asante for his understanding, patience, encouraging words and support through this process. You have been crucial in the final stage of this process.

ABSTRACT

Introduction and aims: The bladder urothelium is generally considered to be poorly permeable blood-urine barrier. However, recent studies have shown that the urothelium expresses transmembrane water channels, aquaporins (AQPs). Currently 13 AQPs (AQP0, AQP1, AQP2, AQP3, AQP4, AQP5, AQP6, AQP7, AQP8, AQP9, AQP10, AQP11, AQP12) subtypes have been identified in mammalian tissues, and from these subtypes, AQPs 1-4, AQP7, AQP9 and AQP11 have been found in the urothelium of various species indicating that AQPs could regulate urothelial cell volume and osmolarity, determine the final composition of urine. However, the exact function of AQPs, their cellular regulation and distribution under different osmotic conditions in bladder urothelium remain to be elucidated. Therefore, this study aimed to i) investigate the expression of AQPs in pig urinary bladder, ii) the potential role of AQPs in mediating water transport across pig bladder urothelium in response to osmotic stress iii) investigate the effect of hypotonic and hypertonic solution on AQP3 intracellular localisation

Methods: Bladders obtained from (~6 months old) female pigs, as well as tissues used as positive control were obtained from the local abattoir and used to investigate AQPs. PCR was carried out on mRNA isolated from bladder mucosa and on urothelium cell suspensions, as well as tissues used as positive control to identify AQPs 1-11. Localisation of AQPs was determined using immunohistochemistochemical method on paraffin embedded mucosa sections. Movement of deuterium oxide (D_2O) fluxes across the bladder urothelium/suburothelium (mucosa) membranes were assessed using an Ussing chamber system. AQP3 intracellular localisation in urothelial cells after exposure to changes in tonicity was asses using immunoflourescence.

Results: AQPs 1, 3, 9, 11 mRNA expression was found in the mucosa of pig bladder, AQP 3, 9, 11 expression was also found specifically in urothelium. Immunohistochemistry showed AQP1 labelling in the endothelium of lamina propria blood vessels. AQPs 3 and 11 were expressed throughout the urothelium and AQP9 immunoreactivity was detected in upper region of the urothelium. Ussing chamber experiment shows gradual increase in D_2O concentration on the basolateral side of the mucosa over time when osmotic gradient was created between the apical and basolateral side of the mucosa tissue section with a known D_2O concentration on the apical side. D_2O diffusion rate was halted when tissue was treated with $HgCl_2$. The average diffusion rate for D_2O in absence of $HgCl_2$ and in the presence of $HgCl_2$ was calculated using Newman-keuls test. AQP3 immunoreactivity was detected around the nucleus in untreated urothelial cells, however, after exposure to hypertonic and hypotonic solutions for 4 and 5 hours, AQP3 immunoreactivity was detected mainly in the cell membrane.

Conclusions. Four different AQPs subtypes were identified in adult pig bladder, suggesting that AQPs may play a regulatory role in urothelial cell volume and water transport across the urothelium. Water movement was detected across pig bladder urothelium which was significantly inhibited by $HgCl_2$, demonstrating a possible role of AQPs in mediating transcellular movement of water across bladder urothelium. Immunofluorescent staining revealed cytoplasmic localisation of AQP3 in untreated

urothelial cells and its translocation to the cell membrane under osmotic stress. AQPs in the urinary bladder urothelium may play a regulatory role in urothelial cell volume and modifying the final urine composition depending on the overall fluid homeostasis.

ABBREVIAT IONS

AQP -	Aquaporin
AKAP2 -	A-kinase Anchoring Protein 2
AVP -	Arginine Vasopressin
ADH -	Antidiuretic Hormone
BSA -	Bovine Serum Albumin
BPH -	Benign Prostatic
BOO -	Bladder Outlet Obstruction
CaM -	Calmodulin
Deuterium -	D_2O
DM -	Diabetes Mellitus
DI -	Diabetes Insipidus
ENaC -	Epithelial Na^+ Channel
ER -	Estrogen Receptor
ERE -	Estrogen response element
GAG -	Glycosaminoglycan
GP –	Global Polyuria
GAPDH -	Glyceraldehyde 3-phosphate dehydrogenase
ICS -	International Continence Society
LP -	Lamina Propria
JAMs -	Junction Adhesion Molecules
LUT -	Lower Urinary Tract
MBS -	Membrane binding Solution
NFW -	Nuclease Free Water
NHU -	Normal Human Urothelial
NO -	Nitric Oxide
NP -	Nocturnal Polyuria
OAB -	Overactive Bladder
PKC -	Protein Kinase C

PKA -	Protein kinase A
PCR -	Polymerase chain Reaction
PKG -	Protein kinase G
PBS -	Phosphate Buffered Saline
RT-PCR -	Reverse Transcription PCR
RAS -	Renin-angiotensin System
RT -	Room Temperature
RVD -	Regulatory Volume Decrease
RVI –	Regulatory Volume Increase
RBC -	Reduced Bladder Capacity
SF-	Selectivity Filter
SMMHC -	Smooth Muscle Myosin Heavy Chain
TBS -	Tris buffer Saline
TJs -	Tight Junctions
TRP -	Transient Receptor Potential
TEER -	Transepithelial Electrical Resistance
TRPV4 -	TRP Vanilloid 4
UT -	Urea transporter
VUR -	Vesicoureteral Reflux
Vwf –	von Willebrand Factor

PRESENTATIONS AND PUBLISHED WORKS

Oral presentation

Expression and localisation of aquaporin water channels in adult pig urinary bladder

Postgraduate research forum 2018. University of the West of England (Bristol, UK)

Poster presentations

Expression and localisation of aquaporin water channels in adult pig urinary bladder

CRIB forum 2016. University of the West of England (Bristol, UK)

Expression and localisation of aquaporin water channels in adult pig urinary bladder

The Physiology Society: Physiology Annual Main Meeting 2016 (Cardiff, UK)

E poster presentation

Manso, M., Drake, M. J., Fry, C. H., Conway, M., Hancock, J. T., & Vahabi, B. (2019). Investigating the functional role and cellular localisation of aquaporin water channels in pig bladder urothelium

International Continent Society Conference Gothenburg (2019)

Publications

Manso, M., Drake, M. J., Fry, C. H., Conway, M., Hancock, J. T., & Vahabi, B. (2019). Expression and localization of aquaporin water channels in adult pig urinary bladder. *Journal of Cellular and Molecular Medicine*, *23*(5), pp. 3772-3775

Manso, M., Drake, M.J., Fry, CH., Conway, M., Hancock, J., Vahabi, B. (2020) The functional role of role and cellular localisation of aquaporin water channels in pig bladder urothelium. *The Journal of Physiology.* (Awaiting publication)

Books that my data have been presented in:

Abrams, P, Cardozo, L., Wagg, A., and Wein, A. (2013). Incontinence 6th Edition (2017). *International Consultation on Incontinence− International Continence Society, Bristol UK, ISBN*, 978-0956960733

Contents

FIGURE CONTENTS

CHAPTER ONE - INTRODUCTION AND MAIN AIMS

CHAPTER TWO - INVESTIGATING THE EXPRESSION OF AQP's IN THE UROTHELIAL AND SUB-UROTHELIAL LAYERS OF PIG URINARY BLADDER

CHAPTER THREE - MEASUREMENT OF D_2O FLUXES ACROSS PIG URINARY BLADDER MUCOSA

CHAPTER FOUR - INVESTIGATING THE EFFECT OF TONICITY ON AQP3 LOCALISATION

CHAPTER FIVE - OVERALL DISCUSSION AND CONCLUSION

TABLE CONTENTS

CHAPTER ONE - INTRODUCTION AND MAIN AIMS

CHAPTER TWO - INVESTIGATING THE EXPRESSION OF AQP's IN THE UROTHELIAL AND SUB-UROTHELIAL LAYERS OF PIG URINARY BLADDER

CHAPTER THREE - MEASUREMENT OF D_2O FLUXES ACROSS PIG URINARY BLADDER MUCOSA

Chapter 1

Introduction and Main Aims

1.1 Anatomy of the Urinary Bladder

The urinary bladder is a hollow viscus and a highly distensible organ that consists of a main portion (body) that collects urine, a funnel-shaped extension (neck) that connects with the urethra and single tube through which the urine passes to reach the external environment. The opening between the bladder and urethra is closed by two rings of muscle called sphincters (Figure 1.1B). The internal sphincter is a continuation of the bladder wall and consists of smooth muscle and immediately adjacent is the external sphincter made up of voluntary, mainly slow-twitch striated-muscle fibers (Silverthorn 2010; Boron and Boulpaep, 2012).

The bladder lies in contact with the posterior surface of the lower part of the anterior abdominal wall (Figure 1.1A) (Mahadevan, 2016). The anatomical position, size and shape of the bladder and the relationship of the bladder with nearby structures are determined by the degree to which the bladder is distended by the contained urine and also by the state of the adjacent viscera (Hickling *et al.,* 2015). In the adult, the empty urinary bladder lies entirely within the true pelvic cavity, occupying the anterior part of the pelvic cavity, behind the pubic symphysis and pubic bones (Figure 1.1B). As the bladder distends it ascends above the level of the pelvic brim and thus into the abdomen.

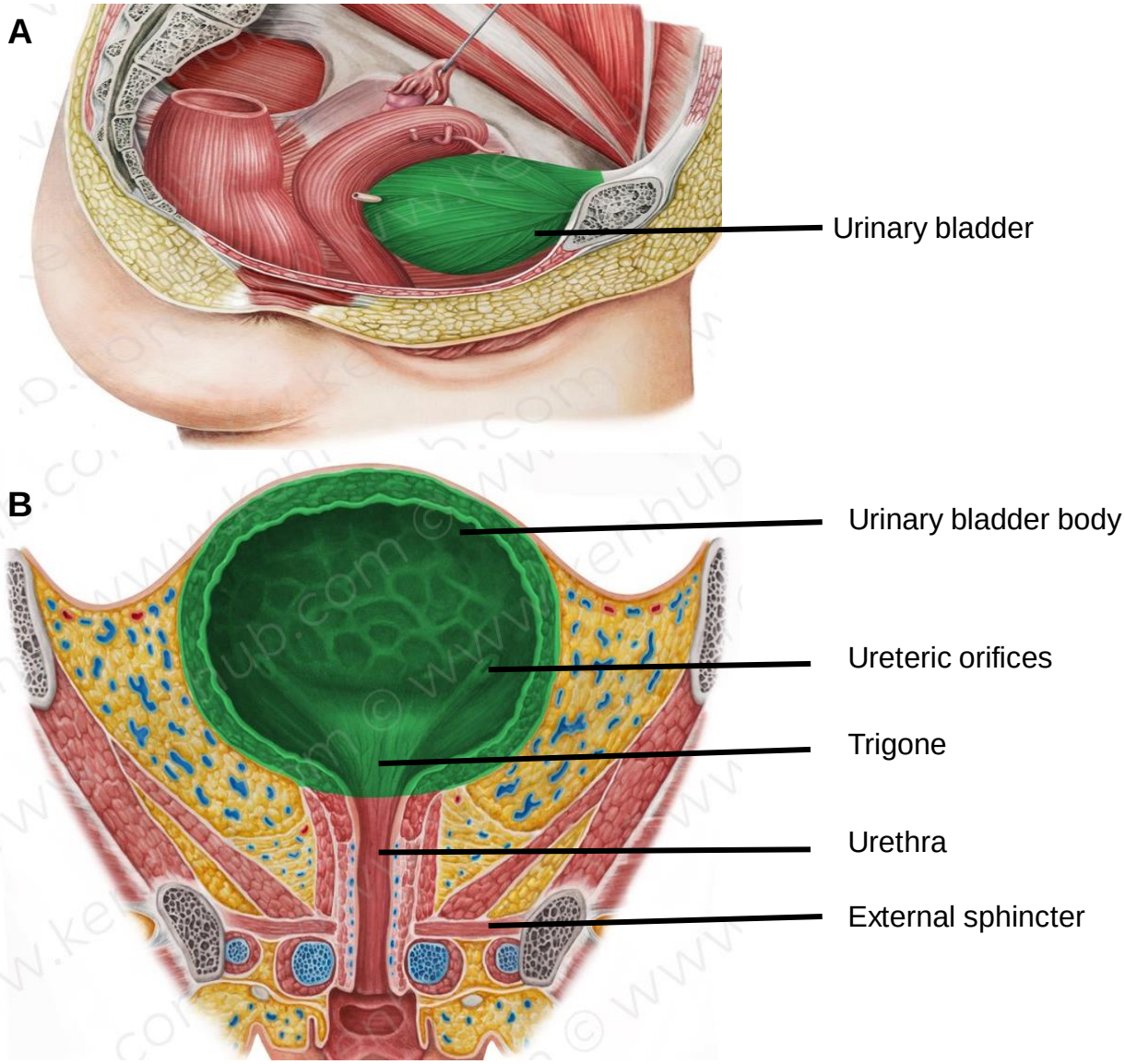

Figure 1.1 Anatomy of the urinary bladder in the human body

A) The Urinary bladder is found to the peritoneum, sitting on the pelvic floor. In females its inferior surface lays on the pubic symphysis and the posterior wall is in contact with the vagina and uterus. **B)** The bladder has four parts: body, which is bounded anteriorly by the apex and the fundus posteriorly, neck, inferiorly located in the region of the internal urethral orifice, emerges from the union of the right and left inferolateral surfaces. The fundus of the bladder contains three openings which form the trigone of the bladder; the internal urethral orifice and the two ureteric orifices (Kenhub, 2020).

1.2 The Function of the Urinary Bladder

The primary functions of a healthy urinary bladder are to act as a reservoir allowing storage of urine whilst maintaining a low intravesical pressure during filling and also to expel urine periodically in a highly coordinated manner when deemed possible (Hill *et al.,* 2015). The high compliance of the bladder wall allows it to expand to hold a volume of about 500ml, and also ensures that the ureters are not forced to transport urine into a pressurised compartment, with the associated risk of retrograde flow (Kohler *et al.,* 2001). Moreover, prevention of reflux into the ureter is helped by the nature of the uretero-vesical junction whereby the ureters do not merely penetrate the bladder wall but make a J-shaped function thus forming a non-return valve (Lescay and Tuma, 2018). The ability of the urinary bladder to store and periodically release urine are dependent on central nervous control, peripheral autonomic and somatic neural pathways.

1.3 Innervation of Bladder and Control of the Micturition Reflex

The micturition cycle is divided to two phases, urine storage and voiding. The bladder and urethra function reciprocally to maintain the cycle. The control of the micturition cycle is dependent upon neural circuits located in the brain, spinal cord and peripheral ganglia. The bladder has dense innervation of autonomic parasympathetic (pelvic), thoracolumbar sympathetic (hypogastric) and somatic (pudendal) nerves (Reviewed in De Groat, 1997 and Andersson and Arner, 2004), which often have opposing functions. During the storage phase, stretch receptors in the bladder send signals via sensory neurons to the brain through the pelvic nerves. One first senses the urge for voluntary bladder emptying at a volume of ~150 ml and senses fullness at ~500 ml.

Nevertheless, until it is socially acceptable to void, efferent impulses from the brain, inhibit presynaptic parasympathetic neurons in the sacral spinal cord that would otherwise stimulate the smooth muscle cells of the bladder wall. Voluntary contraction of the external urethral sphincter, which are controlled by the somatic motor neurons, also contributes to storage (Silverthorn 2010; Boron and Boulpaep, 2012). The voiding phase begins with a voluntary relaxation of the external urinary sphincter, followed by the internal sphincter. When a small amount of urine reaches the proximal (posterior) urethra, afferents signal the cortex that voiding is imminent. The micturition reflex now continues as pontine centres in the brain which no longer inhibit the parasympathetic preganglionic neurons leading to bladder smooth muscle contraction and expulsion of urine. At the same time, the cortical centres inhibit the external sphincter muscles. Voluntary urination also involves the voluntary contraction of abdominal muscles, which further raises bladder pressure and thus contributes to voiding and complete bladder emptying (Silverthorn 2010; Boron and Boulpaep, 2012).

1.4 The Structure of the Bladder Wall

The bladder wall is organized into three different layers (from outside to inside); the serosa/adventitia, detrusor muscle, and mucosa comprising of lamina propria (LP) and the urothelium (Figure 1.2A).

The serosa/adventitia forms a partial covering for the bladder dome. The superior part of the bladder is lined by the peritoneal membrane – the bladder itself is therefore an extraperitoneal organ. The serosa is a protective layer that will indeed allow the bladder to expand relatively independently of other lower abdominal organs. In

addition, the serosa serves as a protective barrier for the urinary bladder detrusor muscle (Mutsaers, 2003; Fry and Vahabi, 2016).

The main component of the bladder wall consists of smooth muscle called the detrusor muscle (Figure 1.2A). The detrusor muscle is composed of three different layers: the longitudinal inner layer which becomes circular in the middle followed by outer longitudinal layer. This muscle is well defined around the neck of the urinary bladder whilst in the rest of the bladder wall the detrusor muscle runs more randomly with little orientation. (Dixon and Gosling, 1987; Sam and Lagrabge, 2018).

The LP, is the suburothelial layer separating the urothelium and underlying detrusor muscle (Figure 1.2B). It is separated from the overlying urothelium by a basement membrane and is composed of an extracellular matrix with elastic fibres, capillaries, lymphatics, immune cells, afferent and efferent nerve endings, fibroblasts, adipocytes, interstitial cells, and indistinct smooth muscle layer, known as the muscularis mucosae (Drumm *et al.,* 2014).

The urothelium, is a transitional epithelium and lines the inner surface of the renal pelvis, the ureters, the urinary bladder and the urethra and forms a barrier to urine and the underlying tissues or the suburothelium and detrusor layers (Bolla and Jetti, 2019). The urothelium is composed of at least three layers; a basal cell layer attached to a basement membrane, an intermediate layer and apical layer composed of large hexagonal cells called the umbrella cells (Figure 1.2B) (Birder and Andersson, 2013). The apical umbrella cells have a diameter of 60-120 µM and are roughly cuboidal in an empty bladder, but they become squamous-like in morphology as the bladder fills. The intermediate layer is formed from two to three layers of polygonal cells which have a diameter of 20 µM, and the basal layer is made up from two to three layers of small cuboidal cells, each with a diameter of 5-10µM (Keshtkar *et al.,* 2007; Bolla and jetti,

2019). In a relaxed urinary bladder, the urothelium is five to seven layers of cell thick. When the urinary bladder fills with urine, it greatly expands stretching the bladder wall. In the distended bladder, the urothelium becomes two to three layers thick without any structural impairment

It was generally assumed that the urothelium is just a passive barrier against urine solutes, pathogens and noxious compounds. Many studies have now demonstrated that the urotheium has additional and important physiological roles (Apodaca *et al.,* 2007; Birder and de Groat, 2007).

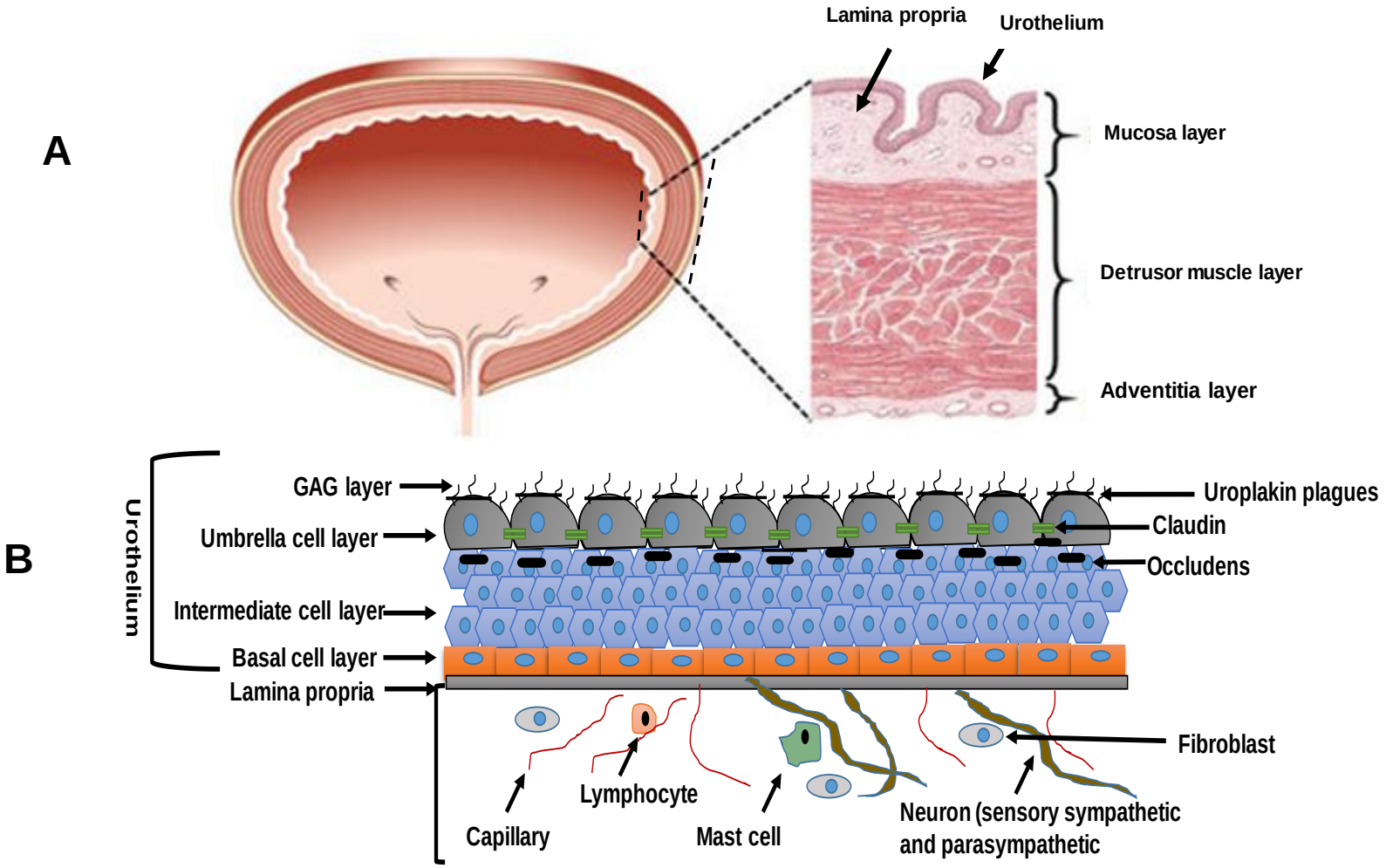

Figure. 1.2 The structure of the bladder wall and schematic drawing of the bladder mucosa. A) an overview of a cross sectioned bladder and a diagram of different layers of urinary bladder wall demonstrating the mucosal layer that lines the bladder and consist of urothelium and lamina propria (LP), the detrusor muscle and the adventitia layer that covers the outer surface of the bladder **B)** Mucosa section with urothelial cells and its properties. The LP is located between the basal membrane and the detrusor muscle. (Adapted from Chunhui *et al.,* 2014)

1.5 The Sensory Function of the Urothelium

Emerging evidence indicates that the urothelium has specialized sensory properties and is capable of detecting mechanical or chemical stimuli (such as changes in bladder pressure or tension, and tonicity of urine) and releasing a number of signalling molecules (Apodaca *et al.,* 2007; Birder and de Groat, 2007).

Urothelial cells express a variety of 'sensor molecules' (i.e. receptors and ion channels), similar to those found on sensory neurons, such as receptors for bradykinin purines (P2X and P2Y), norepinephrine (α and β), acetylcholine (nicotinic and muscarinic receptors), protease-activated receptors, amiloride-sensitive and mechanosensitive Na+ channels, and a number of transient receptor potential (TRP) channels. (Birder and de Groat, 2007; Apodaca *et al.,* 2007; Birder *et al.,* 2014; Gonzales *et al.,* 2014)

Moreover, several substances are released from urothelial cells following mechanical, chemical and thermal stimulation such as neurotrophins, neuropeptides, ATP, acetylcholine, prostaglandins, prostacyclin, nitric oxide (NO) and cytokines (Birder and Andersson., 2013; Burnstock, 2013; Gonzales *et al.,* 2014; Merrill *et al.,* 2016) and these molecules are able to communicate in a reciprocal manner with other cell types including bladder nerves, smooth muscle cells, interstitial cells and inflammatory cells which ultimately alter bladder function (Birder and Andersson., 2013). These observations open new exciting avenues for identifying new pharmacologic interventions that aim to target urothelial cell receptors and ion channels or neurotransmitter release mechanisms, leading to new strategies for the clinical management of bladder disorders.

1.6 The Barrier Function of the Urothelium

Urothelium serves as a tight barrier between the urine and underlying layers of the bladder wall and allows storage of urine volume while preventing the unregulated fluxes of substances between urine and blood (Khandelwal *et al.,* 2009). Epithelial tightness is commonly assessed by measurement of transepithelial electrical resistance (TEER) with epithelial displaying TEER >500 $\Omega.cm^2$ classified as tight (Adam *et al*., 2010). TEER is a widely acknowledged quantitative technique used to measure the integrity of epithelial dynamics in cell culture models of endothelial and epithelial monolayers as well as intact tissues (Srinivasan *et al.,* 2015).

According to Frömter and Diamond (1972), the urinary bladder epithelium is a tight epithelium, based on the TEER ranges observed throughout various mammalian urothelial TEER measurements. The umbrella cell layer, which is in close contact to the urine content of the bladder, is primarily responsible for urothelium permeability barrier function and has TEER that ranges between 10,000 and >75,000 $\Omega.cm^2$ (Khandelwal *et al.,* 2009). This extremely high transepithelial resistance is as a result of a high apical plasma membrane transcellular resistance in addition to the paracellular resistance of tight junctions (Lewis *et al.,* 1976; Negrete *et al.*, 1996; Khandelwal *et al.,* 2009). The transepithelial resistance of the blood–brain barrier, which protects the brain from harmful materials circulating in the blood, ranges from 1,000 to 2,000 $\Omega.cm^2$ (Butt *et al.,* 1990), whereas transepithelial resistances of epidermal and intestinal barrier are even smaller, around 400 and 100 $\Omega.cm^2$, respectively (Soler *et al.*, 1999; Schulkze *et al.,* 2009; Kirschner *et al.,* 2009). Based on the measurement of epithelial in different parts of the body, urothelial blood–urine barrier can be therefore considered the tightest and most impermeable barrier in the

body. Urothelial cells, more specifically umbrella cells, have several features that contribute to the high resistance of the urinary bladder urothelium.

1.6.1 The Specific Features of the Umbrella Cells in Aiding Urothelial Barrier Function

The bladder urothelium allows storage of urine for prolonged periods of time whilst limiting the passage of water, electrolytes and highly permeable molecules such as ammonia, as well as preventing noxious compounds entering the systemic circulation (Hicks, 1975; Apodaca, 2004). Several features of the apical surface of terminally differentiated mammalian urothelial umbrella cells aid the bladder in maintaining normal barrier function as the bladder fills and empties. These features include a number of tight-junction proteins such as zona occludens-1, occludins, claudins (Figure 1.2B), glycosaminoglycan (GAG), as well as specialised lipids and uroplakin proteins (Figure 1.2B) expressed by the umbrella cell apical membrane (Apodaca, 2004; Khandelwal *et al.,* 2009; Birder, 2010). These features allow the urothelium to respond to mechanical stretching as a result of an increase in intravesical pressure during bladder filling whilst maintaining an effective barrier.

1.6.1.1 The Urothelium and the GAG layer

The GAG layer is located on the surface of the urothelial and is composed of dermantan, heparin, and the glycosaminoglycans, chondroitin sulfate and hyaluronic acid (Klingler, 2016). The GAG layer provides a protective barrier to prevent unregulated permeability of water and solutes. Dysfunction of the GAG leads to increased permeability into the deep layers of the urothelium and bladder.

1.6.1.2 The Urothelium and Tight Junction Proteins

Tight junctions are located between the surface of urothelial cells and are made up of a dense network of cytoskeletal elements, cytoplasmic proteins, as well as several transmembrane proteins (Figure 1.3A) (Gonzalez *et al.,* 2003). The cytoplasmic proteins, which include zonula occludens-1 (ZO-1) are believed to form a framework that links the tight junction-associated transmembrane proteins to the peri-junctional actin cytoskeleton (Matter & Balda, 2003). Transmembrane proteins that are associated with the tight junctions include junctional-associated membrane protein 1 (Padura *et al.,* 1998), the Coxsackie and adenovirus-associated receptor (Cohen *et al.,* 2001, Walter *et al.,* 2002), the IG8 antigen (Nasdala *et al.,* 2002), as well as the tetraspan proteins including occludin (~65 kDa) and the claudins (~22 kDa) (Furuse *et al.,* 1993; Furuse *et al.,* 2001). The occludins and claudins form continuous dividing fibrils of transmembrane particles that completely surround the apical aspect of the adjacent surface of each cell (Figure 1.3B), forming a multifaceted barrier, which demonstrates ion and molecular size selectivity (Tsukita *et al.,* 2002; Acharya *et al.,* 2003). The tight junctions between the surface epithelial cells play a major role in blocking transepithelial ion flux efficiently so that the epithelium can maintain the very high transepithelial resistances (Lewis *et al.,* 1976; Wang *et al.,* 2003; Acharya *et al.,* 2003).

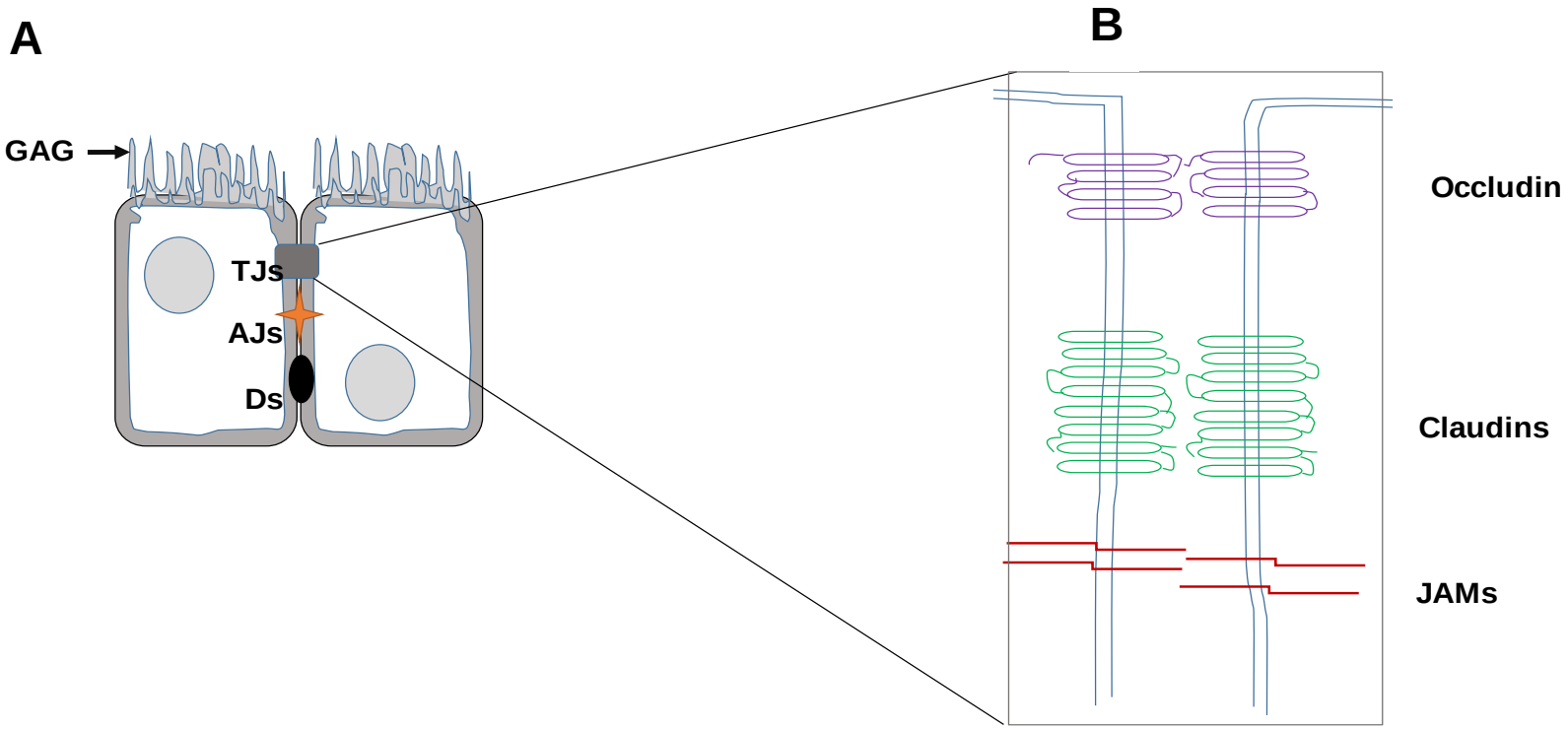

Figure 1.3 The zone of attachment between adjacent urothelial cells A) The zone of attachment between two urothelial cells consists of tight junction (TJs), desmosomes (Ds) and adhered junctions (AJs). **B)** An overview of the structure of a tight junction located between umbrella cells. TJ consist of three members of transmembrane proteins: junction adhesion molecules (JAMs), claudins and occluding, TJs; Tight junctions, AJs; Adherens junctions, Ds; desmosomes, GAG; glycosaminoglycan layer (Adapted from Abrams *et al.,* 2017).

1.6.1.3 The Urothelium and Uroplakins

Another urothelium feature that plays a key role in maintaining tight barrier function of urothelium is the presence of uroplakin (Figure 1.2B). The urothelial umbrella apical surface is entirely covered by folded plaques that are made from uroplakins (Birder and Andersson, 2013). The uroplakins have important functions including maintaining the urothelial barrier, in part by preventing proteins as well as ionic and non-ionic substances from gaining access to the suburothelial area and systemic circulation (Acharya *et al.,* 2004; Apodaca, 2004). Currently, four types of uroplakins have been identified in humans – UPIa, UPIb, UPII, UPIII (Lee, 2011). UPIa, Ib and III are glycoproteins; the sugar residues are important elements in the process of uroplakin synthesis and are necessary for their proper function (Lee, 2011). The role of uroplakins in the urinary bladder remains to be fully elucidated. It has been demonstrated that deletion of the UPII gene leads to a total absence of urothelial plaques, leading to an increased movement of water and solutes of the urine across the urothelium (Wu *et al.,* 2009; Kong *et al.,* 2009). The absence of UPII and UPIIIa also results in the inappropriate development of umbrella cells. These abnormal and underdeveloped umbrella cells undergo hypertrophy that causes urine leakages through the urothelium barrier as well as vesicoureteral reflux (Hu *et al.,* 2002; Kong *et al.,* 2004; Hu *et al.,* 2007; Lee, 2011). Therefore, the presence of uroplakins is key in prevention movement of ion, solutes and water across the urothelium.

1.7 Transport Functions of the Urothelium

Although the urothelium forms a tight barrier, it has been known for many years that the there is a bidirectional movement of water and solutes across this tissue under various osmotic conditions and that the composition of urine changes during passage from the renal pelvis to the bladder (Fellows and Turnbull, 1971; Fellows and Turnbull, 1972; Nelson *et al.,* 1975; Hilson *et al.,* 1990; Negrete *et al.,* 1996). For example, Turnbull and Fellows (1972) investigated Na^+ and water transport across the luminal surface of rabbit urinary bladder urothelium and demonstrated that Na^+ permeability increased when bladders were filled with hypertonic solutions. Moreover, there was apparent net movement of water from the blood stream into the lumen of the bladder (Fellows and Turnbull, 1972). Another study also discovered that during hibernation season in bears, the urinary bladder absorbs heavy water deuterium oxide (D_2O) and urea back into the systemic circulation (Nelson *et al.,* 1975).

Other studies have measured water and Na^+ permeability across the bladder wall in dogs (Rapoport *et al.,* 1960; Hakim *et al.,* 1965), rats (Hicks, 1965) and humans (Fellow and Marshall 1972). These studies collectively have reported a significant net transport (both lumen to blood and blood to lumen) of urinary constituents, primarily water and Na^+ along their respective blood/urine gradients (Levinsky and Berliner 1959; Rapoport *et al.,* 1960; Turnbull and Fellows 1972; Hohlbrugger, 1987: Walser *et al.,* 1988), These studies also concluded that the movement of these solutes and water across the urothelium may not simply rely on passive diffusion but that their active transport is facilitated by transporters and channels.

1.7.1 Transcellular and Paracellular Pathways

Permeability of water and solutes across the urothelium occurs by two main pathways; the paracellular pathway which involves tight junctions located in the intracellular space of urothelial cells (Figure 1.4) and the transcellular pathway which consists of both the apical and basolateral plasma membranes of the terminally differentiated umbrella cells (Figure 1.4) (Carattino *et al.,* 2013).

Paracellular transport of solutes is mainly achieved through diffusion and osmosis where solutes move down their concentration gradients (Bruewer and Nusrat, 2013). This process is heavily influenced by the zone of attachment between flanking urothelial cells (Khandelwal *et al.,* 2009).

The two main barriers involved in transcellular permeability are the apical and basolateral membranes of the umbrella cells (Figure 1.4), with the apical surface of urothelial cells demonstrating the highest TEER of up to 150,000 Ω cm^2, compared to the basolateral surface with a TEER of 1,500 Ω cm^2 (Clausen *et al.,* 1979; Lewis and Kleine, 2000). Whilst paracellular transport of water and solutes is mainly passive, transcellular transport can be both passive and active. Transcellular transport is directional and energy-dependent and is mediated by transporters and channels (Lewis and Kleine, 2000).

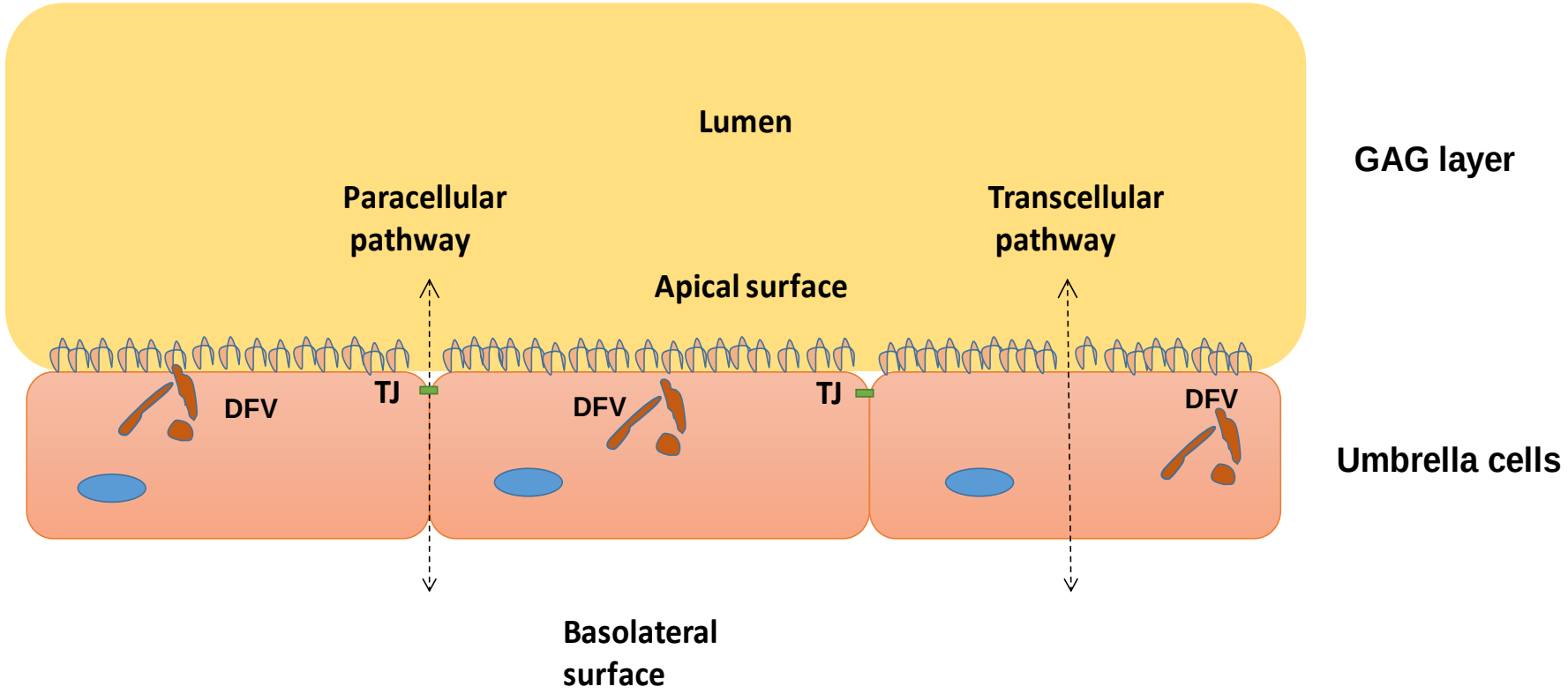

Figure 1.4 Paracellular and transcellular pathways of the urothelium. The paracellular pathway is composed of the intercellular space where tight junctions (TJs) are located. The transcellular pathway, demonstrates movement of solutes across the apical and basolateral plasma membrane of the umbrella cells. The apical plasma membrane contains urothelial plagues and glycosaminoglycan (GAG) layer. DFV, discoical fusiform vesicles; TJ, tight junction; GAG, glycosaminoglycan layer (Adapted from Abrams *et al.,* 2017).

1.8 Mechanisms for Ion, Solute and Water Transport Across the Urothelium

A variety of ion transport mechanisms have been defined in the urothelium. Na^+, K^+ and Ca^{2+} channels, as well as other non-specific cation channels located on the apical surface of the plasma membrane (Lasic *et al.,* 2015). The basolateral plasma membrane, on the other hand, expresses Cl^- channels, Na^+/H^+ and Cl^-/HCO_3^- exchangers, ATPase-dependent pumps as well as Na^+ and K^+ channels (Lasic *et al.,* 2015). Other channels that are also expressed by the umbrella cells include hemmicannels of connexions and pannexin channels (Taruno, 2018; Epifantseva and Shaw, 2019). Na^+/H^+ and Na^+ transporters are known to be responsible for Na^+ and fluid transport across the epithelium of various tissues (Garty and Palmer, 1997). Studies have also demonstrated that Na^+ and K^+ channels channels are involved in cell volume recovery of urothelial cells during changes in intra- and extracellular osmolarity (Lewis and Donaldson,1990).

One of the most studied transport channels is the epithelial Na^+ channel (ENaC). ENaCs are expressed on the apical surface of the terminally differentiated umbrella cells (Figure 1.5). ENaCs facilitate transurethelial Na^+ flux along with Na^+/K^+-ATPase dependent active transport on the basolateral membrane to provide the net electrochemical gradient that promotes Na^+ absorption. During bladder filling, stretch of on the urothelium cells can also stimulate K^+ and Cl^- secretion (Khandewal *et al.,* 2009).

Other ion channels that have also been demonstrated in the urothelium include non-selective TRP channels, permeable to Ca^{2+}, Mg^{2+} and Na^+ (Figure 1.5). (Blanchard *et al.,* 2016). Another family of non-selective cation channels include the purinergic

receptors (P2X) which are activated by the binding of extracellular ATP and have a high permeability to Ca^{2+}, Na^{+}, and K^{+}. (North, 2016).

Solutes such as urea and creatinine are also constantly reabsorbed from urine (or secreted depending on the local environment). Although simple diffusion across the urothelium can be considered for some of these solutes, the magnitude of the quantity of flux and its rapidity of movement indicates that the transport is facilitated or active in nature (Abrahams *et al.,* 2017). For example, two subfamilies of urea transporters (UT)s, UT-A and UT-B, have been identified in the urothelium (Li *et al.,* 2012; Li *et al.,* 2014; Walpole *et al.,* 2014). These transporters are believed to be involved in absorption of urea across the urothelium which leads to alteration of cell volume and osmolality (Li *et al.,* 2012; Li *et al.,* 2014; Walpole *et al.,* 2014).

In addition to ion and solutes, isotopic movement of heavy water (deuterium oxide, D_2O) or isotopically labelled water across mammalian urothelial has been reported (Spector *et al.,* 2002). The mechanism responsible for the bulk movement of water, was under debate until the discovery of aquaporin (AQP) water channels in the bladder (Rubenwulf *et al.,* 2009; Spector *et al.,* 2002; Rubenwulf *et al.,* 2012). The focus of this study is to look at the expression and function of AQP water channels in pig bladder urothelium.

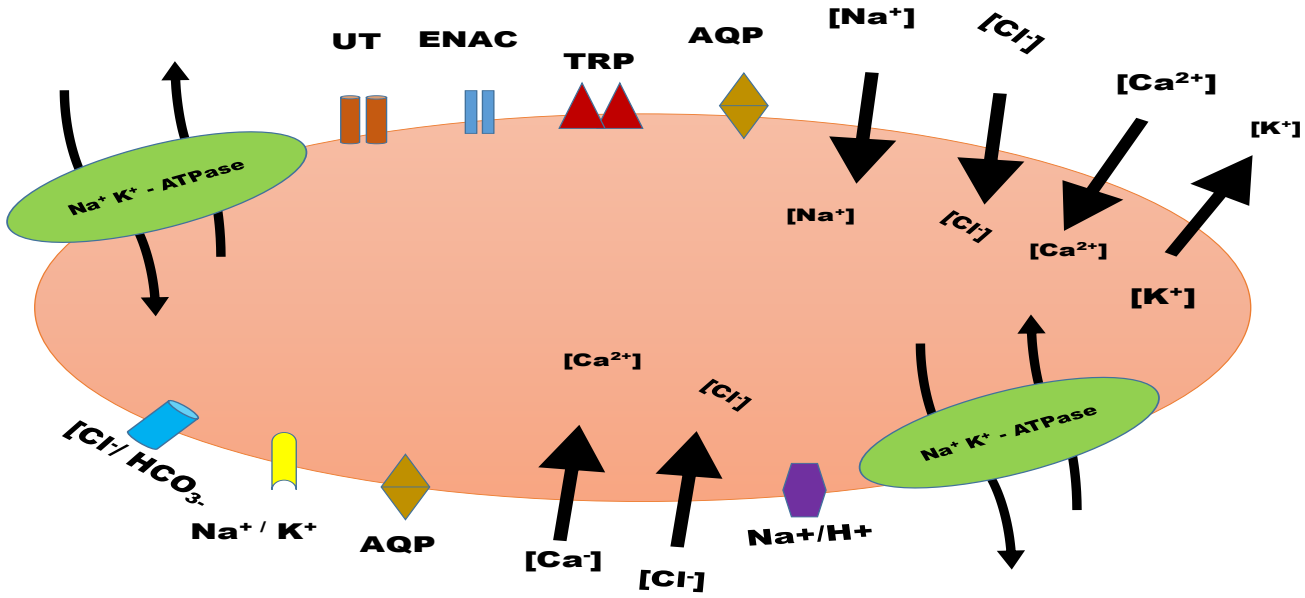

Figure 1.5 A model for ionic, water and solutes homeostasis in urothelial cells.

Distribution of water and ions in cells involve both active and passive transport mechanisms across the plasma membrane. Movement of solutes and ions across urothelial cells are believed to be accommodated by the Influx of water by osmosis and/or through constitutively expressed AQP, leading to cell swelling which induces influx of ions and solutes such as extracellular calcium entry through TRP channels, activation of Na^+ K^+ pump (or ATPase), potassium channels, chloride channels ect, and as a result triggers AQP translocation or water influx. Water subsequently enters or exits the cell to maintain cellular homeostasis. Major channels known to be present on urothelial cells which are involve in maintaining cell homeostasis including volume, osmolarity and pH is shown in the above image. ENAC: Epithelial Sodium Channel, TRP = Transient Receptor Potential, AQP: Aquaporin, Na^+: sodium, K^+: Potassium, Ca^{2+}: Calcium, Cl^- : Chloride, Na^+ H^+ : Sodium Hydrogen exchanger, Na^+ K^+ : Sodium Potassium pump, Cl^-/ HCO^{3-} : Chlorde Bicarbonate exchanger. Since AQPs facilitate solutes such as urea accros cell membrane, Urea Transporter (UT) which transport urea, is believed to work synergistically with AQP channels in facilitating urea transport across uorothelial cells. ENAC is believed to respond to hormonal changes such as aldesteron in regulating Na^+ and as a result triggers water transport through AQP channels (Adapted from Franco *et al.,* 2006, Day *et al.,* 2014)

1.9 AQP Water Channels (Structure and Function)

AQPs, also known as major intrinsic protein (MIPs), are highly conserved ubiquitous integral membrane channels that primarily facilitate the transport of water across cell membranes in various living organisms (Abascal *et al.,* 2014). AQPs mediate water transport across biological membranes in response to osmotic gradients created by active transport of ions and solutes (Patil *et al.,* 2016). Selectivity of AQPs to water and small solutes is determined by their structure, conformational change and conserved motifs. There are currently 12 different AQPs (AQPs 0-11) identified in mammals which are divided into three subfamilies: (i) the classical or orthodox AQPs (AQP1, AQP2, AQP4, AQP5, AQP8) which are responsible for bidirectional movement of water, various ions (CI^-, K^+) and gases (CO_2, NH_3, NO, O_2) across the epithelial barriers even though in general, gas permeability is not limited by the intrinsic cell membrane permeability but by diffusion in so-called 'unstirred layers' outside the membrane (Geers and Gros, 2000) (ii) Aquaglyceroporins (AQP3, AQP7 AQP9 and AQP10), which facilitate the movement of water as well as small solutes such as glycerol, urea, ammonia, and metalloids , and (iii) S-aquaporins or unorthodox superaquaporins (AQP11 and AQP12), which have been identified in animals but their exact role in epithelial barriers remains to be determined (Papadopoulos and Verkman, 2013; Ishibashi *et al.,* 2014; Madeira *et al.,* 2016). All AQPs share the same structural features which consist of six membrane-spanning helical domains (M1, M2, M4, M5, M6 and M8) and two half spanning helices (M3, M7) that surround the cytoplasmic and extracellular vestibules, with the NH_2 and COOH terminals located within the cytoplasm (Figure 1.6) (Verkman, 2011; Nesverova *et al.,* 2019). Four AQP monomers (each is approximately 30kDa in size) are assembled to form tetramers in membranes (Figure 1.6) (Verkman *et al.,* 2014). All AQP channels are characterised

by two asparagine-proline-alanine (NPA) sequences (that are important for the formation of a water-permeating pore) located at loops B and E, that shape short hydrophobic helices participated in substrate selectivity, a single alanine-glutamate-phenylalanine-leucine (AEFL) and histidine-tryptophanvaline-phenylalanine-tyrosine-tryptophan-glycine-proline (HW[V/I][F/Y]WXGP) sequences that are both responsible for water permeability and membrane targeting (Figure 1.6) (Jiang, 2009; Guan *et al.,* 2010; Monsang *et al.,* 2019). The difference between AQPs and aquaglyceroporins is the narrowest constriction point of the channel which is also known as selectivity filter (SF). The radius of the SF in classical AQPs is ~1.1 Å which is slightly smaller than the radius of a molecule of water (~1.4 Å), whereas the radius of the pore for aquaglyceroporins is slightly larger (~1.7 Å) than a molecule of water (Fu D *et al.,* 2000; Tajkhorshid *et al.,* 2002). The SF region is more polar in water selective AQPs and contains conserved histidine whereas in aquaglyceroporins, this region is more hydrophobic with two conserved aromatic residues, usually a tryptophan and a tyrosine (Savage *et al.,* 2010; Verkman *et al.,* 2011). The difference in the SF region of AQPs and aquaglyceroporin contributes to the selectivity of these two different types of channels to water and larger solutes.

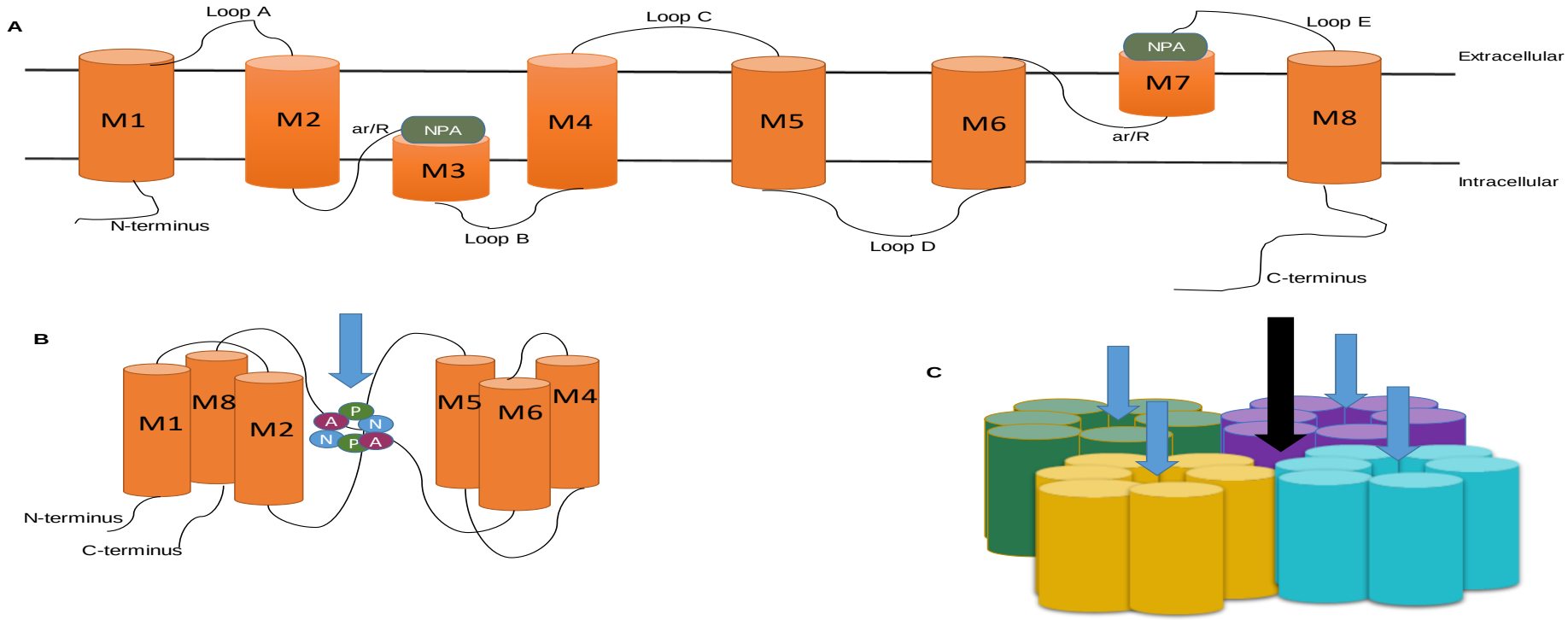

Figure 1.6 The secondary, tertiary, and quaternary structures of Aquaporin proteins

(A) Aquaporin structure contains six α-helices linked together by three extracellular and two intracellular loops. Loops B and E contain asparagine-proline-alanine (NPA) motifs which makes the smallest diameter of AQP pore. In addition, loop E α-helices from each monomer also contains aromatic/arginine (ar/R) motifs which play an important role in H^+ exclusion. **(B)** All six α-helices assemble in a closely connected tertiary monomer structure with both ar/R motifs located internally and interacting at opposite sides of the pore and both NPA motifs interacting within the membrane. A route for water passage exists in the transmembrane pore formed through the centre of the individual monomer three-dimensional barrel. **(C)** Individual AQPs monomers homotetramerise to create a five-pore quaternary structure. The function of the central pore located within the individual monomer, formed by the space between all four monomers, remains largely unknown (Adapted from Halsey *et al.,* 2018).

1.10 AQPs' Regulation

Water is a unique substance and its properties such as being polar allows liquid water to act as a "universal solvent that is able to dissolve many ionic and polar covalent compounds, make it the most central molecule in biology" (Perez and Riveros, 2017). Regulation of the osmotic potential within a cell is fundamental and the water flux across biological membranes is mediated by intrinsic membrane proteins acting as water channels. Eukaryotes have evolved to fine-tune water transport through these water channels (AQPs) by three main regulatory mechanisms: (1) at the transcriptional/translational level (Matsumura *et al.,* 1997); (2) by translocation to the membrane in response to a trigger (Nedvetsky *et al.,* 2009); (3) by conformational change or "gating" (Walz *et al.,* 2009). These regulatory mechanisms can be achieved through phosphorylation, glycosylation or ubiquitination of AQPs (Leitch *et al.,* 2001; Hendriks *et al.,* 2004; Kamsteeg *et al.,* 2006; Buck *et al.,* 2004; Willermain *et al.,* 2014; Duan and Walther, 2015; Nesverova *et al.,* 2019). Phosphorylation of AQPs is the most efficient and studied form of post translational modification of AQP as it allows rapid modification of AQPs membrane water permeability in a reversible manner.

1.10.1 Phosphorylation of AQPs

Phosphorylation of proteins is one of the most important post-translational modifications that allows proteins to be regulated reversibly. About 30% of mammalian proteins are phosphorylated and phosphorylation significantly alters protein activity, protein: protein interactions and protein trafficking (Cohen, 2000; Audagnotto and Peraro, 2017). Effects of phosphorylation are cell specific and thus, enable proteins to be regulated according to the functions of a particular cell type (Cohen, 2000;

Nesverova *et al.,* 2019). In eukaryotes, AQP phosphorylation allows water flow across cellular membranes to be tightly regulated in response to various external and internal signals which are further described in Table 1 (Conner *et al.,* 2013). Trafficking and gating serves as a fast regulatory mechanism by increasing the abundance of AQPs located in the plasma membrane through shuttling of AQP protein, or by increasing water flow through the channel (Kreida and Horsefield, 2015).

1.10.2 Glycosylation of AQPs

Glycosylation is another form of post translational modification in eukaryotes (Lis and Sharon. 1993). Glycans, also referred to as polysaccharide, are mostly attached to secreted proteins as well as membrane proteins. Processing of the glycan occurs in the ER lumen before the protein has been fully synthesised and folded and the protein is subsequently transported to the Golgi apparatus where it is further processed (Jamieson and Palade, 1968; Atkinson and Lee, 1984). Several AQPs are shown to have consensus sequences for N-linked glycosylation and are monoglycosylated in native tissues (e.g; AQP1, AQP3, AQP9, AQP11and AQP10) (Chen *et al.,* 2015). For example, in 50% of purified erythrocytes, AQP1 monomers are glycosylated with polylactosaminyl oligosaccharide at residue N42 in the first extracellular loop (loop A) (van Hoek *et al.,* 1994; Verkman and Mitra 2000; Boury-Jamot *et al.,* 2006). However, the specific functions altered by AQP glycosylation have not been identified. (Helenius, 2001; Spector *et al.,* 2002). Existing reports have suggested that glycosylation of AQPs is not required for water transport function, tetramerization nor for transport from the endoplasmic reticulum to the Golgi complex (Hendriks *et al.,* 2004). Instead, the *N*-linked glycan is important for exit from the Golgi complex and sorting of AQP2 to the

plasma membrane (Hendriks *et al.,* 2004; Buck *et al.,* 2004). AQP glycosylation may be key in AQP maturation and arrangement in the membrane.

1.10.3 Ubiquitination of AQPs

Another less studied form of AQP post translational regulation is ubiquitination. Ubiquitination of membrane proteins is a common way of mediating internalization and promotion of protein degradation by the lysosomal pathway (Piper and Luzio, 2007; Kazazic *et al.,* 2009; Vina-Vilaseca *et al.,* 2011). AQPs have been demonstrated to be ubiquitinated for proteasome degradation (Leitch *et al.,* 2001; Kamsteeg *et al.,* 2006; Willermain *et al.,* 2014). For example, AQP2 phosphorylation sites S256 and S269 play an important role in the translocation of this protein to the membrane. Prevention of S256 phosphorylation causes ubiquitination where ubiquitin protein attaches to AQP2 protein, leading to internalisation of AQP2 irrespective of the S269 phosphorylation status (Kamsteeg *et al.,* 2006). Also, phosphorylation at S261 is involved in AQP2 ubiquitination and degradation (Nedvetsky *et al.,* 2010; Tamma *et al.,* 2011). AQP1 has also been demonstrated to be ubiquitinated for proteasome dependent degradation however, under hypertonic conditions, AQP1 ubiquitination decreases and protein stability markedly increases thereby contributing to overall protein induction (Leitch *et al.,* 2001).

1.10.4 Primary Signals that Stimulate AQP Regulation

Regulation of AQPs through phosphorylation, glycosylation and ubiquitination can be triggered by a number of stimuli including hormones such as vasopressin, adrenaline,

oestrogen, aldosterone (Oliveira *et al.,* 2005; Boone and Deen, 2008; Kwon *et al.*, 2013; Jung and Kwon 2016; Vukicevic *et al.,* 2016;), changes in tonicity (Hoffert *et al.,* 2000, Matsuzaki et al., 2001; Kultz, 2001; Tamas, 2003; Arima *et al.,* 2003, Cahalan *et al.,* 2004; Hasler *et al.,* 2005, Loitto *et al.,* 2007) and activation of TRP ion channels (Benfenati, *et al.,* 2007; Benfenati *et al.,* 2010; Jo *et al.,* 2015) and possible ENaC channels. These primary signals initiate signalling cascades with the ultimate goal of regulation AQP function, depending on the specific need and requirement of the tissue. Although the intracellular signalling pathways used for the control of AQP function have not been conclusively established, a few intracellular signalling components in the regulation of the different types of AQPs have been described (Table 1.2). These include cytoskeletal proteins, Ca^{2+}, protein kinase A (PKA), protein kinase C (PKC), protein kinase G (PKG), and phosphatidylinositol 3-kinase (Table 1.2) (Tietz *et al.,* 2006; Carmosino *et al.,* 2007; Garcia *et al.,* 2001; Ishikawa *et al.,* 2002; Gunnarson *et al.,* 2008; Nesverova *et al.,* 2019). Specific primary signals involved in AQPs regulation have been described in Table 1.1 Studies that have reported on the function, localisation and known intracellular signalling components/pathways for each subtypes of AQPs identified are further discussed in the subsequent sections.

Primary signals	Translocation	AQP	Experimental system	Reference
Vasopressin	PM	AQP2	Native kidney tissue	(Christensen et al., 2009)
	WP	AQP4	Xenopus oocytes	(Moeller et al., 2009)
Histamine	PM	AQP4	Human gastric cells	(Carmosino et al., 2007)
Isoprenaline	PM	AQP3	Human adipocytes	(Rodriguez et al., 2011b)
	PM	AQP7	Human adipocytes	(Rodriguez et al., 2011b)
Hypertonicity	PM	AQP1	Human neutrophils	(Loitto et al., 2007)
	PM	AQP2	Collecting duct cells	(Hasler et al., 2005)
	PM	AQP3	MDCK cells	(Matsuzaki et al., 2001)
	PM	AQP4	Rat astrocytes Lung	(Arima et al., 2003)
	PM	AQP5	epithelial cells Rat	(Hoffert et al., 2000)
	PM	AQP9	astrocytes	(Arima et al., 2003)
Glutamate	PM/WP	AQP4	Astrocytes	(Gunnarson et al., 2008)
Lipopolysaccharide	PM	AQP5	Lung epithelial cells	(Ohinata et al., 2005)
Hypotonicity	PM	AQP1	HEK293/astrocytes	(Conner et al., 2010)
	PM	AQP3	Keratinocytes	(Garcia et al., 2011)
	PM	AQP8	Amnion epithelial cells	(Qi et al., 2009)
Vasoactive intestinal polypeptide	PM	AQP5	Duodenum (Brunner's gland)	(Parvin et al., 2005)
Secretin	PM	AQP1	Cholangiocytes	(Marinelli et al., 1997)
Adrenaline	PM	AQP3	Caco-2 epithelial cells	(Yasui et al., 2008)
	PM	AQP5	Rat parotid cells	(Ishikawa et al., 1999)
Acetylcholine	PM	AQP5	Rat parotid cells	(Ishikawa et al., 1998b)

Table 1.1 Examples of primary signals involved in in AQP regulation

Primary signals that initiate AQP regulation in different cell lines and mammalian tissues are listed PM; aquaporin translocation to the plasma membrane. WP; water permeability. The experimental system used to determine the AQP translocation is included for each primary signal. Adapted from (Conner *et al.,* 2013)

Intracellular component	AQP	Effect	Experimental system	Residue	Reference
PKA	AQP0	WP ↓	Collecting duct	S235	(Reichow and Gonen, 2008)
	AQP2	PM ↑	Kidney tissue	S256	(Christensen et al., 2000)
	AQP4	PM ↓	Human gastric cells	-	(Carmosino et al., 2007)
	AQP5	PM ↓	MDCK	S152	(Karabasil et al., 2009)
	AQP5	PM ↑	Brunner's gland	-	(Parvin et al., 2005)
	AQP6	Uknown	MDCK	-	(Beitz et al., 2006)
	AQP7	Putative	n/a	-	(Kishida et al., 2000)
PKC	AQP0	PM ↑	RK13 epithelial cells	S235	(Golestaneh et al., 2008)
	AQP1	PM ↑	HEK293 cells	T157/T23	(Conner et al., 2012)
	AQP3	PM ↑	Caco-2 epithelial cells	9 T514	(Yasui et al., 2008)
	AQP3	PM ↓	Caco-2 epithelial cells	S660	(Yasui et al., 2008)
	AQP4	PM ↑	Astrocytes	S111	(Gunnarson et al., 2008)
	AQP4	PM ↓	Xenopus oocytes	S180	(Moeller et al., 2009)
	AQP9	PM ↑	Human neutrophils	S11/S222	(Karlsson et al., 2011)
PKG	AQP5	PM ↑	Rat parotid cells	-	(Ishikawa et al., 2002)
Actin	AQP1	PM ↑	Cholangiocytes	-	(Tietz et al., 2006)
	AQP4	PM ↑	Astrocytes	-	(Nicchia et al., 2008)
	AQP5	PM ↑	Salivary gland cells	-	(Tada et al., 1999)
	AQP5	PM ↑	Rat parotid	-	(Ishikawa et al., 1999)
Microtubule	AQP1	PM ↑	HEK293 cells	-	(Conner et al., 2010)
	AQP5	PM ↑	MDCK cells	-	(Karabasil et al., 2009)
+ cAMP	AQP8	PM ↑	Hepatocytes	-	(Garcia et al., 2001)
	AQP5	PM ↑	Lung epithelial cells	-	(Yang et al., 2003)
Ca2+/ Calmodulin	AQP1	PM ↑	HEK293 cells	-	(Conner et al., 2012)
	AQP5	PM ↑	Rat parotid cells	-	(Ishikawa et al., 1998a, Ishikawa et al., 1999, Rabaud et al., 2009)
	AQP6	PM ↑	CHO-K1 cells	-	
TRP channels	AQP1	PM ↑	HEK293 cells	-	(Conner et al., 2012)
RAC1	AQP9	PM ↑	Human neutrophils	-	(Karlsson et al., 2011)
Dynein	AQP1	PM ↑	Cholangiocytes	-	(Marinelli et al., 1997)
Kinesin	AQP1	PM ↑	Cholangiocytes	-	(Marinelli et al., 1997)

Table 1.2 Examples of intracellular signalling components involved in AQP regulation

A summary of the intracellular signalling components involved regulating AQP function. The arrows indicate the direction of the effect. Arrows going down indicate internalisation of AQPs from the membrane as a result of intracellular signalling. Arrows pointing up indicate translocation of AQPs to the membrane and the amino acid residue that the component acts upon is also included where known (Conner *et al.,* 2013)

1.10.4.1 AQP0 Localisation, Function and Regulation

The major intrinsic protein (MIP), also known as AQP0 – was initially identified in 1984 as a water channel and gap junction protein (Gorin *et al.,* 1984). AQP0 is involved in cell-to-cell adhesion of fibre cells and has also been found in kidney collecting ducts and other tissues. Mutations in AQP0 have been associated with individuals suffering from cataracts (Berry *et al.,* 2000). Studies have demonstrated that the C-terminus of AQP0 contains numerous phosphorylation sites; S229 for casein II (Ball *et al.,* 2004), S231 for PKC and S235 for PKA (Schey *et al.,* 2000) and that phosphorylation of these sites is important for gating and translocation of AQP0 to the membrane in various cell.

1.10.4.2 AQP1 Localisation, Function and Regulation

From the 13 identified AQPs, AQP1 was the first protein for which water transport across its channel was assesed. Also it was the first AQP for which the structure was determined (Murata *et al.,* 2000). Since the discovery of AQP1 in erythrocytes, it has been found in a wide range of tissues, including kidneys, eyes, lungs, muscles and brain tissue (Maunsbach *et al.,* 1997; Stamer *et al.,* 2003; Au *et al.,* 2008 Tomassoni *et al.,* 2010; Gao 2013;). No studies have reported AQP1 regulation through gating but it has been shown that changes in tonicity causes trafficking of AQP1 to the membrane in HEK293 cells, mediated by PKC (Conner *et al.,* 2010). It was shown that trafficking was mediated by Ca^{2+} influx through transient receptor potential-canonical 1 (TRPC1) channels, resulting in activation of CaM and PKC, with subsequent phosphorylation of AQP1 (Conner *et al.,* 2010). Two phosphorylation sites with a consensus region for PKC have been identified in AQP1; T157, located in loop

D, and T239 of the C-terminus and they are thought to mediate hypotonicity-induced translocation of AQP1. Phosphorylation of these sites lead to increase water permeability in Xenopus oocytes (Zhang *et al.,* 2007; Tomita *et al.,* 2017). PKA also phosphorylates AQP1 *in vitro* in rat kidney homogenates, and studies carried out in oocytes demonstrated that cAMP and arginine vasopressin (AVP), both known activators of PKA, increase AQP1 membrane abundance (Han and Patil, 2000). The combination of PKA and PKC phosphorylation of AQP1 is not needed for AQP1 translocation to the membrane. This was demonstrated when after inhibition of PKA in HEK293 cells, AQP1 was still trafficked to the plasma membrane. (Zhang *et al.,* 2007).

1.10.4.3 AQP2 Localisation, Function and Regulation

AQP2 was identified soon after the discovery of AQP1, in particular in the renal collecting duct (Fushimi *et al.,* 1993). AQP2 has been identified in a variety of human tissues, including the lungs (Verkman;1998) and intestine (Zhu *et al.,*2016), but is best studied in terms of its function in the collecting duct where it plays a key role in regulating urine volume and concentration, mediated by vasopressin (antidiuretic hormone, ADH). Vasopressin is a peptide hormone that controls plasma osmolality through the regulation of renal water excretion/reabsorption facilitated by AQPs Lee and kwon *et al.,* 2007). When plasma osmolality increases, as would occur in whole body dehydration for example, vasopressin is secreted from the posterior pituitary gland. In the collecting duct, vasopressin binds to G-protein coupled vasopressin V2 receptors on the basolateral membrane which leads to an increase of intracellular cAMP and subsequent phosphorylation of AQP2 by PKA. PKA-mediated

phosphorylation triggers the translocation of AQP2 residing in storage vesicles to the apical membrane, causing increased osmotic water transport across the epithelium of the collecting duct, leading to reabsorption of filtered water back to the blood (Vukicevic *et al.,* 2016). When the levels of vasopressin, which has a short half-life of about 15 mins, are reduced, AQP2 undergoes endocytosis; a fraction of the protein is ubiquitinated and degraded, and the water permeability of the membrane is reduced back to the initial situation (Kamsteeg *et al.,* 2006).

1.10.4.4 AQP3 Localisation, Function and Regulation

AQP3 was initially identified in the basolateral membrane of the collecting duct in the kidney. (Ma *et al.,* 1994, Ishibashi *et al.,* 1994, Echevarria *et al.,* 1994). AQP3 belongs to the aquaglyceroporin family, indicating that it transports not only water, but also glycerol, urea, and other solutes. AQP3 has been identified in various tissues including keratinocytes in the basal layer of the epidermis in human skin (Sougrat *et al.,* 2002). As with many AQPs, the exact role of AQP3 have not been identified, however, a few studies have provided possible roles for AQP3 (Spector *et al.,* 2002; Jamot *et al.,* 2006; Thiagarajah *et al.,* 2017; Rubenwulf *et al.,* 2012). Molecular studies have found that deletion of the AQP3 gene in mice causes a reduction in skin elasticity, slower wound healing, reduced glycerol contents and dry skin (Hara *et al.,* 2002). Another study also revealed that AQP3 null mice causes AQP2 to be down-regulated. Although the mechanism of AQP2 down regulation in the absence of AQP3 is not fully known, a possible suggestion could be proposed. AQP2 is found on the apical surface of collecting ducts to allow reabsorption of water while AQP3 is found on the basolateral surface to allow excretion of water from the cell. Both AQP proteins operate in an

organised manner to reabsorb water as well as restoring the cell volume of collecting duct principal cells, also known as regulatory volume decrease (RVD). It could be hypothesised that, in AQP3 null mice, RVD, a process where cells are restored to their original cell volume, cannot be achieved. Therefore, the increase in cell volume as a result of AQP2 water permeability leadis to cell stretch, initiating an inhibitory mechanism that causes AQP2 to be downregulated as an attempt to prevent the increase in cell volume. AQP3 regulation has not been fully established, however, aldosterone hormone (Kwon *et al.,* 2002), isoprenaline (Rodriguez *et al.,* 2011), adrenaline (Yasui *et al.,* 2008) and tonicity (Matsuzaki *et al.,* 2001; Garcia *et al.,* 2011) have been has been proposed to regulate AQP3 expression and function. Epinephrine was found to promote translocation of AQP3 from the cytoplasmic fraction to the plasma membrane. This increased trafficking of AQP3 was suppressed by phospholipase C and PKC inhibitors and a phorbol ester accelerated the trafficking of AQP3 to the membrane fraction (Yasui *et al.,* 2008).

1.10.4.5 AQP4 Localisation, Function and Regulation

AQP4 was first cloned from rat lung (Hasegawa *et al.,* 1994) and rat brain (Jung *et al.,* 1994a). Since then, AQP4 has also been found in numerous tissues including kidney (Kim *et al.,* 2001). AQP4 is particularly highly expressed in astrocytic glial cells of the brain with a role in maintaining osmotic potential across the blood brain barrier (Passantes-Morales and Cruz Rangel, 2010). Various isoforms for AQP4 have been identified but the isoform identified in the brain is several amino acids longer and it transports water at higher rates. Subsequent publications reported more possible splice variant of the gene (Yang *et al.,* 1995; Lu *et al.,* 1996). AQP4 knock-out in

astrocytic end-feet are protected from cytotoxic brain oedema (Tang and Yang, 2016) and AQP4 antibodies are thought to be key to the onset of neuromyelitis optica (Chan *et al.,* 2012). In addition, the water flux through AQP4 aids in rapid clearance of K^+ thereby contributing to the recovery of normal extracellular K^+ concentration after neuronal activation (Amiry-Moghaddam *et al.,* 2003). AQP4 is also regulated by vasopressin, however, unlike AQP2, vasopressin does not result in AQP4 translocation from internal stores to the plasma membrane. Vasopressin caused AQP4 to be internalised from the cell surface in xenopus oocytes (Gunnarson *et al.,* 2008; Moeller et al., 2009).

1.10.4.6 AQP5 Localisation, Function and Regulation

AQP5 is highly expressed in various tissues including salivary, sweat and lacrimal glands, as well as lungs and airways, and plays a key role in secretion of isotonic fluids (Kitchen *et al.,* 2015). AQP5 has been demonstrated to function together with TRP vanilloid 4 (TRPV4) to control regulatory volume decrease (a process that allows the cells to return to its initial volume) in saliva. AQP5 has the closest homologues to AQP2 and therefore they share similar regulatory mechanisms (Frick *et al.,* 2013). AQP5 has been found to be regulated by cAMP and a PKA-dependent pathway in several cell types. Two consensus PKA sites for phosphorylation have been identified in AQP5; S156 in loop D and T259 in the C-terminus (Woo *et al.,* 2008). The PKA consensus site T259 plays a crucial role in AVP-mediated membrane targeting. Both these sites have been shown to be able to be directly phosphorylated by PKA and S156 was shown to be preferentially phosphorylated in tumour cells (Woo *et al.,* 2008).

1.10.4.7 AQP6 Localisation, Function and Regulation

AQP6 was first cloned from rat kidney and was initially referred to as WCH3 (Ma *et al.,* 1993). AQP6 has been identified in kidney but in contrast to other renal aquaporins, AQP6 is located in intracellular vesicles suggesting that AQP6 is less likely to be involved in water reabsorption. Instead, studies found that acidic pH could serve as the activating mechanism of AQP6 and it could function as an acid-base regulator (Yasui *et al.,* 1999a). Similar to AQP2, AQP6 is retained within intracellular vesicles and studies have found that residues at the N-terminal sequence are required for cytosolic retention (Conner *et al.,* 2013). For example, substitution of the N-terminal sequence on AQP1 for AQP6 N-terminal resulted in intracellular retention of the AQP1/AQP6-N-terminus (Conner *et al.,* 2013). A possible PKA phosphorylation site is also found at the C-terminal but no role has been reported for this site. (Beitz *et al.,* 2006).

1.10.4.8 AQP7 Localisation, Function and Regulation

AQP7 belongs to the aquaglyceroporins, similar to AQP3 AQP9 and AQP10. AQP7 was first cloned from rat testis (Ishibashi *et al.,* 1997a) and was found to transport glycerol. AQP7 expression is also found in both skeletal (Yang *et al.,* 2000; Skowronski *et al.,*2007) and cardiac muscle (Butler *et al.,* 2006; Skowronski *et al.,* 2007).

In humans it was first found expressed in adipose tissue (Kuriyama *et al.,* 1997). In adipocytes, AQP7 supplied the glycerol needed for gluconeogenesis (Lena and Lebeck, 2018). In addition, adult AQP7 null mice have a severe increase in body fat mass indicating a role in obesity (Hara-Chikuma *et al.,* 2005). In the kidney, AQP7 has

also been shown to reabsorb glycerol (Skowronski *et al.,* 2007). PKA has been proposed to be involved in AQP7 translocation in which cells? (Kishida *et al.,* 2000), however, experimental evidence for this is currently lacking.

1.10.4.9 AQP8 Localisation, Function and Regulation

AQP8 has been found in various tissues including colon, placenta, liver, heart (Ma *et al.,* 1997), testis (Ishibashi *et al.,* 1997b) and pancreas (Koyama *et al.,* 1997). As with many of the identified AQPs, AQP8 regulation still remains to be fully established in the different tissues in which it has been identified. However, studies have provided evidence of intracellular components involved in AQP8 trafficking. For example, AQP8 has been shown to be trafficked from intracellular vesicles to the plasma membrane in response to cAMP stimulation in isolated hepatocytes (Garcia *et al.,* 2001). Although AQP8 exhibits similar structure and conserved NPA sequences compared to other AQPs, studies shows that AQP8 lacks the conserved regions essential for phosphorylation via PKA or PKC (Conner *et al.,* 2013). This observation is significant in providing the possibility of an intermediate protein that is independent of the PKA pathway, being involved in phosphorylation of AQP8.

1.10.4.10 AQP9 Localisation, Function and Regulation

AQP9 is expressed in kidney, liver, leucocytes, lung, spleen, brain and testis (Lindskog *et al.,* 2016). Similar to AQP3 and AQP7, AQP9 it belongs to the aquaglyceroporin family and has been shown to transport solutes such as urea and glycerol in addition to water (Ishibashi *et al.,* 1998; Tsukaguchi *et al.,* 1998). In liver, AQP9 mediates the

uptake of glycerol and also participate in the mechanisms of energy sensing in the brain (Badaut *et al.,* 2004). PKC is a possible regulator for AQP9. AQP9/PKC binding or phosphorylation sites have been identified as serine residues 11 and 222 (Loitto *et al.,* 2007). AQP9 has also been shown to be phosphorylated in human neutrophils. PKC-mediated phosphorylation at serine 11 triggered by hyperosmolarity caused trafficking of AQP9 to the plasma membrane which contributed to RVD or a regulatory volume increase (RVI). Of interest, a S11A mutation ablated AQP9 translocation to the plasma membrane (Karlsson *et al.,* 2011).

1.10.4.11 AQP10 Localisation, Function and Regulation

Little is known about AQP10 expression, regulation and function. AQP10 belongs to the aquaglycerolporins localised in human adipose tissue, small intestine, male reproductive system and skin (Li *et al.,* 2006). In the small intestine, two isoforms of AQP10 were identified and both isoforms have been proposed to play different roles in the proximal portion of human small intestine (Li *et al.,* 2006; Laforenza *et al.,* 2015) In adipose tissue, AQP10 is expressed along with AQP7 and it is believed to have similar role as AQP7 in maintaining normal or low glycerol content inside the adipocytes, thus protecting human from obesity (Laforenza *et al.,* 2016). Currently, no studies have been reported on AQP10 regulation in mammals.

1.10.4.12 AQP11 Localisation, Function and Regulation

AQP11 is considered as an S-aquaporin or unorthodox superaquaporin. These have been identified in animals but not fungi, bacteria or plants, and their exact role in epithelial barriers remains to be determined (Madeira *et al.,* 2016; Ishibashi *et al.,*

2014; Papadopoulos and Verkman, 2013). AQP11 null mice develop polycystic kidneys (Ishibashi, 2009). Also, Muller cells expressing AQP11 shows the AQP11 is important during osmotic stress conditions in the rescue from cell shrinking in extracellular hypertonic conditions (Deeg *et al.,* 2016). Immunohistochemical studies have shown AQP11 localisation in intracellular organelles kidney proximal tubes (Morishita *et al.,* 2005). The ability of AQP11 to mediate water transport was investigated in oocytes and reconstituted liposomes. However, these experimental studies showed contrasting data. Oocytes showed no water transport (Gorelick *et al.,* 2006), while transport was observed in artificial liposomes (Yakata *et al.,* 2007). The exact intracellular signalling pathway or signalling components involved in AQP11 activity has currently not been revealed.

1.10.4.13 AQP12 Localisation, Function and Regulation

Similar to AQP11, AQP12 belongs to the S-aquaporins or unorthodox superaquaporins. AQP12 is poorly characterised and little is known about its role. A key signature feature of all identified AQPs is the tandem repeats of highly conserved pore-forming amino acid residues named NPA boxes (Morishita *et al.* 2004). The NPA boxes of the new subfamily, of which AQP12 belongs, however, are very different with an overall homology of less than 20% (Morishita *et al.* 2004). Further, little is known about the functions and physiological relevance of AQP12. AQP12 was selectively localised in the acinar cells of the pancreas and this along with its location in intracellular organelles suggests a role in digestive enzyme secretion such as

AQP	Year Found	Permeable to	Location	Putative Functional Roles
0	1984	Water	Lens fibre gap junctions	Water regulation, structural function
1	1987	Water	Kidney (proximal renal tubule), eye, CNS, lung, erythrocytes	Water homeostasis, fluid reabsorption
2	1993	Water	Kidney collecting duct	Water homeostasis, reabsorption from urine
3	1994	Water, glycerol, urea	Skin, kidney, lung, eye, small intestine, colon	Water homeostasis in renal collecting duct, glycerol/lipid metabolism
4	1994	Water	Brain, lung, muscle, stomach Glial cells, (astrocytes), renal collecting duct	Water regulation, cerebral oedema
5	1995	Water	Salivary-, lacrimal- and sweat gland, lung, eye.	Facilitates isotonic secretions
6	1993	Water, anions	Renal collecting duct	Intracellular water/ion regulation
7	1997	Water, glycerol, urea, arsenite	Adipocytes, kidney, liver, testis	Glycerol/lipid metabolism
8	1997	Water	Liver, kidney, testis, pancreas, heart, colon, placenta, small intestine	Water homeostasis
9	1998	Water, glycerol, urea, small solutes, arsenite	Kidney, liver, leucocytes, lung, spleen, brain, testis	Water/ small molecule homeostasis, glycerol metabolism
10	2001	Water, glycerol, urea	Small intestine (duodenum, jejunum), kidney	Water regulation
11	2000/2005	Water	Kidney, testis, brain, pancreas, leucocytes, smooth muscle , liver	Unknown
12	2000/2005	Unknown	Pancreas	Unknown

Table 1.3 Expression, localisation, function and discovery of AQP 0-12

This table present the different types pf AQPs identified in mammalian cells, their subcategories, function and their discovered roles (where known) in different tissues. Adapted from Conner *et al.,* 2012

1.11 AQPs and the Urinary Bladder

The notion that the kidney is not exclusively responsible for determining the final concentration of urine has existed for many years. Several studies have demonstrated that the composition of urine sampled at the renal pelvis is different from samples taken from the bladder (Englund 1956; Levinsky and Berliner 1959; Cahill *et al.,* 2003; Shafik *et al*. 2004; Shafik *et al.* 2005), suggesting that for the duration that urine is present in the bladder, the urothelium contributes to modifying urine composition.

AQPs (and aquaglyceroporins) have been identified in the urothelium of various species such as rats, hibernating bears and humans (Spector *et al.,* 2002; Rubenwulf *et al.,* 2009; Rubenwulf *et al.,* 2012), indicating that AQPs might generally be involved in modification of urine concentration. Changes to the extracellular osmolarity of urothelial cells are also a form of stress, which results in release of transmitters such as ATP, acetylcholine and Nitric oxide (NO) (Birder and Andersson, 2013). Release of these transmitters has a significant effect on the contractile function of the bladder and transduction mechanisms underlying the activation of afferent fibres during bladder filling (Vlaskovska *et al.,* 2001; Yu and de Groat, 2010). However, the exact role of AQPs in mediating the sensory and contractile functions of the bladder wall, and the mechanisms by which their expression and function in the urothelium is regulated, remains unclear. A better understanding of the role of AQPs in modulating water and solute movement across the bladder urothelium should aid in the development of novel therapeutic interventions for the treatment of conditions, such as nocturia.

1.12 Pathologies Associated with Urothelium Barrier Dysfunction

As with many other organs, the cause of bladder disorders cannot be attributed to one single source. However, there is emerging evidence to support the involvement of

bladder urothelium abnormalities in a variety of these disorders (Curhan *et al.,* 1999; Held *et al.,* 1990; Johansson and Fall, 1990; Tomaszewski *et al.,* 2001). One of these abnormalities is nocturia. Nocturia is a lower urinary tract (LUT) disorder that is currently defined by the International Continence Society (ICS) as waking up from the main period of sleep one or more times to void (Bergman *et al.,* 2015). Morbidity associated with nocturia, mainly due to its impact on sleep, includes increased prevalence of depressive symptoms in men and woman, tiredness, mood changes, cognitive dysfunction with poor concentration and performance (Jin and Moon, 2008; Kupelian *et al.,* 2012; Dani *et al.,* 2016).

The prevalence of nocturia increases with age (Kim *et al.,* 2010), so another important associated morbidity is an increased risk of falls and fractures in the elderly (Friedman and Weiss, 2013). These complications collectively result in direct, indirect and intangible costs to health-care systems that are often overlooked. Direct annual costs of nocturia, including those associated with falls and fractures, were estimated to be approximately $1.5 billion in the United States (US) and €1 billion in the largest fifteen European countries (Larsen, 2014). Loss or impairment of work productivity, which is categorized as an indirect impact of nocturia, was calculated to cost $62.5 billion and €29 billion annually in US and in the 15 largest European countries respectively (Oelke *et al.,* 2014). Intangible costs, such as behavioural modifications, feelings of loss of control and poor mood, prove difficult to be evaluated as they affect the quality of life of patients and are not immediately equivalent to an economic cost (Larsen, 2014). In view of these financial and social impacts of nocturia, it is important to research and develop better treatments and management options for this condition.

1.12.1 Aetiology and Pathophysiology of Nocturia

Nocturia is considered as one of the hallmarks symptoms of lower urinary tract (LUT) disorders such as overactive bladder (OAB) syndrome and benign prostatic hyperplasia (BPH) (Kerrebroeck and Andersson, 2014). Treatment options provided for patients with LUTs disorders such as OAB and BPH do not significantly improve nocturia (Smith and Wein., 2011), indicating that although nocturia is hallmark for LUTs, it is a condition in its own right with various aetiologies unrelated to bladder or prostate disorders. Thus, treatment regimens should be designed to treat nocturia and not other LUT disorders in the hope of improving nocturia. While bladder outlet obstruction (BOO) or prostate enlargement may cause nocturia in some patients, in many non-urological factors play a major role. Hormonal imbalance, uncompensated heart disease, sleep disorder and lifestyle choices, such as fluid intake before bed time, are a few examples of non-urological factors (Van Kerrebroeck *et al.,* 2002). In addition to bladder storage disorders, other urological causes may be related to kidney disorders that leads to overproduction of urine throughout the day or during sleep (global or nocturnal polyuria) (Kerrebroeck and Andersson, 2014).

1.12.2 Urological Causes of Nocturia

The general accepted categories for the classification of nocturia includes nocturnal polyuria (NP), reduced bladder capacity (RBC), global (24 hour) polyuria (GP) and a combinations of these conditions. Under the category of RBC, altered salt/water reabsorption from the bladder is a possible cause (Weiss *et al.,* 1998).

1.12.3 Nocturnal polyuria Nocturnal polyuria (NP)

NP is excessive urine production at night (33% of total daily urine output) caused by water diuresis, solute diuresis or both, and it affects up to 82% of patients with nocturia (Young *et al.,* 2015). Lifestyle and behavioural choices such as excessive fluid intake in the evening (diuretic beverages; alcohol, caffeine) (Figure 1.7) or a defect in vasopressin secretion and function causes NP. Alternatively, the condition may be idiopathic (Kerrebroeck and Andersson, 2014). The primary causes of solute diuresis include congestive heart failure, sleep apnoea, renal insufficiency, autonomic neuropathy, venous insufficiency and neurological disease (Kujubu 2009).

1.12.4 Global polyuria (GP)

GP is defined as a continuous overproduction of urine (more than 40ml/kg over a 24 hr period) and may result from several different pathologies (Kerrebroeck and Andersson, 2014). GP usually occurs as a result of polydipsia (Figure 1.7) which in turn leads to increased urine production. This form of urine production is not limited to sleep hours and occurs during the day and the night-time (Jin and Moon, 2008). Polydipsia may simply be behavioural or secondary to dehydration due to a poorly controlled disorder such as diabetes mellitus (DM) or diabetes insipidus (DI) (Jin and Moon, 2008; Kerrebroeck and Andersson, 2014).

1.12.5 Reduced Bladder Capacity (RBC)

RBC is usually due to bladder storage problems caused by benign prostatic hyperplasia (BPH), overactive bladder (OAB), interstitial cystitis or bladder pain syndrome (Hofmeester *et al.,* 2014). RBC is a feature of neurogenic bladder, which

may be due to conditions such as Parkinson's disease, multiple sclerosis, spinal cord injury, or stroke (Figure 1.7). Voiding disorders associated with OAB lead to urine retention that affects the functional storage capacity and leads to increased urinary frequency (Hajdinjak and Leskovar, 2013). Patients with RBC could also be presented with NP. Thus, in order to improve the condition, treatment options for patients with RBC usually take into account the possibility of existing NP (van Kerrebroeck and Anderson, 2014).

1.12.6 Non-urological Causes of Nocturia (sleep impairment)

Sleep disorders such as insomnia, restless leg syndrome and narcolepsy can also cause nocturia (Figure 1.7). Neurological and psychiatric conditions such as depression, anxiety and chronic pain disorder may also cause secondary sleep disorders associated with nocturia (Jin and Moon, 2008; Ancoli-Isreal *et al.,* 2011). Increased alcohol consumption and drugs such as cardiac glycosides and lithium use can contribute to sleep impairment that in turn leads to nocturia (Wyman *et al.,* 2009).

1.12.7 Circadian Clock Disorders

A circadian clock is an internal self-sustained molecular oscillator that is responsible for controlling behavioural, physiological and metabolic daily rhythms in mammals (Ko and Takahashi, 2006). The bladder has been identified to be influenced by circadian genes and it has been demonstrated that the voiding micturition cycle of an organism is caused by adaptation to the day-night cycle of the environment (Figure 1.7) (Kim *et al.,* 2016). Men with bladder obstruction, that causes reduced voiding volume and

shorter voiding time in the afternoon compared to mornings and overnight, have a dysregulated circadian clock (van Kerrebroeck and Anderson, 2014). Considering nocturia as a circadian disorder that simply leads to voiding at the wrong time, warrants a different approach into the investigation in the pathophysiology of nocturia.

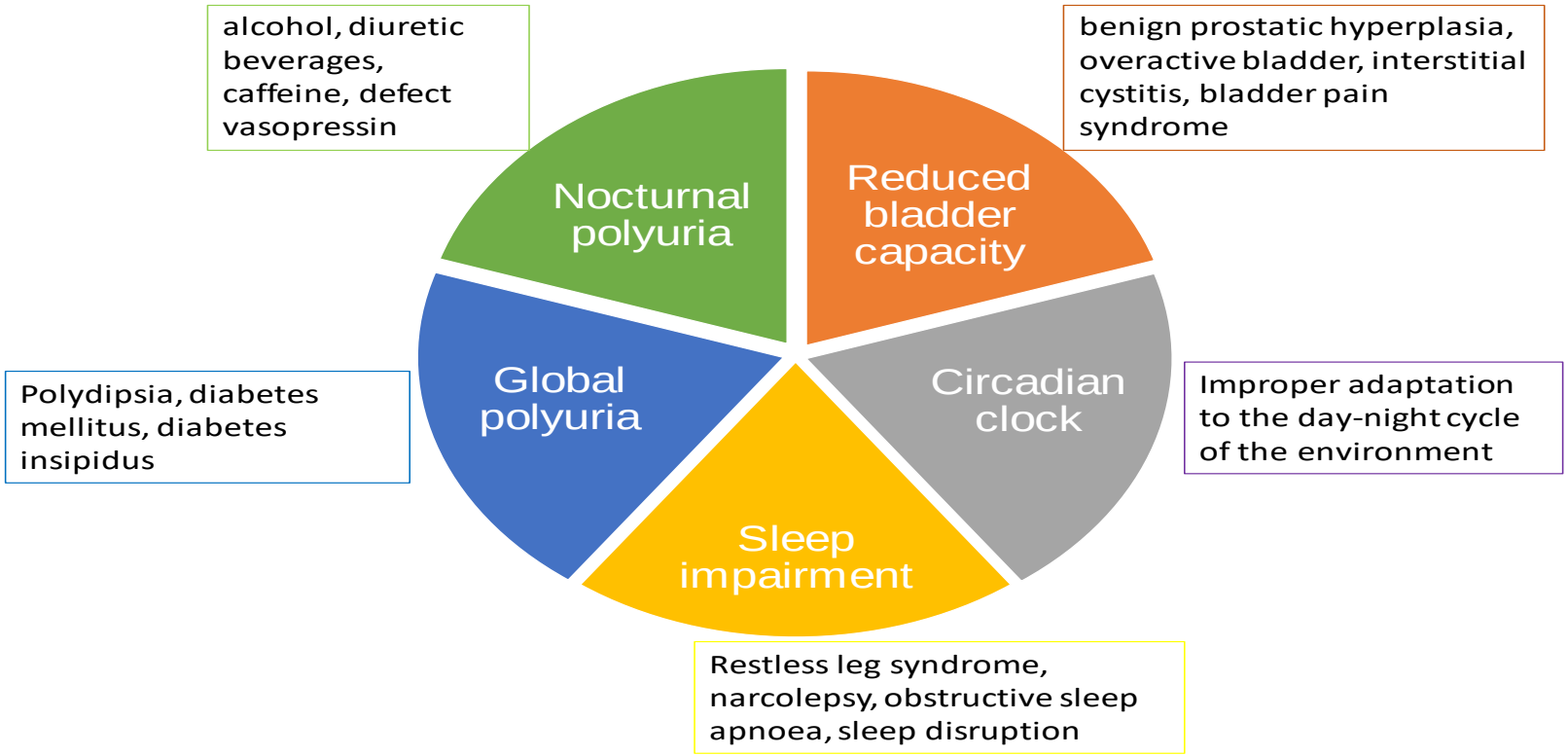

Figure 1.7 Urological and non urological causes of nocturia.

The general accepted categories for nocturia is devided into five classification: nocturnal polyuria (NP), reduced bladder capacity (RBC), global (24 hour) polyuria (GP) and a combinations of these conditions where the causes are non urological, such as circadian clock disorder, sleep imparment. The figure presented above demonstrates the different causes of nocturia.

1.13 Treatment Options for Nocturia

The current available treatments for nocturia include alpha-blockers, 5-alpha reductase inhibitors and anti-muscarinics, which are not generally effective because these drugs do not primarily manage nocturia, but rather target other LUT disorders such as OAB, BHP that are associated with nocturia (Friedman and Weiss, 2013). Desmopressin, a synthetic analogue of vasopressin, is a key compound for the treatment of nocturia, as it increases renal reabsorption of water via AQP2, thereby reducing the fluid load delivered to the LUT (Cvetković and Plosker, 2005; Rezakhaniha *et al.,* 2011; Friedman and Weiss, 2013). However, desmopressin is highly specific in its function and thus cannot effectively be used in the treatment of certain types of nocturia including the type caused by reduced functional bladder capacity (Weiss, 2013). Thus, better treatment options are desirable, as many people have nocturia that is refractory to available licensed options.

A new concept of bladder absorption to avoid nocturia has been reported. It has been demonstrated that during the “sleep-flat pattern,” the bladder reaches its functional capacity shortly after sleep onset and is maintained steadily at the functional capacity until wake time in the morning (Watanabe *et al.,* 2016). In the process, a temporary reduction in bladder volume occurs without micturition, which further supports the notion that water is absorbed from the bladder. Therefore, there is increasing evidence that the bladder plays an active role in both solute and fluid reabsorption and is able to modify the final composition of urine. Since AQPs have been identified in the bladder urothelium, their exact role in mediating water transport across the bladder wall needs to be further explored in order to target these proteins for increasing bladder capacity during sleep and treatment of nocturia.

In this study, the possibility of a new approach to moderate the balance between fluid accumulation and bladder reservoir function by investigating the role of the bladder urothelium in mediating transmural water transport was evaluated

1.14 The Use of Animal Models to Study Bladder Pathologies

Animals have been used for medical and scientific research for a long time. The anatomical and physiological resemblance between human and animals, predominantly mammals, have allowed researchers to conduct the majority of scientific research involving the study of mechanisms and in the assessment of novel therapies in animal models before application to humans (Sinoussi and Montagutelli, 2015). However, not all results obtained on animals can be directly translated to humans. This observation is emphasised by the variation in the complex network of hormones, circulating factors such as epidermal growth factor, as well as cross-talk between cells in the different species, particularly in small rodents such as rat and mouse (Sinoussi and Montagutelli, 2015). The use of animal models to study lower urinary tract dysfunction can be challenging due to the fact that bladder symptoms cannot be determined in an animal. Therefore surrogate physiological and behavioural observations have to be utilised. To date, a variety of animals, mainly small rodents, along with cell culture models, have been used to study lower urinary tract pathophysiology. However, extrapolating findings generated using small laboratory animals to the physiology of urine storage and voiding in large animals is difficult. Studies have evaluated the urodynamic properties of pig *in vivo*, demonstrating comparable urodynamic (Sibley, 1984; Crowe and Burnstock, 1989; Mills *et al.,* 2000b; Moore and Brading, 2007) and structural (Dixon and Gosling, 1983; Teufl

et al., 1997) characteristics to humans, and potential clinical relevance. We have also developed a novel perfused model using isolated pig urinary bladder to study the integrative physiology of the bladder.

1.15 Hypothesis, Aims and Objectives of the Study

1.15.1 Hypothesis

The overall hypothesis of this study is that pig urinary bladder expresses AQP channels and these channels are responsible for absorption of water across the bladder urothelium in response to different osmotic conditions

1.15.2 Aims of the study

The adult pig bladder offers a viable animal model as it has comparable structural and physiological properties to the human bladder. Based on existing data, the expression and function of AQPs in pig urinary bladder has not been investigated. Therefore, the overall aims of this study were to investigate whether AQPs are expressed in pig bladder urothelium and explore their role in mediating water flux across the urothelium under various osmotic condition

1.15.3 The overall objectives of this study

- To identify the different subtypes of AQPs in pig urinary bladder using polymerase chain reaction (PCR)
- To identify the localisation of AQP substypes in the different layers of pig urinary bladder using PCR and immunohistochemistry and western blot
- To determine whether the identified AQPs are functional in pig urinary bladder using Ussing chamber
- To determine whether changes in osmolarity affect the rate of water movement of across pig mucosa section using using chamber
- To determine whether AQPs are translocated to the membrane in respond to changes in osmolarity using immunoflourescense

Chapter 2

Investigating the Expression of AQP's in Urothelial and Sub-urothelial Layers of Pig Urinary Bladder

2.1 Introduction

The presence of AQPs has now been reported in the urinary bladder of various species and it is hypothesised that AQPs are involved in modifying the final concentration of urine (Rubenwulf *et al.,* 2009; Spector *et al.,* 2002; Rubenwulf *et al.,* 2012). Studies have now confirmed the presence of AQPs in human (Rubenwolf *et al.,* 2009), rat (Spector *et al.,* 2002) and American black bears urothelium (Spector *et al.,* 2015)

2.1.1 AQPs in Human Urinary Bladder

AQPs have been identified in human bladder. AQP3, AQP4, AQP7 AQP9 and AQP11 were constitutively expressed at the transcript level in freshly isolated human urothelial cells and a normal human urothelial (NHU) cell line (Rubenwolf *et al.,* 2009). Immunolableling demonstrated an intense production of AQP3 protein in the basal cell layer. AQP4 and AQP7 showed less intense cytoplasmic expression throughout the urothelium. No immunoreactivity was found with the antibody against AQP9 whereas AQP11 protein production could not be assessed due to the lack of suitable antibodies (Rubenwolf *et al.,* 2009). The expression of both “orthodox” aquaporins and aquaglyceroporins may be of significance with regards to physiological function of these channels in human urothelial cells.

2.1.2 AQPs in Rat Urinary Bladder

In rat bladder AQP1, AQP2 and AQP3 have been identified. It was shown that AQP1 was expressed in endothelial cells of capillaries and small arteries, whereas AQP2 and AQP3 were expressed in cell membranes of rat urothelium with the exception of the apical surface of umbrella cells. AQP2 was also present in the cytoplasm of urothelial cell. (Spector *et al.,* 2002). It was further demonstrated that dehydration

induced upregulation of AQP2 and AQP3 but not AQP1, suggesting that changes to urine osmolarity can directly impact AQP2 and AQP3 expression and function. AQP1 was not affected by the hydration status of the animal, which is in keeping with a study showing that in vascular endothelium, renal cortex and inner and outer medulla, AQP-1 is not regulated by hydration status or circulating AVP (Terris *et al*., 1996).

2.1.3 AQPs in American Black Bears Urinary Bladder

Studies with American black bears, which undergo winter hibernation, have shown that these animals do not urinate for months. However, despite continuous production of urine during the hibernation state, these animals do not become uraemic and blood urea levels remain constant (Nelson *et al.,* 1973). In subsequent studies, radioactively-labelled urea and deuterium oxide (D_2O), were instilled into the bladder of these animals during the hibernation period and it was observed that both D_2O and urea could be detected in the plasma, demonstrating reabsorption of these compounds across the bladder wall (Nelson *et al.,* 1975). Of interest, a recent study with hibernating American black bears reported AQP1 protein production in suburothelial capillaries and arterioles and AQP3 in the basolateral membrane of basal and intermediate cells (Spector *et al.,* 2015) which further supports an association between the presence of AQPs and their potential involvement in mediating urea and D_2O reabsorption across the bladder urothelium.

Although not many studies have investigated the expression of AQPs and their function in the urinary bladder, these studies collectively provide strong evidence for a complex role of the urinary bladder urothelium in regulating osmolality and

composition of the urine with the possibility of contributing to the overall fluid homeostasis in the body.

2.1.4 Potential Regulatory Mechanism Mediating AQP Expression and Function in Bladder Urothelium.

Some of the potential receptors and channels responsible for mediating AQP function and expression in various tissues were described in chapter 1. As there are numerous potential primary signals involved in regulating AQP function, the expression profile of only a few of these proteins were investigated in this study.

2.1.4.1 Transient receptor potential (TRP) Channels and AQPs

Studies have shown that TRP channels regulate AQP channels (Benfenati *et al.,* 2011; Jo *et al.,* 2015; Kitchen *et al.,* 2015). In astrocytes, regulatory volume decrease (RVD), a mechanism for volume control that serves to prevent detrimental swelling in response to hypo-osmotic stress, is mediated by interaction between AQP4 and TRPV4 (Benfenati *et al.,* 2011). Also, hypotonicity-induced calcium influx through TRPC1 has also been shown to be important for translocation of AQP1 (Conner *et al.,* 2012). In addition, calcium influx through TRPV4 mediates AQP5-dependent regulatory volume decrease in acinar cells (Kitchen *et al.,* 2015). TRP channels may therefore be important in regulating AQP function. Therefore the presence of TRP channels in pig urinary bladder was investigated.

2.1.4.2 Estrogen Receptors and AQPs

Estrogen receptor (ER) has been demonstrated to regulate AQP function. An estrogen response element (ERE) has been identified in the promoter region of the AQP1, AQP3, AQP2 and AQP5 genes (Zou *et al.*, 2011; Jiang *et al.*, 2015; Cui *et al.,* 2018). AQPs expression appears to be influenced (up or downregulation of AQPs) by the changes in estrogen levels during menstrual cycle in human epithelial endometrial cells (Cui *et al.,* 2018). AQP3 expression in the mid- and late-secretory phases of the human endometrium is significantly higher than in other phases. Progesterone up-regulates AQP3 by directly targeting the promoter of the AQP3 gene (Cui *et al.,* 2018). As female pigs were used throughout this study, changes in AQPs expression and function in the urinary bladder could be expected depending on the phase of estrus cycles of the pigs. Therefore, the presence of ERs was also investigated in pig urothelium.

2.1.4.3 ENaC Channels and AQPs

Another type of channel that is hypothesized to regulate AQP function indirectly are ENaC channels. Numerous studies have reported AQP involvement in regulatory volume decrease (Liu et al., 2006; Benfenati *et al.,* 2007; Day et al., 2014) a mechanism that involves the transport of water and ions including Na^+ to regulate intracellular and extracellular osmolarity. According to the proposed RVD mechanism by Day et al., (2014) ENaC are involved in this process (Day *et al.,* 2014)

Therefore, identifying the presence of these channels and receptors in pig urinary bladder mucosa could suggest a possible regulatory mechanism involved in AQP expression and function.

2.2 Aims and Objectives

The aim of this study was to investigate the expression of AQPs in the urothelial and sub-urothelial layers of pig urinary bladder and to determine the expression of some of the potential channels and receptors reported to be involved in AQP expression, trafficking and function.

2.2.1 Specific objectives

- Accurate qualitative mapping of aquaporin channels in the pig bladder tissues using PCR molecular technique
- Accurate qualitative mapping of aquaporin channels in the different layers of pig bladder tissues using immunological techniques
- Accurate qualitavie mapping of possible AQP regulators in different layers of the pig urinary bladder using PCR molecular technique

2.3 Materials and Methods

2.3.1 Tissue Preparation

Bladders, kidney (cortex, medulla and pelvis), stomach antrum, lung, liver, duodenum, rectum and testis from ~6-months old female pigs (*Sus scrofa domestica*), were obtained from a local abattoir (with permission of Langford Abattoir, University of Bristol, Bristol, UK), immediately after the animals were killed.

Pig bladders were used to investigate AQP expression. Kidney (cortex, medulla and pelvis), stomach antrum, lung, liver, duodenum, rectum and testis, collectively referred to as positive control tissue, were used to validate AQP primers.

Kidney and liver samples were also obtained from 8-week female Wistar rats (210-223g) euthanised for other studies (University of Bristol, Bristol, UK). Rat kidney and liver were placed in 10% neutral buffered formailne (Formaldehyde, 37%, 900ml deionized water, NaH_2PO_4; 4.0g/L, Na_2HPO_4; 6.5g/L) and used as positive controls for validation of AQP antibodies used immunohistochemical experiments.

The animals used in this experiment for AQP studies using molecular and immunohistochemical techniques were in accordance with UK Government regulations (Animals Scientific Procedures Act 1986). This study did not require a UK Home Office project license, because no regulated procedures were carried out.

Tissues were placed in ice-cold Krebs solution containing (mM): NaCl, 118.4; $NaHCO_3$, 24.9; KCl, 4.7; $CaCl_2$, 1.9; $MgSO_4$, 1.1; KH_2PO_4, 1.15; glucose, 11.7; 95% O_2/5% CO_2, pH 7.4. The warm ischaemia time (time between sacrificing the animal and placing the required organs in cold buffer) was kept to 15-30 min. Samples of bladder and kidney from pigs and rats were also placed in 10 % neutral-buffered

formalin (37% formaldehyde solution, Nacl 0.8 g, KH_2PO_4 0.4 g, K_2HPO_4 0.65 g, Distilled water 90ml) for immunohistochemistry. From each bladder, mucosa samples (urothelium and lamina propria; 30-50 mg) were obtained by blunt dissection from the lateral wall of the dome using the natural plane of division between the lamina propria and the underlying smooth muscle layer. In addition, 30-50 mg of urothelial cell suspension (consisting of basal, intermediate and umbrella cells) in lysis buffer (Promega, UK) was obtained by gentle scraping of a separate luminal part of the mucosa with a scalpel. 30-50 mg of the positive control tissues were obtained by blunt dissection ensuring that each sample consists of all the different layers of the tissue.

All procedures were performed at room temperature (RT) with tissues bathed in Krebs solution. Mucosa samples and those from positive control tissues, were washed four times in phosphate buffered saline (PBS) composed of 137 mM NaCl, 2.7 mM KCl, 8 mM Na_2HPO_4, and 2 mM KH_2PO_4 (with the exception of urothelium cells which were suspended in lysis buffer) prior to RNA extraction. All chemicals were from Promega (UK).

2.3.2 RNA Isolation and Reverse Transcription PCR

Bladder mucosa and urothelial samples from 25 different pigs as well as positive control tissue samples of different organs from one pig were homogenised at 12000 x g with TissueRuptor (Qiagen, UK) for 30 sec to 1 min in 500 µl RNA lysis buffer (Promega, UK). Total RNA was extracted from tissue samples using Promega SV total RNA isolation kit (Promega, UK) according to the manufacturer's instructions, including the removal of trace genomic DNA which was part of the RNA extraction process.

Homogenised samples were centrifuged at 13,000 x g for 5 min followed by aspiration of clear lysate. Chloroform (200 µl) was added to clear lysate and centrifuged at 900 x g for 10 min at 4℃. Ethanol (100% , 200 µl) was then added to 400 µl clear lysate and vortexed immediately. The lysate was transferred to a pre-assembled spin basket and centrifuged at 13,000 x g for 1 min. The RNA was subsequently bound to the silica membrane in the spin basket column and was then washed twice with 700 µl and 500 µl of RNA washing solution, respectively for 1 min at RT at 13,000 x g. Spin basket columns containing silica bound RNA was treated with Promega DNase treatment solution containing 24 µl yellow core buffer, 3 µl of $MnCl_2$ (0.09 M), 3 µl of DNase-1 enzyme for 30 min at RT. The DNase treatment was then inactivated by addition of 50 µl DNase stop solution to the spin basket column containing silica bound RNA to terminate the reaction. Two additional washings were performed using 600 µl and 400 µl of RNA washings solutions at each 13,000 x g for 1 min and 5 min. Total RNA sample was eluted from the spin basket column using 20-30 µl nuclease free water. RNA integrity and concentration was determined using a NanoDrop-1000 spectrophotometer (Thermofisher, UK). The ratio of absorbance at 260 nm and 280 nm was used to assess the purity of RNA and a ratio above 1.80 was the acceptable to avoid sample contamination with DNA and protein.

2.3.3 Complementary DNA (cDNA) Synthesis

Total RNA (1 µg) was reverse transcribed to single-stranded cDNA using GoScript™ enzyme along with oligo dT primers in two separate steps as per manufacturer's instructions (Promega, UK). In the first step, 1 µg of total RNA was added to a reaction mixture containing 0.5 µg Oligo $(dT)_{15}$ Primer and nuclease free water (NFW) to reach

a final volume of 10 µl. The reaction mixture was heated at 70 ºC using a heating block for 5 min and immediately chilled on ice for 5 min. The reaction mixture was subsequently centrifuge for 10 seconds in a micro-centrifuge and then stored on ice.

A second reaction mixture containing 4 µl of GoScript™ 5X Reaction Buffer, 1.5 µl of 1.5 mM $MgCl_2$, 1.5 µl of 0.5 mM PCR Nucleotide Mix, 1.5 µl of 20 units Recombinant RNasin®, 1.5 µl of GoScript™, 1 µl of Reverse Transcriptase and NFW to reach a final volume of 20 µl, was prepared and added to the initial mixture on ice to reach a final volume of 30 µl. The total mixture was heated at 25ºC for 5 min and 42ºC for 1 hr for annealing and extension, respectively. The reaction was terminated at 70ºC for 15 min. The transcribed RNA to single-strand cDNA was used for the polymerase chain reaction (PCR).

2.3.4 Polymerase Chain Reaction (PCR)

Primers specific for pig AQP1-11, smooth muscle myosin heavy chain (SMMHC), ER 1, TRPC4, TRPV4, Claudin-2, Claudin-4, ENaCs, vWF, Uroplakin were designed using the primer-3 design tool (http://primer3.ut.ee/).

To ensure that the urothelial samples obtained from the pig bladder were pure and did not contain cells from the sub-urothelial or smooth muscle layers cell, smooth muscle specific genes vWF and SMMHC were designed to test for the presence of smooth muscle cells in extracted urothelial cell samples using PCR. Primers for endothelial specific gene vWF was also designed to use as a control measure for cross contamination of sub urothelial blood vessels in extracted urothelium cell samples.

Uroplakin primers served to determine the presence of umbrella cells in extracted urothelial samples.

To ensure that the urothelial samples obtained from the pig bladder contain all the relevant layers, uroplakin and Claudin primers were designed as urothelial specific cell gene.

Primers were also designed to amplify potential AQPs regulatory channels and receptor TRPC4, TRPV4, AG-2R and ER 1.

To optimise PCR conditions for the primers, pig bladder tissue samples were subjected to gradient PCR using annealing temperatures of 53ºC, 54ºC , 55ºC , 56ºC , 56.5ºC , 57ºC , 58.2ºC , 59.4ºC, 60ºC , 61ºC with all the different primers. The PCR reaction mixture contained 3 µl of 1 µg cDNA, 12.5 µl GoTaq® G2 Hot Start Colorless, 3 µl of 0.8 mM of forward and reverse primers and NFW to reach a final mixture volume of 30 µl. This mixture was used in the following PCR conditions: 5 min denaturation at 94 °C; 35 cycles of 94 °C for 30 s; annealing temperature for 1 min (different annealing temperatures, Table 2.1); 1 min at 70 °C and a 5 mins final extension at 70 °C. cDNA samples were first amplified using Glyceraldehyde 3-phosphate dehydrogenase (GAPDH) forward and reverse primers (Table 2.1) to confirm successful reverse transcription (positive control). Absence of genomic DNA contamination was confirmed using RNA samples in PCR reaction (negative control). Sterile water reaction was also included instead of cDNA template as an additional negative control. Following confirmation of the presence of amplifiable cDNA, samples were amplified using primers specified in Table 2.1. The PCR products were loaded onto 2% (w/v) agarose gels containing 1 µl of 0.4 µg ethidium bromide. Electrophoresis was carried out at 100 V for approximately 40 min. The bands were visualised using the Syngene

gel imaging and analysis system (Cambridge, UK). The PCR products were identified by comparison with DNA ladder covering the range of 100-1000 bp. The PCR products were purified using the Wizard® SV Gel and PCR Clean-Up System (Promega, UK). The separated DNA bands were excised from the gel and transferred into 1.5 ml Eppendorf tubes. Membrane binding solution (MBS) was added to the excised gel at ratio of 10 µl MBS to 10 mg of excised gel. The mixture was incubated at 65 ºC for 10 min to dissolve the gel in the MBS, transferred into a minicolumn-collection tube system and centrifuged at 12000 x g for 1 min. The DNA in the column was washed by adding 700 µl of membrane wash solution to the column followed by centrifugation at 12000 x g for 5 min. Elution of DNA from the column into new DNase-free tube was performed by adding 40 µl of nuclease-free water followed by centrifugation at 12000 x g for 1 min. The purified PCR products were sent for sequencing at the concentration of 10 ng/µl and the primers concentration was 10 pmol/µl per sequencing reaction (Eurofins MWG, Ebersberg, Germany). Sequence data were verified by comparison with the genome database using BLAST from the NCBI website (http://blast.ncbi.nlm.nih.gov/blast.cgi).

Table 2.1. List of pig specific primer sequences, gene accession numbers and the expected product size. The corresponding annealing temperatures for pig specific AQPs, SMMHC, transporters, ER-1, TRPC4, TRPV4, Claudin-2, Claudin-4, ENaC α, β, γ uroplakin, vWF and GAPDH. The primers were based on mRNA sequences accessed from DDBJ/EMBL/GenBank database and the primers designed using Primer 3 software. The purpose of the gene amplification was to determine the presence of AQPs, SMMHC, transporters, ER-1, TRPC4, TRPV4, Claudin-2, Claudin-4, ENaC α, β, γ uroplakin, vWF and GAPDH in the tissue sampe collected.

Name of primer/Accession number	Forward primer (5'-3')	Reverse primer (5'-3')	Base pairs	Annealing temperature (°C)
AQP 1 (NM_214454.1)	AGCTGCCAGATCAGTGTCCT	CCAGTGGTCCTGGAAGTTGT	375	60.9
AQP 2 (NM_001128476.1)	GCTGCCATGTCTCCTTTCTC	TCATGGAGCAGCCAGTGTAG	318	59.04
AQP 3 (NM_001110172.1)	GGGACCCTTATCCTCGTGAT	AGAAGCCATTGACCATGTCC	394	58.2
AQP 4 (NM_001110423.1)	TTGCTTTGGACTCAGCATTG	TGACATCAGTCCGTTTGGAA	332	57.5
AQP 5 (NM_001110424.1)	GAAGGAGGTGTGCTCTCTGG	CGTGTTGTTGTTGAGCGAGT	373	59.5
AQP 6 (NM_001128467.1)	TGGATGACTGTCAGCAAAGC	CCTCAGGTATGACCCCGTAA	316	58.3
AQP 7 (NM_001113438.1)	AGAGTTCTTGGCCGAGTTCA	ACCGGTCACTGTCAGCTTTC	346	59.6
AQP 8 (NM_001112683.1)	GCCTGTCGGTCATTGAGAAT	GGATGATCTCTGCCACCACT	333	58.6
AQP 9 (XM_005659551.1)	TGCATTTGCAGACCAGGTAG	CTGGTTTGTCCTCCGATTGT	380	58.7
AQP 10 (NM_001128454.1)	TTGTGCTCATGCTCTTCACC	GGATAGGTGGCAAAGATGGA	355	57.7
AQP 11 (NM_001112682.1)	CGCTTTCGTCTTGGAGTTTC	GGAGCAGATGGCCTCTATCA	388	58.4
GAPDH (XM_005658673.2)	CACGTTGGGGGTGGGGACAC	ACCCAGAAGACTGTGGATGG	171	60.0
Uroplakin 2 (XM_005667407.1)	TGTCCCCTGCGTTAACTGAG	TTCGAGGAAGCGTGGACATT	315	59.6

TRPV4 (XM_013986922.1)	GCCTGTGTATTCCTCGCTCT	CTGGTAGTAAGCGGTGAGGG	241	59.5
TRPC4 (NM_001145868.1)	AGCCCCAAGTCTCTCTGGTA	CTCTGATCATAGCGGCCACA	187	59.5
Oestrogen receptor 1 (NM_214220.1)	GTGTCCAGCTACCAACCAGT	GATCATCTGGTCGGCTGTCA	289	56.6
Claudin-4 (XM_013995522.1)	GCCTTCCTTCCAGCTCCTAG	GATGTTGCTGCCGATGAAGG	160	59.5
Claudin-2 (NM_001161638.1)	ATCTTCATGGGATCCTGCGG	CTTGGCTTTGGGTGGTTGAC	239	59.6
Von Willebrand factor (NM_001246221.1)	TCCAGAACAACGACCTCACC	TCCTGGAAAATGTCGCTGGT	205	59.6
Smooth muscle myosin heavy chain (XM_013991919.1)	GACCTCGTTCGTTCCCTCAA	CCGGGTTTGGTTTTGTCCTG	156	59.6
Epithelial sodium channel SCNN1B transcript variant X1 (NC _010452)	TTCAGGCCTGTATTCGCTCC	TTGTACTGGGTGTCGTTGCA	214	59.8
Epithelial sodium channel SCNN1A (NM_213758.2)	AGGACGGGAGGTAGGATCAG	TGGCCTCTCTGTTGCTTCTC	236	59.8
Epithelial sodium channel SCNN1G (XM_003124543)	CTGTCTCAACACCAACACGC	ACGGCGGGAAAATCTAGCTT	195	59.7

2.3.5 Immunohistochemistry

Fixed bladder and kidney samples from pigs and rats in 10 % neutral buffered formaline were processed and embedded in paraffin. Tissue sections (3 µm) were placed on (3-aminopropyl) triethoxysilane coated slides and placed in a 60 °C oven overnight prior to immunohistochemical staining to aid adhesion. Sections were dewaxed in clearance (2 x 5 min) and dehydrated in 100 % ethanol (2 x 3 min). Endogenous peroxidase activity was blocked by incubation in 0.3 % H_2O_2 prepared in 100% methanol for 30 mins at ~20 °C. Citrate buffer (10 mM sodium citrate, 0.05% Tween 20, pH 6.0) was used for antigen retrieval of tissue sections by bringing the citrate buffer to the boil twice in a 750 W microwave and allowing to cool for 5 min and 15 min respectively. Slides were subsequently washed (2 x 3 min) in phosphate buffered saline (PBS (mM): NaCl, 154; $NaH_2PO_4.12H_2O$, 1.86; $Na_2HPO_4.2H_2O$, 7.48; pH 7.1) and blocked with 10% horse serum in PBS (20 min) to block non-specific binding sites, followed by incubation with the specific primary antibody (AQP1, 3, 9 and 11 polyclonal antibodies, used at 1:1000-1:1500 (Table 2.2) dilutions in PBS, (Almone Laboratories, Israel) overnight at 4°C. Negative controls replaced the primary antibody with the relevant peptide (Alomone Laboratories, Isreal). Relevant peptide is where primary antibody (Table 2.2) was mixed with the control peptide (1:4 ratio) in 1 ml Tris buffer saline (TBS) and was incubated for an hour at RT before applying to tissue sections overnight at 4 °C. Subsequent to overnight incubation, the slides were washed in PBS (2 x 3 min) and a biotinylated antibody raised to mouse IgG was applied (prepared as per Vectastain ABC kit instructions) (20 min). The slides were washed again in PBS (2 x 3 min) followed by application of avidin biotin complex in PBS (as per Vectastain ABC kit instructions) (20 mins). Slides were washed in PBS (2 x 3 min), developed with DAB/H_2O_2 in distilled water (as per DAB substrate kit

instructions) for 10 min and then washed in running water for 10 min. Sections were counterstained with Harris's haematoxylin (25% Gill haematoxylin) (30 s) and washed in running tap water (10 min). Finally, the sections were dehydrated in 100% ethanol (2 x 3 min), cleared in 100% clearene (2 x 5 min) and mounted in Clearium® Mounting Media. Sections were examined at x40 magnificationusing a Nikon Eclipse 50i microscope (Nikon Instruments Inc., USA).

2.3.6 Immunoblotting

2.3.6.1 Preparation of Protein Lysate

Mucosa and urothelial (50-100 mg) from the urinary bladder of 3 different pigs were homogenised in 1 ml of RIPA lysis buffer (400 µl of 5 M NaCl; 200 µl of 1M Tris-HCl; two tablets of 1x protease inhibitor (Sigma, UK); 2 ml of 10% SDS; 17 ml of distilled water) with TissuesRuptor (Qiagen, USA)

2.3.6.2 Protein Concentration Determination by the Bradford Assay

For protein estimation, a stock dye of Coomassie blue G was prepared (330 mg Coomassie blue G dye dissolved in 100 ml of phosphoric acid/ethanol (2:1) mixture). This was diluted to a working solution from 1.5 ml stock dye 4 ml phosphoric acid, 1.9 ml ethanol and 92.6 ml water. Appropriate dilutions of 0.2, 0.4, 0.6, 0.8, 1.0 and 1.2 µg/µl bovine serum albumin (BSA) in deionised water were prepared and 5 µl of diluted sample was pipetted into 96 triplicate wells. Unknown concentration protein samples were diluted between 1:5 and 1:50 in deionised water. Working solution of Coomassie blue G dye (200 µl) was pipetted into each well and the absorbance was measured at

OD_{620nm} with a Fluostar Optima plate reader (BMG Labtech, Aylesbury, UK). The OD_{620nm} is directly proportional to protein concentration over this range of standards, a standard curve (Figure 2.1) was constructed and using linear regression the concentration of protein in the samples was calculated using their OD_{620nm}.

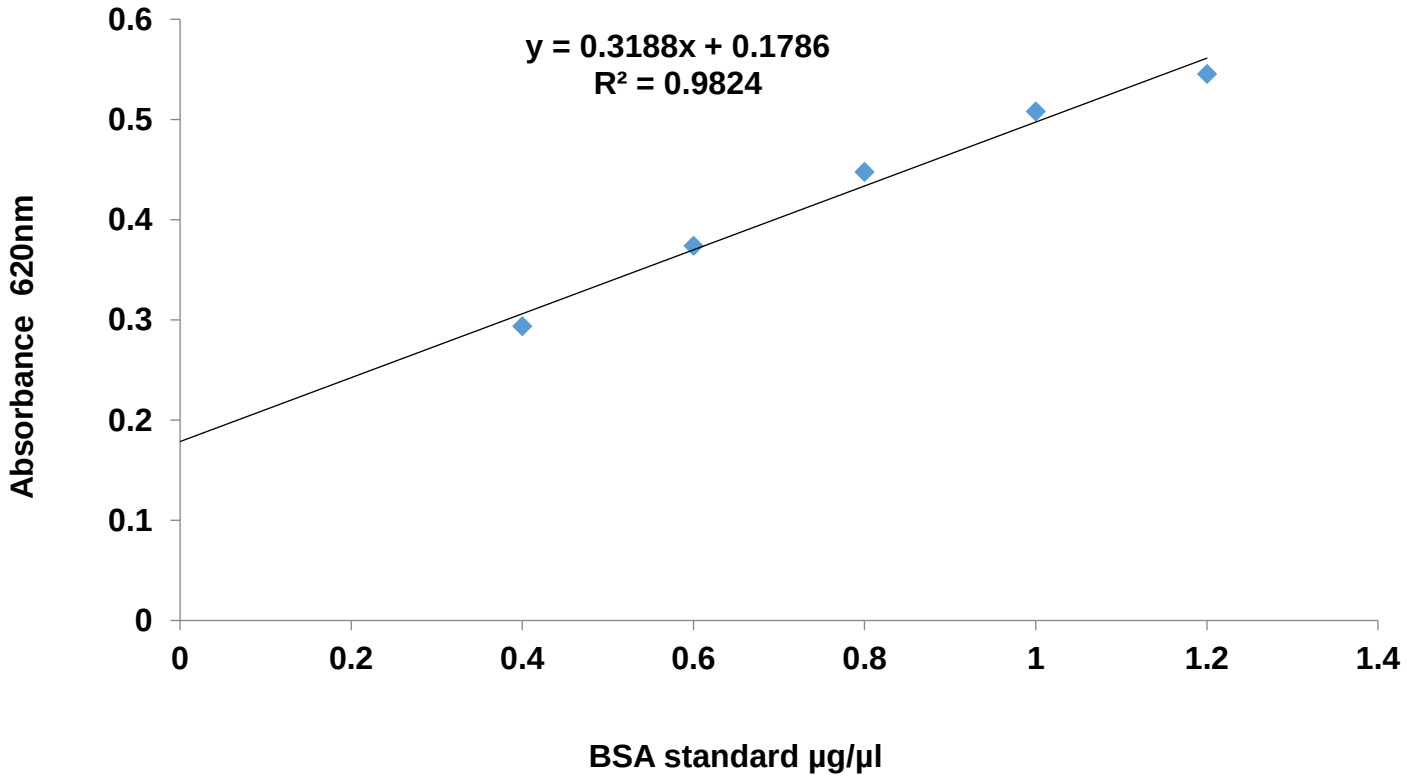

Figure 2.1 Bradford assay standard curve of BSA concentration versus absorbance.

The concentration of protein (µg /µl) was determined using the equation y=0.3188x+0.1786 generated from the BSA standards prepared with an R^2 value of 0.982, where y is absorbance and x is concentration. The calibration curve is needed to calculate samples concentration.

2.3.6.3 SDS-polyacrylamide gel electrophoresis

Protein lysate prepared from bladder mucosa and urothelium (20µg) was added to loading dye NuPAGE LDS Sample Buffer (4x bromophenol blue dye in 200 mM Tris, pH 6.8; 4x SDS-glycerol containing 40% glycerol and 8% SDS; 5% β-mercaptoethanol) (Life Technologies, Paisley, UK). Diluted samples were denatured by heating at 95 °C for 5 min and protein separated by electrophoresis alongside Spectra Multicolour Broad Range Protein Ladder (Fisher Scientific UK Limited, Loughborough, UK) on a NuPAGE 4–12 % Bis–Tris precast gel (Life Technologies, Paisley, UK) using the NuPAGE MES SDS Running Buffer (Life Technologies, Paisley, UK) in a XCell SureLock transfer tank for 1 h at 100 V. Proteins on the gel were subsequently transferred onto a polyvinylidene difluoride (PVDF) membrane in trans-Blot SD wet transfer (Biorad, Hertfordshire, UK) using XCell SureLock™ system.

Once the transfer was complete, the PVDF membrane was washed twice in 1X TBS-tween (TBST) (50 mM Tris-HCl, 150 mM NaCl; pH 7.4; 0.1% (v/v) Tween 20) for 5 min, then blocked in 5 % (w/v) non-fat dried milk powder in 1X TBST 1 hour and incubated overnight at 4 ºC with primary antibodies diluted in 5 % milk and 1X TBST (Table 2.2). The membrane was then washed 6 x 5 min in TBST and incubated at RT for 45 mins with anti-rabbit horseradish peroxidase (HRP) conjugated secondary antibody (Vector Laboratories) (dilution 1:5000) in 5 % (w/v) non-fat milk dissolved in 1X TBST. The blot was then subjected to a further wash cycle with TBST and then incubated with 2 ml of HRP substrate for 1 min. Immunolabelled proteins was visualisation using Luminata Forte Western HRP Substrate (Millipore) applied for 2 min, followed by exposure to Amersham Hyperfilm ECL (GE Healthcare, UK).

Table 2.2. Primary antibodies and their respective concentrations.
Primary antibodies used to probe for AQP1, AQP3, AQP9, AQP11 in immunoblot and immuhistochemistry. Different concentration were used to improve specificity. Peptide control was four fold the initial diluted antibody. The listed antibodies were obtained from Alomone Laboratories (Jerusalem, Israel)

Primary antibody	Dilution (5% milk and TBST) IHC	Dilutions (in 5% milk and TBST) WB	Species (polyclonal)	Reactivity and peptide sequence
Anti- AQP1 (AQP-001) (Kim *et al.,* 2013)	1:1000	1:200	Rabbit	Mouse, human, rat (C)KVWTSGQVEEYDLDADDIN
	Peptide control (PC) 1:1000+ 4000 pc	Peptide control (PC) 1:1000+ 800 pc		
Anti- AQP3 (AQP-003) (Zheng and Bollinger,2003)	1:1000	1: 200	Rabbit	Mouse, human, rat (C)STEAENVKLAHMKHKEQI
	Peptide control (PC) 1:1000+ 4000 pc	Peptide control (PC) 1:1000+ 800 pc		
Anti- AQP9 (AQP-009) (Sales *et al.,* 2016)	1:1000	1: 300	Rabbit	Mouse, rat (C)EKDGAKKSLMQRLALK
	Peptide control (PC) 1:1000+ 4000 pc	Peptide control (PC) 1:1000+ 1200 pc		
Anti- AQP11 (AQP-011) (Yasui *et al.,* 1999)	1:1500	1:500	Rabbit	Mouse,rat (C)SLSLTKYHFDER
	Peptide control (PC) 1:1000+ 6000 pc	Peptide control (PC) 1:1000+ 2000 pc		

2.4 Results

2.4.1 Amplification of Urothelial Specific genes to Determine Cross Contamination of Mucosa in Urothelial Samples

RT-PCR was used to investigate the expression of various urothelial specific genes such as Claudin-2, Claudin-4 (tight junction proteins) and uroplakin 2 to ensure that all the cell layers of the urothelium were indeed present in the collected urothelial cell suspensions as these are urothelial specific genes.

SMMHC and vWF served as a control measure for urothelial extraction technique to confirm the absence of smooth muscle cells contamination in urothelial sample.

GAPDH as a housekeeping gene was used to confirm successful RNA isolation and reverse transcription.

Claudin-4, but not Claudin-2, was expressed in both urothelial and mucosa samples (Figure 2.2). Uroplakin and GAPDH was expressed in both mucosa and urothelial samples (Figure 2.2). SMMHC and vWF expression was identified in the mucosa samples only (Figure 2.2). Urothelial samples containing SMMHC and vWF was excluded from the experiment.

The presence of vWF and SMMHC in mucosa sample but not in urothelial sample suggest successful urothelial extraction technique. The presence of Claudin 4 and Uroplakin suggest the presence of umbrella cells in extracted urothelial sample. The experiment was repeated 25 times to ensure that variabilities such as diet, age, variation in different pigs had no influence on the expression of AQPs present in pig urinary bladder. Sterile water replaced cDNA template as a negative control. Samples of interest, control samples and negative control samples were run on the same gel

but in different lanes. For the purpose of the thesis, the relevant bands from the different lanes are joined together to illustrate PCR product at the expected size.

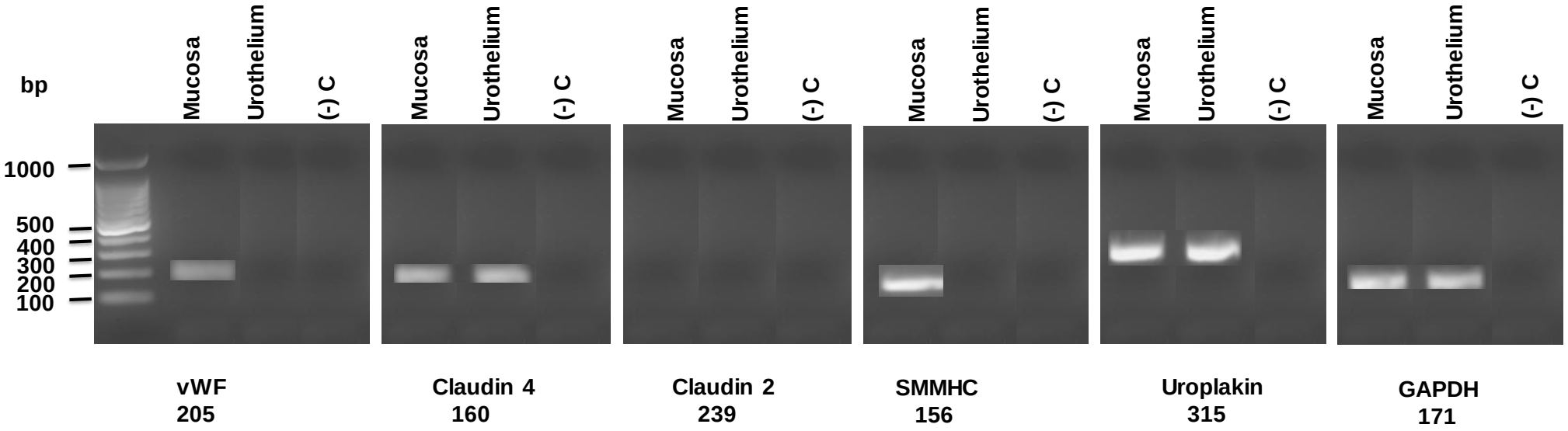

Figure 2.2: Expression of vWF, Claudin-4, Claudin-2, SMMHC, GAPDH and uroplakin mRNA in pig urinary bladder. Expression of vWF Claudin-4, Claudin-2, SMMHC, GAPDH and uroplakin transcripts in a representative pig bladder mucosa and corresponding urothelium found at the expected size. The negative controls is substitution of reverse transcriptase with nuclease-free water in the amplification process. bp= base pair (-) C = negative control, representative image of n=25.

2.4.2 Amplification of AQPs 1, 3, 9 and 11 mRNA in Adult Pig Bladder

RT-PCR demonstrated the expression of AQP1 in the mucosa but not the urothelium of the pig bladder (Figure 2.3). In addition, AQP3, AQP9 and AQP11 were expressed in the mucosa and the urothelium of pig bladder with only a faint band for AQP9 in the mucosa (Figure 2.3). The expression of AQP2, AQP4, AQP5, AQP6, AQP7, AQP8, AQP10 and AQP11 could not be detected in either mucosa or urothelium preparations of the pig bladder (n=3) (Figure 2.3).

RT-PCR demonstrated the expression of all 11 AQP subtypes in different pig tissues (Figure 2.4). This demonstrates that the absence of expression of AQP2, AQP4-8, AQP10, 11 in the pig bladder does not represent a failure of the protocol to amplify any mRNA for these particular AQP subtypes.

Sterile water replaced cDNA template as a negative control. Samples of interest, control samples and negative control samples were run on the same gel but in different lanes. For the purpose of the thesis, the relevant bands from different lanes are joined together to illustrate PCR product at the expected size.

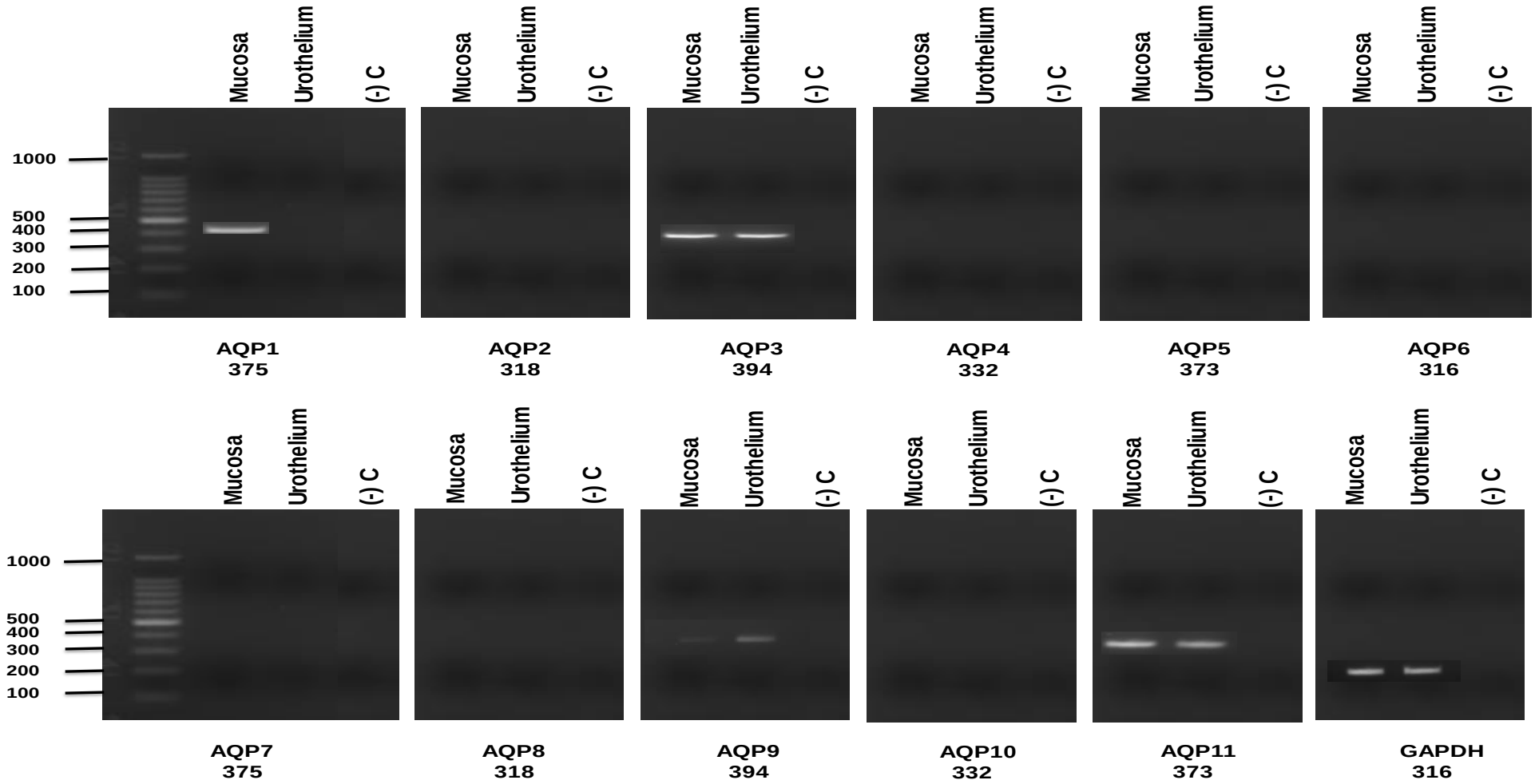

Figure 2.3: AQP mRNA expression of AQPs in pig bladder urothelium and mucosa

Expression of AQP1-11 transcripts in a representative pig bladder mucosa and the corresponding urothelium sample; the red arrow in AQP9 mucosa demonstrate a faint band. The negative controls are where nuclease-free water substituted reverse transcriptase in the amplification process. (representative image of n=25)

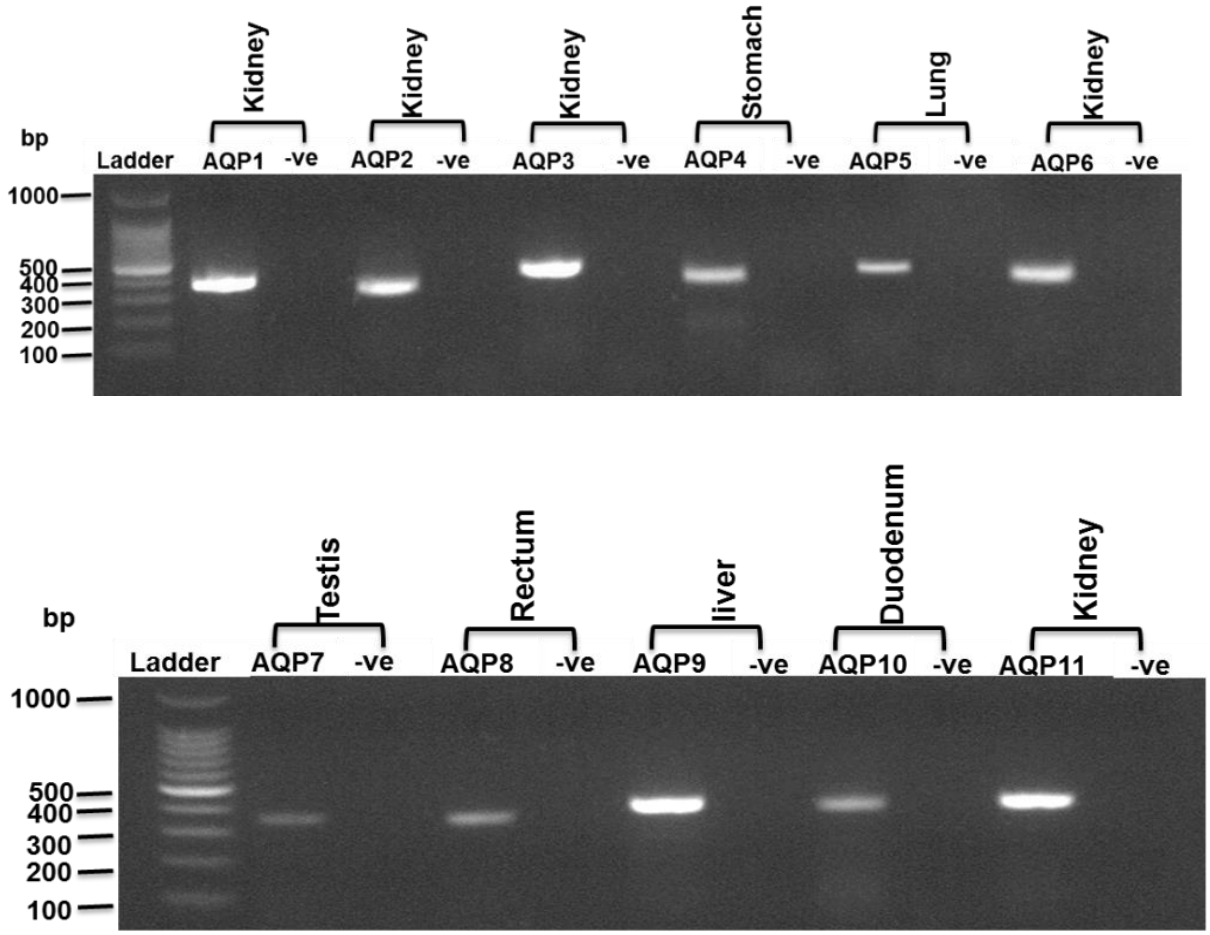

Figure 2.4: AQP transcript expression in positive control tissues
Expression of AQP1-11 transcripts in positive control tissues: pig kidney, stomach, lung, testis, rectum, liver and duodenum. The negative controls are where nuclease-free water substituted reverse transcriptase in the amplification process. bp= base pair (-)C = negative control (representative image of n=3).

2.4.3 Amplification of TRPC4, TRPV4, ER-1 ENaC-α ENaC-β ENaC-γ, Transcripts in Adult Pig Bladder

TRPC4, TRPV4, ER-1 ENaC-α ENaC-β ENaC-γ were investigated to determine their presence in pig bladder as they could serve as potential regulatory channels, receptor for AQP regulation.

RT-PCR demonstrated the expression of TRPV4, ER-1 ENaC-β and ENaC-γ in the mucosa and urothelium of the pig bladder (Figure 2.5). Faint band for TRPC4 was found in the mucosa only and a faint band for ENaC-α was expressed in the urothelium only (Figure 2.5). (n=3). Sterile water replaced cDNA template as a negative control. Samples of interest, control samples and negative control samples were run on the same gel but in different lanes. For the purpose of the thesis, the relevant bands from different lanes are joined together or pasted to illustrate PCR product at the expected size.

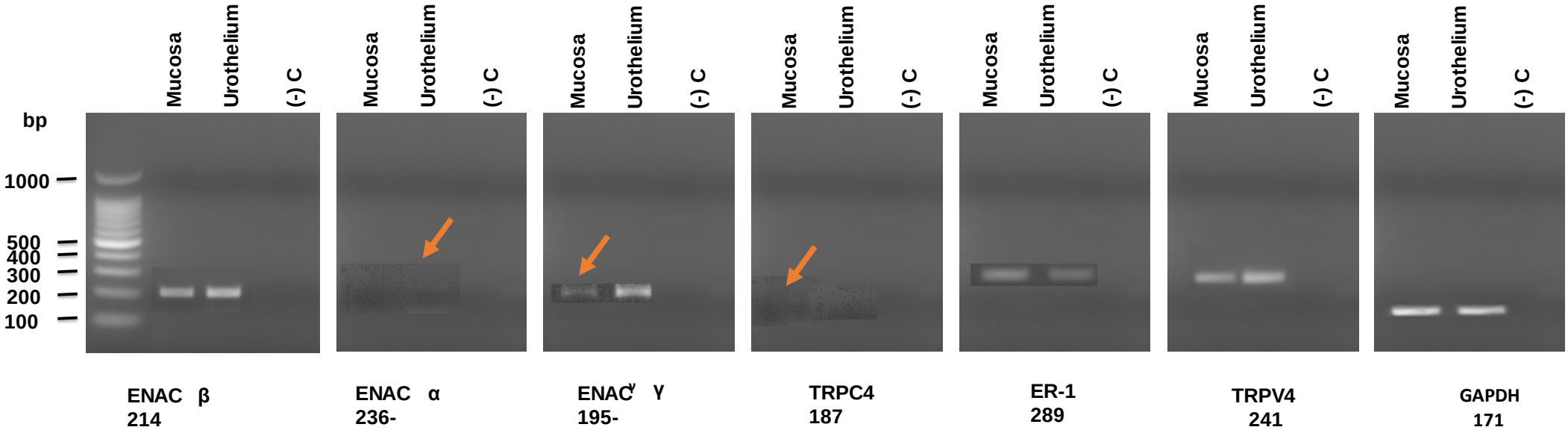

Figure 2.5 Expression of TRPC4, TRPV4, ER-1 ENaC-α ENaC-β ENaC-γ, AG-2R transcripts in pig urinary bladder.

Expression of TRPC4, TRPV4, ER-1 ENaC-α ENaC-β ENaC-γ, AG-2R GAPDH and uroplakin transcripts in a representative pig bladder mucosa and the corresponding urothelium sample. Red arrows demonstrate faint bands. The negative controls are where nuclease-free water substituted reverse transcriptase in the amplification process. bp= base pair (-)C = negative control (representative image of n=3)

2.4.4 Immunihistochemical Detection of AQP1, 3, 9 and 11 protein in Adult Pig Bladder from Tissue Extract

The presence of AQP1, 3, 9 and 11 proteins in adult pig bladder was investigated using Western blotting and antibodies specific for AQP1, 3, 9 and 11. Immunoblotting of AQP proteins showed band for AQP1 in the samples prepared from mucosa layer at expected size around 28 kDa (Figure 2.10), AQP3 was also detected in both mucosa and isolated urothelial extracts at around 28 kDa (Figure 2.10). Additional bands were detected on the immunoblot for AQP3 with protein sizes of around 55 kDa, 65 kDa and 70 kDa which could be phosphorylated forms of AQP3 (Yasui *et al.,* 2008).

A band for AQP9 was found in the urothelial protein extract 35 kDa (Figure 2.10) and AQP11 was also detected in both urothelium and mucosa layer with urothelium at around 40 kDa (Figure 2.10). All the repeats are n=1. Protein quantification was not performed due to the low *n* number. In addition, the purpose of the immunoblot was to determine the size of AQP protein.

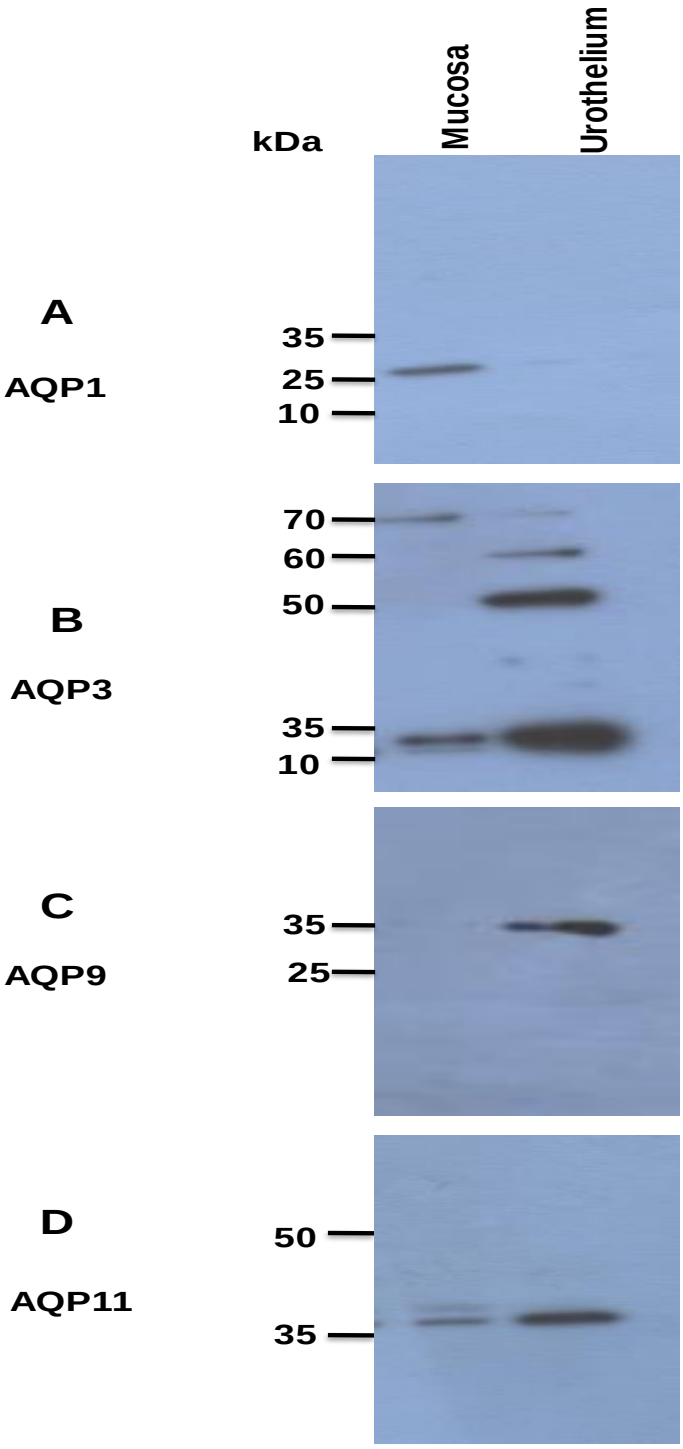

Figure 2.6 Investigation of AQP1, 3, 9, 11 protein in pig urinary bladder mucosa and urothelium.

The presence of AQP1, AQP3, AQP9 and AQP11 protein was detected in pig bladder mucosa and urothelium on immunoblots with anti AQP1, AQP3, AQP9 and AQP11 specific rabbit polyclonal antibodies at 1:200, 1:200, 1:300 and 1:500 dilution repectively. 20µg sample protein was loaded in each well of SDS-polyacrylamide gel. A) AQP1 was detected in the mucosa layer at 28 kDa, B) AQP3 was detected at 28 kDa, in mucosa and urothelium, C) AQP9 was detected around 35 kDa in urothelium only, D) AQP11 was detected at around 40 kDa in pig in mucosa and urothelium. n=1.

2.4.5 Immunoperoxidase Labelling of AQP1, 3, 9 and 11 in Adult Pig Bladder Extracts

AQP1, AQP3, AQP9 and AQP11 expression was detected in different regions of the urothelium and lamina propria in 12 adult pig bladder using immunohistochemistry.

AQP1 immunoreactivity was present in the lamina propria, localised to endothelial cells in capillaries and arterioles (Figure 2.7A). AQP1 negative control using a peptide control (Table 2.2) showed no labelling in the bladder (Figure 2.7B) suggestion that the antibody used is specific in detecting AQP1. Positive control experiments using rat kidney cortex demonstrated localisation of AQP1 to proximal tubules (Figure 2.7C, peptide control, Figure 2.7D).

AQP3 labelling was detected throughout the urothelium (Figure 2.8A, negative control using a peptide control, Figure 2.8B). The positive control experiments in rat kidney medulla demonstrated AQP3 labelling in the collecting tubules (Figure 2.8C, peptide control, Figure 2.8D).

AQP9 labelling was identified in the upper layers of the urothelium which would include umbrella and intermediate cells (Figure 2.9A, peptide control, Figure 2.9B). The positive control experiments using rat liver demonstrated AQP9 labelling in the hepatic lobules (Figure 2.9C, peptide control, Figure 2.9D).

AQP11 labelling was also detected throughout the urothelial layer (Figure 2.10A, peptide control, Figure 2.10B). A positive control shows labelling in rat kidney cortex (Figure 2.10C, peptide control, Figure 2.10D).

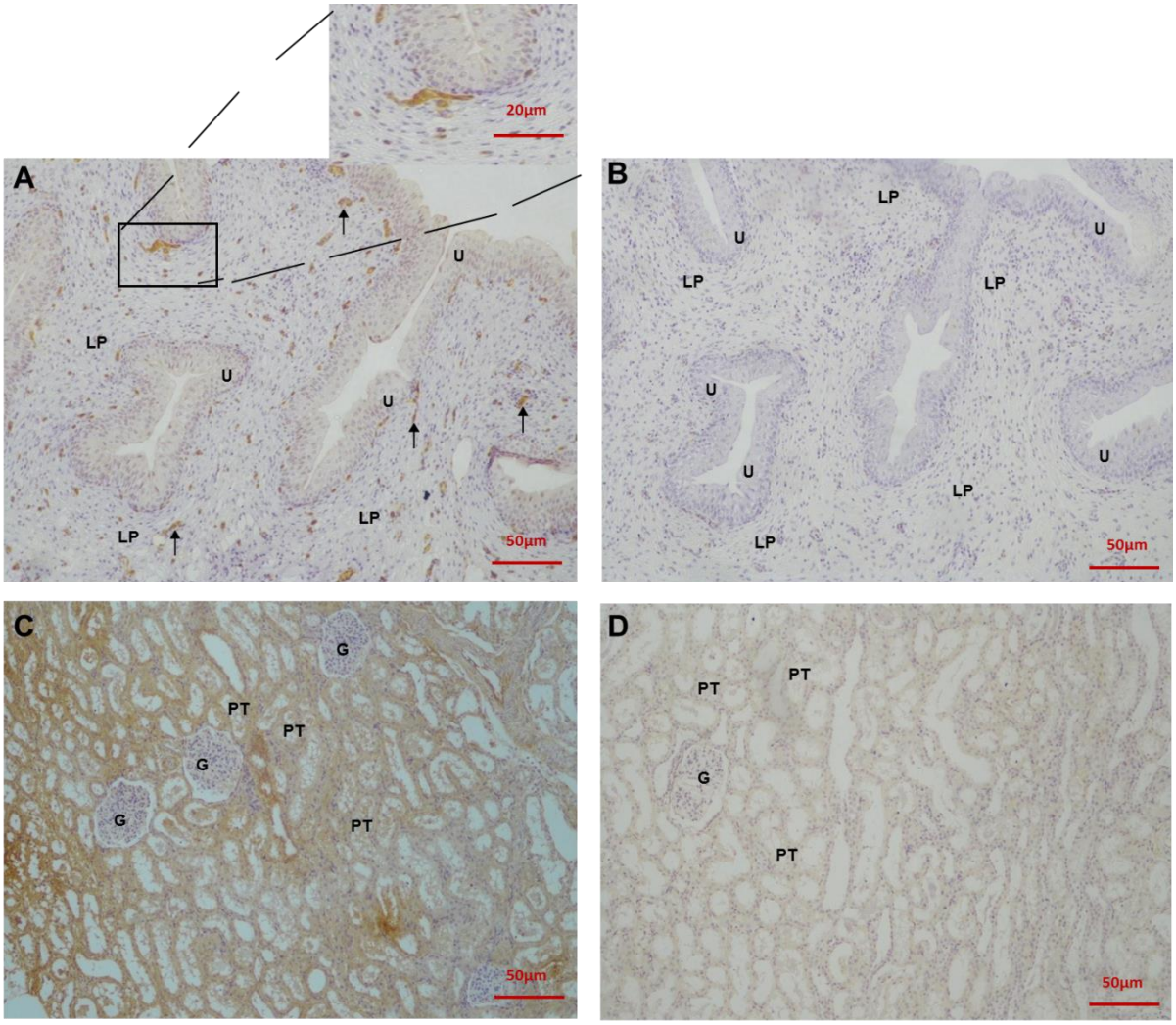

Figure 2.7 Immunoperoxidase labelling of AQP1 in pig bladder and positive control tissue, **rat kidney.**

Rabbit polyclonal anti-AQP1 antibody was used at a dilution of 1:1000 to detect AQP1 in pig mucosa tissue section. **A:** bladder mucosa with AQP1 immunoreactivity in the lamina propria. The inset shows a small blood vessel immediately below the urothelium at a larger magnification. **B:** mucosa, peptide negative control. **C**: AQP1 immunoreactivity in rat kidney; apical and basolateral membranes of cells of the proximal tubule and descending thin limb. **D:** rat kidney, peptide negative control. U, urothelium; LP, lamina propria; G, glomerulus, PT, proximal tubule. Bladder mucosa, representative image of n=12; kidney, representative image of n=3.

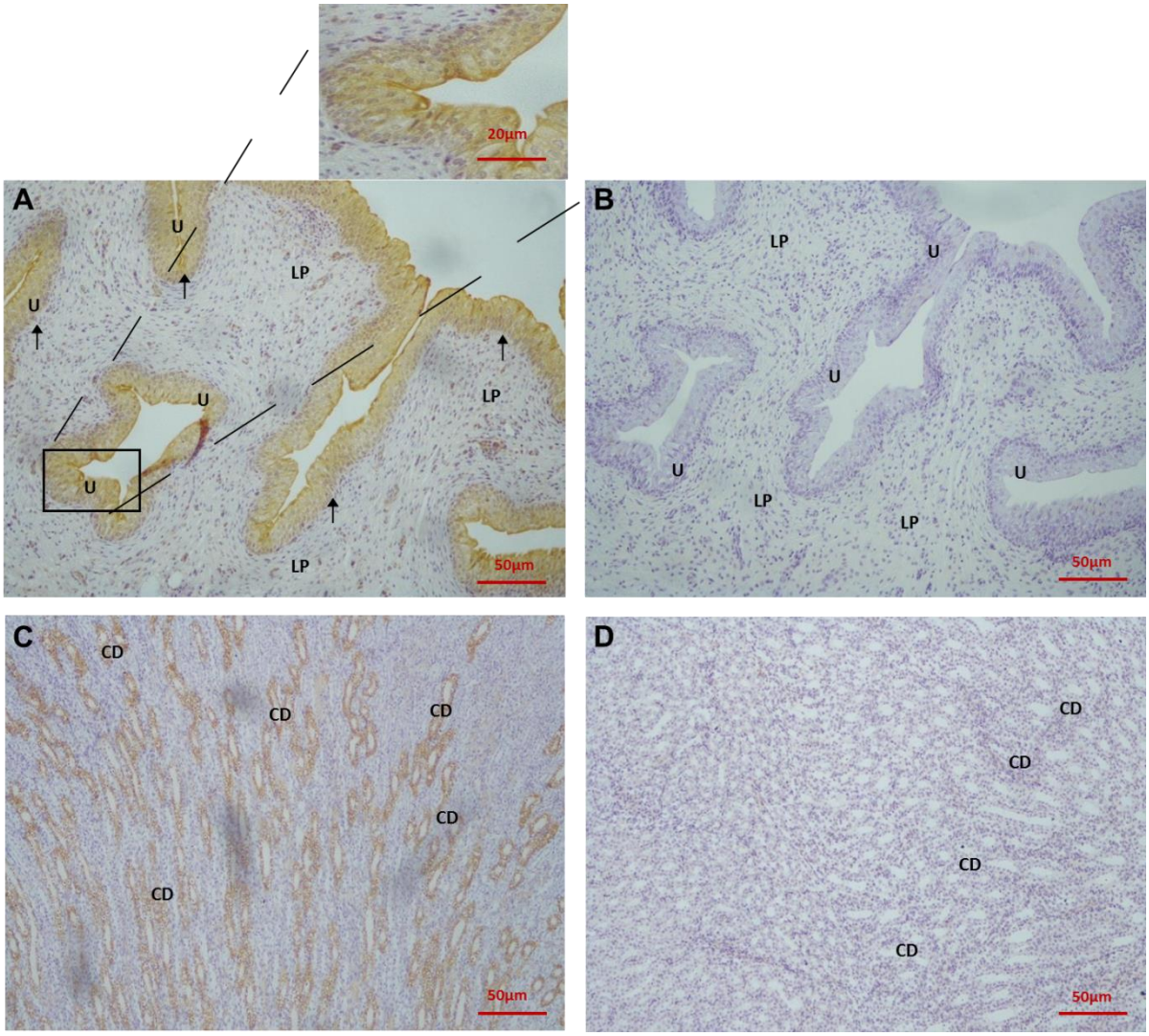

Figure 2.8 Immunoperoxidase labelling of AQP3 in pig bladder and positive control tissue, rat kidney medulla.

Rabbit polyclonal anti-AQP3 antibody was used at a dilution of 1:1000 to detect AQP3 in pig mucosa strip. **A:** bladder mucosa with AQP3 immunoreactivity in the urothelium, the inset shows the urothelium at a larger magnification. **B**: mucosa, peptide negative control. **C**: AQP3 labelling in rat kidney medulla; collecting duct cells; **D**: rat kidney, peptide control**.** U, urothelium; LP, lamina propria; G, glomerulus, CD, collecting duct. Bladder mucosa, representative image of n=12; kidney, representative image of n=3.

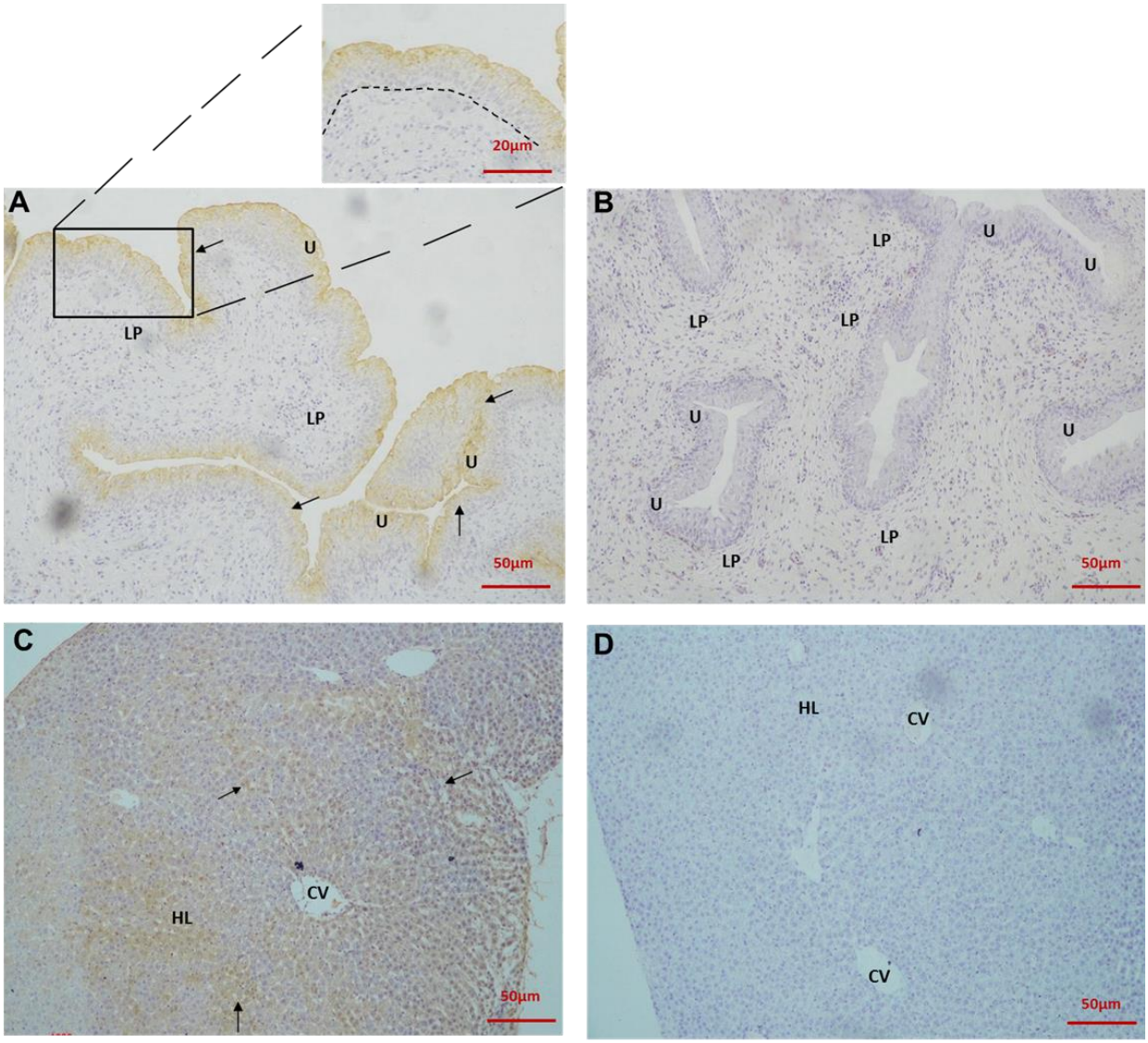

Figure 2.9 Immunoperoxidase labelling of AQP9 in pig bladder and positive control tissue, rat liver

Rabbit polyclonal anti-AQP9 antibody was used at a dilution of 1:1000 to detect AQP9 in pig mucosa strip. **A**: bladder mucosa with AQP9 immunoreactivity in the urothelium. The inset shows the urothelium at a larger magnification. The dotted line demonstrates the boundary between the urothelium and the suburothelium region. **B:** mucosa, peptide control. **C**: AQP9 labelling in rat liver; perivascular hepatocytes, **D**: rat liver, peptide negative control. U, urothelium; LP, lamina propria; CV, central vein; HL, hepatic lobule. Bladder mucosa, representative image of n=12; kidney, representative image of n=3.

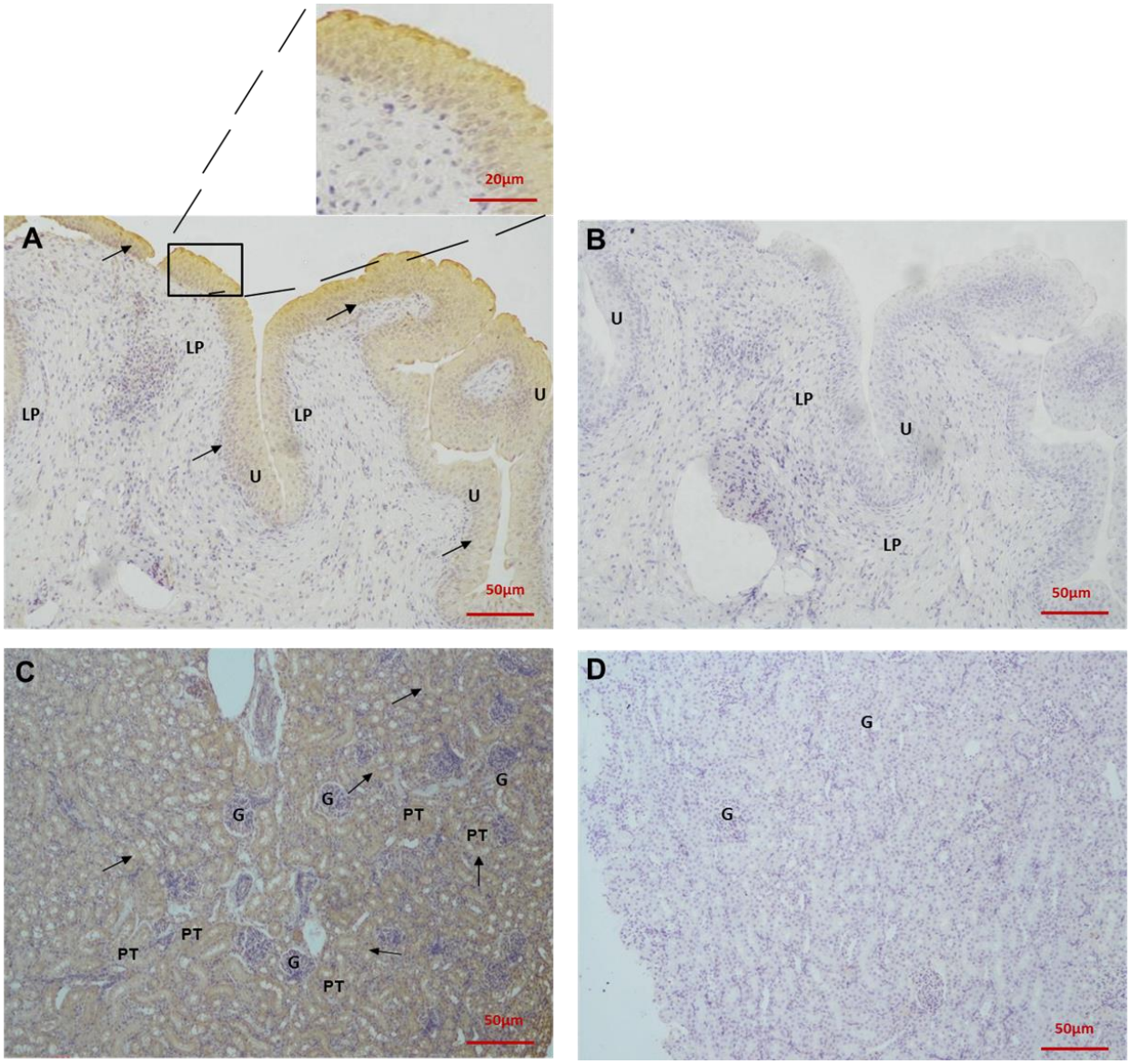

Figure 2.10 Immunoperoxidase labelling of AQP11 in pig bladder and positive control tissue, rat kidney

Rabbit polyclonal anti-AQP11 antibody was used at a dilution of 1:1500 to detect AQP11 in pig mucosa strip. **A:** bladder mucosa with AQP11 immunoreactivity in the urothelium. The inset shows the urothelium at a larger magnification. **B:** mucosa, peptide control. **C:** AQP11 labelling in rat kidney medulla intracellularly in the proximal tubule. **D:** rat kidney, peptide negative control. U, urothelium; LP, lamina proria; G, glomerulus, PT, proximal tubule. Bladder mucosa, representative image of n=12; kidney, representative image of n=3.

2.5 Discussion

2.5.1 Expression of AQPs in the Urinary Bladder

The main aim of this study was to determine the expression profile of AQPs in the adult pig bladder whether it can be used as a model to describe human bladder function. mRNA expression and protein production of AQP1, AQP3, AQP9 and AQP11 were observed in the urothelial and suburothelial layers of pig bladder. However, AQP4, AQP7 which are reported to be expressed in human (Rubenwulf *et al.,* 2009) and AQP2, AQP5, AQP6, AQP8 and AQP10 were not detected.

AQP1 was confined to lamina propria blood vessels and not to the urothelium (Fig 2.3 & 2.7) as observed in rat bladder and ureter (Spector *et al.,* 2002). The functional role of AQP1 in proximal tubular and the descending limb of the loop of Henlé epithelium is to mediate water fluxes (Boassa *et al.,* 2006). AQP1 is also found in blood vessels of many tissues, where it may also gate K^+ channel activity (Boassa *et al.,* 2006). AQP1 multifunctional channel suggests it is a potential therapeutic target for pathological conditions involving altered fluid homeostasis as well as in mice airways and lungs where it facilitates osmotic water transport across alveolar microvascular endothelium (Verkman, 2002). However, AQP1 knockout in transgenic mice had no impact on alveolar fluid absorption, impaired humidification or lung CO_2 transport (Song *et al.,* 2001; Yang *et al.,* 2000; Fang *et al.,* 2002). Similarly, deletion of AQP1 in the microvascular endothelial cells of salivary gland in mice had no effect on the secretion of saliva (Ma *et al.,* 1999). It appears that AQP1 has limited physiological function in fluid movement in the endothelium, but its functional role in the microvasculature of the bladder mucosa is unknown. AQP2, the subtype responsible for AVP mediated water fluxes of the distal tubule and collecting duct of the nephron

in human was absent in pig bladder mucosa. Whiles AQP2 has been identified in rat bladder (Spector *et al.,* 2009), similar to this study AQP2 is absent in human bladder.

AQP3 was expressed in the urothelium of pig urinary bladder, consistent with data from human and rat bladder urothelium (Spector *et al.,* 2002; Rubenwolf *et al.,* 2009). Rubenwolf *et al*. (2009) also reported that AQP3 was located especially at the intercellular borders of basal and intermediate cells, but in the pig bladder it was demonstrated that distribution was homogeneous throughout the urothelium (Fig 2.3 & 2.8). AQP3 transports several neutrally-charged solutes, including water, glycerol, urea and H_2O_2 (Hara-Chikuma *et al.,* 2015). Distribution of AQP3 on both apical and basolateral membranes of bladder urothelium suggests bidirectional movement of water and solutes. AQP3 expression is responsive to changes of local osmolality (Spector *et al.,* 2002). Exposure of human urothelial cells to hyperosmolar NaCl (500 mosm/kg) solutions increased AQP3 expression, as well as increased water fluxes (Rubenwulf *et al.,* 2012). These suggest that AQP3 expression and translocation to the plasma membrane is part of a mechanism to regulate urothelial cell osmolarity and volume during increased osmotic stress as caused by exposure to urine of variable osmolality. AQP3 is a member of the aquaglyceroporin family and thus also transports urea and other solutes (Litman *et al.,* 2009). Based on the similarities in the function of AQP3 and urea transporter B, which has also been found in the urothelium (Timmer *et al.,* 2001; Yang *et al.,* 2002; Dong *et al.,* 2013), it may be postulated that AQP3 also facilitates the transfer of urea across the bladder urothelium.

AQP9 was detected more on the apical surface of the pig urothelium, i.e. umbrella and intermediate cells (Fig 2.3 & 2.9). Basal cells differentiate into intermediate and umbrella cells (Papafotiou *et al.,* 2016) and other studies have shown that AQP9

expression is also evident in differentiated keratinocytes (Sugiyama *et al*., 2001), freshly isolated urothelium and differentiated urothelial cultures (seen as urothelial cells expressing ZO-1 and Claudin-4 to tight junction complex) (Rubenwolf *et al.,* 2009), whereas AQP3 is localised in both differentiated and proliferating urothelial cells (Rubenwolf *et al.,* 2009). These data including this current study suggest that whiles AQP3 expression is required throughout the different cell types of the urothelial cells, AQP9 expression is mostly seen in differentiated cells (umbrella cells) located in the lumen of the bladder where it may serve to be important for modifying urine. AQP9 also belongs to the aquaglyceroporin family and is involved in glycerol influx and urea efflux during increased liver gluconeogenesis (Carbrey *et al.,* 2003). A 3D-structural analysis of APQ9 showed a larger pore size compared to other AQPs and can explain its ability to transport larger molecules such as lactate, purines and pyrimidines (Tsukaguchi *et al.,* 1998; Viadiu *et al.,* 2007). Thus, AQP9 could modify the final composition of urine by facilitating transport of various solutes across the bladder urothelium.

AQP11 was identified throughout the urothelium (Fig 2.3 & 2.10) and its expression has been reported in different mammalian tissues including: rat testis, mouse brain and kidney (Yeung *et al.,* 2010; Koike *et al.,* 2016). AQP11 is mainly present in the endoplasmic reticulum and only a fraction migrates to the cell membrane to facilitate glycerol and water transport (Morishita *et al.,* 2005; Madeira *et al.,* 2014; Ikeda *et al.,* 2011). AQP11 expression has also been shown in human adipocytes where it functions as a water and glycerol channel (Madeira *et al.,* 2014). Thus, AQP11 may act as a water and glycerol transporter in bladder urothelium under osmotic stress.

2.5.2 Potential Regulatory Mechanism Mediating AQP Expression and Function in Bladder Urothelium

2.5.2.1 Expression of TRP Channels in Pig Urinary Bladder

Various studies have demonstrated that the expression/ function/ translocation of AQPs in different cell types is dependent on an increase in intracellular calcium levels (Benfenati *et al.,* 2011; Jo *et al.,* 2015). This increase in intracellular Ca^{2+} levels seems to be dependent on activation of various Ca^{2+} channels expressed in the cell membrane rather than elevation of intracellular calcium levels. One of the key families of ion channels responsible for mediating the flux of Ca^{2+} from extracellular space to the intracellular space in response to osmotic/ chemical or mechanical stresses are the TRP channels

TRPV4 mRNA expression was found in both mucosa and urothelium whilst TRPC4 expression was limited to the mucosa (Fig 2.5). Previous studies have demonstrated that different subtypes of TRP channels such as TRPV1, TRPV2, TRPV4, TRM4, TRPM8 and TRPA1, are expressed in the urinary bladder of rats, pigs and humans (Vahabi *et al.,* 2013; Anderson, 2019) in the urothelial cells similar to this current study. TRPC4 was found to be expressed in the submucosa.TRPC4 have also been identified in the vascular endothelial cells (Kim *et al.,* 2012).Therefore the identification of TRPC4 could suggest that in pig bladder, TRPC4 is also expressed in vascular endothelial cells.

Currently, no studies have reported an interaction between TRP channels and AQPs in the urinary bladder, however, a few studies have reported an interaction between TRP channels and AQPs in different tissues and cell lines (Benfenati *et al.,* 2011; Jo *et al.,* 2015; Conner *et al.,* 2012). TRPC1, also part of the canonical family as TRPC4

is shown to regulate AQP1 translocation to the plasma membrane in rat astrocytes (Conner *et al.,* 2012) therefore the identification of AQP1 in blood vessels capillaries and endothelial cells in the suburothelial and the expression of TRPC4 in the lamina propria could suggest that TRPC1 is involved in regulating AQP1 translocation.

The presence of different types of TRP channels detected in pig urinary bladder in this study in addition to the clear association of TRP channels in various subtypes of AQP regulation suggest that TRP cahnnels could also regulate AQP channels in pig urinary bladder. These channels could be further explored as part of future work in AQP regulation in the bladder.

2.5.2.2 Expression of ER-1 in Pig Urinary Bladder

In this study, the expression of ER-1 was detected in the mucosa and the urothelium of the female pig bladders (Figure 2.5). The association between oestrogen receptors and AQPs, in particular AQP1, AQP3, and AQP9 have been characterised extensively in other tissues (Jablonski *et al.,* 2003; Kim *et al.,* 2010; Oliveira *et al.,* 2005). Oestrogen receptor response element has been identified in the promoter region of AQP3 gene and oestrogen has been demonstrated to directly upregulate AQP3 expression by activating oestrogen response element found within AQP3 gene (Huang *et al.,* 2015). In rat efferent ductile epithelium and the initial segment of the epididymis, oestrogen and 5α- dihydrotestosterone were found to upregulate AQP9 expression (Oliveira *et al.,* 2005). Similarly, an increase water permeability was observed in mouse uterus (expressing AQP2 and AQP3) treated with oestrogen (Jablonski *et al.,* 2003). These studies collectively demonstrate that changes in estrogen levels impact AQP expression and function. In the current study, female pig bladder were used throughout the experiment and transcripts for ER-1 was identified in the urinary

bladder. ER receptors are also found in human bladder (Losif *et al.,* 1981), since estrogen is shown to upregulate AQPs expression, the identification of ER in pig bladder could suggest a potential mechanism for estrogen mediated up and down regulation of AQP expression depending on the reproductive cycle of the pig. Further studies to investigate the protein levels, localisation and interaction of ER-1 with AQPs in bladder urothelium are required.

2.5.2.3 Expression of ENaC in Pig Urinary Bladder

ENaCs are major regulatory channels of Na^+ and water reabsorption (Butterworth, 2010) and paracellular transport of water across cell membrane in response to Na^+ transport has been established (Tripathi and Boulpaep, 1989). In some cell types, constitutive expression of AQPs in the plasma membrane has been reported and thus we hypothesised that in addition to paracellular movement of water in response to Na^+ transport, transcellular water transport facilitated by constitutively expressed AQPs can occur in the event of increase in Na^+ transport. Therefore the expression of the different subtypes of ENaC channels in the urinary bladder was explored

Three homologous ENaC subunits were identified in the pig urinary bladder. ENaC β and ENaC γ were identified in the mucosa and urothelium whilst ENaC α subunit was only found in the urothelium (Figure 2.5).

In a study investigating the distribution of electrolytes and water transport pathways in human cortical distal nephron, AQP3 and AQP2 were found to be co-localized with ENaCs within the same cells of the cortical collecting duct (Biner *et al.,* 2002) suggesting a possible direct or indirect interaction between AQP2 AQP3 and ENaC channels. In mammalian urinary bladder, ENaC isoforms (α-, β-, and γ-ENaC) are also present in the apical plasma membrane and function as trans-epithelial sodium

reabsorption channels (Smith *et al.,* 1998). Stretch of the bladder in response to increasing urinary volume or aldosterone levels caused an increase in the number of ENaCs in the apical membrane of rabbit urinary bladder urothelium (Smith *et al.,* 1998). Rabbit bladder urothelium has the ability to reabsorption up to ~80 µmol/h of Na^+, indicating that the urothelium is involved in modifying the final concentration of urine (Smith *et al.,* 1998). Currently, no studies have reported the involvement of ENaC in AQPs function or expression. However, ENaC could indirectly influence AQPs' function via the reabsorption of Na^+ to regulate urothelial cell volume. This assumption is in line with studies by Rubenwolf *et al.* (2012), where they demonstrated that an increase in the osmolarity of tissue culture medium achieved through increasing the concentration of NaCl up to 500 mosm/kg caused an increase in AQP3 expression (Rubenwulf *et al.,* 2012).The general principle of Na^+ reabsorption is the movement of water alongside Na^+. Therefore, an increase in Na^+ reabsorption will cause changes in extracellular and intracellular osmolarity. These changes could initiate water reabsorption mediated by active transport through AQP channels or passive diffusion to regulate osmolarity.

2.5.3 Control Experiments Implemented in this Study

In this study, it was important to determine the expression profile of AQPs in both the urothelial and suburothelial layers as AQPs localisation in the different layers of the bladder wall could help detemine their physiological role in water homeostasis. Therefore, in order to ensure that both urothelial and mucosa samples obtained from the pig bladder were not contaminated with cells from other layers of the bladder wall, various markers such as vWF and SMMHC were used ensure that the urothelial samples did not have any cross contamination from the suburothelial layer. SMMHC

are smooth muscle cells specific markers (Lu *et al.,* 2011; Sadegh *et al.,* 2012). SMMHC expression was seen in the mucosa only in this study (Fig 2.5). The expression of SMMHC in mucosa was expected as mucosa contains muscularis mucosa which are smooth muscle cells. Urothelial samples containing SMMHC bands were excluded from the experiment. vWF is an endothelial specific marker (Zanetta *et al.,* 2000) was used as a control to check the urothelial samples for cross contamination with vascular endothelial cells. vWF was identified in the mucosa but not the urothelium samples as the mucosa contains a rich network of capillaries and arterioles (Fig 2.5). Urothelial samples positive for vWF were excluded from all the experiments.

Also, to ensure that the urothelial and mucosa samples extracted contained all the different cell layers in particular the umbrella cells as these are known to easily dissociate with minimum shear stress (Carattino *et al.,* 2013), which could have happened during transport of the bladder, the expression of terminally differentiating urothelial markers such as Claudin-2 and Caludin-4, uroplakin (Smith *et al.,* 2015) were investigated in all samples. Uroplakin, Claudin-2, Claudin-4 mRNA was detected in the bladder urothelium and mucosa (as the mucosa also contains the urothelial layer), demonstrating that all layers of the bladder urothelium were indeed present in the samples and were not dissociated during the dissection technique.

These controlled experiments before each experiment demonstrated that no cross contamination was introduced to the different samples. Moreover, they confirm that the isolated cell extract were indeed of urothelial and mucosa cells. Therefore the data generated was reliable.

2.6 Summary

Four different AQP mRNA's (AQP1, AQP3, AQP9, and AQP11) were detected in adult pig bladder, suggesting that AQPs may regulate urothelium cell volume and also determine the final urine composition. Changes to the extracellular osmolality of urothelium cells may also generate membrane stress, and release various transmitters from the bladder urothelium that affect bladder contractility and sensory nerve transduction. However, the exact role of AQPs in mediating the sensory and contractile functions of the bladder wall, and the mechanisms by which their expression and function in the bladder is regulated is unknown.TRPC4, TRPV4, ER-1 and ENaC transcript was detected in pig urinary bladder. These proteins have previously been shown to be directly or indirectly involved in regulating AQP expression and function in other tissue types. Therefore, they may also be important in modulating AQP function in the urinary bladder. The exact role of AQPs in mediating the sensory and contractile functions of the bladder wall, and the mechanisms by which their expression and function in the bladder is regulated is unclear and remains to be elucidated.

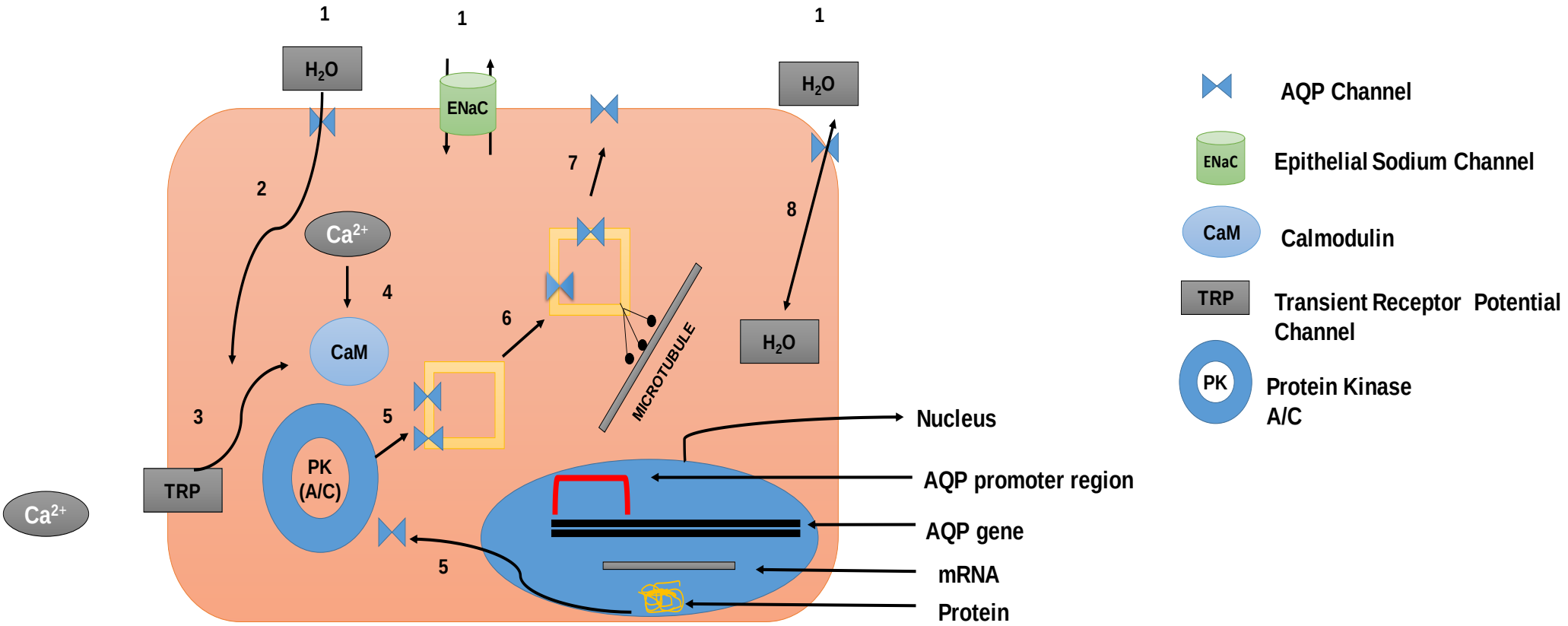

Figure 2.11 A proposed model for the regulation of rapid cellular water flow.

Regulation of osmolarity through influx of AQP channels in conjunction with solute channels such as ENaC. **1)** Continue adjustment of intracellular osmolarity in response to small changes in extracellular environment is achieved through transcellular influx of solutes such as sodium through ENaC and water through constitutively expressed AQP channels. **2)** In the event of rapid osmotic changes caused by influx of water through AQP channels leading to cell swelling, **3)** TRP channels are activated to allow extracellular calcium entry and as a result triggers additional AQPs translocation to the plasma membrane **4, 5, 6, 7).** The translocation to the plasma membrane is believed to be along microtubules which is dependent on the activation of calmodulin (CaM) followed by AQP protein phosphorylation and insertion in the cell membrane. To increase the amount of plasma membrane AQPs, **5)** AQP synthesis is initiated in response to prolonged extracellular osmotic challenges (such as trauma) or hormonal changes such as oestrogen leading to the activation of oestrogen response element, for example in the promoter region of AQP3. The increased amount of AQPs in the cell membrane facilitate water entry or exit from the cell to maintain cellular homeostasis **8)**. Adapted from Conner *et al.,* 2012.

Chapter 3

Measurement of D_2O Fluxes Across Pig Urinary Bladder Mucosa

3.1 Introduction

The tightness of the urothelial barrier is important for a healthy bladder function as disruption of this barrier has been associated with various urothelial bladder disorders such as interstitial cystitis and bladder pain syndrome (Parsons, 2010; Jiang and Kuo., 2017). Various techniques such as real time transepithelial electrical resistance (TEER) measurement with microinjection of fluorescently-labelled molecules imaged with epifluorescent microscope (Hill *et al.,* 2017), impedance spectroscopy and conductance scanning (Krug *et al.,* 2009) TEER measurement with epithelial volt ohm meter chop-stick electrodes the TEER (Srinivasan *et al.,* 2015) or the Ussing chamber technique (Li *et al.,* 2004) have been used in the laboratory to study the barrier function of various tissues (Li *et al.,* 2004; Clark,2009). Out of these various techniques, the Ussing chamber system is frequently used in measuring TEER of many epithelial tissues. The Ussing chamber system is widely used to measure paracellular and transcellular movement of ions across tissues, including intestinal transport during the processes of homeostasis, damage (Li *et al.,* 2004; Clark, 2009) and restitution (Riegler *et al.,* 2000).

3.1.1 History of the Ussing Chamber

The Ussing chamber was originally designed around 1950 by Hans Ussing to measure the short-circuit current as an indicator of net ion transport across frog skin (Ussing and Zerahn, 1951). Prior to the development of the Ussing chamber, Na^+ transport influx across the frog skin was established to be higher than the efflux of Na^+ using double labelling with Na^+ isotopes (Levi and Ussing, 1949). The Ussing chamber allowed the first investigation of ion (Na^+) transport physiology of an epithelium.

Ussing chamber uses a biological membrane, across which salts and water are transported, to separate two chambers containing test solutions (Li *et al.,* 2004). If the composition and volume of solutions in the two chambers is identical paracellular movements would be minimised if the electrical potential gradient across the membrane was also set to zero by an external voltage-clamp. (Clarke *et al.,* 2009). .

This external current is termed the short-circuit current (I_{sc}). Therefore, by eliminating transepithelial diffusion forces (osmotic and electrochemical gradients), the movement of ions as measured by isotopic tracers or the I_{sc} in the Ussing chamber is due to active transport (Clarke *et al.,* 2009).

The Ussing chamber method also enables continuous validation of the integrity and viability of the tissue or cells by measuring electrophysiological parameters such as transepithelial electrical resistance (R), transmembrane potential difference (V_{te}) and short circuit current (I_{sc}) using the following equation (Li *et al.,* 2004):

Equation 3.1

$$R_{te} = \left(\frac{V_{te}}{I_{sc}} \right)$$

3.1.2 Ussing Chamber Experiments in the Urinary Bladder

The Ussing chamber system has been used to characterise the transport properties of bladder urothelium in different species (Miyake *et al.,* 2013; Mani *et al.,* 2013; Burshtein *et al.,* 2013; Arnold *et al.,* 2019). With rabbit urinary bladder, the Ussing

chamber was used to measure water, urea, ammonia and H^+ permeability of the urothelium (Negrete *et al*., 1996).

A study investigated the effects of cAMP on epithelial Na^+ channel activity in rabbit bladder by measuring the amiloride-sensitive short-circuit current across bladders mounted in Ussing chambers (Burton *et al.,* 2000). In this study, they discovered that cAMP stimulates the insertion of new Na^+ channels into the apical membrane of the rabbit bladder urothelium.

Ussing chamber has also been a valuable technique in measuring water transport across the urinary bladder urothelium using urothelial cells established on permeable Snapwell™ to measure radioisotopic flux of [^{3}H] water (Rubenwulf *et al.,* 2012). Rubenwolf *et al.* (2012) have previously looked at AQPs responsiveness to changes in osmolarity using *in vitro*-differentiated normal human urothelial cell culture systems in hemi-chambers (Rubenwulf *et al.,* (2012). In their study, they demonstrated that changes in osmolarity in particular increase in NaCI causes increase water and urea movement across the urinary bladder. AQP blockade with $HgCl_2$ resulted in decreased water and urea flux. No other study have reported the use of Ussing chamber in the study of urinary bladder since however, these studies previous collectively demonstrate that Ussing chamber is a powerful tool to investigate urinary bladder urothelium.

3.1.3 The use of D_2O in Measuring Transurothelial Water Movement

D_2O (heavy water) is used as a moderator in nuclear reactors. Its biological effects have both “solvent isotope effects,” those due to the special properties of D_2O as a solvent, and “deuterium isotope effects” (DIE), which result when D replaces H in many biological molecules have been studied extensively (Kushner *et al.,* 1999). D_2O has a low toxicity toward mammals and therefore widely used in research for measuring water movement in humans and animals.

Since H_2O is thought to interact with specific amino acid residues Phe-56 and Agr-195 in AQP pore via hydrogen bonding (Mamonov *et al.,* 2007;Miloshevsky and Jordan, 2004) to allow H_2O to be transported across membranes, D_2O which has similar properties as H_2O, might interact with AQPs in a similar way (Mamonov *et al.,* 2007).

Previously, D_2O permeability through AQPs such AQP1 has been studied to determine whether AQP1 selectivity to water is limited to H_2O only and not other heavier water such as D_2O. It was demonstrated that D_2O permeability through AQP1 is similar to that of H_2O (Mamonov *et al.,* 2007). Therefore, D_2O was used as a maker to determine water movement in this study

3.1.4 Potential AQP Inhibitors

A number of ions and molecules have been tested as AQP inhibitors (Jeyaseelan *et al.,* 2006). However, the existing compounds are non-specific and can block numerous transporters, channels and enzymes. Therefore they cannot be considered as specific inhibitors of AQP channels and the effect on water movement is secondary to altered ion transport. Heavy metal compounds such as gold and silver or mercury chloride were the first to be identified as non-selective AQPs inhibitors (Savage and Stroud 2007).

$HgCl_2$ was used in this current Ussing chamber experiment as it is commonly used to inhibit AQP channels in a variety of tissues and cells. $HgCl_2$ has previously been demonstrated to reduce water transport in the red blood cell membrane by inhibiting AQP channels (Preston *et al.,* 1993). This selective inhibition subsequently allowed for aquaporin isolation, cloning, membrane transport characterization, and mercury sensitivity mutational analysis (Savage and Stroud 2007). The purpose of this study was to determine the role of AQPs in mediating water flux across the bladder urothelium, therefore, the effect of $HgCl_2$, specific AQP inhibitor on D_2O movement across the pig bladder urothelium was assessed. (Preston *et al.,* 1993; Rubenwulf *et al.,* 2012)

The need for an effective and specific AQP inhibitor is important in studying the functional role of AQP channels in mediating water and solute transport. In addition to this, AQP specific inhibitors are important as AQPs have been implicated in a variety of diseases such as nephrogenic diabetes insipidus and polycystic kidneys (Morishita., 2005; Loonen *et al.,* 2008) including disorders in the urinary bladder urothelium such as bladder outlet obstruction (BOO) (Kim *et al.,* 2010).

3.2 Aims of the Study

Little is known about the functionality of AQPs in the urinary bladder. The aim of this study was to investigate the potential role of AQPs in mediating water transport across pig bladder urothelium in response to osmotic stress

3.2.1 Objectives of the D_2O flux experiments were:

- To determine the rate of water (D_2O) flux from apical to basolateral chambers across pig bladder mucosa strip
- To determine is the rate of water flux was dependent on the transmembrane osmotic gradient
- To determine if the rate of water flux was dependent on functional aquaporin channels - this was done by using the non-selective aquaporin inhibitor 300 µM $HgCl_2$
- To determine if the rate of water flux was dependent different osmotic gradient - this was done by exposing the basolateral and apical side of the tissue to different osmotic solutions containing D_2O on the apical side in the presence of $HgCl_2$.

3.3 METHODS

3.3.1 Tissue Preparation for Ussing Chamber Experiments

Female pig (*Sus scrofa domestica*) bladders were obtained from a local abattoir. Whole bladders were placed in PBS for transportation on ice. From each bladder, two paired strips of circular orientated mucosa were dissected from the bladder dome at room temperature using dissection forceps and fine-tip pointed stainless steel scissors with curved blades. One mucosal strip was used for control experiments and the other one was used to investigate the effect of $HgCl_2$ on movement of D_2O.

The paired tissue sections were immediately stretched and mounted on a 14.6 mm by 5.0 mm rectangular chamber and secured by six fine needles located at the edges of the chamber. Chambers containing tissue sections were placed in an Ussing chamber system. Twelve pairs of mucosal strips from twelve different bladders were used for Ussing chamber experiments.

3.3.2 The Structure of an Ussing Chamber System

An Ussing chamber supports an epithelial membrane in such a way that each side of the membrane is isolated and faces a separate chamber-half (Figure 3.1). The Ussing chamber system used in this study was made from a solid acrylic block cut into cylindrical halves. Each half consisted of a hollow chamber open at one end, so that when the two halves were brought together a single chamber was formed. A parafilm O-ring fitted into a groove at the open end of each half-chamber to ensure a watertight seal. When an experimental tissue preparation was stretched across the hole the only connection between the two chambers was via the preparation itself (Figure 3.1). Each

half of the chamber had several ports: for connection to a water-jacketed circulation system; for introduction and drainage of superfusing solution; and for making electrical connections to the system. Ports to measure transmembrane potential were closest to the tissue while ports for current injection electrodes were furthest from the tissue (Figure 3.1). Electrical connections were made with Ag-AgCl pellet electrodes that fitted into the ports. The electrodes were connected to a high input impedance amplifier to record the potential difference and pass current. The voltage and current electrodes made contact with the superfusing solution via 2% agar bridges filled with 3 M KCl through Luer ports. The remaining ports allowed superfusing fluid to make contact with the two faces of the epithelial membrane preparation.

The face of one chamber-half was imbedded with sharp stainless-steel pins which mated with corresponding holes in the other chamber-half face. These pins puncture the preparation to hold it in place across the hole (radius 5 mm) in each half-chamber. A modified Krebs solution (Table 3.2) superfused the tissue from reservoirs on each side of the chamber. Each horizontal reservoir arm had an inlet and outlet port for access to the water jacket. Water at the desired temperature was pumped through a jacket from a water bath (37ºC). Each reservoir had a separate air/gas inlet to drive the circulation system, in these experiments 95% O_2/5% CO_2 was used to maintain a constant pH of 7.40±0.05.

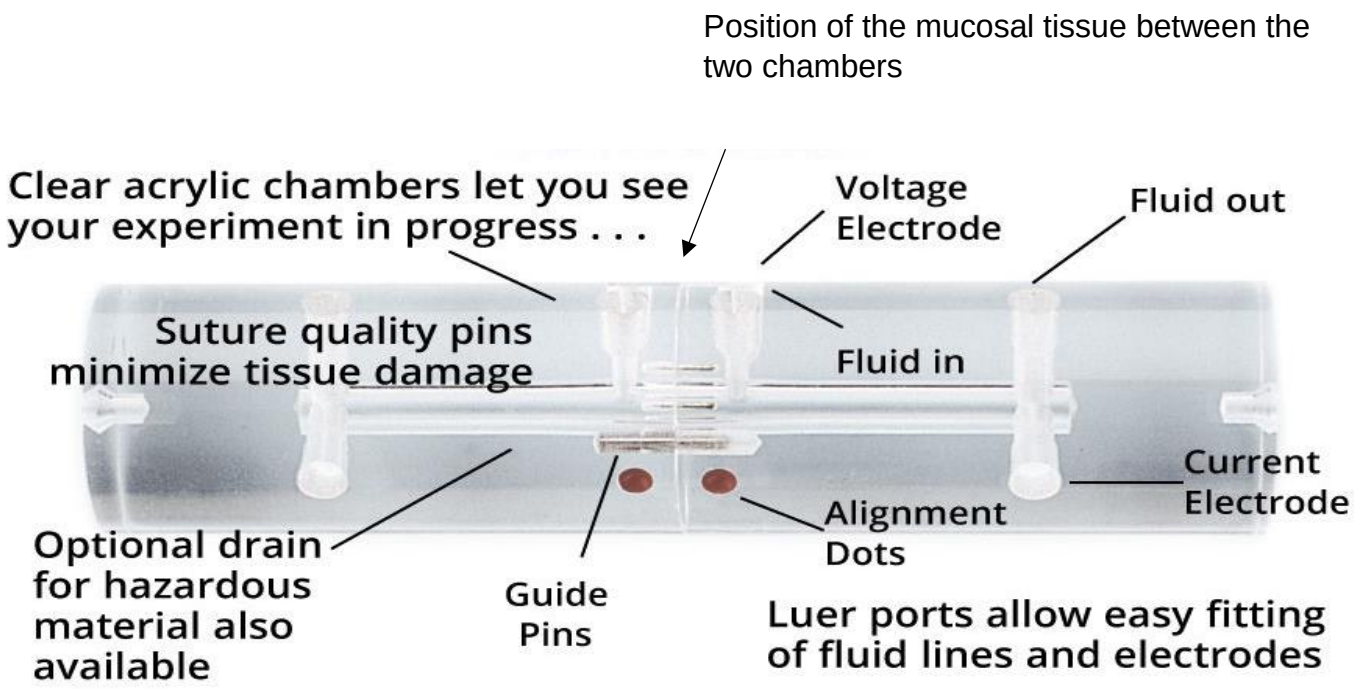

Figure 3.1: The Ussing chamber

Schematic diagram of an Ussing chamber. The Ussing consisted of two chambers to allow the tissue to be placed inbetween the chambers. The guide pins ensure the tissue is held in place and alignment dots allow the chambers to be assembled in the right orientation. Each half-chamber has voltage and current electrode connecting ports to pass current and measure the transmembrane potential. Additional ports in the chamber allows constant perfusion of the tissue preparation with experimental solution and 95% O_2 and 5% CO_2 to ensure a steady oxygen perfusing to tissue. Other ports serve to enable fluid sampling. The chamber is a clear acrylic that allows the observation of the experimental progress. (Adapted from WPI, 2015)

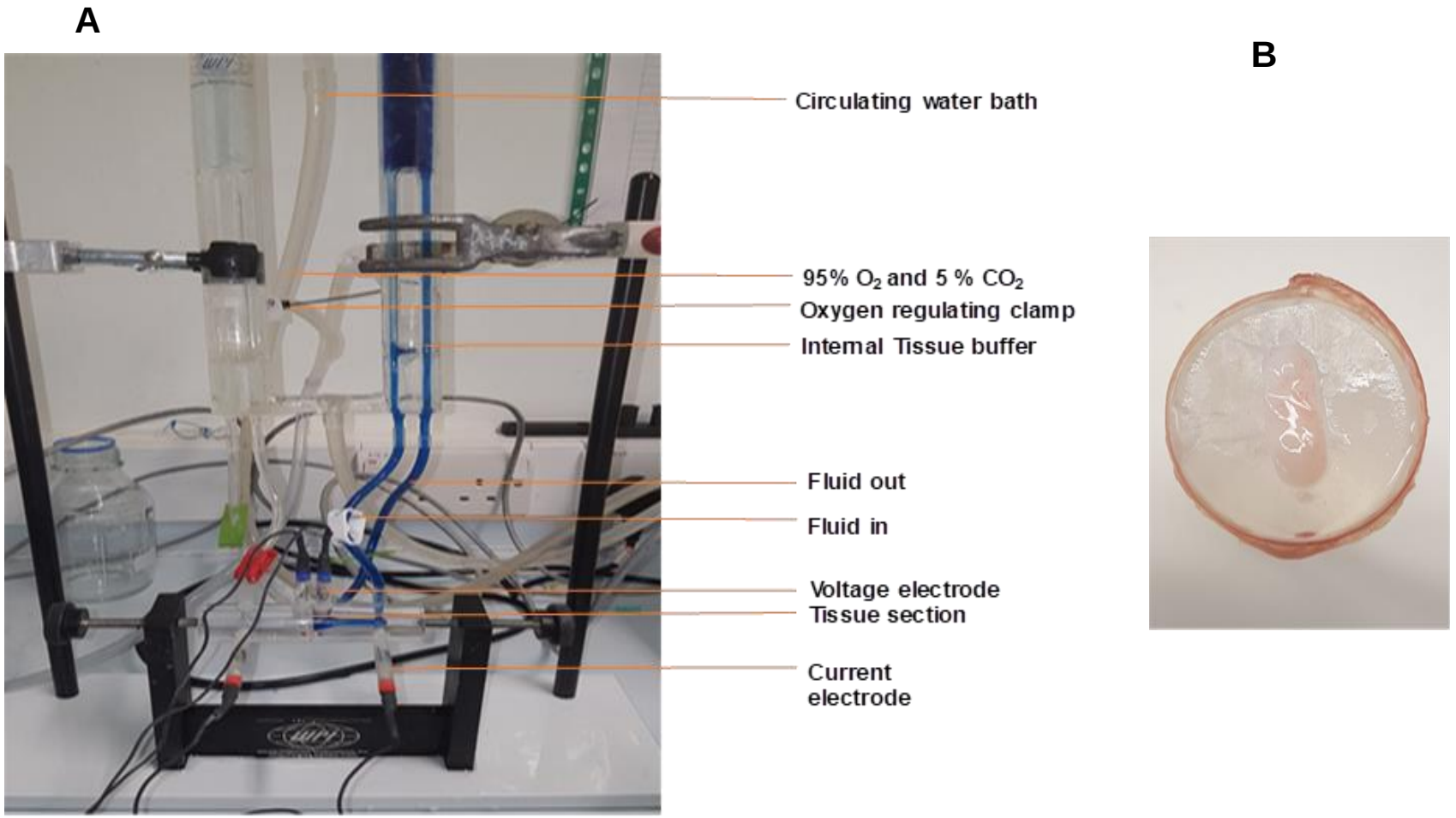

Figure 3.2 The Ussing chamber system: A) Representative image of an assembled Ussing chamber system used in this experiment. The Ussing chamber system consisted of oxygen regulating clamp; to regulate the flow of oxygen to the tissue preparation, circulating water bath; to water jacket internal tissue buffer and maintain desired temperature at 37ºC, tissue section; pig bladder mucosa tissue preparation used to determine the rate of D_2O movement, internal tissue buffer; to provide a physiological condition for the tissue to stay viable, fluid out/fluid in; ports that allow internal tissue buffer to circulate in and from the tissue, voltage electrode/current electrode; to allow TER measurement. **B)** Representative image of pig mucosa tissue preparation used during the experiments.

3.3.4 Noise and Offset Voltage Control

The chambers, superfusing solutions and solid agar bridges of 3M KCl in 2% agar were prepared before each experiment. The Ussing chamber was assembled (Figure 3.2) without any tissue and the whole system was flushed with Krebs solution).

A watertight system was established (without tissue preparation) with superfusate in the central chamber and the temperature of the circulating water bath was adjusted to 37ºC. Current and voltage electrodes were inserted into each half-chamber to test for intrinsic noise and any voltage offsets (Figure 3.2). The electrodes were connected to a commercial system (Model: U9500/U9520. WPI UK) to inject current and record potential difference and to test for intrinsic noise and any voltage offsets. Noise and offsets generally arose from bubbles in the agar bridges connecting the current/voltage electrodes to the superfusate; bubbles were removed by gently tapping the agar bridges. The potential difference (p.d.) between the two voltage electrodes was measured and should have been <0.1 mV; when greater agar bridges were again cleaned until the p.d. was acceptable. Current pulses, I, were then injected (<0.1 mA) and the p.d. (V) recorded; the resistance of the superfusate-filled chamber, R, was calculated from the relationship $R=V/I$. The value of V was then offset to 0 mV by passing a current from the control system.

3.3.5 The Ussing Chamber Experimental Set Up

After noise and offset corrections were carried out as described above, the two separate chambers, one chamber for control experiment and the other chamber for $HgCl_2$ treatment, were disconnected from the superfusate solution and a sheet of two

paired mucosa was stretched across the mouth of the central chamber of one half-cell and then connected to the second half-cell both chambers were filled with superfusate. At this time, the system was checked visually for leaks. After reassembly of the system, each reservoir was filled with the same volume of modified Krebs superfusate (20 ml) to maintain equal hydrostatic pressure across the preparation. Ballooning of the preparation into one half-chamber indicated unequal hydrostatic pressure between the two half-chambers. Agar bridges previously prepared with their respective electrodes, were inserted in the wells of the two half chambers to record the potential difference across the preparation. The current electrodes were then inserted in preparation for the measurement of transmembrane resistance. The chamber was again checked for leakages and the time of the chamber assembly was recorded. The system was then allowed to equilibrate for an hour to recover from the mounting procedure until an acceptable value of transmembrane potential was recorded. The respective chambers facing the apical and baso-lateral faces of the mucosa membranes was carefully recorded and are henceforth referred to as the apical and baso-lateral chambers.

3.3.6 Transient Epithelial Electrical Resistance Measurement

The electrical resistance of the tissue preparation was measured under voltage-clamp conditions using EVC400 and EVC3 preamplifiers which is part of the commercial system. The measurement of the electrical resistance was only performed for the initial tissues used in the experiment to establish a tight urothelial barrier. The short-circuit current (I_{sc}) is that required to offset the existing transmembrane potential to 0 mV. The transmembrane potential (V_{te}) of the preparation was initially recorded in current-clamp mode. Current was then passed in voltage-clamp mode to offset V_{te} to 0 mV

and the value of I_{sc} recorded. The transmembrane resistance, r_{te}, was than calculated from Ohm's Law:

Equation 3.2

$$r_{te} = \frac{V_{te}}{I_{sc}}$$

To normalise resistance, (Ω,cm^{-1}) values to be independent of membrane area values were normalised to specific resistances (Ω.cm) by the relation:

Equation 3.

$$R_{te}=r_{te}.A$$

Where *A* is the cross-sectional area of the preparation covering the hole between the two-half chambers.

3.3.7 Establishing the Optimum Time for D_2O Flux Measurements Across Pig Bladder Mucosa

Initially, to determine the optimum time scale for measuring D_2O concentration on the basolateral side of the mucosal membrane, samples were taken i) during 6 hours of initial equilibration (samples were taken every hour) ii) during 13 hours of equilibration

(samples taken every hour after the 6th hour) after 19 hours of equilibration (samples were taken every 10 mins for 1 hour) and iii)

3.3.7.1. Measurement of Transmembrane D_2O Fluxes for Six Hours

The reservoirs supplying the apical and the basolateral half chambers were both filled with 20 ml PBS for each experiment, a tissue preparation was mounted between the chambers and was allowed to equilibrate for an hour. Subsequently, the apical chamber reservoir was emptied and loaded with an hypotonic solution but dissolved in water containing 40% deuterium oxide, (D_2O). The basolateral membrane of the reservoir was loaded with a hypertonic solution without D_2O. Samples (1ml) of superfusate were taken from the basolateral chamber every 1h over a period of six hours, and the concentration of D_2O was determined.

In order to maintain the transmembrane hydrostatic pressure across the mucosal membrane, an equal volume of fluid was also taken at each sampling time point from the apical reservoir.

3.3.7.2. Measurement of Transmembrane D_2O Fluxes for 20 Hours

Similar method described above was used for 20 hours experiment. The reservoirs supplying the apical and the basolateral half chambers were both filled with 20 ml PBS for each experiment, a tissue preparation was mounted and was allowed to equilibrate for an hour. Subsequently, the apical chamber reservoir was emptied and loaded with an hypotonic solution but dissolved in water containing 40% D_2O. The basolateral membrane of the reservoir was loaded with a similar hypertonic solution but without

D_2O. The system was allowed to equilibrate overnight (19 hours) and then a 1 ml sample of superfusate was taken from the basolateral chamber every 10 min over a period of 1 hour for analysis of D_2O content.

An equal volume was also taken each time from the apical reservoir to maintain the transmembrane hydrostatic pressure. The measurement of D_2O in the basolateral sample showed high amount of D_2O detection however the changes in D_2O concentration overtime with each sample remained the same suggesting that the concentration had plateaux. Therefore, a decision was made to look at the period of D_2O movement between the two time points

3.3.7.3 Measurement of Transmembrane D_2O Fluxes for 13 Hours

Similar method described above was used for 13 hours experiment. The reservoirs supplying the apical and the basolateral half chambers were both filled with 20 ml PBS for each experiment, a tissue preparation was mounted and was allowed to equilibrate for an hour. Subsequently, the apical chamber reservoir was emptied and loaded with an hypotonic solution but dissolved in water containing 40% D_2O. The basolateral membrane of the reservoir was loaded with a similar hypertonic solution but without D_2O. The system was allowed to equilibrate for 5 hours and then a 1 ml sample of superfusate was taken from the basolateral chamber every 1 h over a period of eight hours for analysis of D_2O content.

An equal volume was also taken each time from the apical reservoir to maintain the transmembrane hydrostatic pressure. A gradual increase in D_2O diffusion rate was observed in this time period and therefore, all the subsequent experiments were done performed within this time point.

3.3.7.3 Measurement of Transmembrane D_2O Fluxes

The same experiment described above in the 13 hours was used for this experiment. The reservoirs supplying the apical and the basolateral half chambers were both filled with 20 ml PBS for each experiment, a tissue preparation was mounted and was allowed to equilibrate for an hour. Both apical and basolateral sided on each chamber were subsequently emptied and washed with PBS 5 times and the apical half chamber and the basolateral half chamber was loaded with the following solution gradient separately:

- Hypertonic on the basolateral/Hypotonic on the apical
- Isotonic on the basolateral/Hypertonic on the apical
- Isotonic on the basolateral/Hypotonic on the apical
- Isotonic on the basolateral/Isotonic on the apical

The system was allowed to equilibrate for five hours and then a 1 ml sample of superfusate was taken from the basolateral chamber every hour over a period of eight hours for analysis of D_2O content. An equal volume was also taken each time from the apical reservoir to maintain the transmembrane hydrostatic pressure. At the end of each experiment, 3% v/w Evans Blue dye diluted in PBS was added to the apical reservoir to test for any leaks between the two half-chambers via the preparation for an hour to determine the integrity of the tissue preparation (Figure 3.3). Samples collected from leaking tissue preparations were excluded from the data analysis. This experimental set up served as a control.

Table 3.8: Establishing the optimum time for D_2O flux measurement across pig bladder mucosa. To determine the optimum time and incubation period needed for D_2O flux measurement, three different experimental set up protocols indicated below were applied.

Experimental Set Up	**Tissue Incubation Period (h)**	**Sample Collection Duration**	**Volume of sample collection each time (ml)**
Measurement of Transmembrane D_2O Fluxes for Six Hours	1	5h	1
Measurement of Transmembrane D_2O Fluxes for 20 Hours	19	Every 10m for 1h	1
Measurement of Transmembrane D_2O Fluxes for 13 Hours	5	8h	1

3.3.7.4 Measurement of Transmembrane D_2O Fluxes in the Presence of $HgCl_2$

To determine whether the movement of D_2O was attributed to passive diffusion or the presence of AQP channels in the urinary bladder, a second using chamber system was set up where AQP channels are inhibited with $HgCl_2$. The exact same approach was used. The reservoirs supplying the apical and the basolateral half chambers were both filled with 20 ml PBS for each experiment, a tissue preparation was mounted and was allowed to equilibrate for an hour.

The apical and side on each chamber was subsequently emptied and washed with PBS 5 times, 20 ml PBS containing 300uM $HgCl_2$ was loaded to the apical side of the tissue for an hour. Both apical and basolateral sided on each chamber were subsequently emptied and washed with PBS 5 times and the apical half chamber and the basolateral half chamber was loaded with the following solution gradient separately:

- Hypertonic on the basolateral/Hypotonic on the apical
- Isotonic on the basolateral/Hypertonic on the apical
- Isotonic on the basolateral/Hypotonic on the apical
- Isotonic on the basolateral/Isotonic on the apical

The system was allowed to equilibrate for five hours and then a 1 ml sample of superfusate was taken from the basolateral chamber every hour over a period of eight

hours for analysis of D_2O content. An equal volume was also taken each time from the apical reservoir to maintain the transmembrane hydrostatic pressure. At the end of each experiment, 3% v/w Evans Blue dye diluted in PBS was added to the apical reservoir to test for any leaks between the two half-chambers via the preparation for an hour to determine the integrity of the tissue preparation (Figure 3.3). Samples collected from leaking tissue preparations were excluded from the data analysis.

Table 3.2 Krebs buffer solutes. Composition of solutions used to measure the influence of osmotic pressure on transmembrane D_2O flux Hypotonic solution; 96mOsM, Hypertonic solution; 407mOsM, Isotonic solution 283mOsM;

Chemicals (mmol/l)	**NaCl**	**D Glucose**	**$NaHCO_3$**	**KCl**	**$MgSO_4$**	**KH_2PO_4**	**$CaCl_2$**	**Tris base**	**Sucrose**
Hypotonic	**47**	**12**	**25**	**4.6**	**2.4**	**1.2**	**2.6**	**0**	**0**
Isotonic	**47**	**12**	**25**	**4.6**	**2.4**	**1.2**	**2.6**	**71**	**0**
Hypertonic	**94**	**12**	**25**	**4.6**	**24**	**1.2**	**2.6**	**0**	**160**

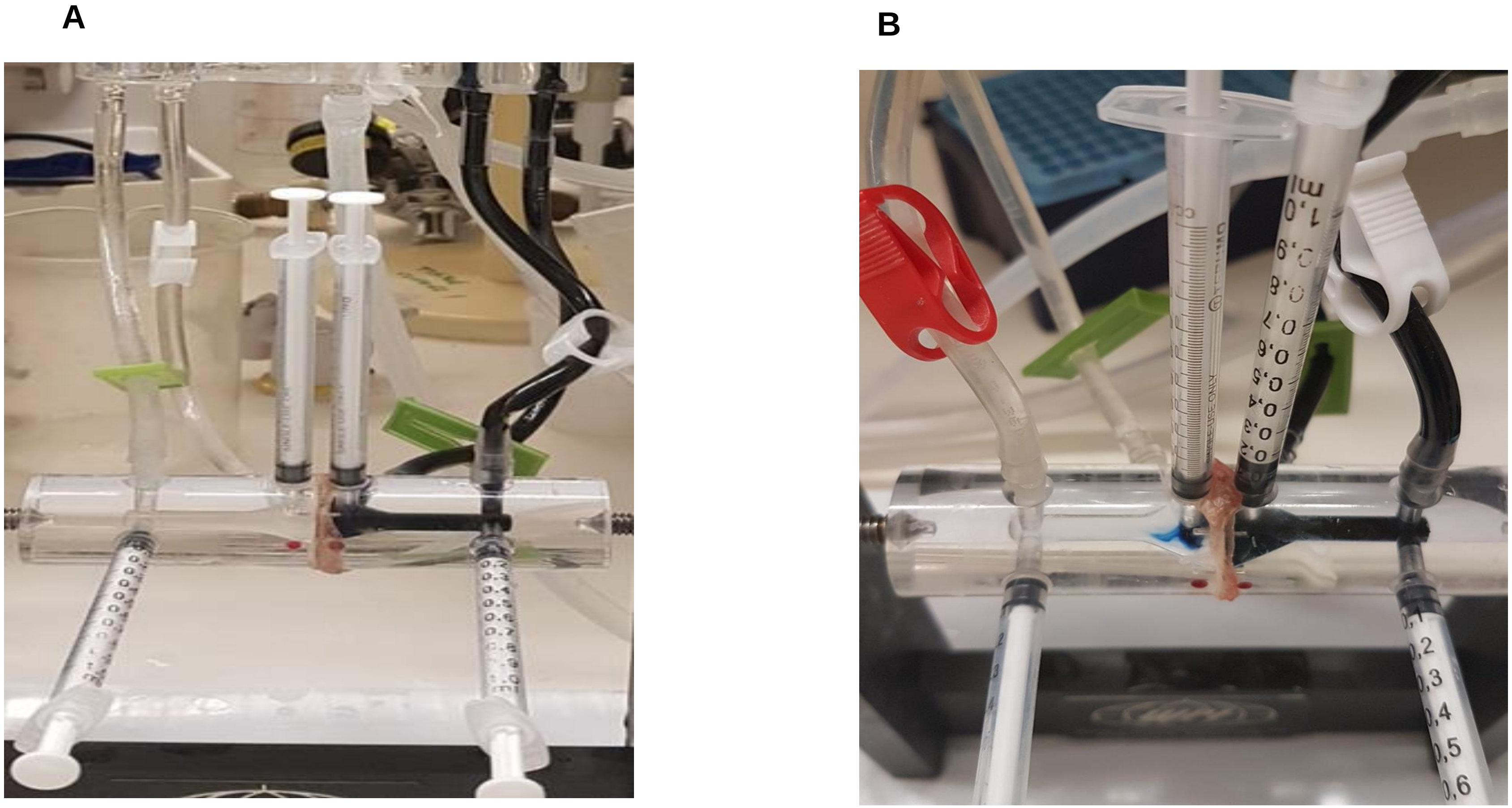

Figure 3.3 Tissue integrity assessment using Evans Blue dye. A) Close up image of the Ussing chamber with urinary bladder mucosa tissue preparation. 3% Evans Blue dye diluted in PBS was loaded on the apical reservoir/half chamber. **A)** No visible movement of Evans Blue dye detected on the basolateral half chamber after 1 hour. **B)** Movement of Evans Blue dye was detected on the basolateral half chamber after 10 minutes indicating leaking tissue preparation.

3.3.8 Infrared Detection of D_2O and Calculation of Flux Rate

Sample (1 ml each) collected from the basolateral side of the chamber were loaded on fourier-transform infrared spectroscopy reader and the sample were analysed using a Fourier-transform infrared spectrometer (FT-IR spectrometer) peak signals detected around a wavenumber of 2501 cm^{-1} were interpreted as D_2O values. Figure 3.5 shows a spectrometer reading of D_2O solution of known concentrations. A standard curve of concentration (0.4%, 0.5%, 1%, 2%, 6% is this v/v) against wave length was generated (Figure 3.5). The relationship between peak amplitude and D_2O concentration was linear and fitted to a straight-line equation:

$$y = mx + c$$

where y = optical density @ 2501 cm wavelength); m = gradient of the relationship; c a non-zero intercept constant; x = D_2O percentage.

The change in concentration of D_2O on the basolateral side of the mucosa over time, in the presence and absence of $HgCl_2$, was used to estimate the permeability (diffusion) coefficient (P_D) using the equation:

$$P_D = \phi/(A.\Delta C)$$

Where ϕ is the flux of the tracer across the membrane and is calculated from the net increase of the tracer in the basolateral surface, A is the area of the apical membrane, and ΔC is the concentration gradient for the D_2O across the membrane

3.3.9 Statistical Analyses

All data are presented as mean ± standard error of the mean (SEM) of three repeats (n=3). The number of separate experiments from different animals are denoted as *n.* Comparisons between the total D_2O diffusion, $HgCl_2$ dependent D_2O diffusion and $HgCl_2$ independent D_2O diffusion used repeated measures analysis of variance (ANOVA) with *post-hoc* tests (Newman-keuls test) for any differences between pairs of conditions.

The rate of D_2O diffusion amongst the different tonicities was compared using one-way ANOVA followed by a post hoc test (Tuckeys test). Straight-line fits used an iterative algorithm to calculate the best-fit values of slope and intercept. $p<0.05$. All analyses were performed in GraphPad Prism.

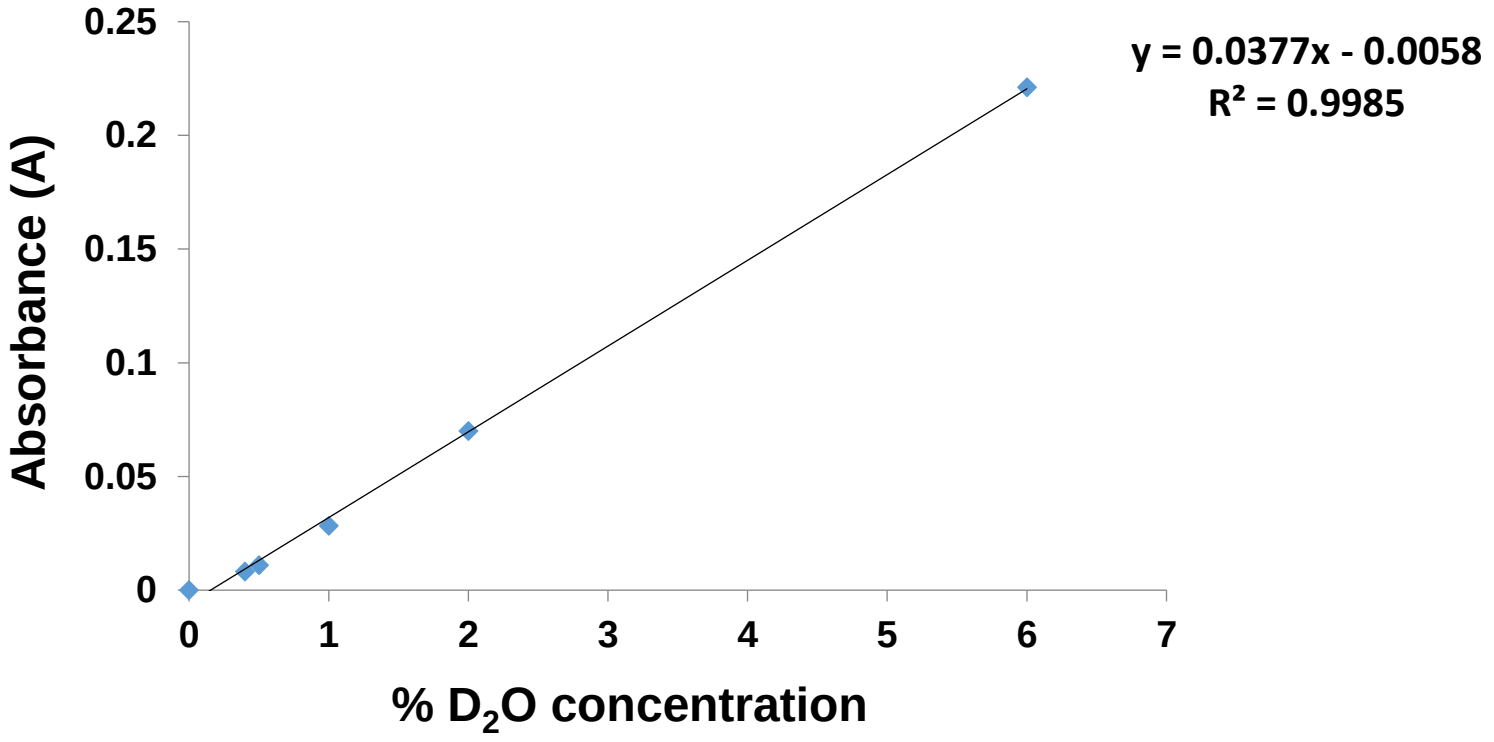

Figure 3.4 Representative graph of known D2Ostandard cencentrations against peak height in absorbance. A standard curve of concentration against absorbance for D_2O was generated. The relationship between absorbance on the y axis and D2O concentration ((%) 0, 0.4, 0.5, 1, 2, 6) on the x axiswas linear and fitted to a straight-line equation.

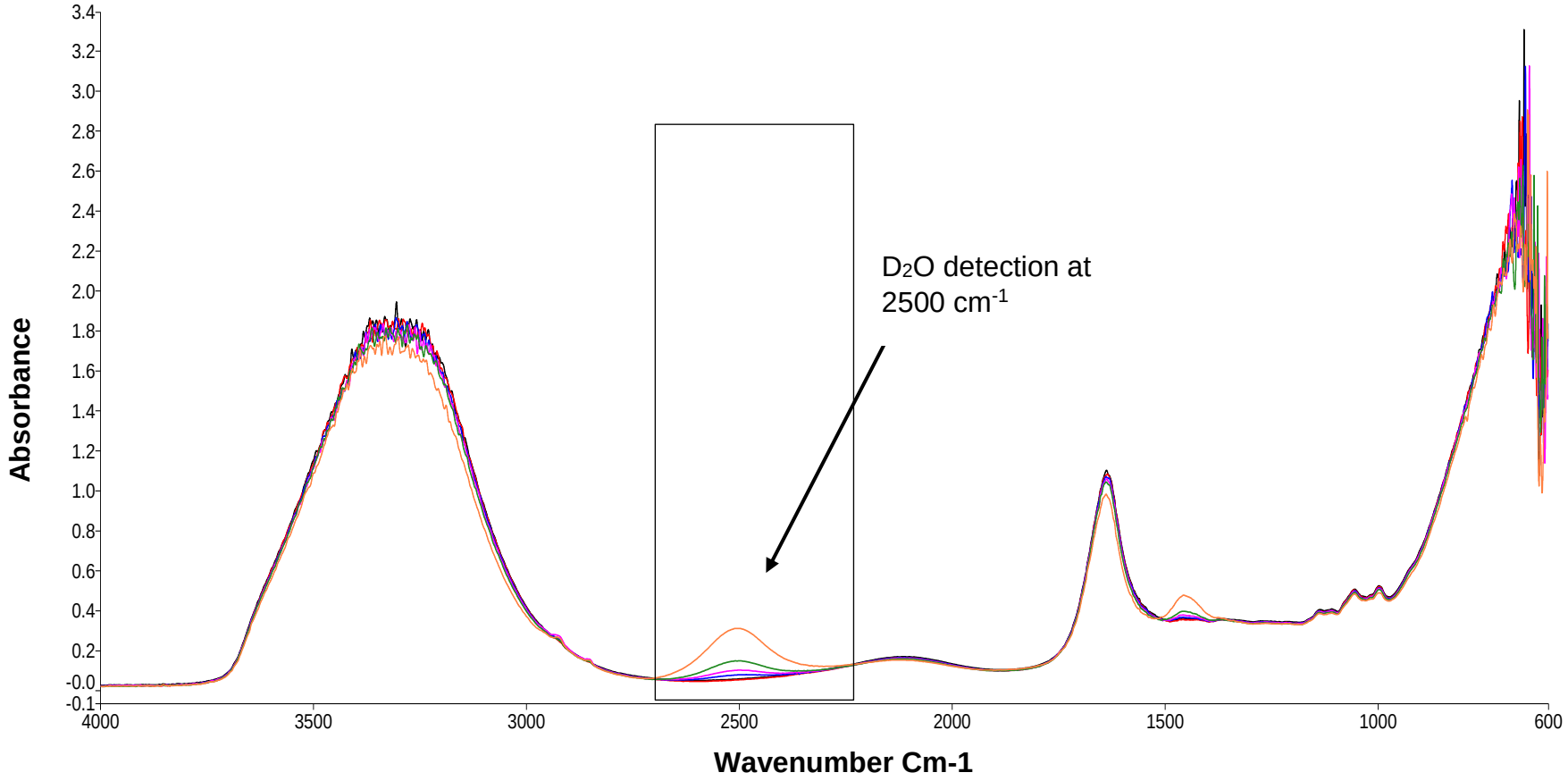

Figure 3.5 The fourier-transform infrared spectroscopy (FT-IR) spectrum of D_2O

Experimental samples of different D_2O concentrations were analysed using a PerkElmer FT-IR spectrometer. D_2O peak was detected at 2500 cm^{-1} wavenumber region. Wavenumberof 2500 cm^{-1} were interpreted as D_2O values.

3.4 RESULTS

3.4.1 Establishing transient epithelial resistance (TER) and the Optimum Time for D_2O Flux measurements across pig bladder mucosa

To determine the tightness of the dissected mucosa strip, the permeability properties of 5 mucosa constructs of bladder were determined by TER measurements. The mean TER was 1303.4 $\Omega.cm^2$, indicating a 'tight' urothelium. Once a tight barrier was established, the TER was not measured for subsequent experiments.

To determine optimum time scale for measuring D_2O movement across pig bladder urothelium, the concentration of D_2O on the basolateral side was measured under maximum osmotic gradient (i.e. hypotonic solution on the apical side and the hypertonic solution on the basolateral side) over 3 time scales: 6 hours, 13 hours and 20 hours.

Experiments were performed initially where samples was taken every 1 h for six hours. However, the concentration of D_2O was too low for detection (Fig 3.6). Therefore, a longer experimental time was chosen. Tissue was allowed to incubate overnight (19 hrs) and samples were collected every 10 min for 1 hour on the 20^{th} hour (Figure 3.7). Although the movement of D_2O was detected, there was no change in the concentration of D_2O over time in these samples. Therefore, a decision was made to allow the tissue to equilibrate for five hours and samples taken every hour after the sixth hour for an additional eight hours. This resulted in a total of 13 hours experiment with five hours tissue equilibration time and eight hours sampling time.

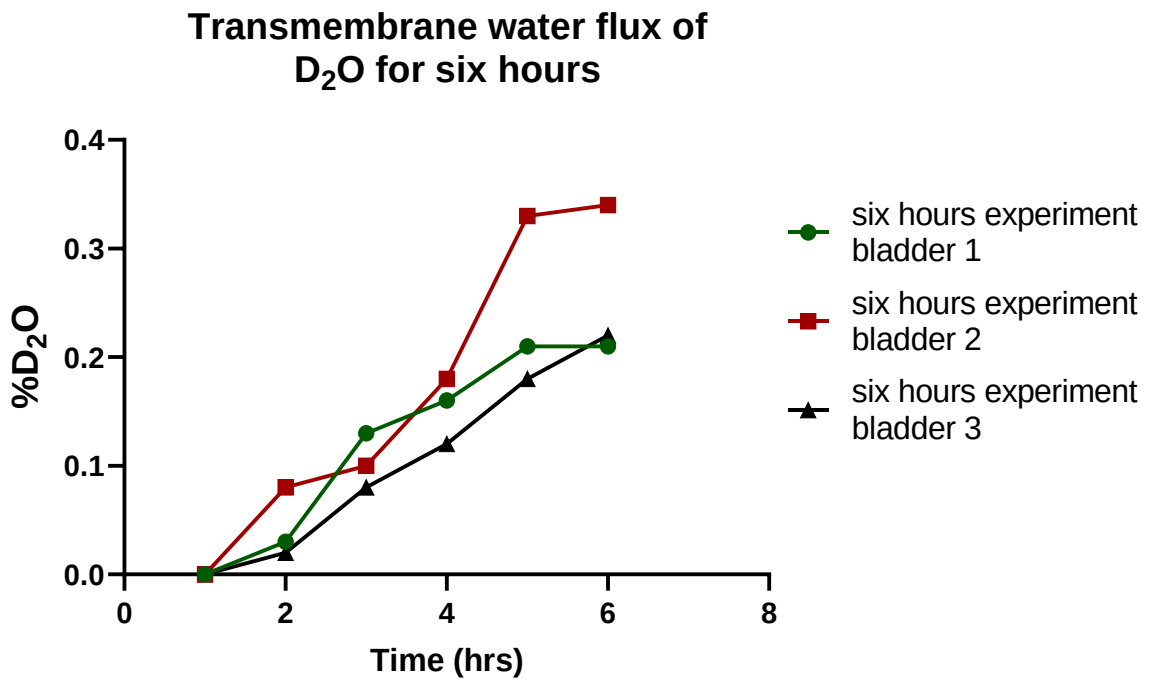

Figure 3.6. Measurement of transmembrane D_2O flux for six hours

Graph represent three different repeats of six hours experiment of D_2O against time. Small quantities of D_2O was detected over the period of six hours with an increase in D_2O concentration with each hour of sampling.

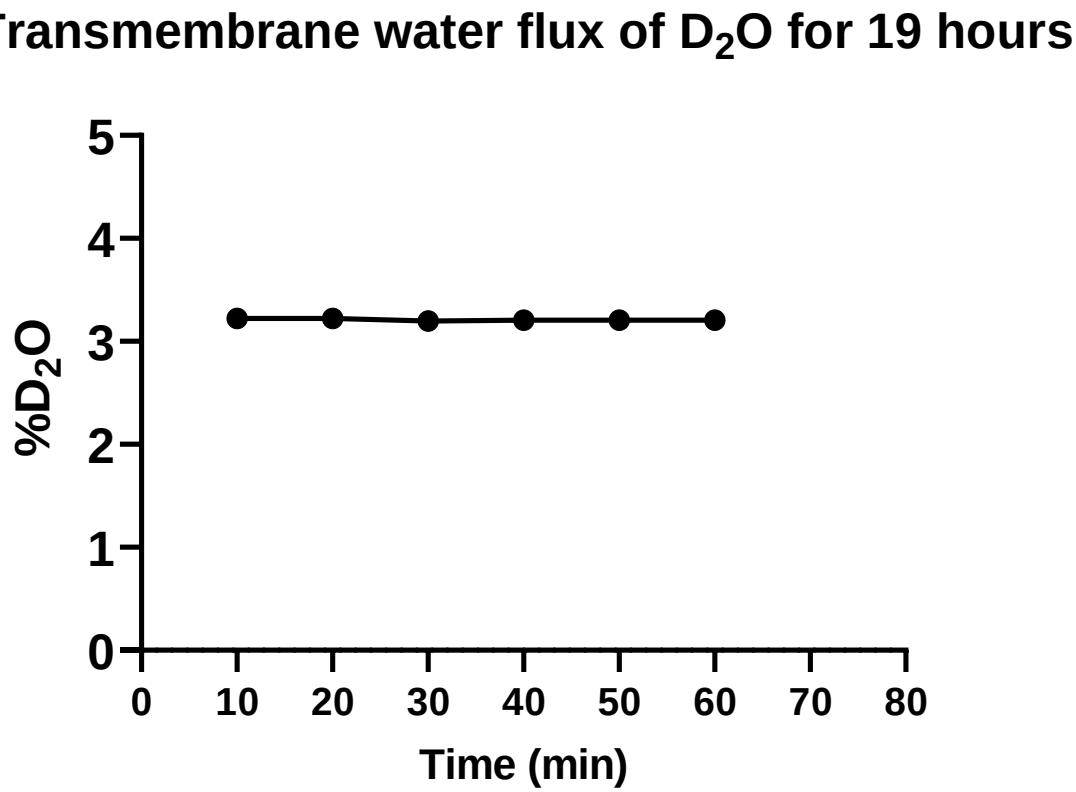

Figure 3.7. Measurement of transmembrane D_2O flux for 1 hour after 19 hours incubation time

Graph represent one bladder strip of one hour experiment of %D_2O against time. After 19 hours of incubation, samples were taken from the basolateral side every 10 minutes for one hour. Almost equal amount of D_2O concentrations were detected with each sampling every 10 minutes for one hour.

3.4.2 Rate of D_2O Diffusion when isotonic solutions was used at both basolateral and apical side of the tissue strip.

In order to determine whether there was any basal diffusion of D_2O across pig bladder mucosa in the absence of an osmotic gradient, both the apical and basolateral sides of the mucosa membrane were bathed in isotonic Krebs solution (Table 3.4). The concentration of D_2O (% D_2O) measured on the basolateral side of three mucosa membranes is shown in Table 3.4. No D_2O movement was detected across the first mucosa sample (Table. 3.4). Very low concentrations of D_2O were detected from the 6^{th} to 8^{th} hour on the basolateral side of the second mucosa sample. No D_2O movement was detected across the third mucosa sample (Table. 3.4). This data demonstrates that there was hardly a driving force for D_2O movement across the barrier without an osmotic gradient even though concentration gradient for D_2O was present.

As the movement of D_2O was minimal when both the apical and basolateral sides of the mucosa membrane were exposed to isotonic solution, a concentration gradient was created across the mucosa membrane by bathing the apical and basolateral side of the tissue with solutions of different osmolarity.

Statistical analysis could not be performed due to the absence of sample detection.

Table 3.4 Concentration of D_2O measured on the basolateral side of the mucosa when both apical and basolateral sides of the membrane were bathed in isotonic solution.

As a control, isotonic Krebs solution was loaded on the basolateral and apical sides of the membrane in three different repeat experiments with three different samples. Movement of D_2O was not detected in the first and third repeat. Movement of D_2O was detected in the second repeat at the 6^{th} 7^{th} and 8^{th} hours.

Time	%D_2O movement Bladder 1	%D_2O movement Bladder 2	%D_2O movement Bladder 3
1	**0**	**0**	**0**
2	**0**	**0**	**0**
3	**0**	**0**	**0**
4	**0**	**0**	**0**
5	**0**	**0**	**0**
6	**0**	**0.33**	**0**
7	**0**	**0.41**	**0**
8	**0**	**0.53**	**0**

3.4.3 Calculation of D_2O Diffusion Rate in Absence and Presence of $HgCl_2$

To determine the diffusion rate of D_2O across the pig urinary bladder mucosa in the presence and absence of $HgCl_2$, the concentration of D_2O on the basolateral side of pig bladder mucosa strips mounted in Ussing chambers was measured over eight hours (after five hours of equilibration). The rate of diffusion under different osmotic conditions in the absence and presence of $HgCl_2$ was calculated

3.4.3.1. Hypertonic Solution on the Basolateral Side and Hypotonic Solution on the Apical Side

In this experiment, the basolateral side of the mucosa strip was bathed in hypertonic solution and the apical side was bathed in hypotonic solution, aim to maximise the osmotic gradient created across the mucosa

The linear regression analysis of D_2O concentration against time in the absence (total D_2O movement, n=3) and presence of $HgCl_2$ ($HgCl_2$-independent D_2O movement n=3; Figure 3.8) was used to calculate the D_2O diffusion rate across each mucosal strip. (Table 3.5) The $HgCl_2$-independent D_2O concentration at each time point was subtracted from the total D_2O concentration to determine the $HgCl_2$ dependent D_2O movement and the diffusion rate (Figure 3.8 and Table 3.5)

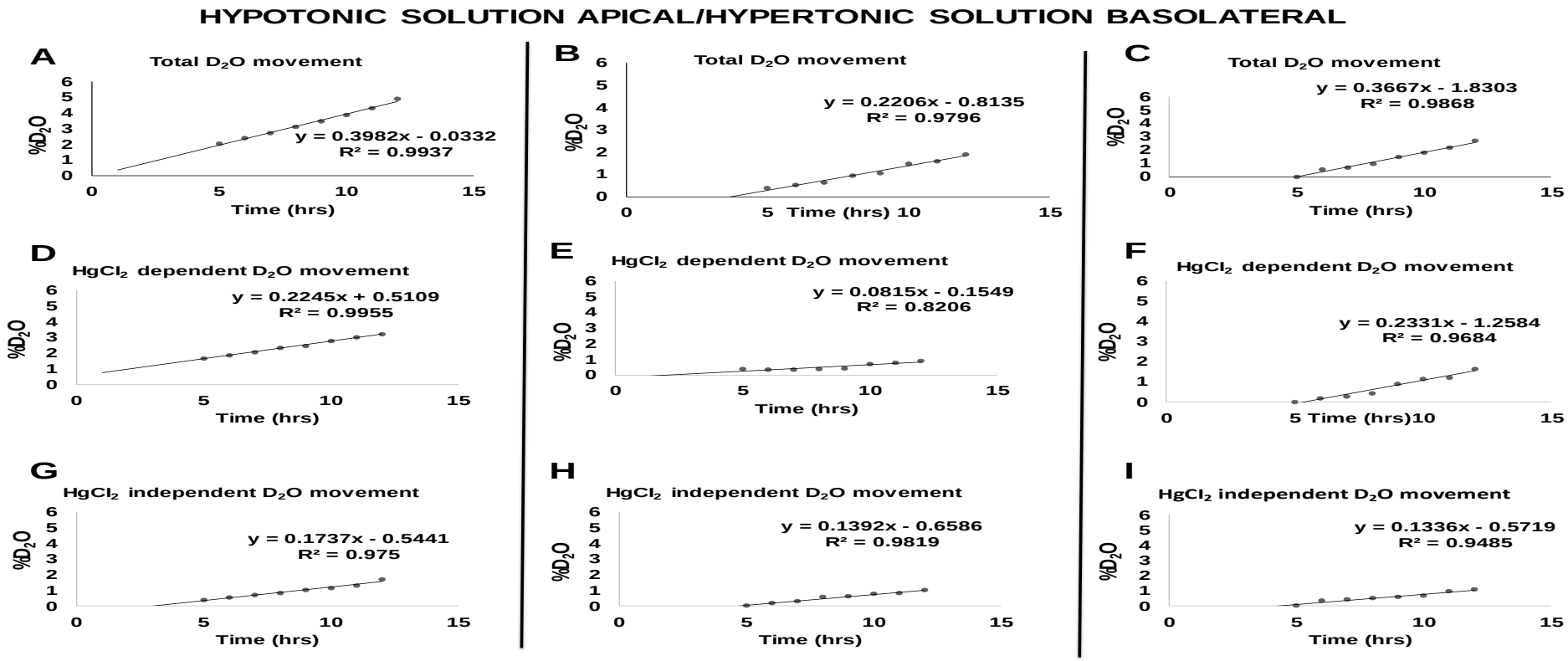

Figure 3.8 Linear regression analysis of D_2O concentration against time in presence and absence of $HgCl_2$ with hypotonic solution on the apical and hypertonic solution on the basolateral side of pig bladder mucosa. A, B and C) Linear regression analysis of total D_2O concentration against time in 3 mucosa strips. G, H and I) Linear regression analysis of D_2O concentration against time in presence of $HgCl_2$ ($HgCl_2$-independent D_2O movement) in 3 mucosa strips. The $HgCl_2$-independent D_2O concentration at each time point was subtracted from the total D_2O concentration at that time point in paired mucosa strips to determine the $HgCl_2$ dependent (AQP dependent) D_2O concentrations D, E and F) Linear regression analysis of $HgCl_2$ dependent D_2O concentration against time. The diffusion rate was calculated using % D_2O over time from these graphs

Table 3.5 The rate of diffusion of total, $HgCl_2$ dependent, $HgCl_2$ independent D_2O movement for each repeat

The slopes for total D_2O movement, $HgCl_2$ dependent D_2O movement and $HgCl_2$ independent D_2O movement for hypotonic solution on the apical and hypertonic on basolateral

Conditions	Rate of diffusion (slope of the linear regression analysis)
Bladder strip 1	
Total movement	0.3982
$HgCl_2$ independent D_2O movement	0.1737
$HgCl_2$ dependent D_2O movement	0.2245
Bladder strip 2	
Total movement	0.2206
$HgCl_2$ independent D_2O movement	0.1392
$HgCl_2$ dependent D_2O movement	0.0815
Bladder strip 3	
Total movement	0.3667
$HgCl_2$ independent D_2O movement	0.1336
$HgCl_2$ dependent D_2O movement	0.2331

A comparison between the total, $HgCl_2$ dependent and $HgCl_2$ independent D_2O diffusion rates is presented in Figure 3.9. There was a noticeable, but a non-significant (p = 0.0664) reduction in D_2O diffusion rate when the tissue was treated with 300µM $HgCl_2$, a non-selective AQP inhibitor (Figure 3.9) There was also no significant difference (p = 0.0664) between the $HgCl_2$ dependent and $HgCl_2$ independent D_2O diffusion rates. (Figure 3.9).

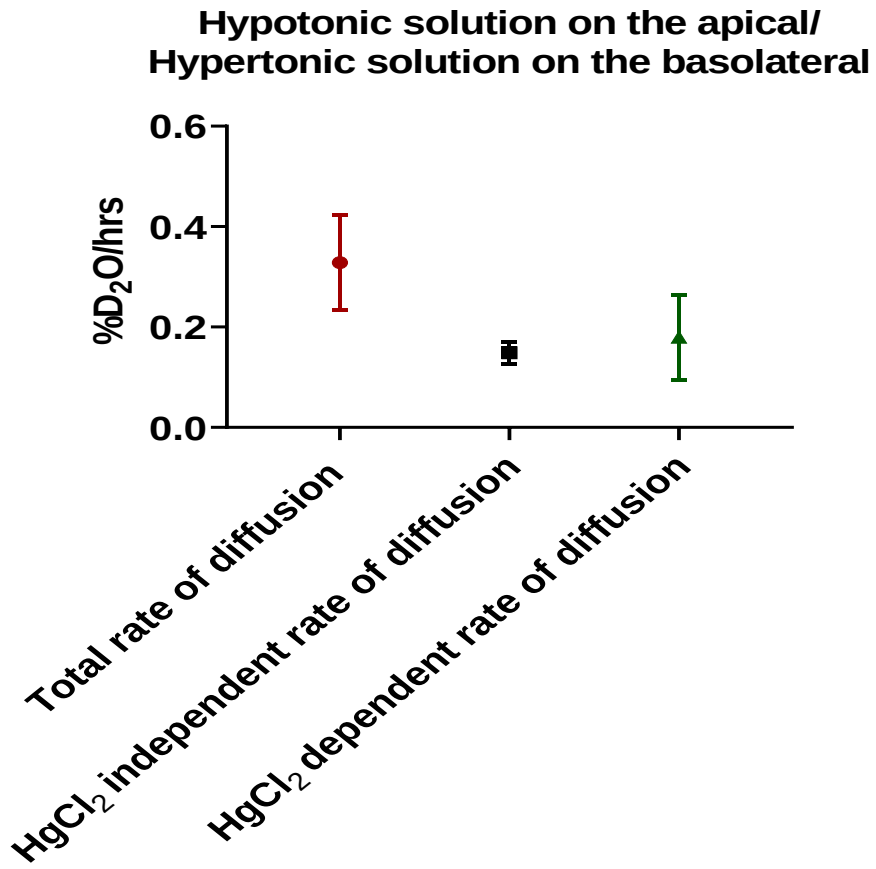

Figure 3.9. Comparison of the mean D_2O diffusion rates in absence and presence of $HgCl_2$ with hypotonic solution on the apical and hypertonic solution on the basolateral side of the pig bladder mucosa strip.

There was no significant difference between the total, $HgCl_2$ dependent and $HgCl_2$ independent D_2O diffusion rates. The different D_2O diffusion rates were compared using a repeated measures one-way ANOVA followed by a Newman-Kleus post-hoc test. p value=0.0664, Data are expressed as mean ± SEM of 3 independent repeats (n=3).

3.4.4 Calculation of D_2O Diffusion Rate in Absence and Presence of $HgCl_2$

To determine the diffusion rate of D_2O across the pig urinary bladder mucosa in the presence and absence of $HgCl_2$, the concentration of D_2O on the basolateral side of pig bladder mucosa strips mounted in Ussing chambers was measured over eight hours (after five hours of equilibration). The rate of diffusion under different osmotic conditions in the absence and presence of $HgCl_2$ was calculated

3.4.4.1. Isotonic Solution on the Basolateral Side and Hypotonic Solution on the Apical Side

In this experiment, the basolateral side of the mucosa strip was bathed in isotonic solution and the apical side was bathed in hypotonic solution, aim to simulate the osmotic gradient created across the mucosa in over hydrated condition.

The linear regression analysis of D_2O concentration against time in the absence (total D_2O movement, n=3) and presence of $HgCl_2$ ($HgCl_2$-independent D_2O movement n=3; Figure 3.10) was used to calculate the D_2O diffusion rate across each mucosal strip. (Table 3.6) The $HgCl_2$-independent D_2O concentration at each time point was subtracted from the total D_2O concentration to determine the $HgCl_2$ dependent D_2O movement and the diffusion rate (Figure 3.10 and Table 3.6)

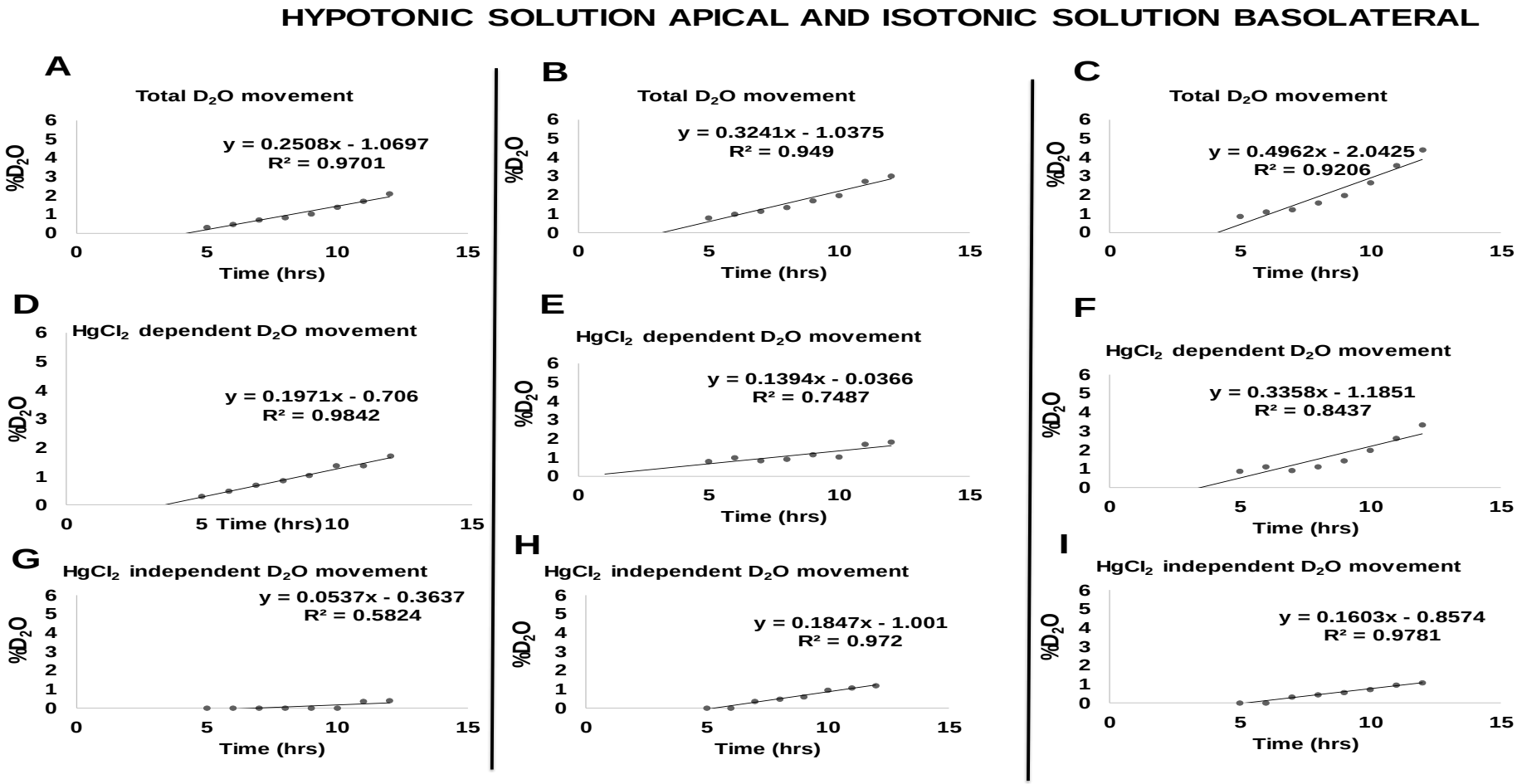

Figure 3.10 Linear regression analysis of D_2O concentration against time in presence and absence of $HgCl_2$ with hypotonic solution on the apical and isotonic solution on the basolateral side of pig bladder mucosa. A, B and C) Linear regression analysis of total D_2O concentration against time in 3 mucosa strips. G, H and I) Linear regression analysis of D_2O concentration against time in presence of $HgCl_2$ ($HgCl_2$-independent D_2O movement) in 3 mucosa strips. The $HgCl_2$-independent D_2O concentration at each time point was subtracted from the total D_2O concentration at that time point in paired mucosa strips to determine the $HgCl_2$ dependent (AQP dependent) D_2O concentrations D, E and F) Linear regression analysis of HgCl2 dependent D_2O concentration against time. The diffusion rate was calculated using % D_2O over time from these graphs

Table 3.6 the rate of diffusion of total, $HgCl_2$ dependent, $HgCl_2$ independent D_2O movement for each repeat. The slopes for total D_2O movement, $HgCl_2$ dependent D_2O movement and $HgCl_2$ D_2O independent movement for hypotonic solution on the apical and isotonic on basolateral with representative equilibration time show the length of duration before D_2O could be sampled.

Conditions	**Rate of diffusion (slope of the linear regression analysis)**
Bladder strip 1	
Total movement	0.2508
$HgCl_2$ independent D_2O movement	0.0537
$HgCl_2$ dependent D_2O movement	0.1971
Bladder strip 2	
Total movement	0.3241
$HgCl_2$ independent D_2O movement	0.1847
$HgCl_2$ dependent D_2O movement	0.1394
Bladder strip 3	
Total movement	0.4962
$HgCl_2$ independent D_2O movement	0.1603
$HgCl_2$ dependent D_2O movement	0.3358

A comparison between the total, $HgCl_2$ dependent and $HgCl_2$ independent D_2O diffusion rates is presented in Figure 3.11. There was a noticeable, but a non-significant ($p=0.0645$) reduction in D_2O diffusion rate when the tissue was treated with 300µM $HgCl_2$, a non-selective AQP inhibitor (Figure 3.11) There was also no significant difference ($p=0.0645$) between the $HgCl_2$ dependent and $HgCl_2$ independent D_2O diffusion rates. (Figure 3.11).

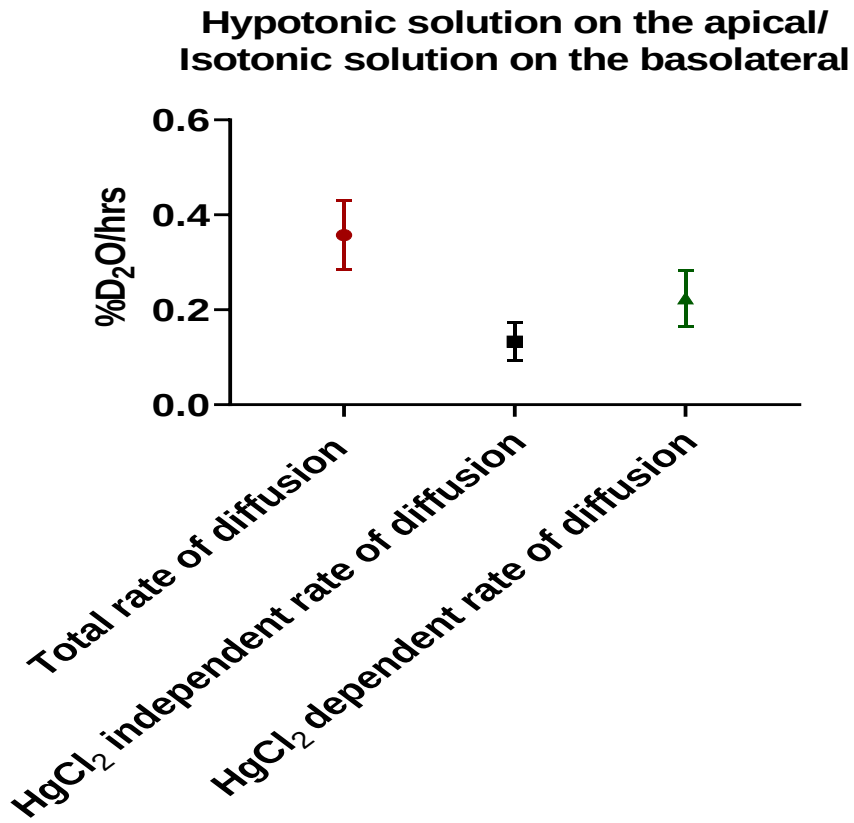

Figure 3.11 Comparison of the mean D_2O diffusion rates in absence and presence of $HgCl_2$ with hypotonic solution on the apical and isotonic solution on the basolateral side of the pig bladder mucosa strip.

There was no significant difference between the total, $HgCl_2$ dependent and $HgCl_2$ independent D_2O diffusion rates. The different D_2O diffusion rates were compared using a repeated measures one-way ANOVA followed by a Newman-Kleus post-hoc test. p value=0.0645, Data are expressed as mean ± SEM of 3 independent repeats (n=3). Data are expressed as mean ± SEM of 3 independent repeats.

3.4.5 Calculation of D_2O Diffusion Rate in Absence and Presence of $HgCl_2$

To determine the diffusion rate of D_2O across the pig urinary bladder mucosa in the presence and absence of $HgCl_2$, the concentration of D_2O on the basolateral side of pig bladder mucosa strips mounted in Ussing chambers was measured over eight hours (after five hours of equilibration). The rate of diffusion under different osmotic conditions in the absence and presence of $HgCl_2$ was calculated.

3.4.5.1. Isotonic Solution on the Basolateral Side and Hypertonic Solution on the Apical Side

In this experiment, the basolateral side of the mucosa strip was bathed in isotonic solution and the apical side was bathed in hypertonic solution, aim to simulate the osmotic gradient created across the mucosa in severely dehydrated condition.

The linear regression analysis of D_2O concentration against time in the absence (total D_2O movement, n=3) and presence of $HgCl_2$ ($HgCl_2$-independent D_2O movement n=3; Figure 3.12) was used to calculate the D_2O diffusion rate across each mucosal strip. (Table 3.7) The $HgCl_2$-independent D_2O concentration at each time point was subtracted from the total D_2O concentration to determine the $HgCl_2$ dependent D_2O movement and the diffusion rate (Figure 3.12 and Table 3.7)

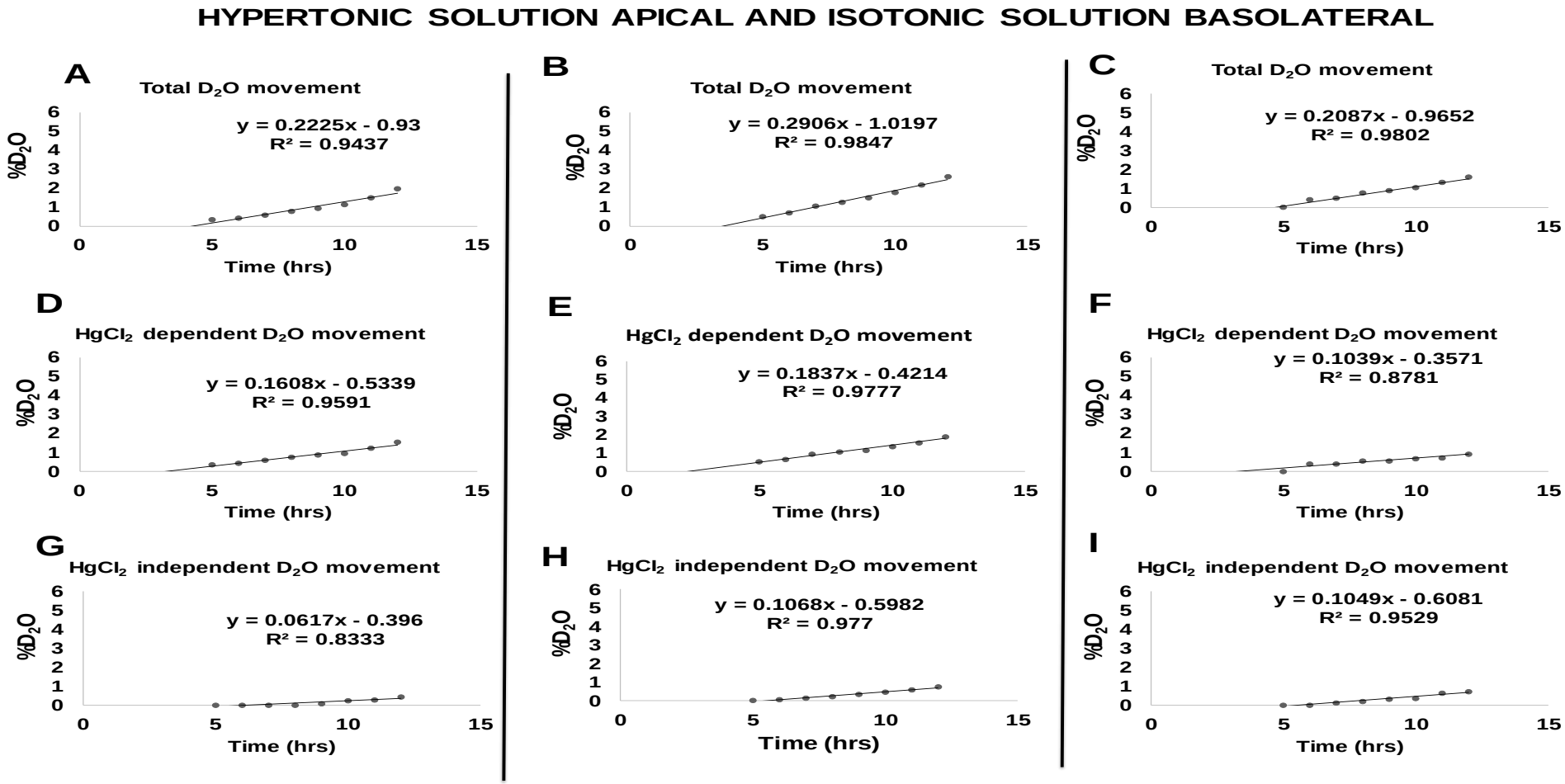

Figure 3.12 Linear regression analysis of D_2O concentration against time in presence and absence of $HgCl_2$ with hypertonic solution on the apical and isotonic solution on the basolateral side of pig bladder mucosa. A, B and C) Linear regression analysis of total D_2O concentration against time in 3 mucosa strips. D, E and F) Linear regression analysis of D2O concentration against time in presence of $HgCl_2$ (AQP-independent D_2O movement) in 3 mucosa strips. The $HgCl_2$-independent D_2O concentration at each time point was subtracted from the total D_2O concentration at that time point in paired mucosa strips to determine the $HgCl_2$ dependent (AQP dependent) D_2O concentrations G, H and I) Linear regression analysis of $HgCl_2$ dependent D_2O concentration against time. The diffusion rate was calculated using % D_2O over time from these graphs

Table 3.7 the rate of diffusion of total, $HgCl_2$ dependent, $HgCl_2$ independent D_2O movement for each repeat. The slopes for total D_2O movement, $HgCl_2$ dependent D_2O movement and $HgCl_2$ D_2O independent movement for hypotonic solution on the apical and isotonic on basolateral with representative equilibration time show the length of duration before D_2O could be sampled.

Conditions	Rate of diffusion (slope of the linear regression analysis)
Bladder strip 1	
Total movement	0.2225
$HgCl_2$ dependent D_2O movement	0.1608
$HgCl_2$ independent D_2O movement	0.0617
Bladder strip 2	
Total movement	0.2906
$HgCl_2$ dependent D_2O movement	0.1837
$HgCl_2$ independent D_2O movement	0.1068
Bladder strip 3	
Total movement	0.2087
$HgCl_2$ dependent D_2O movement	0.1039
$HgCl_2$ independent D_2O movement	0.1049

A comparison between the total, $HgCl_2$ dependent and $HgCl_2$ independent D_2O diffusion rates is presented in Figure 3.13. There was a significant difference ($p=0.0263$) between the total versus $HgCl_2$ dependent and independent D_2O diffusion rates (Figure 3.13). However, there was also no significant difference ($p=0.0263$) between $HgCl_2$ dependent versus $HgCl_2$ independent D_2O diffusion rates (Figure 3.13)

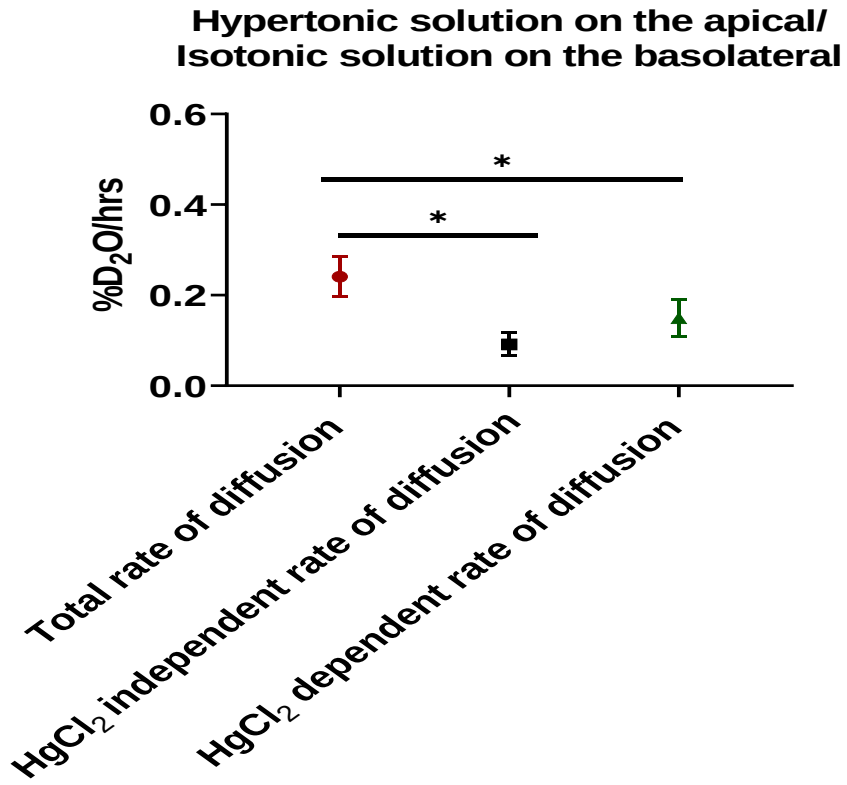

Figure 3.13 Comparison of the mean D_2O diffusion rates in absence and presence of $HgCl_2$ with hypertonic solution on the apical and isotonic solution on the basolateral side of the pig bladder mucosa strip.

There was a significant difference between the total versus $HgCl_2$ dependent and $HgCl_2$ independent D_2O diffusion rates. There was no significant difference between the $HgCl_2$ dependent versus $HgCl_2$ independent D_2O diffusion rates. The mean D_2O diffusion rates were compared using a repeated measures one-way ANOVA followed by a Newman-Kleus post-hoc test. *$p<0.05$, Data are expressed as mean ± SEM of 3 independent repeats (n=3).

3.4.6 Comparison of Total, $HgCl_2$ Dependent and $HgCl_2$ independent D_2O Diffusion Rates across Pig Bladder Mucosa under Different Osmotic Conditions

The calculated mean D_2O diffusion rates (total, $HgCl_2$ dependent and $HgCl_2$ independent) were compared between mucosa strips subjected to different osmotic conditions (Figure 3.14). There were no significant differences ($p=0.3558$) detected when comparing the total D_2O diffusion rates between hypotonic apical/ hypertonic basolateral versus hypertonic apical/isotonic basolateral versus hypotonic apical/ isotonic basolateral treatments (Figure 3.14A). There were also no significant differences ($p=0.5537$) in $HgCl_2$ dependent D_2O diffusion rates between hypotonic apical/ hypertonic basolateral versus hypertonic apical/isotonic basolateral versus hypotonic apical/ isotonic basolateral treatments (Figure 3.14B). There were also no significant differences ($p=0.3306$) in $HgCl_2$ independent D_2O diffusion rates between hypotonic apical/ hypertonic basolateral versus hypertonic apical/isotonic basolateral versus hypotonic apical/ isotonic basolateral treatments (Figure 3.14C).

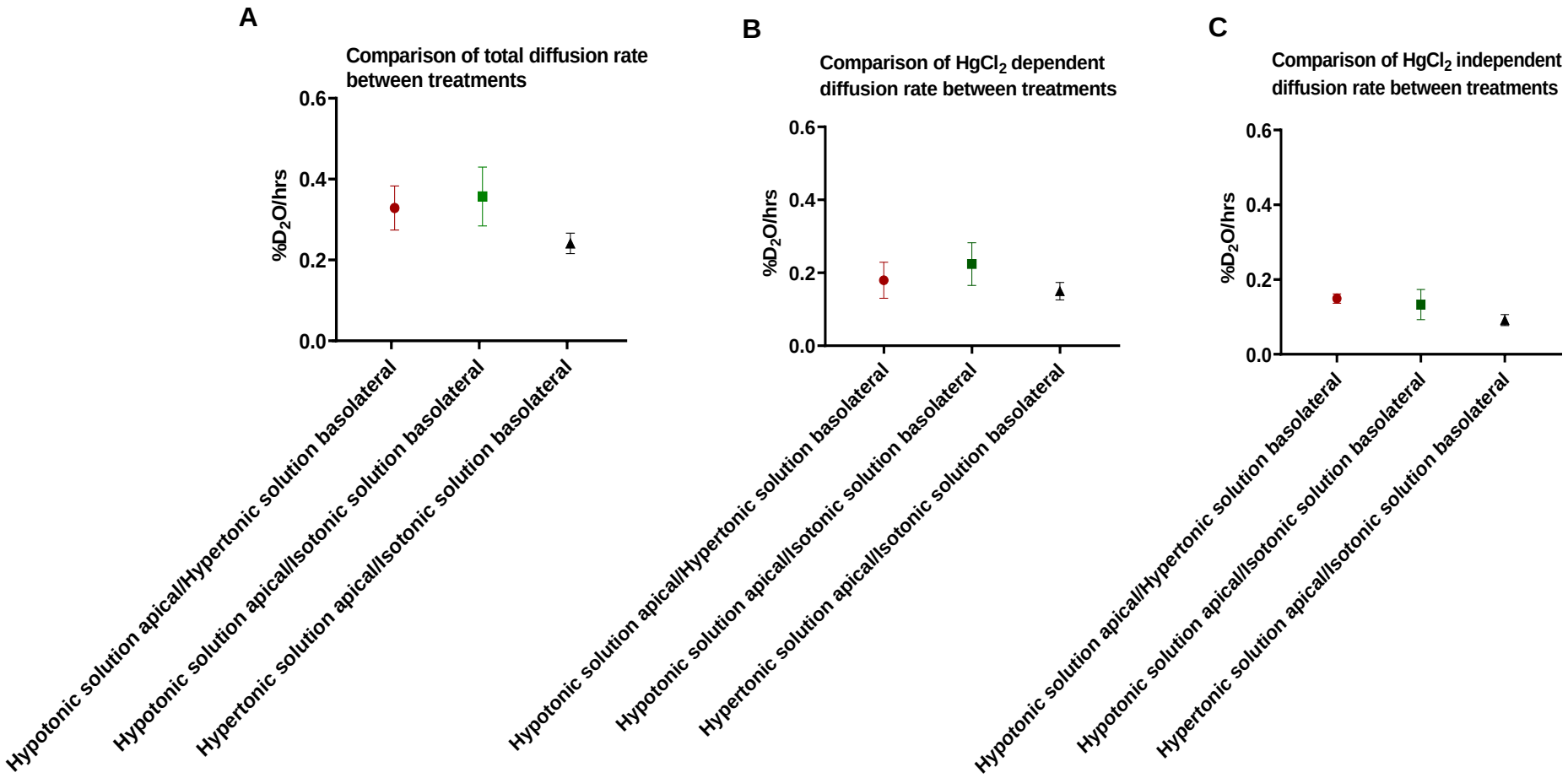

Figure 3.14 Comparison of mean total, $HgCl_2$ dependent and $HgCl_2$ independent D_2O diffusion rates across pig bladder mucosa under different osmotic conditions A) Comparison of mean total D_2O diffusion rates between different treatments, **B)** A Comparison of mean $HgCl_2$ dependent D_2O diffusion rates between different treatments, **C)** Comparison of mean $HgCl_2$ independent D_2O diffusion rates between different treatments,. D_2O diffusion rates were compared by one-way ANOVA followed by a Tuckey's post hoc test (n=3).Data are presented as mean+/- SEM

3.5 Discussion

The bidirectional movement of water and solutes has been demonstrated across the bladder urothelium of various species (Cahill et al., 2003; Englund 1959; Levinsky and Berliner 1959; Shafik et al., 2006; Shafik et al., 2005; Shafik et al., 2004; Walser et al., 1988). However, no studies so far have investigated the movement of water across pig bladder urothelium. In this study, movement of water across pig bladder mucosa mounted in an Ussing chamber setup was detected using isotopically labelled water (D_2O). However, this movement was only detected when the mucosa was subjected to an osmotic gradient, achieved by bathing the apical and basolateral sides of the mucosa in different osmotic solutions. The movement of D_2O was very low or nearly undetectable in absence of an osmotic gradient (when both apical and basolateral sides of the mucosa were bathed in isotonic solution), although a concentration gradient for D_2O existed across the mucosa membrane. This could suggest that without an osmotic gradient, there was not a strong enough driving force for movement of D_2O across the mucosa membrane. The low transurothelial D_2O flux under isotonic conditions could be due to the special properties of the urothelial cells. These cells contain junctional complexes which is a zone of attachment between adjacent urothelial cells and is located at the intersection of their apical and lateral membranes (Khandelwal *et al.,* 2009). The zone of attachment includes tight junctions and adherens junctions, both of which form continuous belts around the cell, as well as desmosomes (structure that allows adjacent cell to be attached) (Khandelwal *et al.,* 2009). Claudins also play an important role in regulating paracellular transport (Montalbetti *et al.,* 2015). These proteins provide a mechanism to limit paracellular water and ion flow across the uroepithelial tissue (Khandelwal *et al.,* 2009).

By introducing the mucosa strip to an osmotic gradient (achieved by bathing the apical and basolateral sides of the mucosa with different osmotic solutions) movement of D_2O was detected after nearly 6 hours of equilibration. Many studies have reported that changes in osmotic gradient causes increase water fluxes which is facilitated by AQPs (Yasui *et al.,* 2008; Benfenati *et al.,* 2011; Rubenwulf *et al.,* 2012; Kitchen *et al.,* 2015). Also, several studies have demonstrated that AQPs are translocated from the intracellular compartment to cell membrane when osmotic gradient is created between intracellular and extracellular osmolarity (Benfenati *et al.,* 2011; Kitchen *et al.,* 2015). This suggesting that AQPs are involved in restoring the changes in osmolarity.

It was observed in this study that 6 hours equilibration time was needed before D_2O could be detected on the basolatareal side. Studies that have looked at AQP mediated water fluxes and AQP translocation to the cells membrane have all reported different time of duration before water fluxes of AQP trafficking could be detected (Yasui *et al.* ,2008; Conner *et al.,* 2010; Garcia *et al.,* 2001; Kitchen *et al.,* 2015). An explanation for the variation in time amongst all these experiments including this current study could suggest different signalling processes and pathways for both AQP protein phosphorylation and AQP protein synthesis in different cell lines and tissues.

3.5.1 AQP dependent D_2O movement across pig bladder urothelium

In this current study, D_2O movement across pig bladder mucosa under three different osmotic conditions was demonstrated: (i) hypotonic solution on the apical side and hypertonic solution on the basolateral side of the mucosa membrane; (ii) hypertonic solution on the apical side and isotonic solution basolateral; (iii) hypotonic solution on the apical side and isotonic solution on the basolateral.

The movement of D_2O observed in all three conditions is believed to be transcellular D_2O movement facilitated by AQP channels. This conclusion was drawn by the observation that when the mucosa strip was exposed to $HgCl_2$, which is known as AQP selective inhibitor, a noticeable reduction in D_2O movement was seen. Rubenwulf et *al* (2012) has also reported similar finding. They demonstrated that AQPs contribute to transurothelial permeability *in vitro* and the transurothelial permeability was modulated by exposing cells to 500mosm/kg NaCl supplemented medium for 48 hours (Rubenwulf *et al.,* 2012). Movement of water and urea was detected after 25 minutes which was sustained for six hours. AQPs function was abolished when urothelial cells were exposed to $HgCl_2$ (Rubenwulf *et al.,* 2012). Their study in addition to this current study suggest that AQPs present in the urinary bladder urothelium are able to respond to the continuous changes in osmolarity and as a result, water is transported through AQP channels across the urothelium.

In this current study, there was no significant difference in the movement of D_2O between hypotonic/isotonic, hypertonic/hypotonic and hypotonic/hypertonic experimental set up in the presence and absence of $HgCl_2$. This finding reported herein was considered in the light of some limitations. A key limitation in this study was the sample size. Three reapeats were performed for each experimental set up and the calculated diffusion rate values for two repeats were similar with the third value showing a large deviation. Due to the small sample size, interpretation of the results, in particular confidence interval and p-value may not demonstrate the true effect and as a result, false positive or false negative conclusion can be made. Therefore, these results were interpreted with caution and will served as groundwork for larger confirmatory studies where the sample number is larger (six or above) to generate more accurate and reliable results.

AQPs are inhibited by ‘mercury salts’ and other metal ion inhibitors but few other and more specific, organic AQP inhibitors have been defined (Brooks *et al.,* 2000; Huber *et al.,* 2007; Huber *et al.,* 2009; Migliati *et al.,* 2009; Mola *et al.,* 2009). All AQPs channels are structurally comparative (Nesverovs *et al.,* 2019) and thus similar mechanisms of inhibition of AQPs identified in pig urinary bladder is likely. Though $HgCl_2$ inhibition of AQPs in this study and in Rubenwulf *et al.,* (2012) study was seen, previous studies have also shown that water movement occurs through channels other than AQPs and some of these channels are not inhibited by $HgCl_2$. Therefore, in this study, a second transcellular mechanism for D_2O movement other than AQPs needs to be considered.

3.5.2 Other possible channels involved in D_2O transport

The absence of complete inhibition of D_2O movement with $HgCl_2$ in this current study has been attributed to paracellular transport of D_2O but studies have shown that transcellular movement of water can be mediated by available surface channels other than AQPs (Fischbarg *et al.,* 1990; Fischbarg *et al.,* 1990; Solomon *et al.,* 1983) Transport of water across the plasma membrane are in part controlled by additional proteins located in the membrane that may include ion pumps, ion channels and ion exchange proteins as well as transient receptor potential (TRP) channels. It has been demonstrated that water transport also occurs through certain membrane transport proteins such as the glucose transporter (Fischbarg *et al.,* 1990) and Cl^- channel (Solomon *et al.,* 1983). Glucose transporters and Cl^- channels are found in most mammalian cells including urinary bladder urothelial cells (Haines, 1994). These channels transport only small amounts of water, firstly as there are few channels in the membrane and secondly because the gating of these Cl- channels open briefly

(Haines, 1994). However they provide another possible explanation for D_2O movement independent of AQP water channel and passive diffusion.

3.5.3 Comparison of mean Total, $HgCl_2$ Dependent and $HgCl_2$ independent D_2O Diffusion Rates across Pig Bladder Mucosa under Different Osmotic Conditions

Previous studies have reported that transurothelial permeability is modulated by NaCl (Rubenwulf *et al.,* 2012). Therefore, because changes in solutes were introduced in the solution used in this experiment where NaCl was normal in hypertonic solution but it was halved for isotonic solution and hypotonic solution, AQP mediated D_2O diffusion rates between the different treatments conditions used above were compared. The two experimental conditions (i) isotonic condition on the basolateral side, hypotonic condition on the apical side; ii) isotonic condition on the basolateral side, hypertonic condition on the apical side were design to in part simulate the physiological condition of mammals. No significant differences were seen between these two conditions. Rubenwulf e*t al.,* (2012) study reported a significant increase in water and urea flux across an osmotic gradient when urothelial cells were exposed to hypertonic conditions. Their studies did not include hypotonic solution studies (Rubenwulf *et al.,* 2012). In their study, AQP3 expression was also upregulated by increased osmolality (Rubenwulf *et al.,* 2012). The observation in this current study does not reflect the same findings observed in Rubenwulf *et al.,* (2012) studies, because, here we demonstrated that both hypertonic and hypotonic caused increase movement of D_2O. Earlier studies done by Presten *et al.* (1992) showed that transfection of AQPs in *Laevis* oocytes that were exposed to hypotonic medium resulted in immediate swelling (Preston *et al.,* 1992; Agre, 2006).

Moreover, HEK293 cells exposed to hypotonic solution (107-125 mOsm/kg) for one hour caused AQP1 to translocate to the cell membrane which eventually caused an increase in cell volume after 30 seconds of hypotonic solution exposure, suggesting that hypotonic solutions could be involved in the immediate translocation of AQPs to the cells membrane as an immediate response to regulate intracellular and extracellular fluid homeostasis and to balance the osmotic stress exposed to cells. Therefore, in this study, the increase diffusion rate in of D_2O hypertonic and hypotonic solution could be due to increase AQP trafficking to the plasma membrane to regulate the urothelial cell volume exposed to in particular hypotonic shock.

In addition, previous studies have shown that AQP proteins in urothelial cells are located surrounding both the apical and basolateral membrane of the cells (Rubenwulf *et al.,* 2009), suggesting that although water permeates from the apical luminal side of the umbrella cells, regulatory volume decrease in the urothelial cells may occur via basolateral movement of water back to the systemic circulation to achieve homeostatic balance. While existing data have not reported AQP-mediated water movement to the systemic circulation, a body of data prior to the discovery of AQPs have shown that bidirectional fluid movement across mammalian urinary bladder urothelium occurs (Hohlbrugger 1987; Levinsky and Berliner, 1959; Rapoport *et al.,* 1960; Turnbull and Fellow, 1972; Walser *et al.,* 1988).

This study demonstrates consistant water movment between all mucosa strips after 5 hours incubation with various tonicity when a gradient was created between the apical and basolateral side. This study adds on to the existing knowledge on emerging roles of the urinary bladder urothelium in regulating urinary bladder function.

Chapter 4

Investigating the Effect of Tonicity on AQP3 Localisation

4.1 Introduction

Similar to many other proteins, regulation of AQP abundance and function can be achieved by several mechanisms: 1) direct regulation of AQP gene expression or protein degradation 2) altering the number of AQP proteins present in the cell membrane via exo- or endocytosis (Balkom *et al.,* 2002, Nedvetsky *et al.,* 2009) and 3), by altering the gating of AQP channels via conformational changes where AQP channels are opened and closed (Sorensen *et al.,* 2013; Reichow *et al.,* 2013; Kalman *et al.,* 2008). Regulation of cellular osmolarity to maintain osmotic homeostasis despite the influence of external factors can be achieved through short-term and long-term regulation of AQPs, (Halsey *et al.,* 2018). Most AQPs were previously considered to be constitutively expressed in the plasma membrane of various cells (Verkman, 2011). This assumption was largely based on the fact that the first AQP protein discovered (AQP1) was identified in the membrane of erythrocytes (Preaston *et al.,*1992). Moreover, because earlier studies investigating AQPs reported AQPs expression on membrane of different cells, AQPs were predominantly referred to as "constitutively" expressed plasma membrane channels with the exception of AQP2 and AQP6 (Verkman., 2005) AQP2 and AQP6 studies showed that these channels reside in the membrane (Yasui *et al.,* 1999; Verkman, 2005). However, emerging studies shows that subcellular localisation of various AQPs are observed in some tissues and these AQPs are translocated to the plasma membrane in response to external stimuli such as changes in osmolarity (Gradilone *et al.,* 2005; Calamita *et al.,* 2005; Conner *et al.,* 2012; Huebert, *et al.,* 2002). Changes in osmolarity in HEK293 cells showed that AQP1 can be trafficked reversibly to the plasma membrane in response to altered tonicity (Conner *et al.,* 2010). This process was identified to be mediated by PKC and microtubule. Membrane localisation of AQP1 was found to increase in a time

dependent manner when HEK293 cells were exposed to diluted DMEM (Conner *et al.,* 2010). They demonstrated that membrane localization of AQP1, was 26 ± 3% in control experiment exposed to non-diluted DMEM. Following replacement of DMEM with diluted DMEM, the relative level of membrane expression in the same cells was 77 ± 2% (Conner *et al.,* 2010). The increase in AQP1 abundance in the cell membrane induced by hypotonic solution occurred over a span of 10 secs demonstrating rapid intracellular signalling process in AQP1 translocation to the membrane. When the HEK293 cells were removed from diluted DMEM and placed in normal DMEM, these HEK293 cells showed a cytoplasmic expression profile for AQP1 similar to that initially observed in the non-diluted DMEM (relative level of membrane expression of 26 ± 3%) (Conner *et al.,* 2010) suggesting a rapid reversible trafficking of AQP1 to membrane in response to osmotic stress (hypotonic) and internalisation of AQP1 from the membrane upon removal of osmotic stress.

A different study also investigated AQP3 localisation in keratinocyte and found AQP3 cytoplasmic localisation. AQP3 was translocated to the cell membrane of cultured human keratinocytes following a 2 h osmotic stress with 200 µM sorbitol (Garcia *et al.,* 2011). The study further revealed that AQP3 was localized near the plasma membrane shortly after an osmotic stress, but that the effect was no longer observed 24h after removal of the osmotic stress (Garcia *et al.,* 2011) demonstrating similar reversible trafficking of AQP3 in response to hypertonicity. These two studies also demonstrate that both hypotonic and hypertonic solution causes trafficking of AQP and that changes in osmolarity is a key factor in regulating AQP trafficking.

Subcellular localisation of AQP and trafficking of AQP to the plasma membrane as a response to external influence other than changes in osmolarity has also been reported for AQP4. AQP4 is known to be highly expressed in glial cells of the central

nervous system and facilitates the osmotically driven pathological brain swelling associated with stroke and traumatic brain injury. Cell surface expression of AQP4 was demonstrated to be rapidly and reversibly regulated in response to changes of tonicity in primary cortical rat astrocytes and in transfected HEK293 cells (Kitchen *et al.,* 2015). AQP4 membrane localization increased 2.7-fold after ten min of hypotonic challenge at 85 mosM/kg of H_2O but did not change significantly after ten min of hypotonic challenge with another hypotonic solution of 140 mosM/kg of H_2O (Kitchen *et al.,* 2015) Demonstrating that hypotonic condition can induce sub cellular localisation of AQP4 to traffic to the membrane. The translocation mechanism was found to involve PKA activation, influx of extracellular calcium, and activation of calmodulin (Kitchen *et al.,* 2015).

Epinephrine has also been found to translocation of AQP3 from the cytoplasmic fraction to the plasma membrane in Caco-2 cells within 60 min. Epinephrine induced membrane trafficking of AQP3 was found to be mediated through the signal pathway GqPCR–PLC–PKC in Caco-2 cells (Yasui *et al.,* 2008). Though, the primary signal in this study was not changes in osmolarity, this study demonstrate subcellular localisation of AQP3 and perhaps epinephrine induces AQP3 synthesis and trafficking to the plasma membrane.

AQPs identified in the urothelium of human urinary bladder cells lines showed increase transurothelial water movement upon exposure to hypertonic solution. Furthermore, the expression of AQP3 was found to be increased in hypertonic solution as a result of increased NaCl (Rubenwulf *et al.,* 2012). Although this study did not focus on AQP3 trafficking but rather increased AQP3 protein levels, the study further support the influence of changes in osmolarity on AQP.

It is interesting to note that these studies collectively reported that translocation of AQPs to the plasma membrane was observed at different time points. Kitchen *et al.,* (2015) showed hypotonic induced AQP4 trafficking to the membrane in ten min, Gracia *et al.,* (2011) showed hypertonic induced AQP1 trafficking to the membrane in 2 hrs, Yasui *et al.,* (2008) showed epinephrine induced AQP3 trafficking to the membrane in one h and Conner *et al.,* (2010) demonstrated hypotonic induced AQP1 trafficking to the membrane in ten sec. The time variation observed in these studies could suggest different intracellular signalling pathways. Moreover, while these studies collectively shows AQP trafficking as a result of changes in osmolarity, considering osmotic induce AQP synthesis as reported by Rubenwulf *et al.,* (2012) followed by AQP trafficking to the plasma membrane in some of these studies could also explain the variation in time for AQPs translocation to the plasma membrane reported by the different studies.

Although these studies have demonstrated that changes in osmolarity is involved in AQP function, expression and translocation, the mechanism by which AQPs that have been identified in the urinary bladder are regulated is still unknown. To date, no studies have reported if increase or decrease osmolarity results in AQP gating or translocation in the urinary bladder. In chapter 2, AQP1, 3, 9 and 11 were identified in the urinary bladder of pig urothelium with AQP1 expressed in the suburothelial area and AQP3, 9 and 11 in the urothelial cells. Here, AQP3 appeared to be most abundantly expressed in the urothelial cells, therefore, a decision was made to investigate the osmotic effect on AQP3 in the urinary bladder.

4.2 Aims of the Study

Hypotonic effect on AQPs localisation have been reported in other studies in different tissues. Though AQP3 expression in response to hypertonicity have been reported in Normal Human Urothelial (NHU) cell line, the effect of hypertonic and hypotonic solution on AQP3 localisation within urothelial cell has not been reported. Therefore, this chapter is to identify the effect of hypotonic and hypertonic solution on AQP3 localisation.

4.2.1 Specific objectives

- To Isolate urothelial cells from pig bladder containing all the different population of urothelial cells (umbrella cells, intermediate cells, basal cells)
- To determine the localisation of AQP3 within urothelial cells in untreated cells using immunochemical experiments
- To determine the localisation of AQP3 within treated urothelial cells using immunohistochemistry
-

4.2 Methods

4.2.1 Tissue Preparation

Female pig (*Sus scrofa domestica*) bladders were obtained as previously described. The bladder was immediately filled with 20 ml Hank's Balanced Salt Solution (HBSS) digestion buffer that consisted of 1% HBSS, 5 mM EDTA and 10 mM hepes (pH was adjusted to 7.4 using sodium bicarbonate) for transportation. From each whole bladder dome, the trigone region was dissected off the bladder body and was then folded inside out so that the urothelium was facing outwards. The bladder base was sealed with a 22 G 2 inches syringe needle and submerged in 100 ml HBSS digestion buffer

4.2.2 Isolation of Cells from the Urinary Bladder Urothelium

Urothelial cells were isolated from the whole bladder of five different pigs by gentle titration during the incubation time where the tissue was submerged in 100 ml of HBSS digestion buffer for one hour at RT. After gentle titration, a cell scrapper was used to scrape off the urothelial cells to ensure maximum collection of basal cells. The whole bladder was discarded and the collected cells suspended in HBSS digestion buffer was initially allowed to sit in a 50 ml falcon tube for 1 min to remove the bottom heavy debris followed by 25 min to allow the cells to set at the bottom. About 80 ml of the top HBSS digestion buffer was gently removed ensuring the bottom HBSS digesting buffer containing the cells was not disturbed. The cell suspension was centrifuge at 600g for five min. Clear lysate liquid at the top was removed and the cell pellet at the bottom was resuspended in 1 ml of PBS.

4.2.3 Cell Counting

A sample was taken from each preparation and counted using an improved Neubauer haemocytometer stage. The percentage of viable cells was visually determined by the proportion excluding Trypan blue (0.4 % solution) purchase from ThermoFisher scientific (UK): 100 µl added to a 100 µl sample of the cell suspension. The three urothelial cell population large (umbrella cells), medium (intermediate cells) and small-sized (basal cells) assessed visually with each experiment to ensure all of the different cell populations were present.

4.2.4 Treatment of Isolated Urothelial Cells

The isolated pig bladder urothelial cells were suspended in PBS. The cell suspension in PBS was subsequently divided into 15 ml falcon tube containing 10 ml of 407 mosM/kg hypertonic, 96 mOsM/kg hypotonic and 289 mOsM/kg isotonic solutions with the composition described (table 3.2) at RT. Additional 15 ml falcon tubes were made containing duplicate of the hypertonic, hypotonic and isotonic solution. Isotonic solution served as a negative control as it had a physiological osmolarity of 289 mOsM/kg. Isolated urothelial cells in 407 mosM/kg hypertonic and 96 mOsM/kg hypotonic was allowed to incubate for 4 and 5 hrs at RT. 4^{th} and 5^{th} hours incubation time was chosen because in chapter 3, movement of water (D_2O) was observed after the 5^{th} hour (Figure 3.6). The 4^{th} hour incubation time was included to determine whether an ealier time point will show any significant differences in AQP3 staining profile compared to the 5^{th} hour time point. Cells in 289 mOsM/kg isotonic solution were

allowed to incubate for five hours. These control cells in isotonic solution are further referred to as non-treated cells.

4.2.5 Immunocytochemistry

After each incubation period with 407 mosM/kg hypertonic 96 mOsM/kg hypotonic 289 mOsM/kg isotonic and a negative control Krebs solution, isolated cell suspensions were centrifuge at 600 g for five min and then washed three times with PBS followed by fixing with 250-500 µl of ice-cold methanol, depending on the cell density, for ten min. The cell suspension were washed three times with PBS and centrifuged at 600 g for five min each time. The cells were then incubated with 100 mM glycine (pH 8.5 in PBS) followed by incubation with 10% foetal bovine serum (FBS) in PBS for 5 min. The cells were permeabilised with 0.2% Triton X-100 in PBS for 20 min, then washed 3x with PBS. Cell suspension was incubated with 3% BSA in PBS at RT for one hour to block non-specific binding sites. With the exception of the negative control cells, all the cells were then incubated with Cytokeratin 7 primary antibody raised in mouse, and AQP3 primary antibody raised in rabbit (cytokeratin 7, 1:1000, AQP3 1:500, prepared in 3% BSA/PBS) separately for 1 hour each at room temperature with each antibody. The cells were then washed 3x 5 min with PBS. Secondary antibodies, Alexa Fluor 488 goat anti-rabbit (dilution) and Alexa Fluor 647 donkey anti-mouse (dilution), were prepared in 3% BSA/PBS and then added to all the samples including the negative control cells and incubated for one hour for each secondary antibody at room temperature. Excess secondary antibodies were removed by 3x 5 min PBS washing after incubation and the cell suspension was incubated with DAPI nuclear stain for ten min. Excess DAPI was removed by washing cell suspension 3x with PBS. 20 µl of

labelled cell suspension were placed on slides and mounted using VECTASHIELD® Antifade Mounting Medium. Imaging was performed using Nikon Ti Eclipse x 40 magnification.

4.3 Results

4.3.1 AQP3 Localisation in Non-Treated Pig Urinary Bladder Urothelial Cells

The expression of AQP3 in isolated primary urothelial cells were investigated in non-treated cells where the cells were incubated in 289 mOsM/kg isotonic solution for five hours. Immuno staining with anti-AQP3 antibody demonstrated cytoplasmic localisation of AQP3 with distinct localisation around the nucleus. DAPI was used to stain the nucleus and is shown in blue. Figure 4.1 is a representative image of non-treated primary urothelial cells (n=3) all displaying a similar intracellular localisation profile.

The ratio of urothelial cells containing AQP3 and cells which did not contain AQP3 was not quantified due to the blurriness of some areas of the prepared slide. Therefore, accurate quantification could not be done.

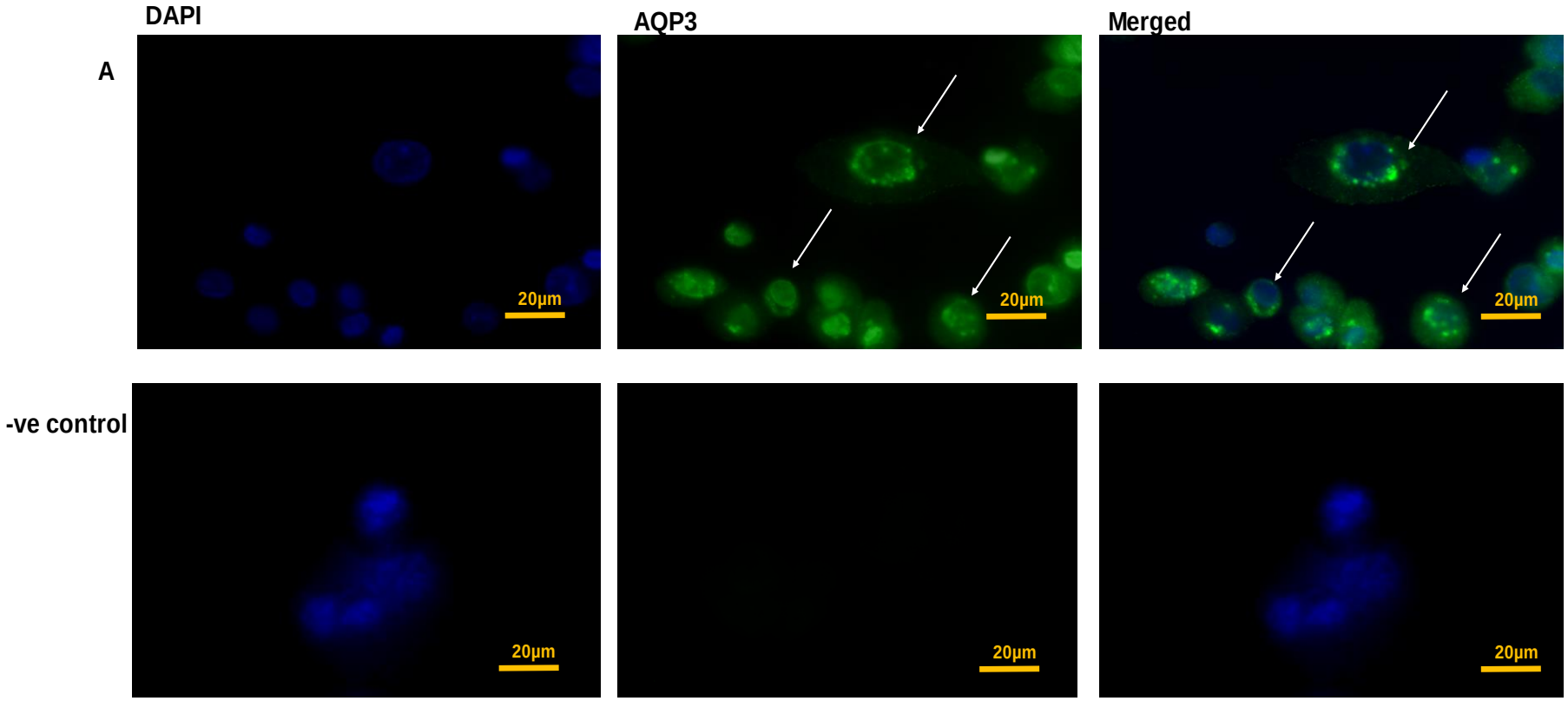

Figure 4.1 AQP3 immunofluorescence labelling of non-treated isolated pig urothelial cells

Isolated urothelial cells kept in 289 mOsM/kg isotonic solution for five hours were stained with rabbit polyclonal anti-AQP3 antibody in 1:500 dilution, and DAPI nucleuse stain. **A)** AQP3 was detected throughout the cytoplasm of the isolated urothelial cells, with distinct localisation around the nucleus. –ve control is in the absence of AQP3 primary antibody. The images shown above are representative of three independent experiments.

4.3.2 AQP3 localisation/ Immunofluorescence Labelling in Isolated Pig Urothelial Cells Following Four Hours Incubation in Hypotponic Krebs Solution

To test the effect of hypotonicity on AQP3 localisation, urothelial cells isolated from pig bladders were incubated in hypotonic Krebs solution for four hours. Cytokeratin 7, urothelial specific marker, was used to identify the isolated urothelial cells. Immunostaining with an anti-AQP3 antibody suggested increased trafficking and plasma membrane localization of AQP3 following incubation of isolated urothelial cells in hypotonic solution. Figure 4.2 is a representative image of four hours treatment of primary urothelial cells (n=3) all displaying a similar intracellular localisation profile.

The ratio of urothelial cells containing AQP3 and cells which did not contain AQP3 was not quantified due to the blurriness of some areas of the prepared slide. Therefore, accurate quantification could not be done.

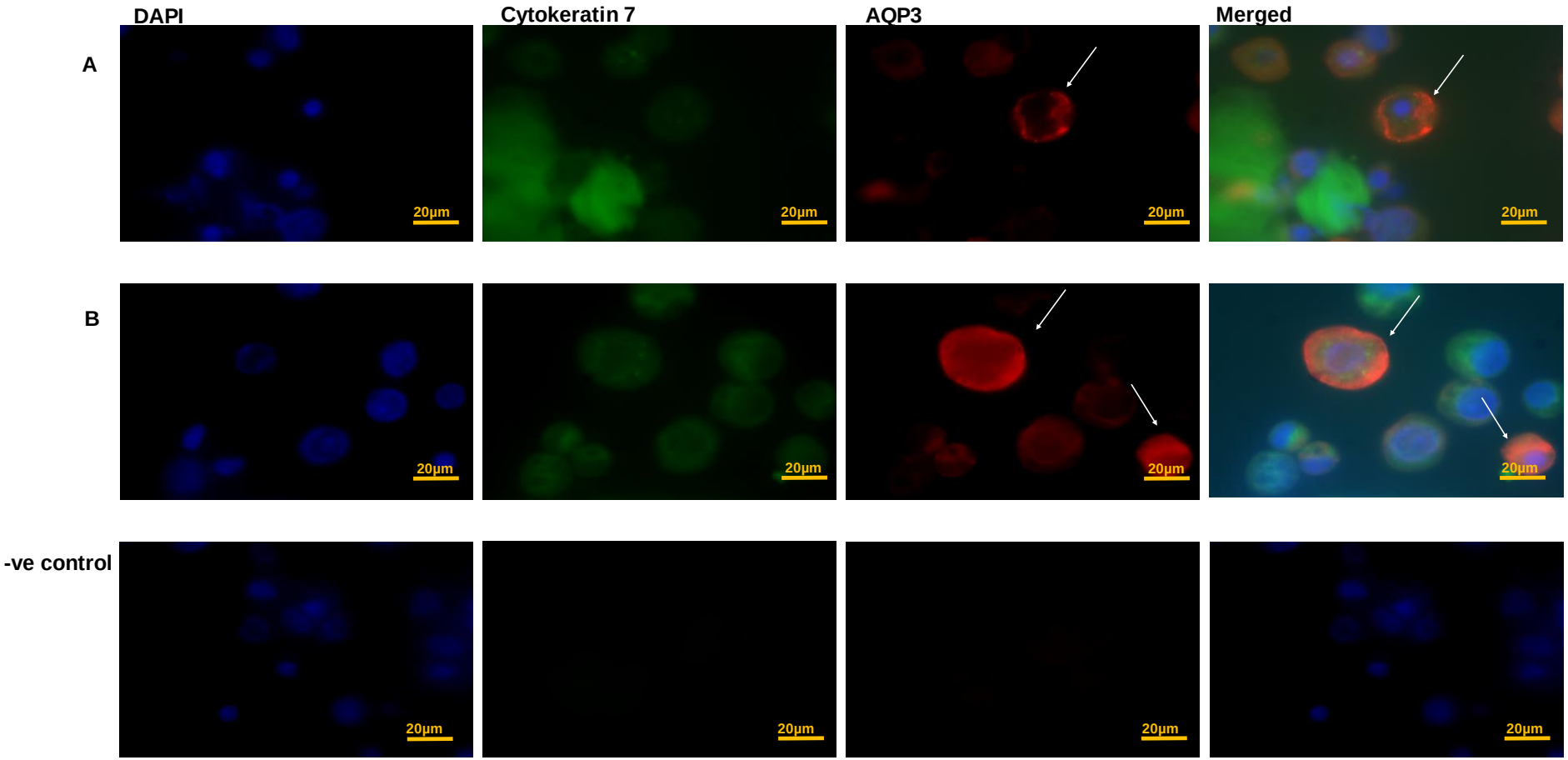

Figure 4.2 AQP3 immunofluorescence labelling in isolated pig urothelial cells following incubation with hypotonic Krebs solution

Isolated urothelial cells kept in 96 mOsM/kg hypotonic Krebs solution for four hours were stained with rabbit polyclonal anti-AQP3 (red) antibody in 1:500 dilution, mouse monoclonal anti-cytokeratin 7 (green) antibody in 1:1000 dilution and DAPI (blue). **A&B)** AQP3 labelling suggested increased trafficking and plasma membrane localisation. –ve control is in the absence of AQP3 primary antibody. Figures are representative of three independent experiments.

4.3.3 AQP3 Localisation/ Immunofluorescence Labelling in Isolated Pig Urothelial Cells Following Five Hours Incubation in Hypotponic Krebs Solution

To test the effect of hypotonicity on AQP3 localisation, urothelial cells isolated from pig bladders were incubated in hypotonic Krebs solution for five hours. Cytokeratin 7, urothelial specific marker, was used to identify the isolated urothelial cells. Immunostaining with an anti-AQP3 antibody suggested increased trafficking and plasma membrane localization of AQP3 following incubation of isolated urothelial cells in hypotonic solution. Figure 4.3 is a representative image of five hours treatment of primary urothelial cells (n=3) all displaying a similar intracellular localisation profile

The ratio of urothelial cells containing AQP3 and urothelial cells which did not contain AQP3 was not quantified due to the blurriness of some areas of the prepared slide. Therefore, accurate quantification could not be done.

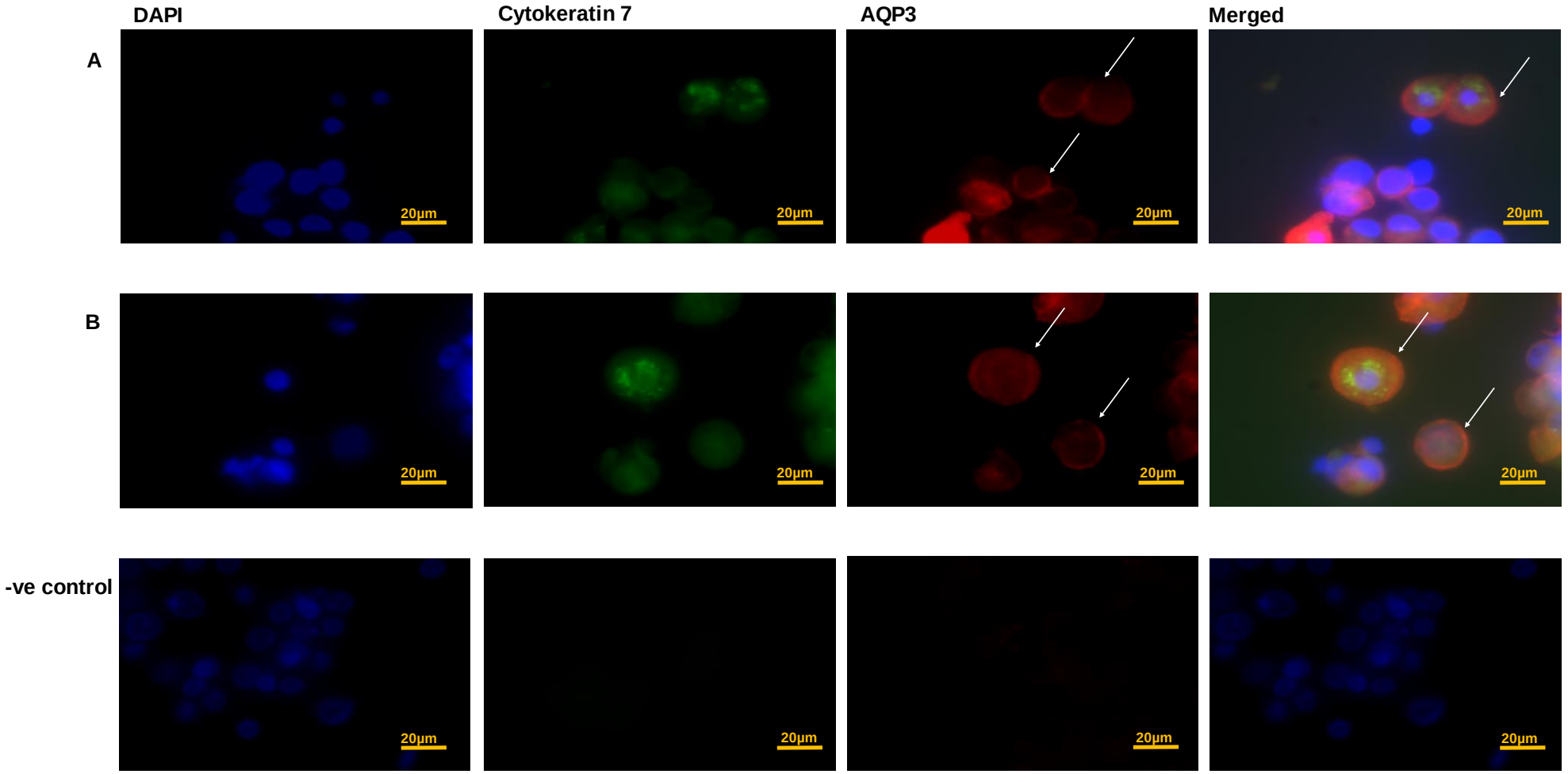

Figure 4.3 AQP3 immunofluorescence labelling in isolated pig urothelial cells following incubation with hypotonic Krebs solution

Isolated urothelial cells kept in 96 mOsM/kg hypotonic Krebs solution for five hours were stained with rabbit polyclonal anti-AQP3 (red) antibody in 1:500 dilution, mouse monoclonal anti-cytokeratin 7 (green) antibody in 1:1000 dilution and DAPI (blue). **A&B)** AQP3 labelling suggested increased trafficking and plasma membrane localisation. –ve control is in the absence of AQP3 primary antibody. Figures are representative of three independent experiments.

4.3.4 AQP3 Localisation/ Immunofluorescence Labelling in Isolated Pig Urothelial Cells Following Four Hours Incubation in Hypertonic Krebs Solution

To test the effect of hypertonicity on AQP3 localisation, urothelial cells isolated from pig bladders were incubated in hypertonic Krebs solution for four hours. Cytokeratin 7, urothelial specific marker, was used to identify the isolated urothelial cells. Immunostaining with an anti-AQP3 antibody suggested increased trafficking and plasma membrane localization of AQP3 following incubation of isolated urothelial cells in hypertonic solution. Figure 4.3 is a representative image of four hours treatment of primary urothelial cells (n=3) all displaying a similar intracellular localisation profile

The ratio of urothelial cells containing AQP3 and urothelial cells which did not contain AQP3 was not quantified due to the blurriness of some areas of the prepared slide. Therefore, accurate quantification could not be done.

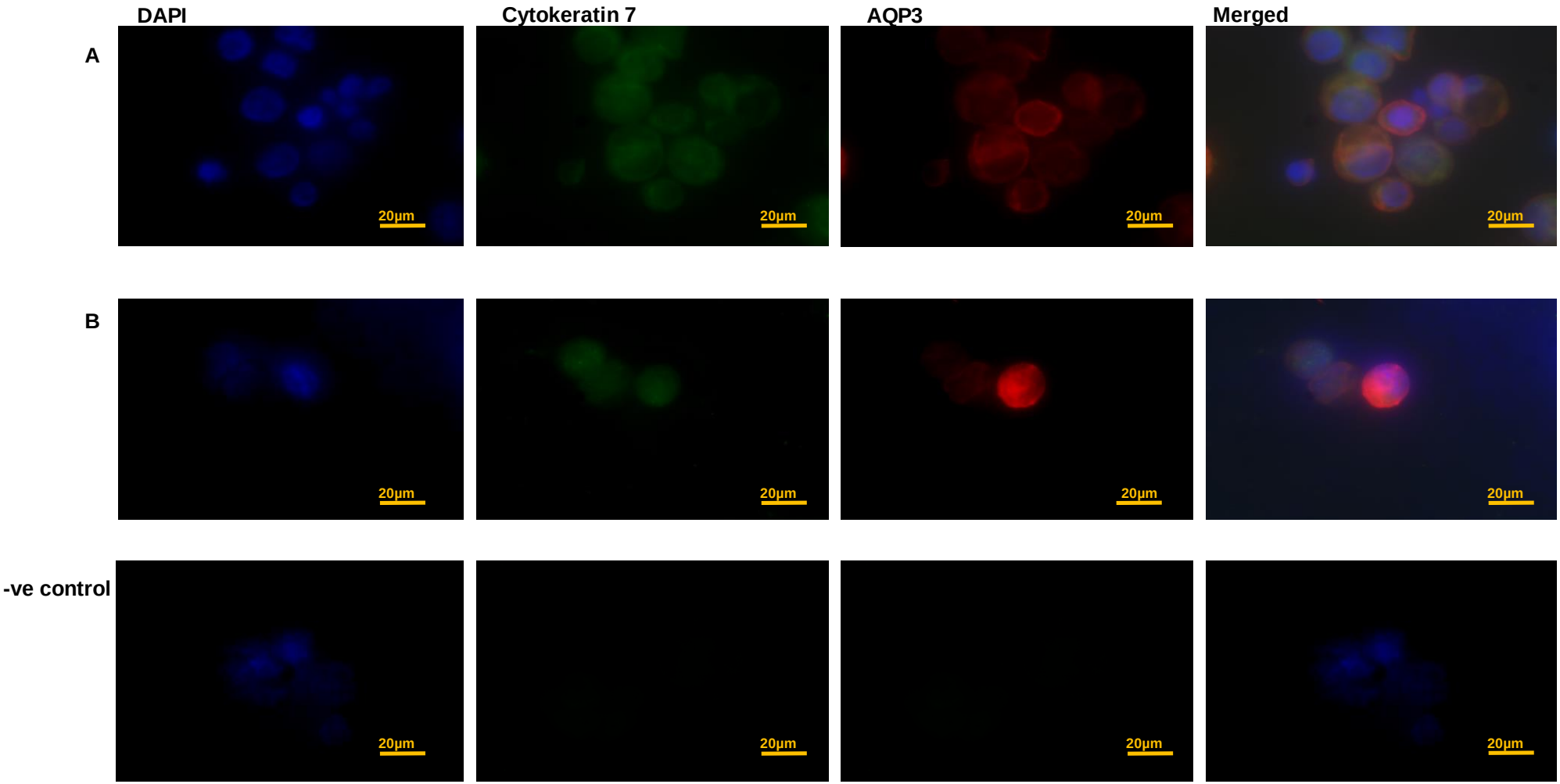

Figure 4.4 AQP3 immunofluorescence labelling in isolated pig urothelial cells following incubation with hypertonic Krebs solution

Isolated urothelial cells kept in 407 mosM/kg hypertonic Krebs solution for four hours were stained with rabbit polyclonal anti-AQP3 (red) antibody in 1:500 dilution, mouse monoclonal anti-cytokeratin 7 (green) antibody in 1:1000 dilution and DAPI (blue). **A&B)** AQP3 labelling suggested increased trafficking and plasma membrane localisation. –ve control is in the absence of AQP3 primary antibody. Figures are representative of three independent experiments.

4.3.5 AQP3 Localisation/ Immunofluorescence Labelling in Isolated Pig Urothelial Cells following five Hours Incubation in Hypertonic Krebs Solution

To test the effect of hypertonicity on AQP3 localisation, urothelial cells isolated from pig bladders were incubated in hypertonic Krebs solution for five hours. Cytokeratin 7, urothelial specific marker, was used to identify the isolated urothelial cells. Immunostaining with an anti-AQP3 antibody suggested increased trafficking and plasma membrane localization of AQP3 following incubation of isolated urothelial cells in hypertonic solution. Figure 4.3 is a representative image of five hours treatment of primary urothelial cells (n=3) all displaying a similar intracellular localisation profile

The ratio of urothelial cells containing AQP3 and urothelial cells which did not contain AQP3 was not quantified due to the blurriness of some areas of the prepared slide. Therefore, accurate quantification could not be done.

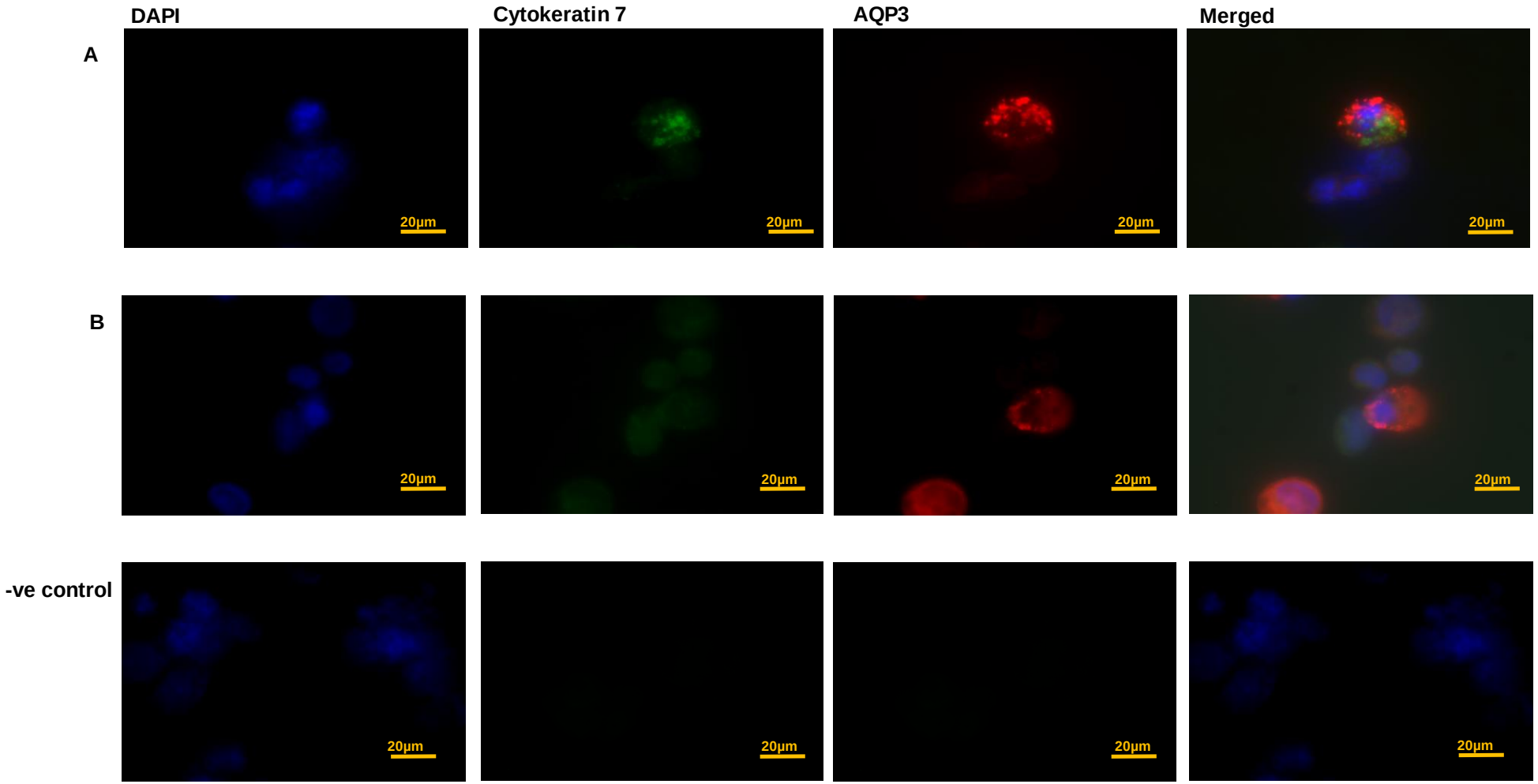

Figure 4.5 AQP3 immunofluorescence labelling in isolated pig urothelial cells following incubation with hypertonic Krebs solution

Isolated urothelial cells kept in 407 mosM/kg hypertonic Krebs solution for five hours were stained with rabbit polyclonal anti-AQP3 (red) antibody in 1:500 dilution, mouse monoclonal anti-cytokeratin 7 (green) antibody in 1:1000 and DAPI (blue). **A&B)** AQP3 labelling suggested increased trafficking and plasma membrane localisation. –ve control is in the absence of AQP3 primary antibody. Figures are representative of three independent experiments.

4.4 Discussion

In this study, different AQPs; AQP3, AQP9 and AQP11 have been identified in pig urinary bladder and they are presented in Chapter 2 results section. Out of these identified AQPs, AQP3 expression and protein levels in all the 3 different cell types of the urothelium was the most abundant. Because of this, AQP3 was chosen as the protein to investigate.

Urinary bladder urothelium is exposed to urine at different levels of osmolarity. AQP3, part of the aquaglycerolporin family and expressed by the urinary bladder urothelium, is continuously exposed to various urine tonicity. AQP3 exposed to different tonicity in the urinary bladder could play an important role in responding to the bladder content and in turn trigger urothelial mediated signalling processes to regulate the bladder function.

AQP3 is a water/glycerol/urea channel abundant in different tissues in the human body such as the kidney, skin, and the urinary bladder (Damiano *et al.,* 2001; Spector *et al.,* 2002; Pavlovic-Djuranovic *et al.,* 2006; Hara and Verkman, 2001; Boury-Jomot *et al.,* 2006) In view of the functional importance of AQP3 in transporting water, as well as solutes, such as glycerol and urea, the effect of different osmolarity on AQP 3 regulation was examined.

In the current study, isolated urothelial cells were exposed to isotonic Krebs solution and immune staining with anti-AQP3 antibody demonstrated cytoplasmic localisation of AQP3 with distinct localisation around the nucleus. This expression pattern of AQPs around the nucleus has also been identified in another study investigating AQP3 in MDCK cell lines (Arnspang *et al.,* 2013). AQP3 tagged with enhanced green fluorescent protein showed AQP3 localisation within the cytoplasm of the cells

(Arnspang *et al.,* 2013). Similar distinct pattern of AQP3 localisation around the nucleus was observed. MDCK cells were stained with Golgi marker G58 K and an overlay of both AQP3 tagged and Golgi staining showed colocalisation (Arnspang *et al.,* 2013). Considerable evidence show that the Golgi complex (Rodriguez-Boulan *et al.,* 2005) regulate sorting of apical and basolateral membrane proteins into separate vesicles in the exocytic and endocytic (recycling) pathways. Because the AQP3 localisation profile in Arnspang *et al.,* (2013) study shows similar AQP3 localisation in the isotonic urothelial cells in this study, It could be assumed that localisation of AQP3 around the nucleus could imply AQP3 localisation in the Golgi. Further studies are required for AQP3 double labelling with Golgi specific markers to confirm this assumption.

The effect of hypotonicity and hypertonicity on AQP3 localisation was examined in this study. Four and five hours as experimental time points were chosen because we found in chapter 3 that movement of water (D_2O) was mostly observed after five hours (Figure 3.6). Moreover, in chapter 3, traces of D_2O was seen in some of the experimental set up after four hours therefore, the fourth hour time point was included to determine whether there was a difference in AQP3 trafficking at fifth and fourth hour. AQP3 labelling suggested increased trafficking and plasma membrane localisation in urothelial cells exposed to both hypotonic and hypertonic solution for four or five hours. No differences were oberserved in AQP3 staining profile between the fourth and fifth hour time points. Two separate studies have reported similar findings in different cells types showing that both hypertonic and hypotonic solution causes AQP3 trafficking to the plasma membrane (Matsuzaki *et al.,* 2001; Garcia *et al.,* 2011).

Matsuzaki *et al.,* (2001) investigated the effect of hypertonicity on AQP3 expression in MDCK epithelial cells by exposing the cells to hypertonic medium containing raffinose

or NaCl. Northern blot and immunoblot analyses revealed that the amounts of AQP3 mRNA and AQP3 protein, respectively, were markedly increased by exposure of cells to hypertonicity (Matsuzaki *et al.,* 2001). In addition to the increased expression of AQP3, Immunofluorescence and immunoelectron microscopy also demonstrated that the abundance of AQP3 protein was increased in cells incubated in hypertonic medium for 24 h and that the protein was localized at the basolateral plasma membrane (Matsuzaki *et al.,* 2001). Garcia *et al.,* 2001 also demonstrated that Immunofluorescence staining of AQP3 in NHK cells revealed a cytoplasmic localization of AQP3 in a controls state when cells were not exposed to hypotonicity. Increased membrane staining was observed in cells that were treated with hypotonic osmotic stress (Garcia *et al.,* 2001)

These two studies suggest that both hypotonicity and hypertonicity causes AQP3 translocation, which is in agreement with this current studies as AQP3 translocation was seen in pig bladder urothelial cells when exposed to both hypertonic and hypotonic Krebs solution. This is not surprising as hypotonicity and hypertonicity are both considered to be a form of osmotic stress. Most cells have the ability to regulated external osmotic stresses by modifying cell volume.

The ability to control cell volume is essential for cellular function of every cell (Lang *et al.,* 1998; Wehner *et al.,* 2003; Hoffmann *et al.,* 2009). The mechanisms involved controlling cell volume include cell membrane proteins such as ion channels, transporters, ionic pumps and cytoskeletal proteins and AQPs (Conner *et al.,* 2012; Day *et al.,* 2013). Hypotonic or hypertonic disturbances in cell volume activate several signalling pathways, resulting in adaptive and protective effects in cells (Hoffmann *et al.,* 2009). Following an osmotic shock, changes in the volume of cells show two dynamic phases. In the first one, which lasts a few seconds to minutes, water rushes

osmotically across the plasma membrane primarily through paracellular water diffusion. In the second phase, the cell undergoes a process of volume regulation; induced cell swelling is followed by regulatory volume decrease (RVD), and induced cell shrinking is followed by regulatory volume increase (RVI) (Lang *et al.,* 1998; Hoffmann *et al.,* 2009). In view of this current study and existing studies of hypotonic and hypertonic effect on AQP3 trafficking, it could be suggested that in the event of hypertonic osmotic stress, urothelium cells respond by initiating RVI mechanism to offset the shrinking of the urothelial cell caused by the increase in tonicity, whereas in the event of hypotinic osmotic stress, urothelial cells respond by initiating RVD mechanism to offset the increase in cell volume caused by the decrease tonicity. Therefore, this process of RVD and RVI could initiate AQP3 translocation to the plasma membrane of the urothelial cell in restoring urothelial cell volume. The signalling pathways associated with regulatory volume control (RVC) appear to be cell-type dependent. The involvement of AQPs in RVC as a result of osmotic stress has been reported previously in other cells.

A study looking at mice fertility found that the sperm of AQP3 −/− mice did not undergo their normal RVD process, and these mice exhibited reduced fertility (Chen *et al.,* 2011; Chen and Duan, 2011). Normally, sperm encounter reduced extracellular osmolality (hypotonicity) which is believed to be a signal that activates sperm mortility (Chen and Duan, 2011). This hypotonic stress also causes the sperm to swell which if not corrected by RVD process, results is impaired fertility caused by excessive bending of the sperm tail with the uterus (Chen *et al.,* 2011). If AQP3 was simply acting passively as a water channel, RVD would not be stopped in AQP3 −/− mice but rather the timescale for which the cell reaches osmotic equilibrium would be increased. Another study done in human and murine salivary gland cells

demonstrated that TRPV4 has a functional interaction with AQP5: in AQP5 knockout cells, the hypotonicity-induced calcium influx through TRPV4 was attenuated and subsequent RVD was abolished. Hypotonicity also increased cell surface expression of both TRPV4 and AQP5 and increased their co-localisation (Liu *et al.,* 2006).

These studies shows that AQP3 is involved in RVC. Therefore, in urothelial cells, prolong exposure to hypotonic or hypertonic solution, which reflect urine content depending on the hydration status of the individual, could initiate AQP3 translocation to the plasma membrane to regulate urothelial cell volume.

Chapter 5

Overall discussion conclusion, and future work

5.1 Overall Discussion and Conclusion

In recent decades, one of the major forces driving lower urinary tract (LUT) research has been the aim of discovering potential new cellular targets for treatment of debilitating conditions such as nocturia. The consequence of these studies has been emergence of new insights into physiological function of the urinary bladder.

The main current treatments for nocturia are vasopressin V2 receptor agonist, Diuretics, selective α_1 adrenoceptor antagonists, antimuscarinics and many other which stimulate water reabsorption, reduce salt and water load, reduce activity in afferent pathways of micturition or reduce the generation of bladder afferent activity and frequency of voiding (Andersson and Kerrebroeck , 2018). These drugs do not directly treat nocturia but target other bladder disorder such as overactive bladder (OAB) and benign prostatic hyperplasia (BPH). However, a new concept of bladder urine absorption to increase the functional capacity of the bladder to avoid nocturia has been proposed (Watanabe and Azuma, 2015). By increasing fluid reabsorption, the need for waking up at night can be reduced significantly and as a result lead to alleviating nocturia symptoms.

It is now clear that bladder is not simply a storage bag that fills and empties with urine, it has an active role in regulating its own function, altering the final composition of urine stored in bladder and sensing the changes in its local environment (Birder, 2010).

The bladder urothelium and the suburothelial layers have been the subject of many studies so far especially in terms of their role in regulating the sensory function of the bladder (Birder, 2010; Birder and Andersson 2013). However, there is a clear lack of understanding on the role of these layers in altering the final composition of urine. The bidirectional movement of water and solutes across the urothelium has been

demonstrated in various studies (Hohlbrugger, 1987; Levinsky and Berliner 1959; Rapoport *et al*., 1960 Walser *et al*., 1988). However there are very limited studies which have looked at the mechanism through which this bidirectional movement is achieved. The discovery of AQPs in the bladder urothelium has provided the researches with a new target to further investigate this phenomenon. However, there are very limited studies in this area.

To date, only six studies have been reported on the relationship between AQPs and the mammalian urinary bladder; in rats and bears (Spector *et al.,* 2002; Spector *et al.,* 2015; Kim *et al.,* 2012) and in isolated human cells and cell lines (Rubenwulf *et al.,* 2009; Rubenwulf *et al.,* 2012; Rubenwulf *et al.,* 2014). Out of these studies, only four studies have focused on the expression profile of AQPs in the urinary bladder (Spector *et al.,* 2002; Spector *et al.,* 2015; Rubenwulf *et al.,* 2009). Rubenwulf *et al.* (2009) identified AQPs in the urinary bladder using freshly isolated urothelial cells and NHU cell lines and identified AQP 3, 4, 7, 9 and 11. (Spector *et al.* (2002) reported the expression of AQP1, 2, 3 in rat urinary bladders using isolated cells and they also demonstrated that dehydration causes an increase in AQP expression (Spector *et al*., 2002). A subsequent study demonstrated that hibernating bears urinary bladder urothelium contain AQP1 and 3, however their exact localisation was not reported.

Therefore in an attempt to further elucidate the role of AQPs in altering the final composition of urine, this study aimed to investigate the expression and possible function of these channels in adult pig urinary bladder, a close model to human bladder function (Parson *et el.,* 2012). In the initial stages of the current study, (Chapter 2) the expression of AQP subtypes was investigated in pig urothelium and suburothelium.

Briefly, in this study, AQP 1 was identified in the arterioles and capillary in the lamina propria which was confined in the mucosa area. This is in line with the studies that have reported AQP expression in the urinary bladder (Spector *et al.,* 2002; Rubenwulf *et al.,* 2012). AQP3 was found evenly distributed across the urothelial in all 3 different cell types (Umbrella, intermediate and basal cells). However, Rubenwolf *et al.* (2009) reported that AQP3 was located especially at the intercellular borders of basal and intermediate cells. The variation in AQP3 distribution in these species could be due to the presence of orthodox AQPs such as AQP4 in NHU cells which was found in all three different urothelial cells types (Rubenwulf *et al.,* 2009). This could suggest that the need for water transport in NHU cells may be much greater than the need for solutes transport. AQP9 was detected more on the apical surface of the pig urothelium, i.e. umbrella and intermediate cells. In NHU cell lines, AQP9 mRNA expression was identified but no immunoreactivity was found for AQP9. Rubenwulf *et al.,* (2009) were unsuccessful in identifying AQP11 protein levels in NHU cells due to the lack of suitable antibodies, this study was able to identify AQP11 protein throughout the urothelium.

Interestingly, the majority of AQPs identified in pig urinary bladder consist of aquaglyceroporins (AQP3, 9 and 11) which, unlike AQP1, are found in the urothelial cells that are exposed to components in urine. It is also interesting to note that, out of all the different subtypes of AQPs currently identified in the urinary bladder of mammals, AQP3 appears to be present in all the different studies which could indicate the crucial role of AQP3 in the urinary bladder. The orthodox AQPs, AQP1, AQP2, AQP4, AQP5, AQP6, which are known to primarily facilitate water could not be identified in in pig bladder urothelium which suggests that the need for water in addition to solute reabsorption is much greater than water only. Reabsorption of urea from

urine during the passage of urine from the kidney to the bladder and in the bladder has been reported in other studies. A number of *in vivo* studies have suggested that many urinary constituents, including water, urea and various ions are reabsorbed through the epithelial (urothelial) lining under certain circumstances (Hohlbrugger, 1987; Levinsky and Berliner 1959; Rapoport *et al*., 1960; Walser *et al*., 1988). Rubenwulf *et al.* (2012) has demonstrated that urea and water in the urinary bladder is reabsorbed by AQPs. Therefore, this study proposed that the expression of AQP3, AQP9 and possibly AQP11 are responsible for water and urea reabsorption and that AQP3, AQP9 and AQP11 function is not limited only in the reabsorption of urea and water but also the loss of other solutes that have previously been reported before the discovery of AQPs. The reabsorption and reutilization of urine nitrogenous wastes (urea, creatinine) is critical for survival in hibernating animals, the advantages of such transport in non-hibernating mammals remains to be clarified. Other studies have proposed that urea and creatinine reabsorption across the urinary bladder is subsequently metabolised and the nitrogen moiety is utilized for protein synthesis in conditions such as low protein, starvation pregnancy and growth in children (Spector *et al.,* 2007). On the other hand, it is also possible that the lower urinary tract urothelium is involved in the pathophysiology of “prerenal azotemia,” a condition defined by relatively high serum levels of urea nitrogen in the state of dehydration and previously believed to be caused by urea reabsorption in the renal proximal tubule and collecting duct only.

Since there are currently very limited studies which have looked at AQPs possible regulatory mechanism in the bladder, the expression of potential regulatory proteins in the pig urinary bladder was investigated. There are many potential receptors and channels that have been shown to be involved in mediating the function, expression

and translocation of AQPs in other tissue types. From these, it was decided to focus on a few of these channels and receptors including TRPC1, TRPV4, ER-2, ENaC, AG-2 to confirm the expression of these channels and receptors in pig urinary bladder. TRPV4 (found in the urothelium) and TRPC1 (found in the mucosa) have not been reported to be expressed pig urinary bladder. Channels such as TRP channels are reported to work directly with AQPs in a synergistic manner by allowing influx of calcium ions in respond to external triggers leading to intracellular signalling cascade which eventually cause AQPs to be trafficked to the membrane (Conner *et al.,* 2010; Day *et al.,* 2013; Benfenati *et al*., 2011). AG-2 receptor (found in the mucosa) has previously been demonstrated in pig bladder but no studies have been done on AG-2 potential interaction with AQP channels (Ilieva *et al.,* 2008). ENAC channels (found mucosa an urotheial layer) are proposed to indirectly influence AQP function by allowing movement of ions across urothelial cells and in turn initiating AQPs to regulate cell volume via a mechanism known as RVC. Therefore, these potential AQP regulatory channels investigated in pig urinary bladder and their presence confirmed could potentially regulate AQP function and expression.

After identifying AQPs subtypes and potential receptors and channels which could regulate these water channels, the second and third objectives of this study were to investigate whether there is evidence of water movement across the pig bladder urothelium and if AQPs were potentially involved in mediating this movement given that no studies have looked at pig bladder and there are very limited studies that have investigating water movement across the bladder urothelium Also, to investigate changes in the effect of tonicity on AQP3 localisation in isolated urothelial cells.

AQP3 was investigate because its expression was the most abundant in this study and it has also been found in all the studies done on AQPs in mammalian bladders (Spector *et al.,* 2002; Rubenwolf *et al.,* 2009).

Since AQP proteins are continuously exposed to changes in urine osmolarity for prolong periods of time, it was hypothesised that AQPs could respond to the changes in osmolarity. For the first time, using an Ussing chamber device, it could be demonstrated that both a hypertonic solution and a hypotonic solution could cause the movement of D_2O across pig urinary bladder mucosa when an osmotic gradient was created, where the basolateral side of the mucosa tissue was exposed to isotonic solution and the apical side of the mucosa was exposed to hypertonic or hypotonic solution. The movement of D_2O is thought to predominantly be mediated by AQP channels. This was demonstrated when the movement of D_2O was noticeably reduced after inhibition of AQPs with $HgCl_2$, a nonspecific AQP inhibitor. Moreover, this study has also demonstrated for the first time in pig urinary bladder that when urothelial cells are exposed to either hypertonic or hypotonic solutions, AQP3 is trafficked to the plasma membrane, indicating that both hypertonic and hypotonic solutions activate AQPs to function and they are translocated to the membrane as demonstrated with AQP3. This observation is important because of the environmental conditions of urothelial cells. Over the course of a day, urothelial cells are exposed to both hypertonic and hypotonic solution on more than one occasion and these cells must adapt to the changes in tonicity each time. While paracellular movement of water occurs as a mechanism to regulate this offset in osmotic imbalance, the rate of paracellular movement of water alone is insignificant to restore the osmotic changes in a limited amount of time (Day *et al.,* 2014). AQPs are proposed to regulate this offset through a common passive mechanism and also cell volume regulation (CVR). AQPs

regulation and cellular distribution varies significantly between systems, specifically in constituent tissues and cells like kidney (Day *et al.,* 2014). This variation in AQP distribution has also been demonstrated in this study for AQP1, 3, 9 and 11 but in particular for AQP3 and AQP9 in urothelial cells. CVR is an important mechanism component of AQP-mediated transcellular water movement. CVR involves regulatory volume decrease (RVD), typically in response to hypotonic induced cell swelling and regulatory volume increase (RVI), predominantly in response to hypertonic induced cell shrinking (Cacace *et al.,* 2014). The mechanism involved in these responses are not fully understood but because this process is cell-type dependent, it is unlikely that there is a single mechanism for CVR. Most cells in the human body has a CVR mechanism to respond to osmotic changes and some cells such as the urothelium cells could have complex CVR mechanisms due to changes in urine osmolarity. As demonstrated in Chapter 3, hypertonic and hypotonic solution both caused movement of D_2O and both modulated tonicity, but also caused AQP3 trafficking as demonstrated in Chapter 4. Therefore, it is hypothesized that trafficking of AQP3 to the plasma membrane and the movement of D_2O could be an important CVR mechanism in the urothelial cells to regulate intracellular osmolarity which is required during both hypertonic and hypotonic conditions (Figure 5.1). This hypothesis is further supported by the observation that when the mucosa strip was exposed to isotonic solution on the basolateral side and isotonic solution on the apical side, small quantities of D_2O was observed on the basolateral side which was lower than that observed when osmotic gradient was created. Also, when isolated urothelial cells were exposed to PBS isotonic solution, AQP3 was found to be localised within the urothelial cell, suggesting that in an isotonic environment, the need for RVI and RVD was not required. The trafficking of AQP3 in response to both hypertonic and isotonic solution has been

reported by two different studies, but both demonstrated the opposite tonicity effects on AQP3 (Garcia *et al.,* 2001; Matsuzaki *et al.,* 2001).

It is important to a acknowledge that Rubenwulf *et al*. (2012) demonstrated increase water fluxes in NHU cells as well as an increase in AQP3 expression in hypertonic condition (500 mOsm/kg). Although water fluxes in hypotonic solution was not reported in their study, increase water fluxes seen in hypertonic solution is in line with this current study. They further demonstrated that hypotonic condition (215 mosm/kg) caused a decreased expression of AQP3 by 30% relative to the control. The decrease in AQP3 protein levels reflects a decrease in AQP3 protein synthesis or increased turnover and not necessary AQP3 trafficking. This distinction is key as the RVC mechanism in urothelial cells is essential in hypertonic as well as hypotonic conditions and thus in their study, available AQP3 within the cytoplasm could be trafficked to the membrane as demonstrated with AQP3 in this study.

Whether the movement of D_2O in this study merely reflects a CVR mechanism to offset osmotic balance or the movement of D_2O is reabsorbed back into the systemic circulation remains to be clarified. However, the use of mucosa strips in this study, where AQP1 resides in endothelial cells and capillaries in the lamina propria as reported in Chapter 2, could suggest a possible D_2O reabsorption to the systemic circulation.

.

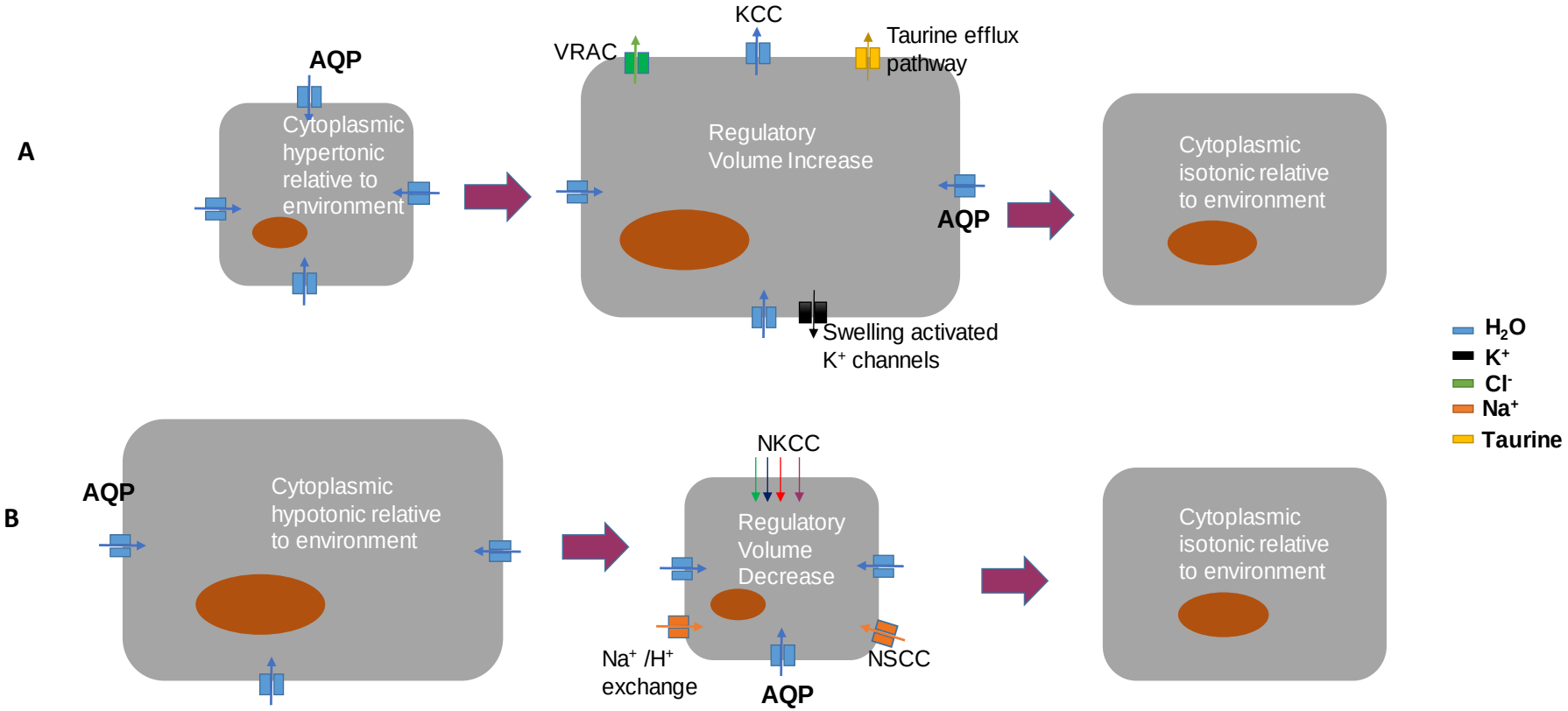

Figure 5.1: Proposed solute transport pathways mediating CVR in Urothelial cells **A)** Represents the pathways for RVD in urothelial cells: the activation of K^+ channels allows efflux of K^+ from the cell and subsequent water loss by osmosis either through AQPs or directly through the lipid bilayer biophysical data demonstrates that AQP expression can increase membrane water permeability by up to ~ 50 fold. Movement of K^+ out of the cell is dependent on the concentration gradient but to maintain the electrostatic membrane potential, volume-regulated anion channel(s) (VRAC) simultaneously move anions (mainly Cl^- during RVD) out of the cell, which could be activated by tyrosine kinases. Four K^+-Cl^- co-transporters (KCCs), known to be activated by cell swelling, are possibly involved in this process.

B) Represents the pathways for RVI in urothelial cells: The activation of Na^+-H^+ exchangers and Na^+-K^+-$2Cl^-$ co-transporters (NKCCs) causes cellular influx of Na^+ and subsequent volume increase by osmotic movement of water.The Na^+-H^+ exchange pump, NHE1, is known to be activated by cell shrinkage, which may be mediated by binding of calmodulin to its carboxy-terminus. The co-transporter, NKCC1, is known to be activated by cell shrinkage, potentially through lysine-deficient protein kinase 1 (WNK1) and proline/alanine-rich protein kinase (SPAK) signalling. Amiloride-sensitive non-selective cation channels (NSCCs) may also play a role. Adapted from Day *et al.* (2014).

To date, no model has been proposed for AQP intracellular signalling pathways with tonicity as a trigger in the urinary bladder urothelium.

Three possible models can be hypothesised for trafficking and function of AQPs in bladder urothelium based on the evidence gathered from this study and other studies on the bladder as well as studies on other tissues

First model: this model is based on a study by Conner *et al*. (2012) who proposed a model for HEK293 cell lines. In HEK293 cell lines, Conner *et al.* (2012) demonstrated that AQP1 exposure to hypotonicity translocated to the cell membrane, a process that is mediated by the influx of calcium ions through TRPC1. Inhibition of mechanosensitive TRPC1 prevented hypotonicity-induced AQP1 translocation. Based on these findings, a model for AQP1 regulation in HEK293 was proposed. Influx of water by osmosis and/or through constitutively expressed AQPs channels causes cell swelling and induces extracellular calcium ion entry through TRP channels, and as a result triggers AQP translocation to the membrane. They demonstrated that AQP1 translocation is dependent on calmodulin (CaM) activation and AQP1 phosphorylation by PKC. Water then exit the cell to maintain cellular homeostasis (Conner *et al.,* 2012). In this current study, it has clearly been demonstrated that AQP 1, 3, 9 and 11 are present in the urinary bladder and that AQP3 is trafficked to the plasma membrane upon exposure to both hypertonic and hypotonic solution. Also, in this study, it was demonstrated that TRPV4, a mechanosensitive ion channel, is also expressed in pig urothelial cells (Figure 4). Moreover, existing data have shown that AQP 1, 3 and 9 contain several putative phosphorylation sites for PKC, PKA (Yasui *et al.,* 2008; Nesverova *et al.,* 2019). In addition, expression of AQP 3 and AQP 9 is shown to be regulated by oleic acid through the PI3K/Akt and p38 MAPK signalling pathways.

Therefore based on existing data and this current data, the model presented in Figure 5.2 is proposed.

Second model: TRPM8 is the only TRP channels that is reported to detect small changes in osmolality, (Quallo *et al.,* 2015). Increasing osmolality evokes depolarization and action potential firing in TRPM8-expressing sensory neurons, whereas inhibition of TRPM8 evokes hyperpolarization (Quallo *et al.,* 2015). TRPM8 expression has also been demonstrated in pig urinary bladders (Vahabi *et al.,* 2013). Whereas in proposed model one, constitutively expressed AQPs in cell membrane initially allows influx of water leading to stretch and which is followed by an influx of calcium ions, in this second model, it is proposed that changes in external osmolarity is detected by TRPC8 which causes an influx of calcium ions, and as a result trigger AQP trafficking to the plasma membrane (Figure 5.2).

Third model: This model is based on RVC mechanisms. Ion channels, such as the Na^+-K^+ pump, help to maintain an osmotic balance across the mammalian cell membrane by keeping the intracellular concentration of Na^+ low (Pirahanchi *et al.,* 2019). In addition to this, reabsorption of urea and other solutes can lead to changes in intracellular and extracellular osmolarity (Schafer, 2004). Therefore, unlike the proposed model one or model two, in this third model, it is hypothesised that in addition to passive diffusion, constitutively expressed AQPs are involved in continuously regulating cell volume by fine tuning of intra- and extracellular osmotic changes. Constitutively expressed AQPs respond to small changes in osmolarity and evoke a mechanism known as RVD/RVI to regulate urothelial cells by allowing bidirectional movement of water and solutes.

In this proposed pathway, TRP channels activation of AQPs trafficking is only important during extreme increase in intra- and extracellular osmotic changes (Figure 5.2).

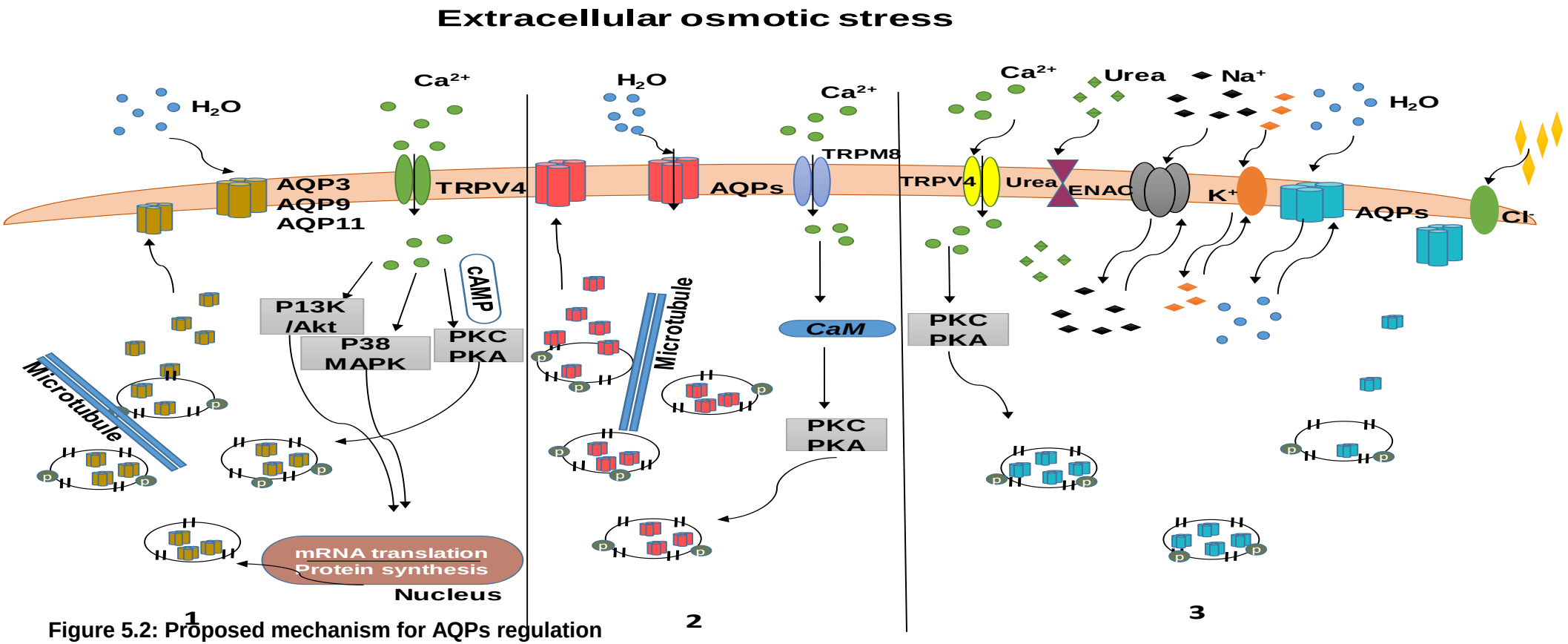

Figure 5.2: Proposed mechanism for AQPs regulation

Proposed model 1: Osmotic changes in extracellular environment causes an influx of H_2O to the cell via constitutively expressed AQPs, the influx of H_2O causes the cell to stretch. TRP channels present respond to the stretch caused by an increased in intracellular water. Calcuim ion influx via the TRP channels result in phosphorylation of AQPs stored in vesicles and trafficking to the cell membrane by protein kinases or AQPs (AQP3/9) synthesis via P13K/Akt and P38 MAPK. When equilibrium is achieved, signalling feedback loop result in down regulation of AQPs expression and de-phosphorylation of AQPs.

Proposed model 2: unlike pathway 1, TRPM8 detect changes in extracellular osmolarity and this leads to influx in calcium to the intracellular space. This is then followed by Influx of water by osmosis and/or through constitutively expressed AQP channels or leads to cell swelling and as a result induces intracellular calcium entry through TRP channels, thereby triggering AQPs translocation. This translocation along microtubules is dependent on calmodulin (CaM) activation and AQP phosphorylation by PKC/PKA. Water subsequently enters or exits the cell to maintain cellular homeostasis.

Proposed model 3: Ion channels such as Na^+-K^+ pump helps maintain an osmotic balance across the cell membrane by keeping the intracellular concentration of Na^+ low. Osmotic changes in extracellular environment causes reabsorption of urea and other solutes and as a result changes in intracellular and osmolarity. This causes constitutively expressed AQPs to allow the permeability of water (bidirectional). These changes are performed continuously in fine-tuning intra and extracellular osmotic changes via as a form of osmosis. TRP channels activation of AQPs is only important during extreme increase in intra and extracellular osmotic changes.

To conclude, knowledge on the mechanisms of water and solute movement across the urothelium is limited and research in this area can help identify novel targets. We have identify AQPs expression for the first time in adult pig bladder urothelium and we have also demonstrated that these AQP channels are functional in the urinary bladder when osmotic gradient is created. We have also demonstrated that AQP3 is trafficked to the membrane after exposure to hypotonic, hypertonic solutions. The presence of AQPs in the urinary bladder can be seen as a new therapeutic target where AQPs can reabsorb water across the bladder urothelium at night as a mechanism to treat Nocturia. Further studies are required to investigate hypotonic and hypertonic intracellular signalling involved in AQPs function, expression and translocation.

5.2 FUTURE WORK

This thesis provides evidence that AQPs are present in the urinary bladder of pigs and also demonstrates that AQPs are function in pig urinary bladder. Furthermore, this thesis shows that the function of these AQPs in mediating water across the urinary bladder could be through trafficking of AQPs, in particular AQP3 to the plasma membrane of urothelial cells. In addition, several regulatory proteins that have been demonstrated to regulate AQPs function in other studies have been demonstrated in this study. To investigate this further, the following experiments could be considered:

- Identification of AQP3 localisation around the nucleus in urothelial cells using cellular organelle markers using AQP3-GFP tagged/EM staining

Investigating the intracellular signalling pathway involved in AQP3 trafficking

- Establish and optimise isolated urothelial cell cultures from pig urothelium for intracellular signalling experiments.
- Exposure of urothelial cells to hypertonic, hypotonic and isotonic Krebs solution followed by inhibition of phospholipase C and PKC and calphostine C respectively and examination of AQP3 cytosolic and plasma membrane fraction proteins levels to determine AQP trafficking.
- Activation of PKC, and phospholipase C to observe AQP3 cytosolic and membrane fraction changes.
- Measurement of intracellular Ca^{2+} using Till photonics-polychrome IV spectrofluorimeter and Olympic microscope and Metaflour imaging system to measure fluorescence traces after urothelial exposure to hypertonic, hypotonic Krebs solution.

- Pharmacological activation and inhibition of TRPV4 and measurement of AQP3 membrane fraction to determine whether an increase in intracellular calcium ions is through TRPV4 after urothelial cells exposure to hypertonic, hypotonic and isotonic solution.
- Investigating the role of AQPs in the release of mediators such as ATP by urothelial cells and bladder contraction.
- Instillation of D_2O in dehydrated, well-hydrated and over-hydrated pig urinary bladders and sampling of blood to determine reabsorption of D_2O back into the systemic circulation under all three conditions.

6.1 REFERENCES

Arnold, Y.E., Thorens, J., Bernard, S., and Kalia, Y.N. (2019). Drug transport across porcine intestine using an Ussing chamber system: regional differences and the effect of P-glycoprotein and CYP3A4 activity on drug absorption. *Pharmaceutics*, *11*(3), p. 139.

Adam, A.P., Sharenko, A.L., Pumiglia, K., and Vincent, P.A. (2010). Src-induced tyrosine phosphorylation of VE-cadherin is not sufficient to decrease barrier function of endothelial monolayers. *Journal of Biological Chemistry*, *285*(10), 7045-7055.

Ancoli-israel, S., Bliwise, D. L., and Nørgaard, J. P (2011). The effect of nocturia on sleep. *Sleep Medicine Reviews*, *15*(2), p. 91-9.

Abir-Awan, M., Kitchen, P., Salman, M.M., Conner, M.T., Conner, A.C. and Bill, R.M. (2019). Inhibitors of mammalian aquaporin water channels. *International journal of molecular sciences*, *20* (7), p. 1589.

Acharya, P., Beckel, J., Ruiz, W. G., Wang, E., Rojas, R., Birder, L. and Apodacas, G. (2004). Distribution of the tight junction proteins ZO-1, occludin, and claudin-4,-8, and-12 in bladder epithelium. *American Journal of Physiology-Renal Physiology*. *287*(2), p. 305-318.

Amiry-moghaddam, M., Williamson, A., Palomba, M., Eid, T., De Lanerolle, N.C., Nagelhus, E.A., and Ottersen, O.P. (2003). Delayed K+ clearance associated with aquaporin-4 mislocalization: phenotypic defects in brains of α-syntrophin-null mice. *Proceedings of the National Academy of Sciences, 100*(23), p. 13615-13620.

Andersson, K.E., and Van Kerrebroeck, P. (2018). Pharmacotherapy for nocturia. *Current urology reports*, *19*(1), p. 8.

Andersson, K.E., and Arner, A. (2004). Urinary bladder contraction and relaxation: physiology and pathophysiology. *Physiological Reviews, 84*(3), p. 935-986.

Abrams, P., Cardozo, L., Wagg, A., and Wein, A. (2013). Incontinence 6th Edition (2017). *ICI-ICS. International Consultation on Incontinence− International Continence Society, Bristol UK, ISBN*, 978-0956960733.

Arima, H., Yamamoto, N., Sobue, K., Umenishi, F., Katsuya, H., and Asai, K. (2003). Hyperosmolar mannitol stimulates expression of aquaporins 4 and 9 through a p38 mitogen-activated protein kinase-dependent pathway in rat astrocytes. *Journal of Biological Chemistry*. *278*(45), p. 44525-44534.

Apodaca, G., and Birder, L.A. (2007). The uroepithelial-associated sensory web. *Kidney international*. *72*(9), p. 1057-1064.

Apodaca, G. (2004). The uroepithelium: not just a passive barrier*. Traffic*, *4*(3), p. 117-128.

Au, C.G., Butler, T.L., Egan, J.R., Cooper, S.T., Lo, H.P., Compton, A.G., and Winlaw, D.S. (2008). Changes in skeletal muscle expression of aqp1 and aqp4 in

dystrophinopathy and dysferlinopathy patients. *Acta Neuropathologica*, *11*(3), p. 235-246.

Agre, P. (2006). The Aquaporin Water Channels*. Proceedings of the American Thoracic Society, 3(1),* p. 5-13.

Arnspang, E. C., Sundbye, S., Nelson, W. J., and Nejsum, L. N. (2013). Aquaporin-3 and aquaporin-4 are sorted differently and separately in the trans-Golgi network. *PloS one*, *8*(9), e73977.

Atkinson, P.H., and Lee, J.T. (1984). Co-translational Excision of Alpha-glucose and Alpha-mannose in Nascent Vesicular Stomatitis Virus G Protein. *The Journal of Cell Biology* [online], 96 (6), p. 2245-2249.

Audagnotto, M., and Dal Peraro, M. (2017). Protein Post-translational Modifications: In Silico Prediction Tools and Molecular Modeling. *Computational and Structural Biotechnology Journal*. 15, p. 309-317.

Abascal, F., Irisarri, I., and Zardoya, R. (2014). Diversity and Evolution of Membrane Intrinsic Proteins. *Biochimica Et Biophysica Acta (Bba)-general Subjects*, *1840*(5), p. 1468-1481.

Birder, L., and Andersson, K.E. (2013). Urothelial signaling. *Physiological Reviews*. *93* (2), p. 653-680.

Badaut, J., Petit, J., M., Brunet, J. F., Magistretti, P. J., Charriaut-Marlangue, C., and Regli, L. (2004). Distribution of Aquaporin 9 in the adult rat brain: preferential expression in catecholaminergic neurons and in glial cells. *Neuroscience*, *128*(1), 27-38.

Balkom Van, B. W., Savelkoul, P. J., Markovich, D., Hofman, E., Nielsen, S., Van der Sluijs, P., and Deen, P. M. (2002). The role of putative phosphorylation sites in the targeting and shuttling of the aquaporin-2 water channel. *Journal of Biological Chemistry*, *277*(44), p. 41473-41479.

Burshtein, G., Friedman, M., Greenberg, S., and Hoffman, A. (2013). Transepithelial transport of a natural cholinesterase inhibitor, huperzine A, along the gastrointestinal tract: The role of ionization on absorption mechanism. *Planta medica*, *79*(03/04), p. 259-265.

Bruewer, M., and Nusrat, A. (2006). Regulation of Paracellular Transport Across Tight Junctions by the Actin Cytoskeleton. *Tight Junctions,* p. 135-145.

Burnstock, G. (2013). Purinergic Signalling in the Lower Urinary Tract. *Acta Physiologica*, *207*(1), p. 40-52.

Buck, T.M., Eledge, J., and Skach, W.R. (2004). Evidence for stabilization of aquaporin-2 folding mutants by N-linked glycosylation in endoplasmic reticulum. *American Journal of Physiology-cell Physiology*, 287(5), p. C1292-C1299.

Birder, L.A., and De Groat, W.C. (2007). Mechanisms of disease: involvement of the urothelium in bladder dysfunction. *Nature Reviews Urology*, *4*(1), p.46.

Brooks, H.L., Regan. J.W., and Yool. A.J. (2000). Inhibition of Aquaporin-1 water permeability by tetraethylammonium: involvement of the loop E pore region. *Molecular Pharmacology*, *57*, p. 1021–1026.

Birder, L, De Goat, W., Mills, I., Morrison, J., Thor, K., and Drake, M. (2010). Neural control of the lower urinary tract: peripheral and spinal mechanisms. *Neurourology and Urodynamics: Official Journal of the International Continence Society*, *29*(1), p. 128-139.

Burton, T. J., Elneil, S., Nelson, C. P., and Ferguson, D. R. (2000). Activation of epithelial Na+ channel activity in the rabbit urinary bladder by cAMP. *European journal of pharmacology*, *404*(3), p. 273-280.

Ball, L.E., Little, M., Nowak, M.W., Garland, D.L., Crouch, R.K., and Schey, K.L. (2003). Water permeability of C-terminally truncated aquaporin 0 (Aqp0 1-243) observed in the aging human lens. *Investigative Ophthalmology and Visual Science*, *44*, p. 4820-4828.

Bolla, S. R., and Jetti, R. (2019). Histology, Bladder. In *StatPearls [Internet]*. StatPearls Publishing.

Butler, T.L., Au, C.G., Yang, B., Egan, J.R., Tan, Y.M., Hardeman, E.C.. and Winlaw, D.S. (2006). Cardiac aquaporin expression In humans, rats, and mice. *American Journal of Physiology-heart and Circulatory Physiology, 291*(2) p. H705-H713.

Butterworth, M. B. (2010). Regulation of the epithelial sodium channel (ENaC) by membrane trafficking. *Biochimica Et Biophysica Acta (BBA)-Molecular Basis of Disease*, *1802*(12), p.1166-1177.

Berry, V., Francis, P., Kaushal, S., Moore, A., and Bhattacharya, S. (2000). Missense mutations in mip underlie autosomal dominant 'polymorphic' and lamellar cataracts linked to 12q. *Nature Genetics*, *2000*(25), p. 15-17

Boron, W. F., and Boulpaep, E. L. (2012). *Medical Physiology, 2e Updated Edition E-Book*. Elsevier health sciences.

Butt, A.M., Jones, H.C. and Abbot, N.J. (1990). Electrical Resistance Across the Blood-brain Barrier in Anaesthetized Rats: A Developmental Study. *The Journal of Physiology,* 429(1), p. 47-62.

Benfenati, V., Caprini, M., Dovizio, M., Mylonakou, M.N., Ferroni, S., Ottersen, O.P., and Amir-moghaddam, M. (2011). An aquaporin-4/transient receptor potential vanilloid 4 (Aqp4/trpv4) complex Is essential for cell-volume control in astrocytes. *Proceedings of the National Academy of Sciences*. *108*(6), p. 2563-2568.

Benfenati, V., Nicchia, G.P., Svelto, M., Rapisarda, C., Frigeri, A., and Ferroni, S. (2007). Functional down-regulation of volume-regulated anion channels in Aqp4 knockdown cultured rat cortical astrocytes. *Journal of Neurochemistry, 100*, p. 87-104.

Biner, H. L., Arpin-Bott, M. P., Loffing, J., Wang, X., Knepper, M., Hebert, S. C., and Kaissling, B. (2002). Human cortical distal nephron: distribution of electrolyte and

water transport pathways. *Journal of the American Society of Nephrology*, *13*(4), p. 836-847.

Boassa, D., Stamer, W. D., and Yool, A. J. (2006). Ion channel function of aquaporin-1 natively expressed in choroid plexus. *Journal of Neuroscience*, *26*(30), p. 7811-7819.

Bergman, A.M., Sih, A.M., and Weiss, J.P. (2015). Nocturia: An Overview of Evaluation and Treatment. *Bladder*. 2 (2)

Boury-jamot, M., Sougrat, R., Tailhardat, M., Le Varlet, B., Bonté, F., and Dumas, M. (2006). Expression and function of aquaporins in human skin: Is Aquaporin-3 Just a Glycerol Transporter?. *Biochim et Biophysica Acta*, *1758*, p. 1034.

Boone, M., and Deen, P.M. (2008). Physiology and pathophysiology of the vasopressin-regulated renal water reabsorption. *Pflügers Archiv-european Journal of Physiology*, *456*(6), p. 1005.

Berry, V., Francis, P., Kaushal, S., Moore, A. and Bhattacharya, S. (2000). Missense mutations in mip underlieautosomal dominant 'polymorphic' and lamellar cataracts linked to 12q. *Nature Genetics,* (25), p. 15-17

Barré-sinoussi, F., and Montagutelli, X. (2015). Animal Models Are Essential to Biological Research: Issues and Perspectives. *Future Science Oa,* 1 (4)

Beitz, E., Lui, K., Ikeda, M., Guggino, W.B., Agre, P., and Yasui M. (2006). Determinants of Aqp6 trafficking to intracellular sites versus the plasma membrane in transfected mammalian cells. *Biology of the Cell, 98*, p. 101-109.

Clarke, L. L. (2009). A guide to Ussing chamber studies of mouse intestine. *American Journal of Physiology-Gastrointestinal and Liver Physiology*, *296*(6), p1151-p1166.

Crowe, R., and Burnstock, G. (1989). A Histochemical and Immunohistochemical study of the autonomic innervation of the lower urinary tract of the female pig. Is the pig a good model for the human bladder and urethra?. *The Journal of Urology*, *141*(2), p. 414-422.

Cahill, D., Fry, C., and Foxall, P. (2003). Variation in urine composition in the human urinary tract: evidence of urothelial function in situ?. *Journal of Urology, 169(*3), p.871-874.

Christensen, B.M., Zelenina, M., Aperia, A., and Nielsen, S. (2000). Localization and regulation of pka-phosphorylated aqp2 in response to V(2)-receptor agonist/antagonist treatment. *American Journal of Physiology-Renal Physiology*

278(1), p. F29-F42

Calamita, G., Ferri, D., Gena, P., Liquori, G. E., Cavalier, A., Thomas, D., and Svelto, M. (2005). The inner mitochondrial membrane has aquaporin-8 water channels and is highly permeable to water. *Journal of Biological Chemistry*, *28*(17), p17149-17153.

Cui, D., Sui, L., Han, X., Zhang, M., Guo, Z., Chen, W., and Kong, Y. (2018). Aquaporin-3 mediates ovarian steroid hormone-induced motility of endometrial epithelial cells. *Human Reproduction*, *33*(11), p. 2060-2073.

Conner, A.C., Bill, R.M., and Conner, M.T. (2013). An emerging consensus on aquaporin translocation as a regulatory mechanism. *Molecular membrane biology*, *30*(1), p. 101-112.

Cvetkovic, R.S., and Plosker, G.L. (2005). Desmopressin. *Drugs*, *65*(1), p. 99-107.

Chan, K.H., Zhang, R., Kwan, J.S.C., Guo, V.Y., Ho, P.W.L., Ho, J.W.M., and Chu, A.C.Y. (2012). Aquaporin-4 autoantibodies cause asymptomatic aquaporin-4 loss and activate astrocytes in mouse. *Journal of Neuroimmunology*, *245*, p. 32-38.

Carattino, M. D., Prakasam, H. S., Ruiz, W. G., Clayton, D. R., McGuire, M., Gallo, L. I., and Apodaca, G. (2013). Bladder filling and voiding affect umbrella cell tight junction organization and function. *American Journal of Physiology-Renal Physiology*, *305*(8), p.1158-1168.

Conner, M.T., Conner, A.C., Brown, J.E., and Bill, R.M. (2010). Membrane trafficking of aquaporin 1 Is mediated by protein kinase C via microtubules and regulated by tonicity. *Biochemistry*, *49*, p. 821-823.

Conner, M.T., Conner, A.C., Bland, C.E., Taylor, L.H., Brown, J.E., and Parri, H.R. (2012). Rapid aquaporin translocation regulates cellular water flow: the mechanism of hypotonicity-induced sub-cellular localization of the aquaporin 1 water channel. *Journal of Biological Chemistry*, *287*(14), p. 11516-25.

Carbrey, J. M., Gorelick-Feldman, D. A., Kozono, D., Praetorius, J., Nielsen, S., and Agre, P. (2003). Aquaglyceroporin AQP9: solute permeation and metabolic control of expression in liver. *Proceedings of the National Academy of Sciences*, *100*(5), p. 2945-2950.

Chen, Q., Peng, H., Lei, L., Zhang, Y., Kuang, H., Cao, Y., and Duan, E. (2011). Aquaporin3 is a sperm water channel essential for postcopulatory sperm osmoadaptation and migration. *Cell research*, *21*(6), p. 922.

Carmosino, M., Procino, G., Tamma, G., Mannucci, R., Svelto, M., and Valenti, G. (2007) Trafficking and phosphorylation dynamics of Aqp4 in histamine-treated human gastric cells. *Biology of the Cell*, 99(1), p. 25-36.

Crook, J., and Lovick, T. (2016). Urodynamic function during sleep-like brain states in urethane anesthetized rats. *Neuroscience,* 313, p. 73-82.

Chen, J.A., Feng, L.R., Lee, S.T., Hsieh, C.Y., and Huang, W.S. (2015). Stress alters the expression of aquaporins in cultured rat intestinal epithelial cells. *Experimental and Therapeutic Medicine*, *10*(5), p. 1967-1972.

Curhan, G.C., Speizer, F.E., and Et A.l. (1999). Epidemiology of interstitial cystitis: a population based study. *The Journal of Urology*, *161*, p. 549-552.

Cacace, V. I., Finkelsteyn, A. G., Tasso, L. M., Kusnier, C. F., Gomez, K. A., and Fischbarg, J. (2014). Regulatory volume increase and regulatory volume decrease responses in HL-1 atrial myocytes. *Cellular Physiology and Biochemistry*, *33*(6), p. 1745-1757.

Chen, Q., and Duan, E. K. (2011). Aquaporins in sperm osmoadaptation: an emerging role for volume regulation. *Acta Pharmacologica Sinica*, *32*(6), p. 721.

Cohen, P. (2000) The Regulation of Protein Function by Multisite Phosphorylation — a 25-year Update. *Trends in Biochemical Science Sci, 25*. p. 595-601.

Cohen, C.J, Shieh, J.T., Pickles, R.J., Okegawa, T., Hsieh, J.T. and Bergelson, J.M. (2001). The coxsackievirus and adenovirus receptor is a transmembrane component of the tight junction. *Proceedings of the National Academy of Sciences*, 98 (26), p. 15191-15196.

Clausen, C., S. A., Lewis, and J. M. Diamond. (1979). Impedance analysis of a tight epithelium using a distributed resistance model. *Biophysical Journal, J. 26* p. 291-318

Dani, H., Esdaille, A., and Weiss, J.P. (2016) Nocturia: aetiology and treatment in Adults. *Nature Reviews Urology.*

Diamond, J.M. (1964) Transport of salt and water in rabbit and guinea-pig gall bladder. *Journal of General. Physiology*, *48*, p. 1-14.

Day, R.E., Kitchen, P., Owen, D.S., Bland, C., Marshall, L., Conner, A.C., and Conner, M.T. (2014). Human aquaporins: regulators of transcellular water flow. *Biochimica Et Biophysica Acta (Bba)-general Subjects*, *1840*(5), p. 1492-1506

Deeg, C. A., Amann, B., Lutz, K., Hirmer, S., Lutterberg, K., Kremmer, E., and Hauck, S. M. (2016). Aquaporin 11, a regulator of water efflux at retinal müller glial cell surface decreases concomitant with immune-mediated gliosis. *Journal of neuroinflammation*, *13*(1), p. 89.

Drumm, B.T., Koh, S.D., Andersson, K.E., and Ward, S.M. (2014). Calcium signalling in cajal-like interstitial cells of the lower urinary tract. *Nature Reviews Urology*, *11*(10), p. 555.

Damiano, A., Zotta, E., Goldstein, J., Reisin, I., and Ibarra, C. (2001). Water channel proteins AQP3 and AQP9 are present in syncytiotrophoblast of human term placenta. *Placenta*, *22*(8-9), p.776-781.

Dixon, J., and Gosling, J. (1987). Structure and innervation in the human. *The physiology of the Lower Urinary Tract,* p. 3-22.

Dong, Z., Ran, J., Zhou, H., Chen, J., Lei, T., Wang, W., and Yang, B. (2013). Urea transporter UT-B deletion induces DNA damage and apoptosis in mouse bladder urothelium. *PloS one*, *8*(10), p. e76952.

Duan, G., and Walther, D. (2015). The roles of post-translational modifications in the context of protein interaction networks. *Plos Computational Biology*, *11*(2).

Dong, Z., Ran, J., Zhou, H., Chen, J., Lei, T., Wang, W., and Yang, B. (2013). Urea transporter UT-B deletion induces DNA damage and apoptosis in mouse bladder urothelium. *PloS one*, *8*(10), p. e76952

Echevarria, M., Windhager, E.E., Tate, S.S., and Frindt, G. (1994). Cloning and expression of Aqp3, a water channel from the medullary collecting duct of rat kidney. *Proceedings of the National Academy of Sciences, 91*(23), p.10997-11001.

Epifantseva, I., and Shaw, R.M. (2018) Intracellular trafficking pathways of Cx43 gap junction channels. *Biochimica Et Biophysica Acta (Bba)-biomembranes*, *1860*(1), p. 40-47.

Epstein, M. (2001). Aldosterone as a determinant of cardiovascular and renal dysfunction. *Journal of the Royal Society of Medicine*, *94*(8), p. 378-383.

Englund, S., Korduner, I., and Westin, B. (1959). Accidental injury to the ureters and the bladder in gynæcological surgery. *Acta Obstetricia et Gynecologica Scandinavica*, *38*(1), p.68-81.

Franco, R., Bortner, C. D., and Cidlowski, J. A. (2006). Potential roles of electrogenic ion transport and plasma membrane depolarization in apoptosis. *The Journal of membrane biology*, *209*(1), p. 43-58.

Fry, C.H., and Vahabi, B. (2016). The role of the mucosa in normal and abnormal bladder function. *Basic & Clinical Pharmacology and Toxicology*, *119*, p. 57-62.

Fu, D., Libson, A., Miercke, L.J., Weitzman, C., Nollert, P., Krucinski, J., and Stroud, R.M. (2000). Structure of a glycerol-conducting channel and the basis for its selectivity. *Science*, *290*(5490), p. 481-486.

Fushimi, K., Uchida, S., Harat, Y., Hirata, Y., Marumo, F., and Sasaki, S. (1993). Cloning and expression of apical membrane water channel of rat kidney collecting tubule. *Nature*, *361*(6412), p. 549.

Frick, A., Eriksson, U. K., de Mattia, F., Öberg, F., Hedfalk, K., Neutze, R., and Törnroth-Horsefield, S. (2014). X-ray structure of human aquaporin 2 and its implications for nephrogenic diabetes insipidus and trafficking. *Proceedings of the National Academy of Sciences*, *111*(17), p. 6305-6310

Fenton, R. A., Brønd, L., Nielsen, S., and Praetorius, J. (2007). Cellular and subcellular distribution of the type-2 vasopressin receptor in the kidney. *American Journal of Physiology-Renal Physiology*, *293*(3), p. F748-F760.

Furuse, M, Hirase, T., Itoh, M., Nagafuchi, A., Yonemura, S., and Tsukita, S. (1993) Occludin: a novel integral membrane protein localizing at tight junctions. *The Journal of cell biology*, *123*(6), p. 1777-1788.

Furuse, M, Hata, M., Furuse, K., Yoshida, Y., Haratake, A., Sugitani, S., and Tsukita, S. (2002). Claudin-based tight junctions are crucial for the mammalian epidermal barrier: a lesson from claudin-1–deficient mice. *The Journal of cell biology, 156*(6), p. 1099-1111.

Fischbarg, J., Kuang, K. Y., Hirsch, J., Lecuona, S., Rogozinski, L., Silverstein, S. C., and Loike, J. (1989). Evidence that the glucose transporter serves as a water channel in J774 macrophages. *Proceedings of the National Academy of Sciences*, *86*(21), p. 8397-8401.

Fowler, C.J., Griffiths, D., and De Groat, W.C. (2008). The Neural Control of Micturition. *Nature Reviews Neuroscience. 9*(6), p. 453.

Fang, X., Yang, B., Matthay, M. A., and Verkman, A. S. (2002). Evidence against aquaporin-1-dependent CO2 permeability in lung and kidney. *The Journal of physiology*, *542*(1), p. 63-69.

Fushimi, K., Uchida, S., Harat, Y., Hirata, Y., Marumo, F., and Sasaki, S. (1993). Cloning and expression of apical membrane water channel of rat kidney collecting tubule. *Nature, 361*(6412), p. 549.

Fischbarg, J., Kuang, K. Y., Vera, J. C., Arant, S., Silverstein, S. C., Loike, J., and Rosen, O. M. (1990). Glucose transporters serve as water channels. *Proceedings of the National Academy of Sciences*, *87*(8), p. 3244-3247.

Friedman, F.M. and Weiss, J.P. (2013). Desmopressin in the treatment of nocturia: clinical evidence and experience. *Therapeutic Advances in Urology, 5*(6), p. 310-317.

Garcia, F., Kierbel, A., Larocca, M.C., Gradilone, S.A., Splinter, P., and Larusso, N.F. (2001). The water channel aquaporin-8 Is mainly intracellular in rat hepatocytes, and its plasma membrane insertion is stimulated by cyclic amp. *Journal of Biological Chemistry*, *276,* p. 12147-12152.

Garcia, N., Gondran, C., Menon, G., Mur, L., Oberto, G., Guerif, Y., and Domloge, N. (2011). Impact of AQP3 inducer treatment on cultured human keratinocytes, ex vivo human skin and volunteers. *International journal of cosmetic science*, *33*(5), p. 432-442.

Groat De, W.C. (1997) A neurologic basis for the overactive bladder. *Urology, 50*(6), p. 36-52.

Gorin, M.B., Yancey, S.B., Cline, J., Revel, J.P., and Horwitz, J. (1984). The Major Intrinsic Protein (Mip) of the Bovine Lens Fiber Membrane: Characterization and Structure Based on Cdna Cloning. *Cell*, *39(*1), p. 49-59.

Geers, C. and Gros, G. (2000). Carbon dioxide transport and carbonic anhydrase in blood and muscle. *Physiological Reviews*, *80*(2), p. 681-715.

Gao, J., Wang, X., Chang, Y., Zhang, J., Song, Q., Yu, H., and Li, X. (2006). Acetazolamide inhibits osmotic water permeability by interaction with aquaporin-1. *Analytical biochemistry*, *350*(2), p. 165-170.

Gao, X., Wang, G., Zhang, W., Peng, Q., Xue, M. and Jinhong, H. (2013). Expression of pulmonary aquaporin 1 is dramatically upregulated in mice with pulmonary fibrosis induced by bleomycin. *Archives of Medical Science*, p. 916-912.

Gunnarson, E., Zelenina, M., Axehult, G., Song, Y., Bondar, A., Krieger, P., and Et Al, (2008). Identification of a molecular target for glutamate regulation of astrocyte water permeability. *Glia*, *56*, p. 587-596.

Garty, H., and Palmer, L.G. (1997). Epithelial sodium channels: function, structure, and regulation. *Physiological Reviews, 77*(2), p. 359-396.

Gradilone, S. A., Tietz, P. S., Splinter, P. L., Marinelli, R. A., and LaRusso, N. F. (2005). Expression and subcellular localization of aquaporin water channels in the polarized hepatocyte cell line, WIF-B. *BMC Physiology*, *5*(1), p. 13.

Guan, X.G., Su, W.H., Yi, F., Zhang, D., Hao, F., Zhang, H.G., and Ma, T.H. (2010). Npa motifs play a key role in plasma membrane targeting of aquaporin-4. *Lubmb Life*, *62*(3), p. 222-226.

Gonzalez-Mariscal, L, Betanzos, A., Nava, P., and Jaramillo, B.E. (2003). Tight junction proteins. *Progress in Biophysics and Molecular Biology*, *81*(1), p. 1-44.

Gorin, M.B., Yancey, S.B., Cline, J., Revel, J.P., and Horwitz, J. (1984). The major intrinsic protein (Mip) of the bovine lens fiber membrane: characterization and structure based on Cdna gloning. *Cell, 39*(1), p. 49-59.

Gorelick, D. A., Praetorius, J., Tsunenari, T., Nielsen, S., and Agre, P. (2006). Aquaporin-11: a channel protein lacking apparent transport function expressed in brain. *BMC biochemistry, 7*(1), p. 14.

Gonzalez, E.J., Arms, L. and Vizzard, M.A. (2014). The role (S) of cytokines/chemokines in urinary bladder inflammation and dysfunction. *Biomed Research International*.

Golestaneh, N., Fan, J.G., Zelenka, P., and Chepelinsky, A.B. (2008). Pkc putative phosphorylation site Ser (235) is required for mip/aqp0 translocation to the plasma membrane. *Molecular Vision, 14*, p. 1 006-1014.

Han, Z. and Patil, R.V. (2000). Protein kinase A-dependent phosphorylation of aquaporin-1. *Biochemical and Biophysical Research Communications, 273*(1), p. 328-332.

Helenius, A., and Aebi, M. (2001) Intracellular functions of N-linked glycans. *Science*, *291*(5512), p. 2364-2369.

Hasegawa, H., Ma, T., Skach, W., Matthay, M.A., and Verkman, A.S. (1994). Molecular cloning of a mercurial-insensitive water channel expressed in selected water-transporting tissues. *Journal of Biological Chemistry,* 269*,* p. 5497-5500.

Hara-Chikuma, M., Satooka, H., Watanabe, S., Honda, T., Miyachi, Y., Watanabe, T., and Verkman, A. S. (2015). Aquaporin-3-mediated hydrogen peroxide transport is required for NF-κB signalling in keratinocytes and development of psoriasis. *Nature Communications*, *6,* p. 7454.

Huang, Y. T., Zhou, J., Shi, S., Xu, H. Y., Qu, F., Zhang, D., and Sheng, J. Z. (2015). Identification of estrogen response element in aquaporin-3 gene that mediates

estrogen-induced cell migration and invasion in estrogen receptor-positive breast cancer. *Scientific reports*, *5*, p. 12484.

Held, P.J., Hanno, P.M., and Et Al, (1990). Epidemiology of interstitial cystitis: 2. *Interstitial Cystitis*, p. 29-48

Huber, V. J., Tsujita, M., Yamazaki, M., Sakimura, K., and Nakada, T. (2007). Identification of arylsulfonamides as aquaporin 4 inhibitors. *Bioorganic & Medicinal Chemistry Letters*, *17*(5), p.1270-1273.

Hohlbrugger, G. (1995). The vesical blood-urine barrier: a relevant and dynamic interface between renal function and nervous bladder control. *The Journal of urology*, *154*(1), p. 6-15.

Hohlbrugger, G. (1987). Changes of hypo- and hypertonic sodium chloride induced by the rat urinary bladder at various filling stages: Evidence for an increased transurothelial access of urine to detrusor nerve and muscle cells with distension. *European Urology*, *13,* p. 83-89.

Halsey, A., Conner, A., Bill, R., Logan, A., and Ahmed, Z. (2018) Aquaporins and their regulation after spinal cord injury. *Cells*, *7*(10), p. 174.

Hasler, U., Nunes, P., Bouley, R., Lu, H.A., Matsuzaki, T., and Brown, D. (2008) Acute hypertonicity alters aquaporin-2 trafficking and induces a mapk-dependent accumulation at the plasma membrane of renal epithelial cells. *Journal of Biological. Chemistry. 283,* p. 26643-26661.

Haines, T. H. (1994). Water transport across biological membranes. *FEBS Letters*, *346*(1), p. 115-122.

Hara, M., Ma, T., and Verkman, A.S. (2001). Verkmanselectively reduced glycerol in skin of aquaporin-3-deficient mice may account for impaired skin hydration, elasticity, and barrier recovery. *Journal of Biological. Chemistry*. *277*, p. 46616-46621.

Huebert, R. C., Splinter, P. L., Garcia, F., Marinelli, R. A. and LaRusso, N. F. (2002). Expression and localization of aquaporin water channels in rat hepatocytes evidence for a role in canalicular bile secretion. *Journal of Biological Chemistry*, *277*(25), p. 22710-22717.

Hilson, A.J., Lewis, C.A., and Harland, S.J. (1990). The permeability of the human bladder to water assessed using tritiated water. *Contrib Nephrol* , p. 41-44.

Hoffert, J. D., Leitch, V., Agre, P., and King, L. S. (2000). Hypertonic induction of aquaporin-5 expression through an ERK-dependent pathway. *Journal of Biological Chemistry*, *275*(12), p. 9070-9077.

Hofmeester, I., Kollen, B.J., Steffens, M.G., Bosch, J.R., Drake, M.J., Weiss, J.P., and Blanker, M.H. (2014) The association between nocturia and nocturnal polyuria in clinical and epidemiological studies: a systematic review and meta-analyses. *The Journal of Urology*, *191*(4), p. 1028-1033.

Hoffmann, E. K., Lambert, I. H., and Pedersen, S. F. (2009). Physiology of cell volume regulation in vertebrates. *Physiological Reviews*, *89*(1), p. 193-277.

Hajdinjak, T., and Leskovar, J. (2013) Comparison of nocturia response to desmopressin treatment between patients with normal and high nocturnal bladder capacity index. *The Scientific World Journal*

Han, Z., and Patil, R.V. (2000) Protein kinase a-dependent phosphorylation of aquaporin-1. *Biochemical and Biophysical Research Communications*, *273*(1), p. 328-332.

Holm-larsen, T. (2014) The economic impact of nocturia. *Neurourology and Urodynamics. 33*, p. S10-S14.

Huber, V.J., Tsujita, M., Kwee, I.L., and Nakada T. (2009). Inhibition of aquaporin 4 by antiepileptic drugs bioorg. *Medical Chemistry.* 17, p. 418–424.

Hickling, D.R., Sun, T.T., and Wu, X.R. (2015) Anatomy and physiology of the urinary tract: relation to host defense and microbial infection. *Microbiology Spectrum*. *3*(4)

Hicks, R.M. (1975). The mammalian urianary bladderan accommodating organ. *Biological Reviews*, *50*(2), p. 215-246.

Hakim, A.A., Lifson, N. and Greevy, C.D. (1965). Fluxes of Na+ and Cl- in the dog urinary bladder. *Investigative Urology, 2*, p. 348-354.

Hicks, R.M. and Ketterer, B. (1970). Isolation of the plasmalemma of the luminal surface of the rat bladder epithelium. *Journal of Cell Biology, 45*, p. 542-553.

Hoek Van, A.N., Wiener, M.C., Verbavatz, J.M., Brown, D., Lipniunas, P.H., Townsend, R.R., and Verkman, A.S. (1995). Purification and structure-function analysis of native, pngase f-treated, and endo-b-galactosidase-treated chip28 water channels. *Biochemistry. 34*, p. 2212-2219.

Hu, H. Z., Granger, N., and Jeffery, N. D. (2016). Pathophysiology, clinical importance, and management of neurogenic lower urinary tract dysfunction caused by suprasacral spinal cord injury. *Journal of Veterinary Internal Medicine*, *30*(5), p. 1575-1588.

Hill, D. R., Huang, S., Tsai, Y. H., Spence, J. R., and Young, V. B. (2017). Real-time measurement of epithelial barrier permeability in human intestinal organoids. *Journal of Visualized Experiments*, (130), p. e56960.

Hill, W.G. (2015) Controle of urinary drainage and voiding. *Clinical Journal of the American Society of Nephrology*. *10*(3), p. 480-492.

Hu, P., Meyers, S., Liang, F.X., Deng, F.M., Kachar, B., Zeidel, M.L., and Sun, T.T. (2002). Role of membrane proteins in permeability barrier function: uroplakin ablation elevates urothelial permeability. *American Journal of Physiology-renal Physiology.* . *283*(6).

Hendriks, G., Koudijs, M., Van Balkom, B.W., Oorschot, V., Klumperman, J., Deen, P.M., and Van Der Sluijs, P. (2004). Glycosylation is important for cell surface

expression of the water channel aquaporin-2 but is not essential for tetramerization in the endoplasmic reticulum. *Journal of Biological Chemistry*, *279*(4), p. 2975-2983.

Ishibashi, K., Tanaka, Y. and Morishita, Y. (2014). The role of mammalian superaquaporins inside the cell. *Biochimica Et Biophysica Acta (BBA)-General Subjects*, *1845*(5), p. 1507-1512.

Ishikawa, Y., and Lida, H. (2002). The muscarinic acetylcholine receptor-stimulated increase in aquaporin-5 levels in the apical plasma membrane in rat parotid acinar cells is coupled with activation of nitric oxide/cgmp signal transduction. *Molecular Pharmacology,* 61, p. 1423-1434.

Ishikawa, Y, Skoronski, M.T., Inoue, N., and Ishida, H. (1999). Alpha(1)-adrenoceptor-induced trafficking of aquaporin-5 to the apical plasma membrane of rat parotid cells. *Biochem Biophys Res Commun*. *265*, p. 94-100.

Ishikawa, Y., Eguchi, T., Skowronski, M.T. and Ishida, H. (1998) Acetylcholine acts on m-3 muscarinic receptors and induces the translocation of aquaporin5 water channel via cytosolic ca2+ elevation in rat parotid glands. *Biochemical Biophysical Research Communications, 245*, p. 835-840.

Itoh, T., Rai, T., Kuwahara, M., Ko, S., Uchida, S., Sasaki, S., and Ishibashi, K. (2005). Identification of a novel aquaporin, AQP12, expressed in pancreatic acinar cells. *Biochemical and Biophysical Research Communications*, *330*(3), p.832-838.

Ikeda, M., Andoo, A., Shimono, M., Takamatsu, N., Taki, A., Muta, K., and Takata, K. (2011). The NPC motif of aquaporin-11, unlike the NPA motif of known aquaporins, is essential for full expression of molecular function. *Journal of Biological Chemistry*, *286*(5), p. 3342-3350.

Jiang, Y (2009). Expression and functional characterization of npa motif-null aquaporin-1 mutations. *Iubmb Life*. *61*(6), p. 222-226.

Jenkins, D., Winyard, P.J. and Woolf, A.S. (2007). Immunohistochemical analysis of sonic hedgehog signalling in normal human urinary tract development. *Journal of Anatomy, 211(*5), p. 620-629.

Jensen, A. M., Li, C., Praetorius, H. A., Nørregaard, R., Frische, S., Knepper, M. A., and Frøkiær, J. (2006). Angiotensin II mediates downregulation of aquaporin water channels and key renal sodium transporters in response to urinary tract obstruction. *American Journal of Physiology-Renal Physiology*, *291*(5), p. F1021-F1032.

Johansson, S.L. (1990) Light microscopic findings in bladders of patients with IC. *Interstitial Cystitis*. p. 83-90.

Jiang, X. X., Fei, X. W., Zhao, L., Ye, X. L., Xin, L. B., Qu, Y., and Lin, J. (2015). Aquaporin 5 plays a role in estrogen-induced ectopic implantation of endometrial stromal cells in endometriosis. *PloS one*, *10*(12), p. e0145290.

Jamieson, J. D., and Palade, G. E. (1968). Intracellular transport of secretory proteins in the pancreatic exocrine cell: IV. Metabolic requirements. *The Journal of Cell Biology*, *39*(3), p. 589-603.

Jung, H.J., and Kwon, T.H. (2016). Molecular Mechanisms Regulating Aquaporin-2 in Kidney Collecting Duct. *American Journal of Physiology-renal Physiology*. *311*(6).

Jung, J.S., Bhat, R.V., Preston, G.M., Guggino, W.B., Baraban, J.M. and Agre, P. (1994). Molecular characterization of an aquaporin cdna from brain: candidate osmoreceptor and regulator of water balance. *Proceedings of the National Academy of Sciences, 91*(26), p. 13052-13056.

Jin, M.H., and Moon, D.A.G. (2008). Practical management of nocturia in urology. *Indian Journal of Urology. 24*(3), p. 289.

Jo, A.O., Ryskamp, D.A., Phuong, T.T., Verkman, A.S., Yarishkin, O., Macaulay, N., and Krizaj, D. (2015). Trpv4 and aqp4 channels synergistically regulate cell volume and calcium homeostasis in retinal müller glia. *Journal of Neuroscience*. *35*(39), p. 13525-13537.

Jiang, Y. H., and Kuo, H. C. (2017). Urothelial barrier deficits, suburothelial inflammation and altered sensory protein expression in detrusor underactivity. *The Journal of urology*, *197*(1), p.197-203.

Jablonski, E. M., McConnell, N. A., Hughes Jr, F. M. and Huet-Hudson, Y. M. (2003). Estrogen regulation of aquaporins in the mouse uterus: potential roles in uterine water movement. *Biology of reproduction*, *69*(5), p. 1481-1487.

Jeyaseelan, K., Sepramaniam, S., Armugam, A., and Wintour, E. M. (2006). Aquaporins: a promising target for drug development. *Expert Opinion on Therapeutic Targets*, *10*(6), p. 889-909.

Kalman, K., Németh-Cahalan, K. L., Froger, A., and Hall, J. E. (2008). Phosphorylation determines the calmodulin-mediated Ca2+ response and water permeability of AQP0. *Journal of Biological Chemistry*, *283*(30), p. 21278-21283.

Kenhub (2019) *Anatomy of the urinary bladder*. Available from: https://www.kenhub.com/en/library/anatomy/urinary-bladder [Accessed 16 January 2020].

Krug, S. M., Fromm, M., and Günzel, D. (2009). Two-path impedance spectroscopy for measuring paracellular and transcellular epithelial resistance. *Biophysical journal*, *97*(8), p 2202-2211.

Kupelian, V., Fitzgerald, M.P., Kaplan, S.A., Norgaard, J.P.K., Chiu, G.R., and Rosen, R.C. (2011). Association of nocturia and mortality: results from the third national health and nutrition examination survey, *The Journal of Urology*. *185*(2), p. 571-577.

Keshtkar, A., Keshtkar, A., and Lawford, P. (2007). Cellular morphological parameters of the human urinary bladder (malignant and normal). *International Journal Of Experimental Pathology*, *88*(3), p. 185-190.

Kreida, S. and Toernroth-Horsefield, S. (2015). Structural insights into aquaporin selectivity and regulation. *Current Opinion in Structural Biology*, *33,* p.126-134.

Kazazic, M., Bertelsen, V., Pedersen, K.W., Vuong, T.T., Grandal, M.V., Rødland, M.S., and Madshus, I.H. (2009). Epsin 1 is involved in recruitment of ubiquitinated receptors into clathrin-coated pits. *Traffic*. *10*(2), p. 235-245.

Köhler, J., Thysell, H., Tencer, J., Forsberg, L., and Hellström, M. (2001). Conservative treatment and anti-reflux surgeryin adults with vesico-ureteral reflux: effect on urinary-tract infection, renal function and loin pain in a lang-term follow-up study. *Nephrology Dialysis Transplantation*, *16*(1), p. 52-60.

Khandelwal, P., Abraham, S.N., and Apodaca, G. (2009). Cell biology and physiology of the uroepithelium. *American Journal of Physiology-renal Physiology*. *297*(6)

Kushner, D. J., Baker, A., and Dunstall, T. G. (1999). Pharmacological uses and perspectives of heavy water and deuterated compounds. *Canadian Journal of Physiology and Pharmacology*, *77*(2), p. 79-88.

Kamsteeg, E.J, Hendriks, G., Goone, M., Konings, I.B., Oorschot, V., van der Sluijs, P., and Deen, P.M. (2006) Short-chain ubiquitination mediates the regulated endocytosis of the aquaporin-2 water channel. *Proceedings of the National Academy of Sciences*. *103*(48), p. 18344-18349.

Kim, H., Kim, J., Jeon, J. P., Myeong, J., Wie, J., Hong, C., and So, I. (2012). The roles of G proteins in the activation of TRPC4 and TRPC5 transient receptor potential channels. *Channels*, 6(5), p. 333-343.

Kim, S. O., Song, S. H., Ahn, K., Kwon, D., Park, K., and Ryu, S. B. (2010). Changes in aquaporin 1 expression in rat urinary bladder after partial bladder outlet obstruction: preliminary report. *Korean Journal of Uurology*, *51*(4), p. 281-286.

Kim, J. I., Kim, J., Jang, H. S., Noh, M. R., Lipschutz, J. H., and Park, K. M. (2013). Reduction of oxidative stress during recovery accelerates normalization of primary cilia length that is altered after ischemic injury in murine kidneys. *American Journal of Physiology-Renal Physiology*, *304*(10), p. F1283-F1294.

Karabasil, M.R., Hasegawa, T., Azlina, A., Purwanti, N., Purevjav, J. and Yao, C. (2009). Trafficking of gfp-aqp5 chimeric proteins conferred with unphosphorylated amino acids at their pka-target motif ((152)srrts) in mdck-ii cells. *Journal of Medical Investigation*, *56*, p. 55-63.

Kwon, T.H., Hager, H., Nejsum, L.N., Andersen, M.L., Frokiaer, J., and Nielson, S. (2001). Physiology and pathophysiology of renal aquaporins. *Seminars in Nephrology*. *21*, p. 231-238.

Kishida, K., Kuriyama, H., Funahashi, T., Shimomura, I., Kihara, S., and Ouchi, N. (2000). Aquaporin adipose, a putative glycerol channel in adipocytes. *Journal of Biological Chemistry*, 275*,* p. 20896-20902.

Kültz, D., Chakravarty, D., and Adilakshmi, T. (2001). A novel 14-3-3 gene is osmoregulated in gill epithelium of the euryhaline teleost fundulus heteroclitus. *Journal of Experimental. Biology*, *204*, p. 2975-2985.

Kong, K.L, Kwong, D.L., Fu, L., Chan, T.H.M., Chen, L., Liu, H., and Law, S.Y.K. (2010). Characterization of a candidate tumor suppressor gene uroplakin 1A in esophageal squamous cell carcinoma. *Cancer research*, *70*(21), p. 8832-8841.

Kerrebroeck Van, P. and Andersson, K.E. (2014). Terminology, epidemiology, etiology, and pathophysiology of nocturia. *Neurourology and Urodynamics* . *33*, p. S2-S5.

Kerrebroeck Van, P., Abrams, P., Chaikin, D., Donovan, J., Fonda, D., Jackson, S., and Robertson, G. (2002). The standardisation of terminology in nocturia: report from the standardisation sub-committee of the international continence society. *Neurourology and Urodynamics, 21*(2), p. 179-183.

Kong, X.T., Deng, F.M., Hu, P., Liang, F.X., Zhou, G., Auerbach, A.B., and Kachar, B. (2004). Roles of uroplakins in plaque formation, umbrella cell enlargement, and urinary tract diseases. *Journal of Cell Biology.* 167 (6), p. 1195-1204.

Koyama, Y., Yamamoto, T., Kondo, D., Funaki, H., Yaoita, E., Kawasaki, K., and Kihara, I. (1997). Molecular cloning of a new aquaporin from rat pancreas and liver. *Journal of Biological Chemistry*, *272*(48), p. 30329-30333.

Karlsson, T., Glogauer, M., Ellen, R.P., Loitto, V.M., Magnusson, K.E., and Magalhaes, M.A. (2011) Aquaporin 9 phosphorylation mediates membrane localization and neutrophil polarization. *Journal of Leukocyte Biology*, *90*, p. 963-973.

Kirschner, N., Poetzl, C., von den Driesch, P., Wladykowski, E., Moll, I., Behne, M. J., and Brandner, J. M. (2009). Alteration of tight junction proteins is an early event in psoriasis: putative involvement of proinflammatory cytokines. *The American Journal of Pathology*, *175*(3), 1095-1106.

Kalman, K., Németh-Cahalan, K. L., Froger, A., and Hall, J. E. (2008). Phosphorylation determines the calmodulin-mediated Ca2+ response and water permeability of AQP0. *Journal of Biological Chemistry*, *283*(30), p. 21278-21283.

Kim, W.U., Min, S.Y., Hwang, S.H., Yoo, S.A., Kim, K.J., and Cho, C.O.S. (2010). Effect of oestrogen on t cell apoptosis in patients with systemic lupus erythematosus. *Clinical & Experimental Immunology. 161*(3), p. 453-458.

Karlsson, T., Glogauer, M., Ellen, R.P., Loitte, V.M., Magnusson, K.E. and Magelhaes, M.A. (2011). Aquaporin 9 phosphorylation mediates membrane localization and neutrophil polarization. *Journal of Leukocyte Biology*. *90,* p. 963-973.

Kitchen, P., ÖBerg, F., Sjöhamn, J., Hedfalk, K., Bill, R.M., Conner, A.C., and Tömroth-horsefield, S. (2015). Plasma membrane abundance of human aquaporin 5 is dynamically regulated by multiple pathways. *Plos One*. *10*(11).

Ko, C.H., and Takahashi, J.S. (2006). Molecular Components of the Mammalian Circadian Clock. Human. *Molecular Genetics. 15*(2), p. 271-277.

Kültz, D., Chakravarty, D., and Adilakshmi, T. (2001) A novel 14-3-3 gene is osmoregulated in gill epithelium of the euryhaline teleost fundulus heteroclitus. *Journal of Experimental. Biology,* 204, p. 2975-2985.

Kujubu, D.A. and Aboseif, S.R. (2008). An overview of nocturia and the syndrome of nocturnal polyuria in the elderly. *Nature Clinical Practice Nephrology*, *4*(8), p. 426-435.

Kwon, T. H., Frøkiær, J., and Nielsen, S. (2013). Regulation of aquaporin-2 in the kidney: a molecular mechanism of body-water homeostasis. *Kidney Research and Clinical Practice*, *32*(3), p. 96-102.

Koike, S., Tanaka, Y., Matsuzaki, T., Morishita, Y., and Ishibashi, K. (2016). Aquaporin-11 (AQP11) expression in the mouse brain. *International Journal of Molecular Sciences*, *17*(6), 861.

Kuriyama, H., Kawamoto, S., Ishida, N., Ohno, I., Mita, S., Matsuzawa, Y., Matsubara, K., and Okubo, K. (1997). Molecular cloning and expression of a novel human aquaporin from adipose tissue with glycerol permeability. *Biochemical and Biophysical Research Communications, 241*(1), p.53-58.

Klingler, C. H. (2016). Glycosaminoglycans: how much do we know about their role in the bladder?. *Urologia Journal*, p. 8311-14.

Karabasil, M.R., Hasegawa, T., Azlina, A., Purwanti, N., Purevjav, J., and Yao, C. (2009). Trafficking of gfp-aqp5 chimeric proteins conferred with unphosphorylated amino acids at their pka-target motif (152) (srrts) in mdck-ii cells. *Journal of Medical Investigation*. *56*, p. 55-63.

Lescay, H.A., and Tuma, F. (2018). Anatomy, abdomen and pelvis, ureter. Statpearls Publishing

Leaf, A. (1962). Actions of neurohypophyseal hormones on a living membrane. *Journal of General. Physiology. 43*, p. 175-189

Loike, J., and Rosen, O.M. (1990). Glucose transporters serve as water channels. *Proceedings of the National Academy of Sciences of the United States of America*. USA 87, 32443247.

Liu, X., Bandyopadhyay, B., Nakamoto, T., Singh, B., Liedtke, W., Melvin, J. E., and Ambudkar, I. (2006). A role for AQP5 in activation of TRPV4 by hypotonicity concerted involvement of AQP5 and TRPV4 in regulation of cell volume recovery. *Journal of Biological Chemistry*, *281*(22), p. 15485-15495.

Lewis, S.A., Eaton, D.C. and Diamond, J.M. (1976). The mechanism of na+ transport by rabbit urinary bladder. *The Journal of Membrane Biology*. 28(1), p. 41-70.

Lewis, S.A. and Klein, T.J. (2000). Urea modified the permeability of the mammalian urothelial *Journal of Urology. 154*(1), p. 219-223.

Lewis, S.A. and Donaldson, P. (1990). Ion channels and cell volume regulation: chaos in an organized system. *Physiology.* 5 (3), p. 112-119.

Lee, B. H., and Kwon, T. H. (2007). Regulation of AQP2 in collecting duct: an emphasis on the effects of angiotensin II or aldosterone. *Electrolyte & Blood Pressure*, *5(*1), p. 15-22.

Lang, F., Busch, G. L., Ritter, M., Volkl, H., Waldegger, S., Gulbins, E., and Haussinger, D. (1998). Functional significance of cell volume regulatory mechanisms. *Physiological Reviews*, *78* (1), p. 247-306.

Lasicˇ, E., Višnjar, T., and Kreft, M.E. (2015). Properties of the urothelium that establish the blood-urine barrier and their implications for drug delivery. *Review of Physiology Biochemistry Pharmacology. 168,* p. 1-29.

Loonen, A. J., Knoers, N. V., van Os, C. H., and Deen, P. M. (2008). Aquaporin 2 mutations in nephrogenic diabetes insipidus. In *Seminars in nephrology 28*(3) p. 252-265.

Lindskog, C., Asplund, A., Catrina, A., Nielsen, S., and Rützler, M. (2016). A systematic characterization of aquaporin-9 expression in human normal and pathological tissues. *Journal of Histochemistry and Cytochemistry*, *64*(5), 287-300.

Losif, C. S., Batra, S., Ek, A., and Åstedt, B. (1981). Estrogen receptors in the human female lower urinary tract. *American journal of Obstetrics and Gynecology*, *141*(7), p. 817-820.

Levi, H., and Ussing, H. H. (1949). Resting potential and ion movements in the frog skin. *Nature*, *164*(4178), p. 928.

Lu, M., Lee, Md, Smith, B.L., Jung, J.S., Agre, P., Verdijk, M.A., Merkx, G., Rijss, J.P., and Deen, P.M. (1996). The human aqp4 gene: definition of the locus encoding two water channel polypeptides in brain. *Proceedings of the National Academy of Science U.S. A*. *93*(20).

Liu, X., Bandyopadhyay, B., Nakamoto, T., Singh, B., Liedtke, W., Melvin, J. E., and Ambudkar, I. (2006). A role for AQP5 in activation of TRPV4 by hypotonicity concerted involvement of AQP5 and TRPV4 in regulation of cell volume recovery. *Journal of Biological Chemistry*, *281*(22), p.15485-15495.

Litman, T., Søgaard, R., and Zeuthen, T. (2009). Ammonia and urea permeability of mammalian aquaporins. *Journal of Molecular Science In Aquaporins* p. 327-358.

Leitch, V., Agre, P., and King, L.S. (2001). Altered ubiquitination and stability of aquaporin-1 in hypertonic stress. *Proceedings of the National Academy of Sciences of the Usa 98,* p. 2894-2898.

Lis, H. and Sharon, N. (1993). Protein glycosylation: structural and functional aspects. *European Journal of Biochemistry*. *218*(1), p. 1-27.

Loitto, V.M., Huang, C., Sigal, Y.J., and Jacobson, K. (2007). Filopodia are induced by aquaporin-9 expression. *Experimental Cell Research*. *313*(7), p. 1295-1306

Lena, F. M., and Lebeck, J. (2018). Implications of aquaglyceroporin 7 in energy metabolism. *International Journal of Molecular sciences*, *19*(1), 154.

Li, H., Sheppard, D. N., and Hug, M. J. (2004). Transepithelial electrical measurements with the Ussing chamber. *Journal of Cystic Fibrosis*, *3*, p. 123-126.

Ilieva, G. S., Tolekova, A. N., Sandeva, R. V., Trifonova, K. J., Tsokeva, Z. I., Ganeva, M. G. and Zezovski, S. (2008). Role of transmembrane calcium current in angiotensin II-mediated contraction of detrusor organ strips from rat urinary bladder. *Bulgarian Journal of Veterinary Medicine*, *11*(2), p. 89-94.

Liu, H. B., Zhang, J., Sun, Y. Y., Li, X. Y., Jiang, S., Liu, M. Y., and Zhang, Z. R. (2015). Dietary salt regulates epithelial sodium channels in rat endothelial cells: adaptation of vasculature to salt. *British Journal of Pharmacology*, *172*(23), p. 5634-5646.

Li, H., Sheppard, D. N., and Hug, M. J. (2004). Transepithelial electrical measurements with the Ussing chamber. *Journal of Cystic Fibrosis*, *3*, p.123-126.

Li, X., Chen, G. and Yang, B. (2012). Urea transporter physiology studied in knockout mice. *Frontiers in Physiology*, *3*, p. 217.

Li, C., Guan, G., Zhang, F., Song, S., Wang, R. K., Huang, Z. and Nabi, G. (2014). Quantitative elasticity measurement of urinary bladder wall using laser-induced surface acoustic waves. *Biomedical Optics Express*, *5*(12), p. 4313-4328.

Lu, S. H., Lin, A. T., Chen, K. K., Chiang, H. S., and Chang, L. S. (2011). Characterization of smooth muscle differentiation of purified human skeletal muscle-derived cells. *Journal of Cellular and Molecular Medicine*, *15*(3), p. 587-592.

Levinsky, N. G., and Berliner, R. W. (1959). Changes in composition of the urine in ureter and bladder at low urine flow. *American Journal of Physiology-Legacy Content*, *196*(3), p. 549-553.

Lee, B. H., and Kwon, T. H. (2007). Regulation of AQP2 in collecting duct: an emphasis on the effects of angiotensin II or aldosterone. *Electrolyte and Blood Pressure*, *5*(1), p. 15-22

Lee, G. (2011). Uroplakins in the lower urinary tract. *International neurourology journal,* 15(1), p. 4.

Laforenza, U., Bottino, C. and Gastaldi, G. (2016). Mammalian aquaglyceroporin function in metabolism. *Biochimica et Biophysica Acta (BBA) - Biomembranes*, *1858*(1), p.1-11

Marinelli, R.A., Pham, L., Agre, P., and Larusso, N.F. (1997). Secretin promotes osmotic water transport in rat cholangiocytes by increasing aquaporin-1 water channels in plasma membrane – evidence for a secretin-induced vesicular translocation of aquaporin-1. *Journal of Biological Chemistry*, *272,* p. 12984-12988.

Ma, T., Song, Y., Gillespie, A., Carlson, E. J., Epstein, C. J., and Verkman, A. S. (1999). Defective secretion of saliva in transgenic mice lacking aquaporin-5 water channels. *Journal of Biological Chemistry*, *274*(29), p. 20071-20074.

Mahadevan, V. (2016). Anatomy of the lower urinary tract. *Surgery (Oxford)*, *34*(7), p. 318-325.

Marinelli, R.A., Pham, L., Agre, P., and Larusso, N.F. (1997). Secretin promotes osmotic water transport in rat cholangiocytes by increasing aquaporin-1 water channels in plasma membrane – evidence for a secretin-induced vesicular translocation of aquaporin-1. *Journal of Biological Chemistry.* 272, p. 12984-12988.

Matter, K., and Balda, M.S. (2003). Signalling to and from tight junctions. *Nature Reviews Molecular Cell Biology*. *4*(3), p. 225.

Madeira, A., Moura, T.F., and Soveral, G. (2016) Detecting aquaporin function and regulation. *Frontiers in Chemistry*. 4

Morishita, Y., Matsuzaki, T., Hara-Chikuma, M., Andoo, A., Shimono, M., Matsuki, A., and Kusano, E. (2005). Disruption of aquaporin-11 produces polycystic kidneys following vacuolization of the proximal tubule. *Molecular and Cellular Biology*, *25*(17), p. 7770-7779.

Ma, T., Frigeri, H., Hasegawa, H., and Verkman, A.S. (1994). Verkmancloning of a water channel homolog expressed in brain meningeal cells and kidney collecting duct that functions as a stilbene-sensitive glycerol transporter. *Journal of Biological Chemistry, 269*, p. 21845-21849.

Moeller, H.B., Fenton, R.A., Zeuthen, T., and Macaulay, N. (2009). Vasopressin-dependent short-term regulation of aquaporin 4 expressed in xenopus oocytes. Neuroscience. *164,* p. 1674-1684.

Miloshevsky, G. V., and Jordan, P. C. (2004). Water and ion permeation in bAQP1 and GlpF channels: a kinetic Monte Carlo study. *Biophysical journal*, *87*(6), p. 3690-3702.

Martin-Padura, I, Lostaglio, S., Schneemann, M., Williams, L., Romano, M., Fruscella, P., and Simmons, D. (1998). Junctional adhesion molecule, a novel member of the immunoglobulin superfamily that distributes at intercellular junctions and modulates monocyte transmigration. The Journal of Cell Biology. *142*(1), p. 117-127.

Montalbetti, N., Rued, A. C., Clayton, D. R., Ruiz, W. G., Bastacky, S. I., Prakasam, H. S., and Carattino, M. D. (2015). Increased urothelial paracellular transport promotes cystitis. *American Journal of Physiology-Renal Physiology*, *309*(12), p. F1070-F1081.

Merrill, L, Gonzalez, E.J., Girard, B.M., and Vizzard, M.A. (2016). Receptors, channels, and signalling in the urothelial sensory system in the bladder. *Nature Reviews Urology* . *13*(4), p. 193.

Mamonov, A. B., Coalson, R. D., Zeidel, M. L., and Mathai, J. C. (2007). Water and deuterium oxide permeability through aquaporin 1: MD predictions and experimental verification. *The Journal of General Physiology*, *130*(1), p. 111-116.

Ma, T., Frigeri, A., Skach, W., and Et Al, (1993). Cloning of a novel rat kidney cdna homologous to chip28 and wch-cd water channels. *Biochemical Biophysical Research Communications.* 197, p. 654-659.

Monsang, S.J., Parhi, J., Choudhury, J., Deka, A., and Pal, P. (2019). Molecular characterisation of carp aquaporin-3a: expression profiling during hormone-induced spawning. *Aquaculture*, 500, p. 569-575

Mani, V., Hollis, J. H., and Gabler, N. K. (2013). Dietary oil composition differentially modulates intestinal endotoxin transport and postprandial endotoxemia. *Nutrition & metabolism*, *10*(1), 6.

Matsumura, Y., Uchida, S., Rai, T., Sasaki, S., and Marumo, F. (1997). Transcriptional regulation of aquaporin-2 water channel gene by camp. *Journal of the American Society of Nephrology*. 8, p. 861-867.

Maunsbach, A.B., Marples, D., Chin, E., Ning, G., Bondy, C., Agre, P., and Nielsen, S.J. (1997). Aquaporin-1 water channel expression in human kidney. *American Society of Nephrology, 8*(1), p. 1-14.

Miyake, M., Toguchi, H., Nishibayashi, T., Higaki, K., Sugita, A., Koganei, K., and Okamoto, S. (2013). Establishment of novel prediction system of intestinal absorption in humans using human intestinal tissues. *Journal of Pharmaceutical Sciences*, *102*(8), p. 2564-2571.

Madeira, A., Fernández-Veledo, S., Camps, M., Zorzano, A., Moura, T. F., Ceperuelo-Mallafré, V., and Soveral, G. (2014). Human aquaporin-11 is a water and glycerol channel and localizes in the vicinity of lipid droplets in human adipocytes. *Obesity*, *22*(9), p2010-2017.

Mola, M. G., Nicchia, G. P., Svelto, M., Spray, D. C. and Frigeri, A. (2009). Automated cell-based assay for screening of aquaporin inhibitors. *Analytical chemistry*, *81*(19), p. 8219-8229.

Matsuzaki, T., Suzuki, T., and Takata, K. (2001) Hypertonicity-induced Expression of Aquaporin 3 in Mdck Cells. *The American Journal Physiology Cell Physiology, 281*

Murata, K., Mitsuoka, K., Hirai, T., Walz, T., Agre, P., Heymann, J.B., and Fuijyoshi, Y. (2000) Structural determinants of water permeation through aquaporin-1. *Nature, 407*, p. 599.

Migliati, E., Meurice, N., DuBois, P., Fang, J. S., Somasekharan, S., Beckett, E.. and Yool, A. J. (2009). Inhibition of aquaporin-1 and aquaporin-4 water permeability by a derivative of the loop diuretic bumetanide acting at an internal pore-occluding binding site. *Molecular Pharmacology*, *76*(1), p. 105-112.

Mills, I.W., Noble, J.G. and Brading, A.F. (2000) Radiotelemetered Cystometry in Pigs: Validation and Comparison of Natural Filling Versus Diuresis Cystometry. *Journal of urology, 164*, p. 1745-1750.

Moore, J.A., and Brading, A.F. (2007) A Porcine model of bladder outlet obstruction incorporating radio-telemetered cystometry. *BJU International*. *100*, p. 1192-1193.

Mutsaers, A. J., Widmer, W. R., and Knapp, D. W. (2003). Canine transitional cell carcinoma. *Journal of Veterinary Internal Medicine*, *17*(2), 136-144.

Nakhoul, N.L., Davis, B.A., Romero, M.F., and Boron, W.F. (1998). *American Journal of Physiology*. *274*, p. 543-548

Nedvetsky, P.I., Tamma, G., Beulshausen, S., Valenti, G., Rosenthal, W., and Klussmann, E. (2009). Regulation of aquaporin-2 trafficking. *Aquaporins*. p. 133-157.

Negrete, H.O., Lavellem J.P., Bergm J., Lewis, S.A., and Zeidel ML. (1996). Permeability properties of the intact mammalian bladder epithelium*. American Journal of Physiology, 271* (4), p. F886-F894

Németh-cahalan, K.L., Kalman, K., and Hall, J.E. (2004). Molecular Basis of Ph and Ca2+ Regulation of Aquaporin Water Permeability. *The Journal of General Physiology. 123*(5), p. 573-580.

Nelson, R.A., Jones, J.D., Wahnerm H.W., McGill, D.B., and Code C.F. (1975). Nitrogen metabolism in bears: urea metabolism in summer starvation and in winter sleep and role of urinary bladder in water and nitrogen conservation. *Mayo Clinic Proceedings. 50* p. 141–146

Nelson, R. A., Wahner, H. W., Jones, J. D., Ellefson, R. D., and Zollman, P. E. (1973). Metabolism of bears before, during, and after winter sleep. *American Journal of Physiology-Legacy Content*, *224*(2), p. 491-496.

North, R. A. (2016). P2X receptors. *Philosophical Transactions of the Royal Society B: Biological Sciences*, *371*(1700), 20150427.

Nesverova, A.S and Törnroth-horsefield, S. (2019). Phosphorylation-dependent Regulation of Mammalian Aquaporins. *Cells* . *8*(2), p. 82.

Negrete, H. O., Lavelle, J. P., Berg, J., Lewis, S. A., and Zeidel, M. L. (1996). Permeability properties of the intact mammalian bladder epithelium. *American Journal of Physiology-Renal Physiology,* 271(4), p. F886-F894.

Nelson, R.A., Jones. J.D., Wahner. H.W., and McGill. D.B. (1975). Code CF.Nitrogen metabolism in bears: urea metabolism in summer starvation and in winter sleep and role of urinary bladder in water and nitrogen conservation. *Mayo Clinic Proceedings, 50* p. 141 146

Nicchia, G.P., Rossi, A., Mola, M.G., Procino, G., Frigeri, A., and Svelto, M. (2008). Actin cytoskeleton remodeling governs aquaporin-4 localization in astrocytes. *Glia*. *56* (17), p.1755-66.

Németh-cahalan, K.L., Kalman, K., and Hall, J.E. (2004). Molecular Basis of Ph and Ca2+ Regulation of Aquaporin Water Permeability. *The Journal of General Physiology*, *123*(5), p. 573-580.

Oelke, M., Adler, E., Marschall-kehrel, D., Hermann, T.R. and Berges, R. (2014). Nocturia: state of the art and critical analysis of current assessment and treatment strategies. *World Journal of Urology*. *32*(5), p. 1109-1117.

Oliveira, C.A., Carnes, K., França, L.R., Hermo, L., and Hess, R.A. (2005). Aquaporin-1 And− 9 are differentially regulated by oestrogen in the efferent ductule epithelium and initial segment of the epididymis. *Biology of the Cell*. *97(*6), p. 385-395.

Ohinata, A., Nagai, K., Nomura, J., Hashimoto, K., Hisatune, A., and Miyata, T. (2005). Lipopolysaccharide changes the subcellular distribution of aquaporin 5 and increases plasma membrane water permeability in mouse lung epithelial cells. *Biochem and Biophysical Research Communications. 326,* p. 521-526.

Parsons, J. K. (2010). Benign prostatic hyperplasia and male lower urinary tract symptoms: epidemiology and risk factors. *Current Bladder dysfunction Reports*, *5*(4), p. 212-218.

Parsons, B. A., Drake, M. J., Gammie, A., Fry, C. H., and Vahabi, B. (2012). The validation of a functional, isolated bladder model from a large animal. *Frontiers in pharmacology*, *3*, 52.

Pirahanchi, Y., and Aeddula, N. R. (2019). Physiology, sodium potassium pump (Na+ K+ Pump). In *StatPearls [Internet]*. StatPearls Publishing.

Passanten-morales, H., and Cruz-rangel, S. (2010). Brain volume regulation: osmolytes and aquaporin perspectives. *Neuroscience. 168* (4), p. 871-884.

Patil, R.V., Xu, S., Van Hoek, A.N., Rusinko, A., Feng, Z., May, J. and Carr, G. (2016) Rapid identification of novel inhibitors of the human aquaporin-1 water channel. *Chemical Biology and Drug Design* [online]. *87*(5), p. 794-805.

Piper, R.C., and Luzio, J.P. (2007). Ubiquitin-dependent sorting of integral membrane proteins for degradation in lysosomes. *Current Opinion in Cell Biology*. *19*(4), p. 459-465.

Parvin, M.N., Kurabuchi, S., Murdiastuti, K., Yao, C., Kosugi-tanaka, C., and Akamatsu, T. (2005). Subcellular redistribution of aqp5 by vasoactive intestinal polypeptide in the brunner's gland of the rat duodenum. *American Journal of Physiology Gastrointest Liver Physiology*, *288*, p. G1283-G1291.

Pavlovic-Djuranovic, S., Kun, J. F., Schultz, J. E., and Beitz, E. (2006). Dihydroxyacetone and methylglyoxal as permeants of the Plasmodium aquaglyceroporin inhibit parasite proliferation. *Biochimica et Biophysica Acta (BBA)-Biomembranes*, *1758*(8), p.1012-1017.

Papafotiou, G., Paraskevopoulou, V., Vasilaki, E., Kanaki, Z., Paschalidis, N., and Klinakis, A. (2016). KRT14 marks a subpopulation of bladder basal cells with pivotal role in regeneration and tumorigenesis. *Nature communications*, *7*, 11914.

Preston, G. M., Jung, J. S., Guggino, W. B., and Agre, P. (1993). The mercury-sensitive residue at cysteine 189 in the CHIP28 water channel. *Journal of Biological Chemistry*, *268*(1), p. 17-20.

Papadopoulos, M.C., and Verkman, A.S. (2013) Aquaporin water channels in the nervous system. *Nature Reviews Neuroscience*. *14*, p. 265.

Qi, H., Li, L., Zong, W., Hyer, B.J., and Huang, J. (2009). Expression of aquaporin 8 is diversely regulated by osmotic stress in amnion epithelial cells. *Journal of Obstetrics Gynaecology Research.* 35, p. 1019-1025.

Quallo, T., Vastani, N., Horridge, E., Gentry, C., Parra, A., Moss, S., and Bevan, S. (2015). TRPM8 is a neuronal osmosensor that regulates eye blinking in mice. *Nature communications*, *6*, 7150.

Riveros-Perez, E., and Riveros, R. (2018). Water in the human body: An anesthesiologist's perspective on the connection between physicochemical properties of water and physiologic relevance. *Annals of medicine and surgery*, *26*, p.1-8.

Rezakhaniha, B., Arianpour, N., and Siroosbakhat, S. (2011). Efficacy of desmopressin in treatment of nocturia in elderly men. journal of research in medical sciences: *The Official Journal of Isfahan University of Medical Sciences* , 16 (4), p. 516.

Reichow, S.L., and Gonen, T. (2008) Noncanonical binding of calmodulin to aquaporin-0: implications for channel regulation. *Structure* , p. 1389-1398.

Rubenwolf, P.C., Georgopoulos, N.T., Clements, L.A., Feather, S., Holland, P., Thomas, D.F., and Southgate, J. (2009). Expression and localisation of aquaporin water channels in human urothelium in situ and in vitro. *European urology*. *56*(6), p. 1013-1024.

Riegler, M., Castagliuolo, I., Wang, C., Wlk, M., Sogukoglu, T., Wenzl, E., and Pothoulakis, C. (2000). Neurotensin stimulates Cl− secretion in human colonic mucosa in vitro: role of adenosine. *Gastroenterology*, *119*(2), 348-357.

Rubenwolf, P.C., Georgopoulos, N.T., Kirkwood, L.A., Baker, S.C., and Southgate, J. (2012) Aquaporin expression contributes to human transurothelial permeability in vitro and is modulated NaCl*. Plos One*. *7*(9)

Rapoport, A., Nicholson, T.F., and Yendt, E.R. (1960). Movement of electrolytes across the wall of the urinary bladder in dogs. *American Journal of Physiology*. 198, p. 191-194.

Rapoport, A., Nicholson, T.F., and Yendt, E.R. (1960). Movement of electrolytes across the wall of the urinary bladder in dogs. *American Journal of Physiology. 198*, p. 191-194.

Rodriguez-Boulan, E., Kreitzer, G., and Müsch, A. (2005). Organization of vesicular trafficking in epithelia. *Nature Reviews Molecular Cell Biology*, *6*(3), 233.

Rodriguez, A., Catalan, V., Gomez-ambros, J., Garcia-navarro, S., Rotellar, F., and Valenti, V. (2011). Insulin- and leptin-mediated control of aquaglyceroporins in human adipocytes and hepatocytes is mediated via the pi3k/akt/mtor signaling cascade. *Journal of Clinical Endocrinology and Metabolism*. 96, p. E586-E597.

Rützler, M., Rojek, A., Damgaard, M. V., Andreasen, A., Fenton, R. A., and Nielsen, S. (2016). Temporal deletion of Aqp11 in mice is linked to the severity of cyst-like disease. *American Journal of Physiology-Renal Physiology*, *312*(2), p. F343-F351.

Reichow, S. L., Clemens, D. M., Freites, J. A., Németh-Cahalan, K. L., Heyden, M., Tobias, D. J., and Gonen, T. (2013). Allosteric mechanism of water-channel gating by Ca 2+–calmodulin. *Nature Structural and Molecular Biology*, *20(*9), p. 1085.

Rabaud, N.E., Song, L., Wang, Y., Agre, P., Yasui, M., and Carbery, J.M. (2009). Aquaporin 6 binds calmodulin in a calcium-dependent manner. *Biochemical and Biophysical Research Communications. 383,* p. 54-57.

Savage, D.F., O'Connell, J.D., Miercke, L.J., Finer-moore, J., and Stroud, R.M. (2010). Structural context shapes the aquaporin selectivity filter. Proceedings of the **National Academy** of **Sciences** of **the United States** of America, [online]. *107,* p. 17164-17169.

Sales, A. D., Duarte, A. B. G., Santos, R. R., Alves, K. A., Lima, L. F., Rodrigues, G. Q., and Figueiredo, J. R. (2016). Modulation of aquaporins 3 and 9 after exposure of ovine ovarian tissue to cryoprotectants followed by in vitro culture. *Cell and tissue research*, *365*(2), p. 415-424.

Schafer, J. A. (2004). Renal water reabsorption: a physiologic retrospective in a molecular era. *Kidney International*, *66*, p. S20-S27.

Soler, A.P, Miller, R.D., Laughlin, K.V., Carp, N.Z., Klurfeld, D.M. and Mullin, J.M. (1990). Increased tight junctional permeability is associated with the development of colon cancer. *Carcinogenesis*. *20*(8), p. 1425-1432.

Sorensen, A. B., Søndergaard, M. T., and Overgaard, M. T. (2013). Calmodulin in a heartbeat. *The FEBS journal*, *280*(21), p. 5511-5532.

Solomon, A. K., Chasan, B., Dix, J. A., Lukacovic, J. M. F., Toon, M. R., and Verkman, A. S. (1983). The aqueous pore in the red cell membrane: band 3 as a channel for anions, cations, nonelectrolytes, and water. *Annals of the New York Academy of Sciences*, *414*(1), p. 97-124.

Sugiyama, Y., Yamazaki, K., Kusaka-Kikushima, A., Nakahigashi, K., Hagiwara, H., and Miyachi, Y. (2014). Analysis of aquaporin 9 expression in human epidermis and cultured keratinocytes. Federation of European Biochemical. Societies *open bio, 4(1)*, p. 611-616.

Stamer, W.D., Bok, D., Hu, J., Jaffe, G.J., and McKay, B.S. (2003). Aquaporin-1 channels in the human retinal pigment epithelium: role in transepithelial water movement. Investive Ophthalmology and Visual Science. 44, p. 2803-2808.

Sibley, G.N. A. (1984). Comparison of spontaneous and nerve-mediate.d activity in bladder muscle from man, pig and rabbit. *The Journal of Physiology, 354*(1), p. 431-443.

Silverthorn, D. U., Ober, W. C., Garrison, C. W., Silverthorn, A. C., and Johnson, B. R. (2010). *Human Physiology: an Integrated Approach* p. 412. San Francisco: Pearson/Benjamin Cummings.

Shafik, A. E.l., Sibai. O., Shafik, A.A., Ahmed, I (2004). Do vesical and voided urine have identical compositions? *Scandinavian Journal of Urology and Nephrology* 38, p. 243–246.

Sougrat, R, Morand, M., Gondran, C., Barré, P., Gobin, R., and Bonté, F. (2002). Functional expression of aqp3 in human skin epidermis and reconstructed epidermis. *Journal of Investigative Dermatology, 118*, p. 678.

Skowronski, M.T., Lebeck, J., Rojek, A., Praetorius, J., Kuchtbauer, E.M., Frøkiær, J., and Nielsen, S. (2007). Aqp7 is localized in capillaries of adipose tissue, cardiac and striated muscle: implications in glycerol metabolism. *American Journal of Physiology-renal Physiology*, *292*(3), p. F956-F965.

Shafik, A., Shafik, IE.l .Sibai, O., and Shafik, A.A (2005). Changes in the urine composition during its passage through the ureter. A concept of urothelial function. *Urology Research, 33*: p 426–428.

Sam, P., and LaGrange, C. A. (2019). Anatomy, abdomen and pelvis, sphincter urethrae. In StatPearls [Internet]. StatPearls Publishing.

Sadegh, M. K., Ekman, M., Rippe, C., Uvelius, B., Swärd, K., and Albinsson, S. (2012). Deletion of Dicer in smooth muscle affects voiding pattern and reduces detrusor contractility and neuroeffector transmission. *PloS one*, *7*(4), p. e35882.

Smith, N. J., Hinley, J., Varley, C. L., Eardley, I., Trejdosiewicz, L. K., and Southgate, J. (2015). The human urothelial tight junction: claudin 3 and the ZO-1α+ switch. *Bladder*, *2*(1), e9.

Savage, D. F., and Stroud, R. M. (2007). Structural basis of aquaporin inhibition by mercury. *Journal of Molecular Biology*, *368*(3), p. 607-617.

Scheiner, S., and Čuma, M. (1996). Relative stability of hydrogen and deuterium bonds. *Journal of the American Chemical Society*, *118*(6), p.1511-1521.

Srinivasan, B., Kolli, A. R., Esch, M. B., Abaci, H. E., Shuler, M. L., and Hickman, J. J. (2015). TEER measurement techniques for in vitro barrier model systems. *Journal of laboratory automation*, *20*(2), p. 107-126.

Schulkze, J.D, Ploeger, S., Amasheh, M., Fromm, A., Zeissig, S., Troeger, H. and Frommc, M. (2009). Epithelial tight junctions in intestinal inflammation. Molecular structure and function of the tight junction: from basic mechanisms to clinical manifestations. *Annals of the New York Academy of Sciences*, *1165*(1), 294-300.

Schey, K. L., Little, M., Fowler, J. G., and Crouch, R. K. (2000). Characterization of human lens major intrinsic protein structure. *Investigative Ophthalmology & Visual Science*, 41(1), 175-182.

Spector, D.A., Wade, J.B., Dillow, R., Steplock, D.A., and Weinam, E.J. (2002). Expression, localization, and regulation of aquaporin-1 to-3 in rat urothelia. *American Journal of Physiology-renal Physiology*, *282*(6)

Spector, D. A., Deng, J., Coleman, R., and Wade, J. B. (2015). The urothelium of a hibernator: the American black bear. *Physiological reports*, 3(6), p. e12429.

Spector, D. A., Yang, Q., and Wade, J. B. (2007). High urea and creatinine concentrations and urea transporter B in mammalian urinary tract tissues. *American Journal of Physiology-Renal Physiology*, 292(1), p. F467-F474.

Song, Y., Jayaraman, S., Yang, B., Matthay, M. A., and Verkman, A. S. (2001). Role of aquaporin water channels in airway fluid transport, humidification, and surface liquid hydration. *The Journal of general physiology*, *117*(6), p. 573-582.

Schey, K.L., Little, M., and Fowler, J.G. (2000) Characterization of human lens major intrinsic protein structure. Crouch Rk Investigative Ophthalmology and Visual Science, 41(1), p.175-82.

Sugiyama, Y., Ota, Y., Hara, M., and Inoue, S. (2001). Osmotic stress up-regulates aquaporin-3 gene expression in cultured human keratinocytes. *Biochimica et Biophysica Acta (BBA)-Gene Structure and Expression*, *1522*(2), p.82-88.

Smith, P. R., Mackler, S. A., Weiser, P. C., Brooker, D. R., Ahn, Y. J., Harte, B. J., and Kleyman, T. R. (1998). Expression and localization of epithelial sodium channel in mammalian urinary bladder. *American Journal of Physiology-Renal Physiology*, *274*(1), F91-F96.

Tajkhorshid, E., Nollert, P., Jensen, M.Ø, Miercke, L.J, O'Connell, J., and Schulten, K. (2002). Control of the selectivity of the aquaporin water channel family by global orientational tuning. *Science, 290*, p. 525-530.

Tang, G., and Yang, G. Y. (2016). Aquaporin-4: A potential therapeutic target for cerebral edema. *International journal of molecular sciences*, *17*(10), p. 1413.

Tomita, Y., Dorward, H., Yool, A., Smith, E., Townsend, A., Price, T., and Hardingham, J. (2017). Role of aquaporin 1 signalling in cancer development and progression. International. *Journal of Molecular Sciences*. *18*(2), p. 299.

Timmer, R. T., Klein, J. D., Bagnasco, S. M., Doran, J. J., Verlander, J. W., Gunn, R. B., and Sands, J. M. (2001). Localization of the urea transporter UT-B protein in human and rat erythrocytes and tissues. *American Journal of Physiology-Cell Physiology*, *281*(4), p. C1318-C1325.

Turnbull, G. J., and Fellows, G. J. (1972). Permeability of the urinary bladder of the rabbit. *Revue Europeenne D'etudes Cliniques et Biologiques. European journal of Clinical and Biological Research*, *17*(8), p. 745-749.

Taruno, A (2018) Atp Release Channels. *International Journal of Molecular Sciences 19*(3), p. 808.

Thiagarajah, J.R., Chang, J., Goettel, J.A., Verkman, A.S., and Lencer, W.I. (2017). Aquaporin-3 mediates hydrogen peroxide-dependent responses to environmental stress in colonic epithelia. *Proceedings of the National Academy of Sciences*, *114*(3), p. 568-573.

Tomaszewski, J.E., Landis, J.R., Russack, V., Williams, Tm, Wang, L.P., Hardy, C., Brensinger, C., Matthews, Y.L., Abele, S.T., Kusek, J.W., and Nyberg, L.M. (2001). Biopsy Features Are Associated with Primary Symptoms in Interstitial Cystitis: Results From the Interstitial Cystitis Database Study. *Urology*, *57,* p. 67-81.

Tomassoni, D., Bramanti, V., and Amenta, F. (2010). Expression of Aquaporins 1 and 4 in the brain of spontaneously hypertensive rats. *Brain Research*, p.155-163.

Tamarappoo, B.K., and Verkman, A.S. (1998). Defective aquaporin-2 trafficking in nephrogenic diabetes insipidus and correction by chemical chaperones. *The Journal of Clinical Investigation. 101*(10), p. 2257-2267.

Tripathi, S., and Boulpaep, E. L. (1989). Mechanisms of water transport by epithelial cells. *Quarterly Journal of Experimental Physiology: Translation and Integration*, *74*(4), p. 385-417.

Tada, J., Sawa, T., Yamanaka, N., Shono, M., Akamatsu, T., and Tsumura, K. (1999). Involvement of vesicle-cytoskeleton interaction in aqp5 trafficking in aqp5-gene-transfected hsg cells. *Biochemical and Biophysical Research Communications*. *266*, p. 443-447.

Terris, J, Ecelbarger, CA, Nielsen, S., and Knepper, M.A (1996). Long-term regulation of four renal aquaporins in rats. *American Journal of Physiology, 271*, p. F414-F422.

Tietz, P.S., McNiven, M.A., Splinter, P.L., Huang, B.Q., and Larusso, N.F (2006). Cytoskeletal and motor proteins facilitate trafficking of aqp1-containing vesicles in cholangiocytes. *Biology of the Cell* , *98*, p. 43-52.

Turnbull GJ, and Fellows G.J (1972). Permeability of the urinary bladder of the rabbit. Rev Eur Etud *Clinical Biology,* 17: p. 745–749.

Tsukaguchi, H., Weremowicz, S., Morton, C. C., and Hediger, M. A. (1999). Functional and molecular characterization of the human neutral solute channel aquaporin-9. *American Journal of Physiology-Renal Physiology*, *277*(5), F685-F696.

Tsukita, S, Furuse, M, and Itoh, M. (2001). Multifunctional strands in tight junctions. *Nature reviews Molecular cell biology*. *2*(4), p. 285.

Tamma, G., Klussmann, E., Maric, K., Aktories, K., Svelto, M., Rosenthal, W., and Valenti, G. (2001). Rho inhibits camp-induced translocation of aquaporin-2 into the apical membrane of renal cells. *American Journal of Physiology-renal Physiology, 281* (6)

Tamas, M., and Et Al, (2003) A short regulatory domain restricts glycerol transport through yeast Fps1p. *Journal of Biological Chemistry.* 278, p. 6337-6345.

Tomita, Y., Dorward, H., Yool, A., Smith, E., Townsend, A., Price, T., and Hardingham, J. (2017). Role of aquaporin 1 signalling in cancer development and progression. *International Journal of Molecular Sciences*, *18*(2), p. 299.

Ussing, H. H. and Zerahn, K. (1951). Active transport of sodium as the source of electric current in the short-circuited isolated frog skin. Reprinted from *Acta. Physiology Scandinavian. 23,* p. 110-127.

Ussing, H.H. (1949). The active ion transport through the isolated frog skin in the light of tracer studies. *Acta Physiology Scandinavian*, 17, p. 1-37.

Vahabi, B., Parsons, B. A., Doran, O., Rhodes, A., Dean, S., and Drake, M. J. (2013). TRPM8 agonists modulate contraction of the pig urinary bladder. *Canadian Journal of Physiology and Pharmacology*, *91(*7), p. 503-509.

Verkman, A.S (2011) Aquaporins at a glance. *Journal of Cell Science, 124*(13), p. 2107-2112.

Verkman, A. S. (2005). More than just water channels: unexpected cellular roles of aquaporins. *Journal of Cell Science*, *118*(15), p. 3225-3232.

Verkman, A.S., Anderson, M.O., and Papadopoulos, M.C. (2014). Aquaporins: Important but elusive drug targets. *Nature Reviews Drug Discovery*, *13*(4), p. 259.

Vlaskovska, M., Kasakov, L., Rong, W., Bodin, P., Bardini, M., Cockayne, D., Ford, A., and Burnstock, G. (2001). P2X3 knock-out mice reveal a major sensory role for urothelially released ATP. *The Journal of Neuroscience*, *21*(15), p.5670-5677.

Verkman, A.S., Anderson, M.O., and Papadopoulos, M.C. (2014). Aquaporins: important but elusive drug targets. *Nature Reviews Drug Discovery*, *13*(4), p. 259.

Verkam, A.S. and Mitra, A.K. (2000). Structure and function of aquaporin water channels. *American Journal of Physiology-renal Physiology*, 278 (1).

Vina-Vilaseca, A, Bender-Sigel, J., Sorkina, T., Closs, E.I. and Sorkin, A. (2011). Protein kinase c-dependent ubiquitination and clathrin-mediated endocytosis of the cationic amino acid transporter Cat-1. *Journal of Biological Chemistry*, *286*(10), p 8697-8706.

Viadiu, H., Gonen, T., and Walz, T. (2007). Projection map of aquaporin-9 at 7 Å resolution. *Journal of molecular biology*, *367*(1), p. 80-88.

Vukićević, T., Schulz, M., Faust, D., and Klussmann, E. (2016). The trafficking of the water channel aquaporin-2 in renal principal cells—a potential target for pharmacological intervention in cardiovascular diseases. *Frontiers in Pharmacology*, 7, p. 23.

Woo, J., Lee, J., Chae, Y.K., Kim, M.S., Baek, J.H., Park, J.C., and Lee, T. (2008). Overexpression of aqp5, a putative oncogene, promotes cell growth and transformation. *Cancer Letters, 264*(1), p. 54-62.

Walz, T., Fujiyoshi, Y., and Engel, A. (2009) The AQP structure and functional implications. *Handbook of Experimental Pharmacology*, p. 31-56.

Wang, F., Daugherty, B., Keise, L.L., Wei, Z., Foley, J.P., Savani, R.C., and Koval, M. (2003) Heterogeneity of claudin expression by alveolar epithelial cells. *American Journal of Respiratory Cell and Molecular Biology*. *29*(1), p. 62-70.

Walser, B.L., Yagil, Y., and Jamison, R.L. (1988). Urea flux in the ureter. *American Journal of Physiology, Renal Fluid Electrolyte Physiol*, *255* (2), F244-F249.

Walters, R. W., Freimuth, P., Moninger, T. O., Ganske, I., Zabner, J., and Welsh, M. J. (2002). Adenovirus fiber disrupts CAR-mediated intercellular adhesion allowing virus escape. *Cell*, *110*(6), 789-799.

Wehner, F., Olsen, H., Tinel, H., Kinne-Saffran, E., and Kinne, R. K. (2003). Cell volume regulation: osmolytes, osmolyte transport, and signal transduction. In *Reviews of Physiology, Biochemistry and Pharmacology* p. 1-80.

Watanabe, H., and Azuma, Y. (2016). Periodical measurement of urine volume in the bladder during sleep: Temporary volume reduction suggestive of absorption. *International Journal of Urology*, *23*(2), p. 182-187.

Weiss, J.P., Wein, A.J., and Kerrebroeck, P. (2014) Future research guidance for nocturia. *Neurourology and Urodynamics*. 33, p. S25.

Wu, X.R, Kong, X.P., Pellicer, A., Kreibich, G., and Sun, T.T. (2009). Uroplakins in urothelial biology, function, and disease. *Kidney international*, *75*(11), p. 1153-1163.

Walz, T., Fujiyoshi, Y., and Engel, A. (2009). The aqp structure and functional implications. *Handbook Experimental Pharmacology*, p.31-56.

Willermain, F., Janssens, S., Arsenijevic, T., Piens, I., Bolaky, N., Caspers, L., and Delporte, C. (2014). Osmotic stress decreases aquaporin-4 expression in the human retinal pigment epithelial cell line, Arpe-19. *International Journal of Molecular Medicine*, *34(*2), p.533-538.

Walpole, C., Farrell, A., McGrane, A., and Stewart, G. S. (2014). Expression and localization of a UT-B urea transporter in the human bladder. *American Journal of Physiology-Renal Physiology*, *307*(9), p. F1088-F1094.

Wu-Pong, S., Livesay, V., Dvorchik, B., and Barr, W. H. (1999). Oligonucleotide transport in rat and human intestine Ussing chamber models. *Biopharmaceutics and Drug Disposition*, *20*(9), p. 411-416.

Yang, B., Fukuda, N., van Hoek, A., Matthay, M. A., Ma, T., and Verkman, A. S. (2000). Carbon dioxide permeability of aquaporin-1 measured in erythrocytes and lung of aquaporin-1 null mice and in reconstituted proteoliposomes. *Journal of Biological Chemistry*, *275*(4), p. 2686-2692

Yang, F., Kawedia, J.D., Menon., and A.G. (2003). Cyclic amp regulates aquaporin 5 expression at both transcriptional and post-transcriptional levels through a protein kinase a pathway. *Journal of Biological Chemistry.* 278, p. 32173-32180.

Yang, B., Bankir, L., Gillespie, A., Epstein, C. J., and Verkman, A. S. (2002). Urea-selective concentrating defect in transgenic mice lacking urea transporter UT-B. *Journal of Biological Chemistry*, *277*(12), p. 10633-10637.

Yasui, M., Kwon, T. H., Knepper, M. A., Nielsen, S. and Agre, P. (1999). Aquaporin-6: An intracellular vesicle water channel protein in renal epithelia. *Proceedings of the National Academy of Sciences*, *96*(10), p. 5808-5813.

Yasui, H., Kubota, M., Iguchi, K., Usui, S., Kiho, T., and Hirano, K. (2008). Membrane trafficking of aquaporin 3 induced by epinephrine. *Biochemical Biophysical Research Communications*. 373, p. 613-617.

Yeung, C. H., and Cooper, T. G. (2010). Aquaporin AQP11 in the testis: molecular identity and association with the processing of residual cytoplasm of elongated spermatids. *Reproduction*, *139*(1), p. 209-216.

Yakata, K., Hiroaki, Y., Ishibashi, K., Sohara, E., Sasaki, S., Mitsuoka, K., and Fujiyoshi, Y. (2007). Aquaporin-11 containing a divergent NPA motif has normal water channel activity. *Biochimica et Biophysica Acta (BBA) - Biomembranes*, *1768*(3), p.688-693.

Yu, Y., and De Groat, W.C. (2010). Effects of stimulation of muscarinic receptors on bladder afferent nerves in the in vitro bladder pelvic afferent nerve preparation of the rat. 1*361*, p. 43-53.

Yang, B., Ma, T., and Verkman, A.S. (1995). Cdna cloning, gene organization, and chromosomal localization of a human mercurial insensitive water channel evidence for distinct transcriptional units. *Ournal of Biological Chemistry*, *270*(39), p. 22907-22913.

Yamamoto, T., Sasaki, S., Fushimi, K. Ishibashi, K., Yaoita, E., Kawasaki, K., and Kihara, I. (1995). Vasopressin increases AQP-CD water channel in apical membrane of collecting duct cells in Brattleboro rats. *American Journal of Physiology-Cell Physiology*, *268*(6), p. C1546-C1551.

Zhang, W., Zitron, E., Hömme, M., Kihm, L., Morath, C., and Scherer, D. (2007). Aquaporin-1 channel function is positively regulated by protein kinase C. *Journal of Biological Chemistry, 282*, p. 20933-20940.

Zou, L. B., Zhang, R. J., Tan, Y. J., Ding, G. L., Shi, S., Zhang, D., and Sheng, J. Z. (2011). Identification of estrogen response element in the aquaporin-2 gene that mediates estrogen-induced cell migration and invasion in human endometrial carcinoma. *The Journal of Clinical Endocrinology and Metabolism*, *96*(9), E1399-E1408.

Zanetta, L., Marcus, S. G., Vasile, J., Dobryansky, M., Cohen, H., Eng, K., and Mignatti, P. (2000). Expression of Von Willebrand factor, an endothelial cell marker, is up-regulated by angiogenesis factors: a potential method for objective assessment of tumor angiogenesis. *International Journal of Cancer*, 85(2), p. 281-288.

Zhu, C., Jiang, Z., Bazer, F.W., Johnson, G.A., Burghardt, R.C., and Wu, G. (2015). Aquaporins in the female reproductive system of mammals. *Frontiers Bioscience*, *20,* p. 838-871.

Zheng, X., and Bollag, W. B. (2003). Aquaporin 3 colocates with phospholipase d2 in caveolin-rich membrane microdomains and is downregulated upon keratinocyte differentiation. *Journal of Investigative Dermatology*, *121*(6), p. 1487-1495.

APPENDIX